PUSHING THE BOUNDARIES OF BIOLUMINESCENCE USING SYNTHETIC LUCIFERINS

A Dissertation Presented

By

David Matthews Mofford

Submitted to the Faculty of the
University of Massachusetts Graduate School of Biomedical Sciences, Worcester
in partial fulfillment of the requirements for the degree of

DOCTOR OF PHILOSOPHY

September 11, 2015

Biochemistry and Molecular Pharmacology

PUSHING THE BOUNDARIES OF BIOLUMINESCENCE
USING SYNTHETIC LUCIFERINS

A Dissertation Presented
By
David Matthews Mofford

The signatures of the Dissertation Defense Committee signify
completion and approval as to style and content of the Dissertation

Stephen C. Miller, Ph.D., Thesis Advisor

Anthony Carruthers, Ph.D., Member of Committee

Celia Schiffer, Ph.D., Member of Committee

Karen Allen, Ph.D., Member of Committee

The signature of the Chair of the Committee signifies that the written dissertation meets
the requirements of the Dissertation Committee

William Kobertz, Ph.D., Chair of Committee

The signature of the Dean of the Graduate School of Biomedical Sciences signifies
that the student has met all graduation requirements of the school.

Anthony Carruthers, Ph.D.,
Dean of the Graduate School of Biomedical Sciences

Program in Biochemistry and Molecular Pharmacology
September 11, 2015

DEDICATION

I dedicate this thesis to my two favorite people:

To my beautiful wife, Christie: Your love and support are endless. I couldn't have done this without you!

To my son and little buddy, Cameron: Mommy and I love you more than we ever thought possible. Thanks for letting Daddy get some sleep while writing!

ACKNOWLEDGEMENTS

First, I would like to acknowledge my thesis advisor, Stephen Miller. Steve's lab was my top choice at UMass and I've always been grateful he let me join. Thank you for the freedom and flexibility I've had over my projects but also for the guidance that has shaped me into the scientist I am today. I have truly enjoyed my time in your lab.

Next, thank you to all of my committee members: Bill Kobertz, Tony Carruthers, Celia Schiffer, and Alexei Bogdanov. Your guidance over the years has been invaluable. I am also grateful to Karen Allen for serving as my outside committee member. Thank you for taking the time to be part of this experience.

Thank you also to all of my lab mates, both past and present: Kate Harwood, Steven Pauff, Randheer Reddy, Kiran Reddy, Adam Choi, and Spencer Adams. Grad school would not have been nearly as fun without hanging out with all of you every day.

Finally, thank you to my wife, Christie. You've always believed in me and I wouldn't be here without you. I love you!

ABSTRACT

Fireflies are beetles that generate yellow-green light when their luciferase enzyme activates and oxidizes its substrate, D-luciferin. This bioluminescent reaction is widely used as a sensitive reporter both in vitro and in vivo. However, the light-emitting chemistry is limited by the properties of the small molecule D-luciferin. Our lab has developed a panel of synthetic luciferin analogs that improve on the inherent characteristics of D-luciferin. My thesis work focuses on harnessing these novel substrates to further expand the utility and molecular understanding of firefly bioluminescence.

The first part of my thesis focuses on using synthetic luciferins to improve bioluminescence imaging beyond what is possible with D-luciferin. Our substrates emit red-shifted light compared to D-luciferin, bringing the wavelength to a range that is more able to penetrate through tissue, but at a cost of lower signal intensity. I developed mutant luciferases that increase the maximal photon flux with the synthetic luciferins over what is achievable with the wild-type luciferase, and furthermore discriminate between substrates based on their chemical structures. Additionally, I have expanded the bioluminescence toolkit by harnessing the intrinsic properties of the luciferins to non-invasively and specifically assay the activity of a single enzyme (fatty acid amide hydrolase) in live mice. Therefore, my work presents an effective way to generally improve

upon bioluminescent reporters, but also to measure the activity of a specific enzyme of interest in the context of a living organism.

The second part of my thesis employs synthetic luciferins to more deeply probe the light-emitting chemistry of bioluminescence. Our synthetic substrates reveal latent luciferase activity from multiple luciferase homologs that are inactive with D-luciferin. These enzymes, the fatty acyl-CoA synthetases, are predicted to be luciferase's evolutionary predecessors, but it was not clear how the light emitting chemistry originated. My work shows that the luciferase must activate the luciferin and provide oxygen access, but the light emitting chemistry is a fundamental property of that activated intermediate. In summary, the work described herein not only expands our understanding of firefly bioluminescence, but also broadens its practical applications to shine bioluminescent light on the dark corners of biology.

TABLE OF CONTENTS

Dedication iii
Acknowledgements iv
Abstract v
Table of Contents vii
List of Tables x
List of Schemes xi
List of Figures xii
List of Third Party Copyrighted Material xvii
Lists of Symbols and Abbreviations xviii
Preface xxi

CHAPTER I: Introduction 1

Firefly bioluminescence 1
The origins of firefly luciferase and light emission 4
Light emission from D-luciferin 6
Firefly luciferase burst kinetics 8
Bioluminescence in biology 9
Limitations of firefly bioluminescence: emission wavelength 12
Red-shifting firefly bioluminescence using the luciferase 14
Red-shifting firefly bioluminescence using the luciferin 15
Limitations of firefly bioluminescence: the properties of D-luciferin 19
Limitations of firefly bioluminescence: other reporter options 19
Firefly luciferase and acyl-CoA ligases 20
Scope of my thesis 25

CHAPTER II: Aminoluciferins extend firefly luciferase bioluminescence into the near-infrared and can be preferred substrates over D-luciferin 28

Summary 28
Introduction 29
Results and Discussion 31
Conclusion 54
Materials and Methods 55

CHAPTER III: Latent luciferase activity in the fruit fly revealed by a synthetic luciferin 62

Summary 62
Introduction 63
Results 65
Discussion 80
Materials and Methods 83

CHAPTER IV: Insect fatty acyl-CoA synthetases exhibit unique latent luciferase activity with synthetic luciferin analogs 91

Summary 91
Introduction 92
Results 96
Discussion 109
Materials and Methods 114

CHAPTER V: Chimeric firefly luciferase / fatty acyl-CoA synthetase enzymes improve substrate selectivity 118

Summary 118
Introduction 119
Results 124
Discussion 142
Conclusion 146
Materials and Methods 147

CHAPTER VI: Luciferin amides enable in vivo bioluminescence detection of endogenous fatty acid amide hydrolase activity 157

Summary 157
Introduction 158
Results and Discussion 161
Materials and Methods 184

CHAPTER VII: Discussion of luciferin amides and imaging in the brain "Luciferins behave like drugs" 192

Summary 192
Viewpoint 193

CHAPTER VIII: Discussion 200

BIBLIOGRAPHY 216

LIST OF TABLES

Table 1.1 Acyl-CoA synthetases used in Figure 1.7.

Table 2.1. Fluorescence and bioluminescence emission wavelengths of all luciferins.

Table 3.1. D-luciferin and long-chain fatty acids competitively inhibit light output from CycLuc2-treated CG6178.

Table 8.1. Optimal enzyme/substrate pairs under various conditions.

LIST OF SCHEMES

Scheme 2.1. Synthesis of CycLuc3 and CycLuc4

Scheme 2.2. Synthesis of CycLuc5 and CycLuc6

Scheme 2.3. Synthesis of CycLuc7−CycLuc10

Scheme 2.4. Synthesis of CycLuc11 and CycLuc12

LIST OF FIGURES

Figure 1.1. Firefly luciferase-catalyzed light emission from D-luciferin.

Figure 1.2. Mechanisms of the adenylate-forming superfamily.

Figure 1.3. All possible keto-enol structures of oxyluciferin.

Figure 1.4. Burst kinetics profile of firefly luciferase injected into D-luciferin.

Figure 1.5. Interaction of light with tissue.

Figure 1.6. Chemical structures of D-luciferin and previously reported synthetic luciferins.

Figure 1.7. Phylogenetic tree of acyl-CoA synthetase genes.

Figure 2.1. Luciferase mechanism and substrates.

Figure 2.2. Initial and sustained bioluminescence intensity with purified WT luciferase.

Figure 2.3. Burst kinetics profiles of all luciferins with each luciferase.

Figure 2.4. Bioluminescence emission spectra for WT luciferase with selected substrates.

Figure 2.5. Normalized emission spectra of all luciferins with each luciferase.

Figure 2.6. Fluorescence peak emission wavelength of each aminoluciferin correlates with the bioluminescence peak wavelength for each luciferase.

Figure 2.7. Burst kinetics profiles of D-luciferin and CycLuc7 treated with purified WT and mutant luciferases.

Figure 2.8. Initial and sustained bioluminescence intensity with purified WT and mutant luciferases.

Figure 2.9. Photon flux from luciferase-expressing CHO cells.

Figure 2.10. Photon flux from live luciferase-expressing CHO cells.

Figure 2.11. Total photon flux from lysed luciferase-expressing CHO cells.

Figure 2.12. Total photon flux from live and lysed luciferase-expressing CHO cells with and without a Cy5.5 bandpass filter.

Figure 2.13. Western blot analysis of luciferase expression.

Figure 3.1. Firefly luciferase and long-chain fatty acyl-CoA synthetases catalyze similar two-step mechanisms.

Figure 3.2. Amino acid alignment between CG6178 (*Drosophila melanogaster*) and FLuc (*Photinus pyralis*).

Figure 3.3. CG6178 is a latent luciferase when treated with the synthetic luciferin CycLuc2.

Figure 3.4. CycLuc2 emits red-shifted light compared with D-luciferin with both FLuc and CG6178.

Figure 3.5. Effect of CycLuc2 chirality and CoA addition on CG6178 bioluminescence.

Figure 3.6. Burst kinetics profiles of D-luciferin, CycLuc2, and their respective adenylates.

Figure 3.7. Burst kinetics profiles of CG6178 and CycLuc2 or CycLuc2-AMP with and without ATP.

Figure 3.8. CG6178 bioluminescence is detected in both live S2 cells and live transfected CHO cells.

Figure 3.9. CG6178 light emission is detectable in both lysed Schneider 2 (S2) cells and lysed transiently transfected CHO cells.

Figure 3.10. Bioluminescence from live *Drosophila* S2 cells treated with CycLuc2 correlates linearly with the number of cells present.

Figure 3.11. Proposed mechanisms of LH_2-AMP oxidation.

Figure 4.1. Fatty acyl-CoA synthetases and firefly luciferase catalyze similar, two-step reactions.

Figure 4.2. Primary sequence alignment of firefly luciferase and three fatty acyl-CoA synthetases.

Figure 4.3. Chemical structures of luciferin substrates.

Figure 4.4. ACSL activity upon treatment with 250 μM of the indicated luciferin analog.

Figure 4.5. ACSL activity upon treatment with 3.91 μM of the indicated luciferin analog.

Figure 4.6. CG6178 activity is reduced by using impure ATP.

Figure 4.7. AbLL activity is reduced by using impure ATP.

Figure 4.8. Firefly luciferase activity is minimally affected by ATP purity.

Figure 4.9. PPi Affects Light Emission from FLuc and CG6178.

Figure 4.10. Burst kinetics of each ACSL with the indicated luciferin analog.

Figure 4.11. CycLuc2 burst kinetics with ACSLs.

Figure 5.1. Parallels between luciferase and fatty acyl-CoA synthetase mechanisms.

Figure 5.2. Amino acid alignment of firefly luciferase and two fatty acyl-CoA synthetases, CG6178 and AbLL.

Figure 5.3. Chemical structures of all luciferin analogs.

Figure 5.4. Luciferase/CG6178 active site chimeras are non-functional luciferases.

Figure 5.5. Luciferase/ACSL C-terminal chimeras are well expressed.

Figure 5.6. CG6178/Luciferase and AbLL/Luciferase C-Terminal Chimeras have lower photon flux compared to their WT counterparts.

Figure 5.7. Normalized photon flux from WT luciferase and each WT chimera.

Figure 5.8. Dose-response curves of WT luciferase and WT chimeras with acyclic luciferins.

Figure 5.9. Dose-response curves of WT luciferase and WT chimeras with cyclic luciferins.

Figure 5.10. Dose-response curves of WT luciferase and WT chimeras with non-traditional core luciferins.

Figure 5.11. Normalized photon flux from R218K luciferase and each R218K chimera.

Figure 5.12. Normalized photon flux from R218K+L286M+S347A luciferase and each triple mutant chimera.

Figure 5.13. Burst kinetics profiles of WT luciferase and WT chimeras with acyclic luciferins.

Figure 5.14. Burst kinetics profiles of WT luciferase and WT chimeras with cyclic luciferins.

Figure 5.15. Burst kinetics profiles of WT luciferase and WT chimeras with non-traditional core luciferins.

Figure 5.16. Burst kinetics profiles of R218K and triple mutant luciferases and their chimeras with select luciferins.

Figure 5.17. Codon optimized CG6178 amino acid and codon sequence.

Figure 5.18. Codon optimized AbLL amino acid and codon sequence.

Figure 5.19. WT luc2 luciferase amino acid and codon sequence.

Figure 5.20. PCR primer design for chimeric constructs.

Figure 5.21. FLuc/CG chimera amino acid and codon sequence.

Figure 5.22. FLuc/Ab chimera amino acid and codon sequence.

Figure 6.1. Enzyme mechanisms and luciferin structures.

Figure 6.2. FAAH inhibitor structures and in vitro FAAH inhibitor screen.

Figure 6.3. Luciferin amides report on rat FAAH activity in vitro.

Figure 6.4. Luciferin amides report on FAAH activity in live mammalian cells.

Figure 6.5. Luciferin amides report on FAAH activity in live cells and improve signal over parent luciferins.

Figure 6.6. Luciferin amides report on inhibitor potency in live cells.

Figure 6.7. Luciferin amides report on FAAH activity in live CHO cells.

Figure 6.8. Luciferin primary amides can inhibit luciferase in vitro.

Figure 6.9. CycLuc1 ethyl ester supports bioluminescence from both live CHO and HeLa cells.

Figure 6.10. Bioluminescence from mice that express luciferase in specific tissues after treatment with luciferins and luciferin amides.

Figure 6.11. CycLuc1 amide increases total photon flux from the brain at 1,000-fold lower dose than D-luciferin.

Figure 6.12. Inhibition of FAAH by PF3845 results in loss of signal from CycLuc1 amide in the brain.

Figure 6.13. Luciferin amides report on FAAH activity in live mice that ubiquitously express luciferase.

Figure 6.14. Bioluminescence from mice that ubiquitously express luciferase after treatment with luciferins and luciferin amides.

Figure 6.15. Ventral view of ubiquitously-expressing luciferase mice treated with CycLuc1 amide.

Figure 6.16. Mice ubiquitously-expressing luciferase treated with high inhibitor dose.

Figure 6.17. FAAH inhibitors do not affect parent luciferins.

Figure 6.18. CycLuc1 amide can be imaged at doses as low as 8 nmol/kg and signal is not saturated at 1 μmol/kg.

Figure 7.1. Enzyme catalyzed reactions.

Figure 7.2. Bioluminescence imaging in luciferase-expressing mice.

Figure 8.1. The loop in firefly luciferase that positions K529 is not well conserved in ACSLs.

Figure 8.2. Proposed bioluminescence MAGL activity assay.

LIST OF THIRD PARTY COPYRIGHTED MATERIAL

Figure 1.4	Dr. Hugo Fraga	3677700332613
Figure 1.5	Dr. Ralph Weissleder	3677690355819
Figure 1.7	Dr. Satoshi Inouyi	Permitted without license number
Table 1.1	Dr. Satoshi Inouyi	Permitted without license number

LIST OF SYMBOLS AND ABBREVIATIONS

α	alpha
Å	angstrom
AAV	adeno-associated virus
ACSL	long-chain acyl-CoA synthetase
ACS	acyl-CoA synthetase
AMP	adenosine monophosphate
ATP	adenosine triphosphate
BBB	blood brain barrier
Boc	*t*-butoxycarbonyl
BRET	bioluminescence resonance energy transfer
BSA	bovine serum albumen
Cd^{2+}	cadmium cation
CCD	charged-coupled device
CHO	chinese hamster ovary
CH_3CN	acetonitrile
CMV	cytomegalovirus
CoA	coenzyme A
CoASH	coenzyme A with a free sulfhydryl group
CO_2	carbon dioxide
Δ	delta
°	degree
DMEM	dulbecco's modified eagle's medium
DMSO	dimethyl sulfoxide
DNA	deoxyribonucleic acid
DSLA	5'-O-[*N*-(dehydroluciferyl)- sulfamoyl]adenosine
DTT	dithiothreitol
ε	molar extinction coefficient
EDTA	ethylenediaminetetraacetic acid
FAAH	fatty acid amide hydrolase
FBS	fetal bovine serum
g	gram
GST	glutathione-S-transferase
HBSS	hank's balanced salt solution
hFAAH	human fatty acid amide hydrolase
HRMS-ESI	high resolution mass spectrometry, electrospray ionization
hr	hour
hv	light
H_2O	water
IC_{50}	The half maximal inhibitory concentration: the inhibitor concentration that is required to decrease the maximal rate by half

IP	intraperitoneal
IPTG	isopropyl β-D-1-thiogalactopyranoside
IR	infrared
K_i	The inhibitory constant: the dissociation constant for the enzyme/inhibitor complex
K_m	The Michaelis-Menten constant: the substrate concentration at which the reaction rate is half of V_{max}
L	liter
L	dehydroluciferin
λ_{max}	wavelength maxima
LH_2	D-luciferin
µ	micro
m	milli
M	molar (mol/L)
MAGL	Monoacylglycerol lipase
Mg	magnesium
min	minute
$MgSO_4$	magnesium sulfate
mol	mole
MW	molecular weight
n	nano
NaCl	sodium chloride
NMR	nuclear magnetic resonance
rFAAH	rat fatty acid amide hydrolase
RLU	relative light unit
ROI	region of interest
RP-HPLC	reverse-phase high pressure liquid chromatography
RPM	rotations per minute
RT	room temperature
PCR	polymerase chain reaction
PET	positron emission tomography
p/s	photons per second
P/S	penicillin/streptomycin
$p/s/cm^2/sr$	photons per second per square centimeter per steradian
PBS	phosphate buffered saline
PDB	protein databank
PMSF	phenylmethylsulfonyl fluoride
PMT	photomultiplier tube
π	pi
PPase	pyrophosphatase
PPi	pyrophosphate
PTS1	peroxisomal targeting sequence
s	second
SD	standard deviation

SDS-PAGE	sodium dodecyl sulfate polyacrylamide gel electrophoresis
SEM	standard error of the mean
S2	schneider 2
TCEP	*tris*(2-carboxyethyl)phosphine
TFA	trifluoroacetic acid
U	unit
UV	ultra violet
V_{max}	The maximum velocity or rate of a reaction catalyzed by an enzyme when all enzyme active sites are saturated with substrate.
WT	wild-type
x g	times gravity
Zn^{2+}	zinc cation

PREFACE

Publications derived from work contained within this thesis:

In CHAPTER II: Mofford, D.M., Reddy, G.R., and Miller, S.C. (2014). Aminoluciferins extend firefly luciferase bioluminescence into the near-infrared and can be preferred substrates over D-luciferin. J. Am. Chem. Soc. *136*, 13277–13282.

In CHAPTER III: Mofford, D.M., Reddy, G.R., and Miller, S.C. (2014). Latent luciferase activity in the fruit fly revealed by a synthetic luciferin. Proc. Natl. Acad. Sci. U.S.A. *111*, 4443–4448.

In CHAPTER VI: Mofford, D.M., Adams, S.T., Reddy, G.S.K.K., Reddy, G.R., and Miller, S.C. (2015). Luciferin Amides Enable in Vivo Bioluminescence Detection of Endogenous Fatty Acid Amide Hydrolase Activity. J. Am. Chem. Soc. *137*, 8684–8687.

In CHAPTER VII: Mofford, D.M., and Miller, S.C. (2015). Luciferins Behave Like Drugs. ACS Chem. Neurosci. *6*, 1273–1275.

I thank Randheer Reddy and Kiran Reddy for their tireless efforts synthesizing all of the synthetic luciferins that formed the basis for my thesis work. I thank Spencer Adams for both teaching and helping me with the mouse imaging in CHAPTER VI.

CHAPTER I:

Introduction

Firefly bioluminescence

Bioluminescence is defined as the production of light from a living organism. Phylogenetic analysis suggests that this fascinating process has evolved independently over 30 times (Greer and Szalay, 2002; Hastings, 1983), in species such as bacteria, dinoflagellates, fungi, and fish. However, some of the best characterized bioluminescent organisms are insects. Light emission from insects is almost exclusively found in beetles from the order Coleoptera, including click beetles (Elateridae family), railroad worm beetle larvae (Phengodidae family), and fireflies and glow worms (Lampyridae family) (Day et al., 2009). While as many as 2,000 bioluminescent beetles have been identified (Herring, 1979), most of the characterization of insect bioluminescence was performed on a single species, the North American firefly, *Photinus pyralis* (Conti et al., 1996; de Wet et al., 1987).

The firefly and all other bioluminescent beetles use an enzyme called luciferase to catalyze light emission (Fraga, 2008; Greer and Szalay, 2002; Hastings, 1998; Wilson and Hastings, 1998). Each beetle has a distinct but homologous version. However, all beetles share the same substrate, D-luciferin. Light emission occurs when luciferase binds D-luciferin, in the presence of Mg-ATP, to catalyze the formation of an intermediate luciferyl-adenylate (Fraga,

2008) (**Figure 1.1**). This activated adenylate allows for the formation of a resonance stabilized carbanion at the C4 carbon of D-luciferin, which can react with oxygen by single electron transfer (Branchini et al., 2015; Mofford et al., 2014a). Oxygen then displaces AMP, forming a high energy dioxetanone ring that spontaneously breaks down to an excited state oxyluciferin by releasing carbon dioxide (Fraga, 2008). Finally, the excited state product relaxes to the ground state by releasing a photon of light, resulting in bioluminescence (**Figure 1.1**). Conversely, the luciferyl adenylate can be oxidized to produce dehydroluciferyl adenylate and hydrogen peroxide via an off-pathway reaction that does not emit light (Fraga et al., 2006) (**Figure 1.1**). Firefly luciferase is able to catalyze light emission with a final quantum yield of 41% (Ando et al., 2008), resulting in the brilliant light emitted by the firefly in the night sky.

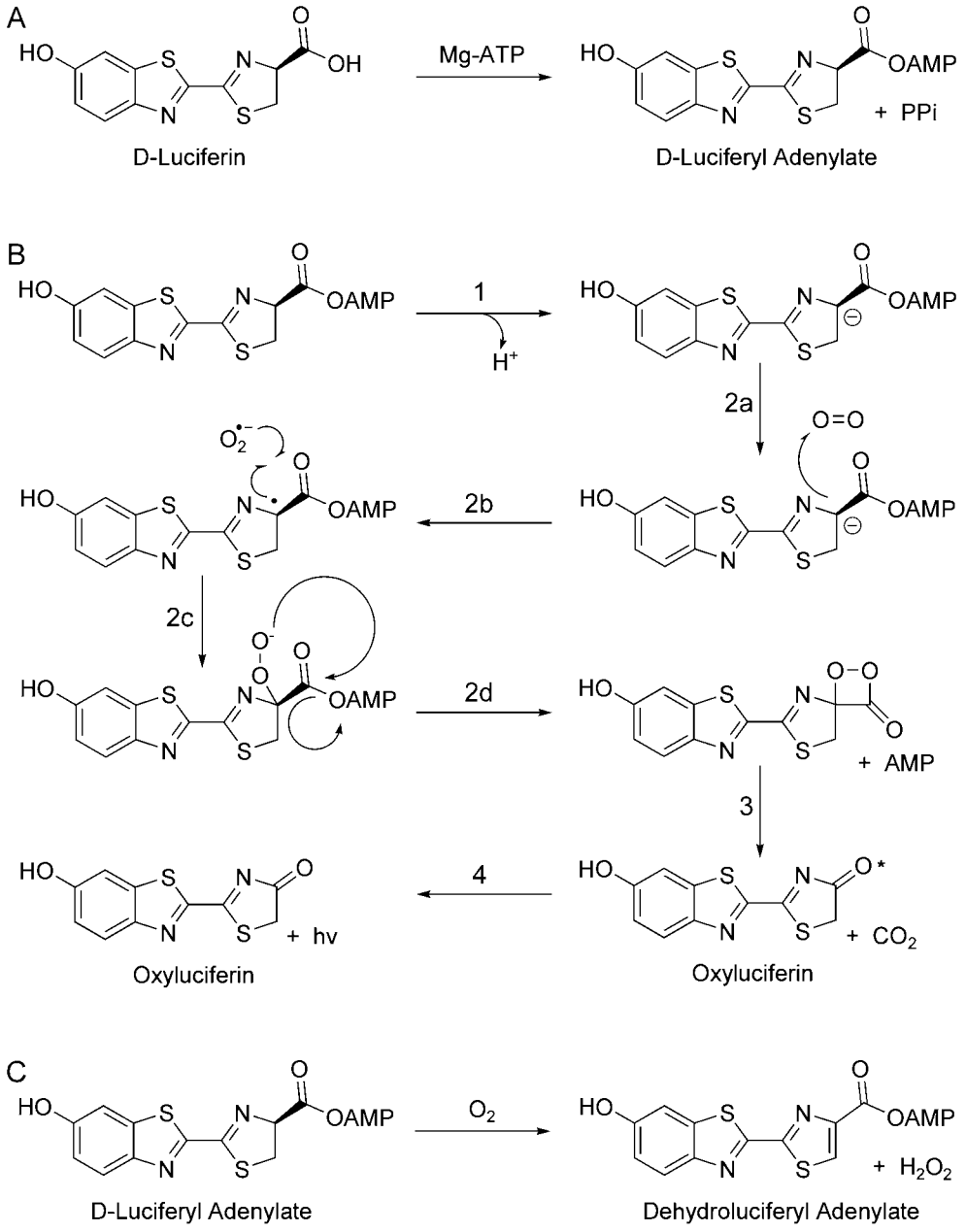

Figure 1.1. Firefly luciferase-catalyzed light emission from D-luciferin. (A) Luciferase binds D-luciferin and Mg-ATP to catalyze the formation of the luciferyl adenylate intermediate. (B) After adenylation: 1) D-luciferyl adenylate stabilizes the formation of a carbanion; 2) the carbanion reacts with oxygen, forms the high energy dioxetanone ring, and releases AMP; 3) the ring decomposes, releasing CO_2 and producing the excited state oxyluciferin; 4) the excited state product relaxes to the ground state via photon emission. (C) Oxidation of the luciferyl adenylate intermediate can also form the off-pathway products dehydroluciferyl adenylate and hydrogen peroxide that do not emit light.

The origins of firefly luciferase and light emission

It has long been apparent that firefly luciferase shares biochemical characteristics with ligases such as acyl-CoA synthetases, aminoacyl-tRNA synthetases, and plant *p*-coumarate-CoA ligases (McElroy et al., 1967; Pietrowska-Borek et al., 2003) (**Figure 1.2**). Indeed, luciferase is able to catalyze the synthesis of dehydroluciferyl adenylate and dehydroluciferyl CoA from dehydroluciferin through a mechanism identical to an acyl-CoA synthetase (**Figure 1.2**). Recently, luciferase was shown to act as a long chain fatty acyl-CoA synthetase (ACSL) (Oba et al., 2003), accepting fatty acid substrates in addition to luciferins. Moreover, the crystal structure of luciferase (Conti et al., 1996; Sundlov et al., 2012) shows similarities to other acyl-CoA synthetases (Conti et al., 1997; Gulick et al., 2003; Reger et al., 2008). Thus, luciferase was classified as a member of the acyl-adenylate/thioester-forming superfamily (Chang et al., 1997; Oba et al., 2005).

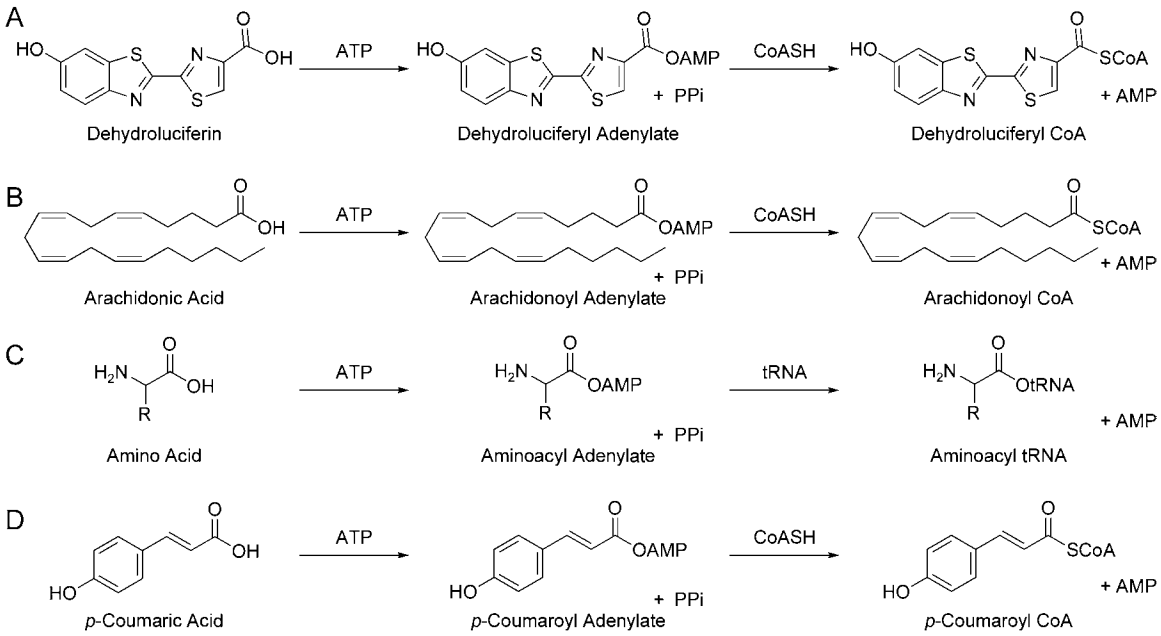

Figure 1.2. Mechanisms of the adenylate-forming superfamily. (A) Luciferase binds dehydroluciferin and Mg-ATP to catalyze the formation of an intermediate adenylate that is then displaced by CoA to produce dehydroluciferyl-CoA. (B) Acyl-CoA synthetases bind fatty acids and Mg-ATP to catalyze the formation of an intermediate adenylate that is then displaced by CoA to produce the acyl-CoA product. (C) Aminoacyl-tRNA synthetases bind their respective amino acid and Mg-ATP to catalyze the formation of an intermediate adenylate that is then displaced by the appropriate tRNA to form the aminoacyl-tRNA product. (D) *p*-Coumarate-CoA ligases bind *p*-coumaric acid and Mg-ATP to catalyze the formation of an intermediate adenylate that is then displaced by CoA to produce the acyl-CoA product.

It is hypothesized that luciferase evolved from a gene duplication event of an ACSL (Oba et al., 2006a). Upon duplication, the original gene retained its native function, leaving the copy free to mutate and evolve a new function (Ohno, 1970). The chemistry to adenylate a free carboxylate is clearly present in an ACSL, yet the origin of the oxidative chemistry of luciferase is less obvious. Originally, oxidation of the intermediate adenylate was proposed to be achieved

non-catalytically (Day et al., 2004), since luciferyl adenylates are readily oxidized without enzyme in basic DMSO (Seliger and McElroy, 1962). However, the level of light generated without enzyme is not sufficient to explain the intense glow that is observed from the firefly, suggesting that the oxidative step must also be catalyzed. Further evidence in favor of catalytic oxidation is the observation that only the D-isomer of luciferin is able to emit light (Fraga, 2008). Moreover, only the D-luciferyl adenylate can be oxidized to form the off-pathway dehydroluciferyl adenylate product (Fraga et al., 2006) (**Figure 1.1**). Oxygen has been shown to generally access ligand binding sites (Baron et al., 2009). The structure of luciferase suggests that oxygen has access from only one direction (Nakatsu et al., 2006); although, a putative oxygen binding site in luciferase has not been identified (Branchini et al., 1998).

Light emission from D-luciferin

In nature, all beetles utilize D-luciferin as the substrate for their respective luciferases. However, the color of light emitted can range from green (530 nm) to red (635 nm) (Hastings, 1996). These variations are due to differences in the local environment of the luciferase binding pocket. It was originally proposed that variations to the binding orientation of D-luciferin caused the different wavelengths. In this model, the angle between the benzothiazole and thiazoline rings would alter the potential energy of the excited state oxyluciferin. It was proposed that an angle of 0° between the two would produce the highest energy

state and emit higher energy green light. An angle of 90° would be the lowest energy state, thus emitting red light. However, subsequent structural studies have invalidated this hypothesis (Nakatsu et al., 2006). Instead, the structure and protonation state of the oxyluciferin determines the wavelength of light emitted. Oxyluciferin can adopt one of six possible conformations (**Figure 1.3**). The phenolic hydroxyl on the benzothiazole can exist as either a protonated phenol or a deprotonated phenolate. The carbonyl on the thiazoline ring can tautomerize to either the keto or enol conformation, and the enol can be further deprotonated to its respective enolate (**Figure 1.3**). Bound to firefly luciferase, the phenolic hydroxyl exists as a phenolate. When the carbonyl is in the keto form, oxyluciferin emits red light (635 nm). The enol and enolate forms emit at 560 nm and 590 nm, respectively (Branchini et al., 2002; Naumov et al., 2009; White et al., 1980). Thus, the local environment in the active site of the luciferase determines the relative abundance of each conformation and the wavelength of light emitted.

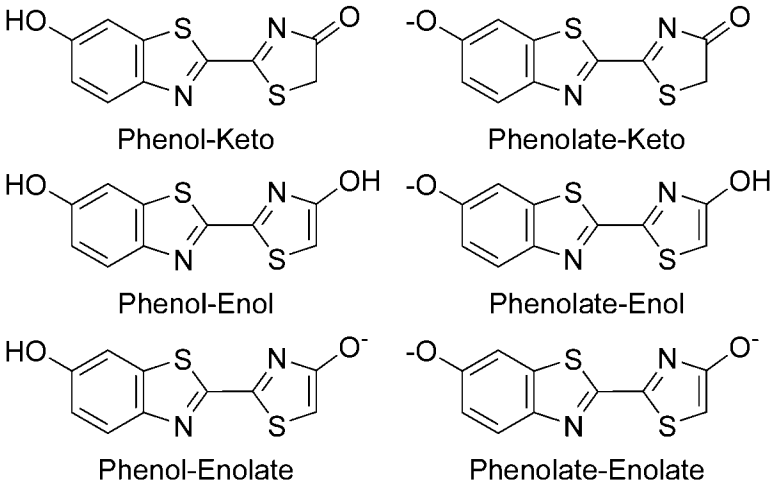

Figure 1.3. All possible keto-enol structures of oxyluciferin.

Firefly luciferase burst kinetics

Luciferase-catalyzed light emission is characterized by "burst kinetics" where, upon rapid injection of enzyme to substrate, there is a burst of light within the first few seconds, followed by a decay in the sustained level of light emission (DeLuca and McElroy, 1974) (**Figure 1.4**). This decay is due to product inhibition, where slow dissociation of the final products inhibits subsequent rounds of catalysis (Fraga, 2008). The slow dissociation of both the oxyluciferin and AMP light emitting products and the "dark" dehydroluciferyl adenylate (L-AMP) product contribute to the inhibition. While L-AMP only accounts for approximately 16% of the oxidized product (Fraga, 2008), it is a much more potent inhibitor than oxyluciferin (L-AMP K_i = 3.8 ± 0.7 nM, oxyluciferin K_i = 0.50 ± 0.03 μM) (Ribeiro and Esteves da Silva, 2008). Its non-competitive inhibition forces luciferase into a

closed conformation (Nakatsu et al., 2006). This inhibition can be relieved by the addition of Coenzyme A (CoA), which reacts with L-AMP to form L-CoA, a less potent inhibitor (Fraga et al., 2006) (**Figure 1.4**).

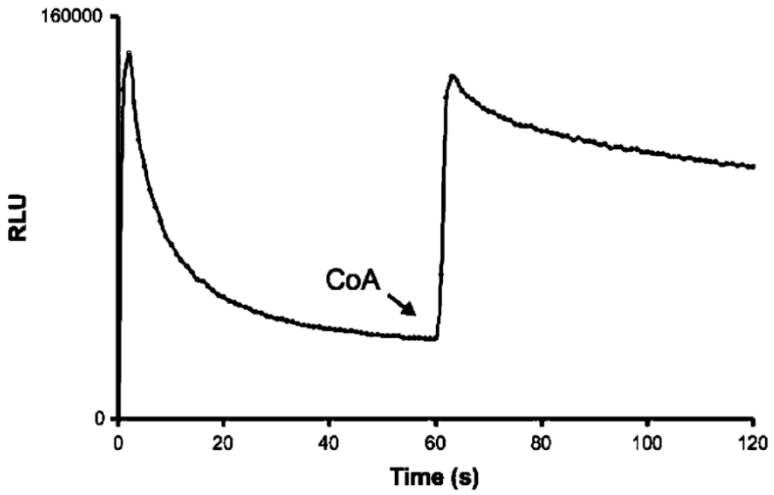

Figure 1.4. Burst kinetics profile of firefly luciferase injected into D-luciferin. Rapid injection of luciferase to D-luciferin produces a burst of light followed by a decay caused by product inhibition. The addition of CoA at 60 s relieves some product inhibition, resulting in a second burst and a decrease in the subsequent decay. Figure adapted from (Fraga, 2008).

Bioluminescence in biology

"Among reaction products, the photon is undoubtedly the most important; few can argue that if not for the light, Luc would not have been rescued from the obscure beetle biochemistry." (Fraga, 2008)

The light-emitting chemistry of bioluminescence has been widely adopted to report on otherwise invisible biological processes (Badr and Tannous, 2011) both in vitro (Fan and Wood, 2007) and in vivo (Prescher and Contag, 2010). For

example, by placing a luciferase gene under the control of a promoter sequence of interest, it is possible to monitor the gene expression controlled by that promoter by luciferase expression and subsequent light emission with D-luciferin (Hill et al., 2001). Conversely, by generating a “pro-luciferin” whose light emitting chemistry is dependent upon enzymatic activity (i.e., linking the luciferin to a short peptide that can be cleaved by a specific protease), the activity of that enzyme can be monitored via light emission (Hickson et al., 2010; Moravec et al., 2009).

Firefly bioluminescence offers several advantages over fluorescence and other optical reporter techniques. Fluorescent proteins can be genetically encoded, much the same way as a luciferase can; and fluorescent dyes can be modified and cleaved by enzymes of interest, similar to a small molecule luciferin (Fernández-Suárez and Ting, 2008). However, all fluorescence-based assays require an external photon to supply the energy needed for the excited state product, as opposed to the chemical reaction used in bioluminescence. It is the need for exogenous light that limits the application of fluorescence compared to bioluminescence. Endogenous molecules such as hemoglobin absorb and even fluoresce visible light (Mobley and Vo-Dinh, 2003; Zhao et al., 2005). Therefore, the external light source will not only excite your target fluorophore, but also the endogenous cellular chromophores, resulting in high background autofluorescence and a low signal-to-noise ratio. Moreover, the absorbed light can also damage these endogenous molecules, causing phototoxicity and cell

death. Without the need for an external photon, bioluminescence does not produce any background autoluminescence or phototoxicity, resulting in a higher signal-to-noise ratio and a lower cell mortality rate.

While bioluminescence offers several advantages over fluorescence, there are relatively few bioluminescent reporters available, compared to the broad pallet of fluorescent proteins and dyes. Indeed, despite the number of organisms that have evolved bioluminescence, the number of luciferase/luciferin systems employed for use as reporters is limited by the number of luciferins discovered (Greer and Szalay, 2002; Welsh and Noguchi, 2012). As mentioned above, all beetle luciferases share D-luciferin as a substrate. The other commonly used luciferin for bioluminescence imaging is coelenterazine, the substrate for many marine luciferases. Most often, the *Renilla* luciferase from the sea pansy, *Renilla reniformis*, is used in conjunction with coelenterazine. However, coelenterate bioluminescence is inferior to beetle bioluminescence due to the coelenterazine substrate: coelenterazine is larger, less water soluble, and more toxic than D-luciferin, limiting its use in live cells and organisms (Welsh and Noguchi, 2012). Additionally, while D-luciferin must be adenylated before oxidation, coelenterazine does not need to be activated, resulting in a low level of auto-oxidation and higher background luminescence. Therefore, D-luciferin in conjunction with firefly luciferase has become the preferred bioluminescent reporter system for use in the biological sciences. *Renilla* luciferase and

coelenterazine are often used as a second/control reporter when investigating multiple biological events simultaneously (Welsh and Noguchi, 2012).

Limitations of firefly bioluminescence: emission wavelength

Undoubtedly, firefly bioluminescence has become an invaluable tool for studying biology. However, it is not without some caveats. First, the wavelength of light that is emitted is not ideal, especially for in vivo imaging. Cellular components and other endogenous molecules such as hemoglobin, absorb visible light (Weissleder and Ntziachristos, 2003; Zhao et al., 2005) (**Figure 1.5**). Therefore, a large portion of the light emitted by luciferase is absorbed by the surrounding tissue and will not penetrate through the animal for detection. Near-infrared (near-IR) light (650-900 nm) is less well absorbed by these endogenous molecules and is able to further penetrate through tissue (Mobley and Vo-Dinh, 2003; Weissleder and Ntziachristos, 2003) (**Figure 1.5**). The broad emission spectrum of luciferase contains a portion of light in this range and is thus still able to be used. However, red-shifting the emission wavelength of luciferase to increase the intensity of near-IR light would make for a more sensitive reporter system. This optimal optical window is another reason that beetle bioluminescence is preferred over coelenterate bioluminescence. Coelenterazine emits blue-shifted light compared to D-luciferin, so even more light will be absorbed by the surrounding tissue (Haddock et al., 2010) (**Figure 1.5**).

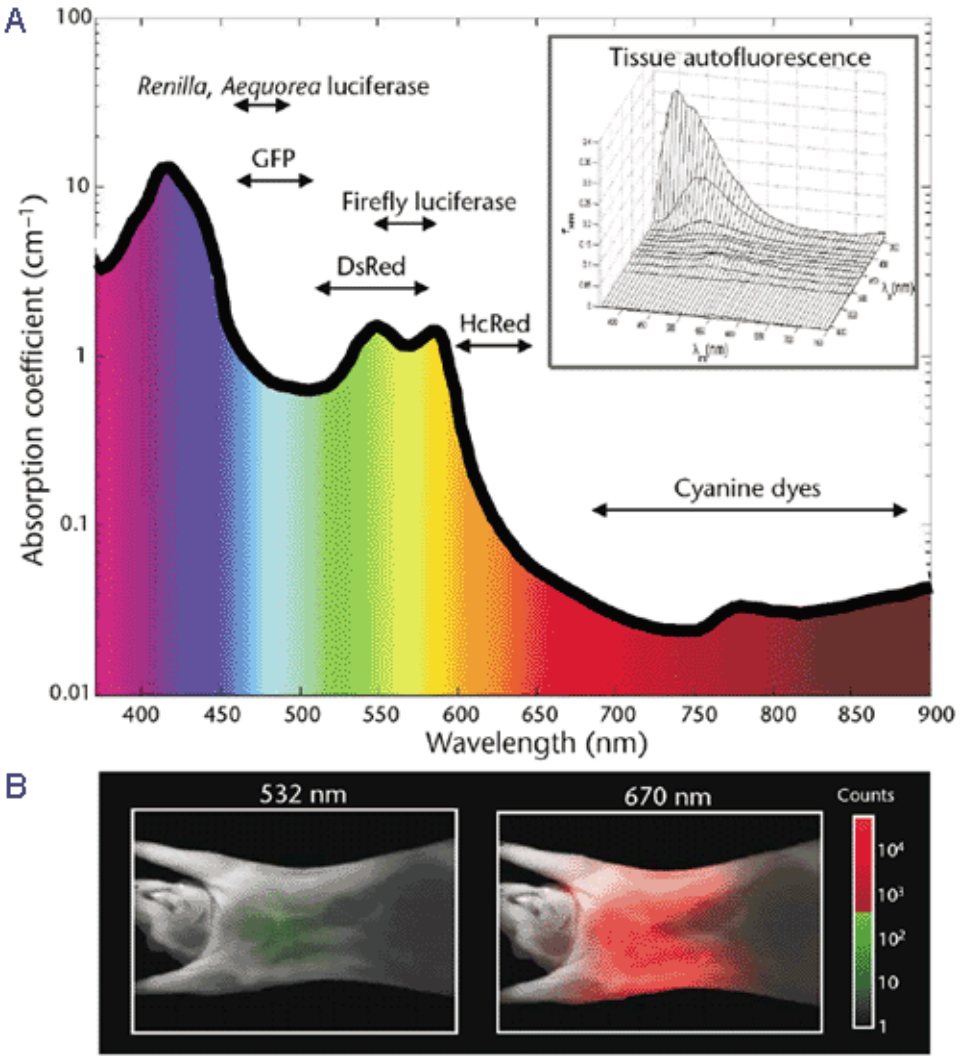

Figure 1.5. Interaction of light with tissue. (A) The absorption coefficient of light in tissue, assuming normally oxygenated tissue (saturation of 70%), 50 mM hemoglobin, and a composition of 50% water and 15% lipids. The emission range of several common imaging reagents are shown. The insert shows autofluorescence spectra obtained in vivo at different excitation wavelengths. (B) The mouse images show experimentally measured photon counts through the body of a nude mouse at 532 nm (left) and 670 nm (right). Figure adapted from (Weissleder and Ntziachristos, 2003).

Diverse factors can impact the wavelength of light emitted with D-luciferin (Seliger and McElroy, 1964). For example, the presence of divalent cations, such as Cd^{2+} and Zn^{2+}, can red-shift the peak wavelength of light emitted with firefly luciferase. Additionally, lowering the pH of the solution to ~6, or increasing the temperature of the solution from ambient to 37 °C also red-shift the emission profile. Finally, the origin of the luciferase can impact the wavelength of light emitted. The railroad worm luciferase from the lateral lanterns of *Phrixothrix vivianii* catalyzes emission of green light (542 nm), while the luciferase from the head lanterns of *Phrixothrix hirtus* results in red light emission (628 nm) (Viviani et al., 1999). In the lab, the environmental parameters can be readily manipulated. However, living organisms hold the concentration of divalent cations, pH, and temperature constant. Therefore, the luciferase and luciferin are the preferred targets for altering the emission profile in vivo.

Red-shifting firefly bioluminescence using the luciferase

Several labs have focused on using red-shifted beetle luciferases from either click beetles (Wood et al., 1989) or railroad worms (Viviani and Ohmiya, 2000). These luciferases favor emission by the keto form of oxyluciferin (**Figure 1.3**), thus emitting red-shifted light relative to firefly luciferase. Others have generated firefly luciferase mutants that also red-shift the light with D-luciferin (Branchini et al., 2005a, 2010a; Mezzanotte et al., 2011). Alternatively, Branchini et al., developed a chimeric enzyme between the luciferases of *Photinus pyralis*

and *Luciola italia* that improves the overall intensity of light with D-luciferin (Branchini et al., 2014). While the chimera may not red-shift the peak wavelength of light emitted, the increased intensity may still improve the level of photon flux that penetrates through the tissue. All of these strategies produce luciferases that catalyze light emission in a more desirable range; however each luciferase is still fundamentally limited by the photophysical properties of D-luciferin itself.

Red-shifting firefly bioluminescence using the luciferin

An alternative strategy is to design and synthesize synthetic luciferin analogs that emit at longer wavelengths than D-luciferin. This can be done in one of two ways: 1) through bioluminescence resonance energy transfer; 2) through chemical alteration of the luciferin structure. Bioluminescence resonance energy transfer (BRET) uses the energy of the excited state oxyluciferin to excite a second fluorophore that will then emit light at an even longer wavelength (Pfleger et al., 2006). This technique is often used to measure protein-protein interactions, since the donor luciferase and the acceptor fluorophore must be in close proximity. Here, by either directly labeling firefly luciferase with a near-IR fluorophore (Branchini et al., 2010b), or conjugating the luciferin to a near-IR dye (Kojima et al., 2013), BRET can be a source of near-IR light. However, the need to modify luciferase with a near-IR dye limits its use as a genetically encodable reporter; and attaching a near-IR dye to the luciferin will limit water solubility and

cell permeability of the luciferin. Also, there is a loss of signal intensity with BRET that may counter any benefit from the red-shift in peak wavelength.

Our lab and others have instead focused on direct chemical modification of the luciferin substrate. The energy difference between the excited and ground states determines the wavelength of light emitted (Naumov et al., 2009), and it is well known that replacing the 6'-hydroxyl of D-luciferin with a more electron-donating amino group red-shifts the peak wavelength of light emitted (White et al., 1966). Our lab therefore designed synthetic luciferin analogs that replace the 6'-hydroxyl of D-luciferin with cyclic alkylamino groups fused to the 5' and 6' positions of the benzothiazole (Reddy et al., 2010) (**Figure 1.6**). These alkylamino substituents are more strongly electron-donating than either the original hydroxyl or the amine, which should red-shift the peak emission wavelength even more. Additionally, by restricting molecular motion of the arylamine by cyclization back to the benzothiazole, the modified luciferins should maintain a high quantum yield. Indeed, these substrates displayed red-shifted light emission relative to D-luciferin, and also increased the total photon flux when used with Promega's Ultra-Glo luciferase (Auld et al., 2009) and P450-Glo buffer (Reddy et al., 2010). However, when used with WT firefly luciferase without the P450-Glo buffer, each of these luciferins displayed much weaker light than D-luciferin, due to an increased affinity for luciferase and corresponding increase in product inhibition (Reddy et al., 2010).

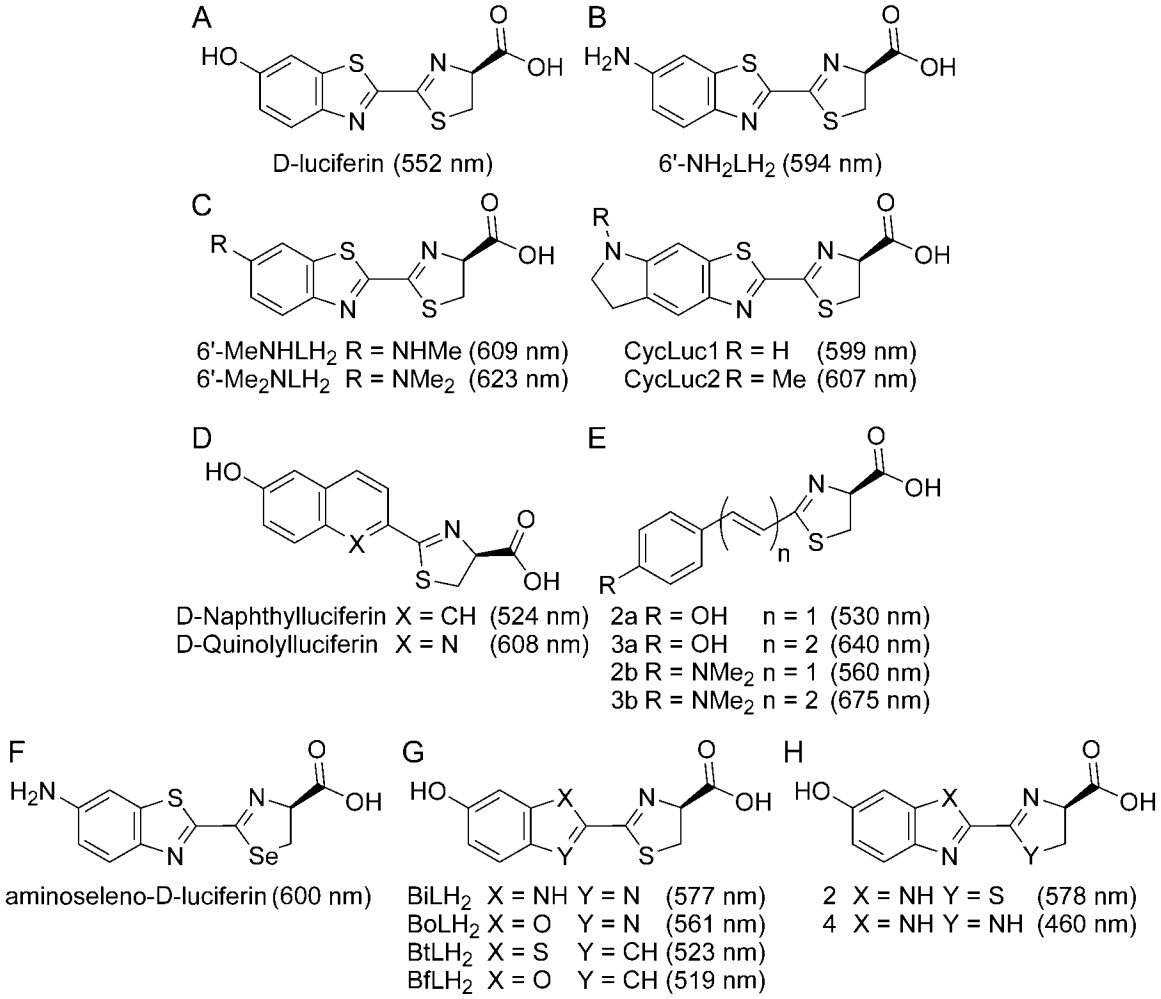

Figure 1.6. Chemical structures of D-luciferin and previously reported synthetic luciferins. (A) D-luciferin. (B) White et al., 1966. (C) Reddy et al., 2010. (D) Branchini et al., 1989. (E) Iwano et al., 2013. (F) Conley et al., 2012. (G) Woodroofe et al., 2012. (H) McCutcheon et al., 2012. Peak emission wavelengths reported are shown in parentheses.

Other groups have more drastically modified the luciferin structure. Branchini et al. was one of the first to alter the core of D-luciferin. They showed that it was possible to exchange the benzothiazole of D-luciferin for either a naphthalene or quinoline (Branchini et al., 1989) (**Figure 1.6**). These luciferins emit light upon treatment with firefly luciferase at 524 nm and 608 nm, respectively, albeit at a lower intensity than D-luciferin. Subsequently, others have developed electronically modified luciferins by substituting single atoms in either the benzothiazole or thiazoline rings of D-luciferin (Conley et al., 2012; McCutcheon et al., 2012; Woodroofe et al., 2012) (**Figure 1.6**). All remain substrates for luciferase and display altered emission profiles, but none improve on the bioluminescence obtained with D-luciferin. Finally, Iwano et al. completely removed the benzothiazole in favor of a simpler aromatic system with extended π-conjugation to the thiazoline ring (Iwano et al., 2013) (**Figure 1.6**). This strategy has produced the first example of a peak emission wavelength in the near-IR, at 675 nm. However, as with all the other synthetic substrates, shifting the peak wavelength is accompanied by a loss of signal intensity. While all of these new substrates demonstrate how promiscuous luciferase is, no example of a synthetic luciferin has shown improvement over WT luciferase and D-luciferin under saturating luciferin and ATP conditions.

Limitations of firefly bioluminescence: the properties of D-luciferin

An added benefit of many synthetic luciferins is increased cell permeability and/or higher affinity for luciferase. When used in live cells and organisms, firefly luciferase will be retained inside the cell. Therefore, a luciferin must first cross the membrane in order to emit light. D-luciferin is small and relatively polar, therefore it is capable of moderate diffusion across cell membranes. However, D-luciferin only has a modest affinity for luciferase (K_m = ~7 μM) (Harwood et al., 2011) and is thus unlikely to reach saturating conditions when used in live cells and organisms. Many of the synthetic luciferins developed thus far show increased hydrophobicity relative to D-luciferin which should increase cell permeability. Cyclic alkylamino luciferins also have increased affinity for luciferase (K_m < 0.1 μM) (Harwood et al., 2011), allowing sufficient substrate to enter the cells to saturate the enzyme.

Limitations of firefly bioluminescence: other reporter options

Finally, as mentioned above, the number of distinct bioluminescent reporters is lacking. There has been some success in spectrally isolating beetle luciferase signals by using luciferases that emit at different wavelengths (i.e., green and red) (Branchini et al., 2005a, 2010a). However, this analysis can be complicated when used in vivo. The light that is emitted from a luciferase within a live mouse is naturally red-shifted by the body temperature of the mouse, and by its tissues absorbing lower wavelength light (Zhao et al., 2005). Thus, the green

luciferase will naturally shift toward the red so the two signals will not be as resolved as they would be in vitro.

Currently, multiplexed assays using bioluminescence can be performed by reporting on one event with firefly luciferase/D-luciferin and on the second with *Renilla* luciferase/coelenterazine. These two systems are completely orthogonal, meaning that there is no activity from a luciferase with the other substrate (e.g., *Renilla* luciferase does not emit light with D-luciferin and vice versa). This technique works very well, despite the flaws of *Renilla* luciferase, but is limited to these two luciferase/luciferin pairs.

Firefly luciferase and acyl-CoA ligases

Apart from using luciferase as a tool to report on biological function, work has also been done to understand the evolution of insect bioluminescence. Firefly luciferase is a member of the acyl-adenylate/thioester-forming superfamily (Chang et al., 1997). Other members of this family include acyl- and acetyl-CoA synthetases, aminoacyl-tRNA synthetases, and plant *p*-coumarate-CoA ligases, none of which emit light (McElroy et al., 1967; Pietrowska-Borek et al., 2003). All members catalyze the synthesis of their respective products via intermediate adenylates after reaction with ATP (**Figure 1.2**). Since the structure of luciferase was solved (Conti et al., 1996), it has become apparent that the members of this family share a similar tertiary structure. Luciferase is divided into two domains: a large N-terminal domain that contains the luciferin and ATP binding pockets, and

a small C-terminal catalytic domain. Catalysis occurs at the interface between the two (Conti et al., 1996; Sundlov et al., 2012). Many other members of this family share this organization (Conti et al., 1997; Gulick et al., 2003; Reger et al., 2008).

In addition to catalyzing light emission from D-luciferin, firefly luciferase is also a long chain fatty acyl-CoA synthetase able to synthesize fatty acyl-CoA from long chain fatty acids, ATP, and CoA (Oba et al., 2003). Analysis of luciferase's fatty acyl-CoA synthetase activity shows a similar substrate preference to mammalian ACSLs, preferring saturated medium-chain fatty acids (C8-C14) and unsaturated long-chain fatty acids (C16-C20) (Oba et al., 2005). However, upon phylogenetic analysis of fatty acyl-CoA synthetases from mammals, insects, plants, fungi, and bacteria, it appears that luciferase is not evolutionarily related to the mammalian enzymes (Oba et al., 2005) (**Figure 1.7** and **Table 1.1**). Oba et al. hypothesize that luciferase and other insect fatty acyl-CoA synthetases share a distinct ancestor from their mammalian counterparts.

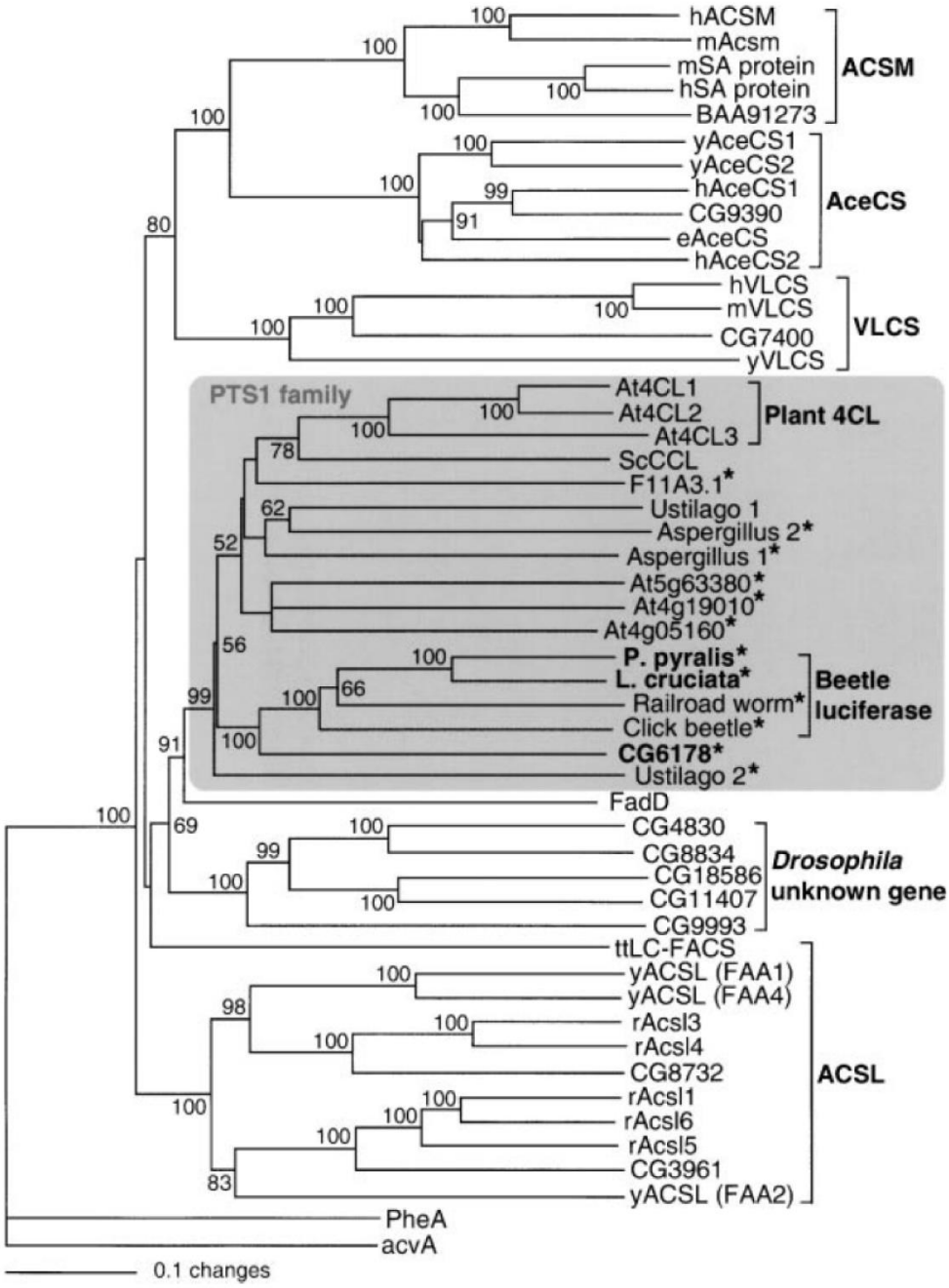

Figure 1.7. Phylogenetic tree of acyl-CoA synthetase genes. The tree was constructed by the neighbor-joining method using amino acid sequences. Abbreviated names are listed in **Table 1.1**. Numbers indicate bootstrap values from 1,000 replicates. Only bootstrap values over 50% are indicated. Horizontal branch lengths indicate genetic distances. The genes that possess a peroxisomal targeting sequence (PTS1) at the C-terminus are marked with *. A shaded clade shows the PTS1 family. Figure adapted from (Oba et al., 2005).

Table 1.1 Acyl-CoA synthetases used in Figure 1.7.

Name	Access. No.	Organism	Function of gene product	PTS1 signal[a]
Mammal				
mAcsm	NP_473435	*Mus musculus*	ACSM	−
mSA protein	NM_016870	*Mus musculus*	ACSM	−
mVLCS	AAB87982	*Mus musculus*	VLCS	−
rAcsl1	NP_036952	*Rattus norvegicus*	Rat ACSL	−
rAcsl3	NP_476448	*Rattus norvegicus*	Rat ACSL	−
rAcsl4	NP_446075	*Rattus norvegicus*	Rat ACSL	−
rAcsl5	NP_446059	*Rattus norvegicus*	Rat ACSL	−
rAcsl6	NP_570095	*Rattus norvegicus*	Rat ACSL	−
hSA protein	NM_005622	*Homo sapiens*	Human SA gene	−
hACSM	NM_052956	*Homo sapiens*	Putative ACSM	−
hVLCS	NP_003636	*Homo sapiens*	VLCS	−
BAA91273	BAA91273	*Homo sapiens*	Unknown	−
hAceCS1	AAF75064	*Homo sapiens*	AceCS	−
hAceCS2	Q9NUB1	*Homo sapiens*	Putative AceCS	−
Insect				
P. pyralis	AAA29795	*Photinus pyralis*	Luciferase and ACSL	+
L. cruciata	M26194	*Luciola cruciata*	Luciferase and ACSL	+
Railroad worm	AF139645	*Phrixothrix hirtus*	Railroad worm luciferase	+
Click beetle	AAQ11720	*Pyrophorus plagiophthalamus*	Jamaican click beetle luciferase	+
CG3961	NP_649067	*Drosophila melanogaster*	Unknown	−
CG4830	NM_141903	*Drosophila melanogaster*	Unknown	−
CG6178	NM_142964	*Drosophila melanogaster*	ACSL	+
CG7400	NM_079984	*Drosophila melanogaster*	Putative fatty acid transporter	−
CG8732	NP_724696	*Drosophila melanogaster*	Unknown	−
CG8834	NM_136935	*Drosophila melanogaster*	Unknown	−
CG9390	S52154	*Drosophila melanogaster*	Putative AceCS	−
CG9993	NP_611518	*Drosophila melanogaster*	Unknown	±
CG11407	NM_142574	*Drosophila melanogaster*	Unknown	−
CG18586	NM_139736	*Drosophila melanogaster*	Unknown	−
Nematode				
F11A3.1	CAA94751	*Caenorhabditis elegans*	Unknown	+
Plant				
At4CL1	U18675	*Arabidopsis thaliana*	*Arabidopsis* 4CL	−
At4CL2	AF106085	*Arabidopsis thaliana*	*Arabidopsis* 4CL	−
At4CL3	AF106087	*Arabidopsis thaliana*	*Arabidopsis* 4CL	−
At5g63380	AY250835	*Arabidopsis thaliana*	*Arabidopsis* 4CL-like protein	+
At4g05160	AY250839	*Arabidopsis thaliana*	*Arabidopsis* 4CL-like protein	+
At4g19010	AY250834	*Arabidopsis thaliana*	*Arabidopsis* 4CL-like protein	+
Fungi				
Ustilago 1	EAK81955	*Ustilago maydis*	Unknown	−
Ustilago 2	EAK85592	*Ustilago maydis*	Unknown	+
Aspergillus 1	EAA57739	*Aspergillus nidulans*	Unknown	+
Aspergillus 2	EAA61507	*Aspergillus nidulans*	Unknown	+
yAceCS1	AAC04979	*Saccharomyces cerevisiae*	Yeast AceCS	−
yAceCS2	P52910	*Saccharomyces cerevisiae*	Yeast AceCS	−
yVLCS	NP_009597	*Saccharomyces cerevisiae*	Yeast VLCS (Fat1p)	−
yACSL (FAA1)	NP_014962	*Saccharomyces cerevisiae*	Yeast ACSL (Faa1p)	−
yACSL (FAA2)	NP_010931	*Saccharomyces cerevisiae*	Yeast peroxisomal ACSL (Faa2p)	−
yACSL (FAA4)	NP_013974	*Saccharomyces cerevisiae*	Yeast putative ACSL (*FAA4*)	−
Bacteria				
PheA	1AMUA	*Brevibacillus brevis*	(See in Materials and methods)	−
acvA	P19787	*Penicillium chrysogenum*	(See in Materials and methods)	−
eAceCS	NP_418493	*Escherichia coli* K12	Putative AceCS	−
ttLC-FACS	AB126656	*Thermus thermophilus* HB8	ACSL	−
FadD	P29212	*Escherichia coli* K12	ACSL	−
SeCCL	NP_628552	*Streptomyces coelicolor* A3(2)	Cinnamate:CoA ligase	−

[a]The PTS1 signal was searched by the PTS1 predictor. Genes were identified as: possess the PTS1 (+), do not possess the PTS1 (-), or could not classify (±). Table adapted from (Oba et al., 2005)

While luciferase may share a common ancestor to insect ACSLs, retain ACSL activity, and emit light via an activated adenylate, it is still a mystery where the oxidation function originated. Only very weak light emission has ever been seen from an ACSL upon treatment with D-luciferin (Viviani et al., 2013). However, Oba et al. have shown that it is possible to elicit light emission from a fatty acyl-CoA synthetase after mutagenesis of the luciferin binding pocket, albeit at much lower intensity than luciferase (Oba et al., 2009). Still, their results suggest that it may just be the binding affinity and/or orientation of D-luciferin limiting light emission from an ACSL, instead of lack of functional ability.

Despite the lack of endogenous light-emitting capabilities, luciferase homologs, such as ACSLs, could be a source of genetic diversity for generating improved bioluminescent reporters. Branchini et al. demonstrated that a chimeric enzyme of the luciferases from *P. pyralis* and *L. italia* could improve the light emitted from D-luciferin (Branchini et al., 2014). This was the first example of an engineered luciferase improving on WT. These enzymes are both luciferases and emit light independently when treated with D-luciferin. However, extending this strategy to luciferase homologs may also produce beneficial effects.

Scope of my thesis

Firefly bioluminescence is a fascinating phenomenon that has been harnessed to report on otherwise invisible biological processes. Our lab has developed a panel of synthetic luciferin analogs based on the general core structure of the native firefly substrate, D-luciferin. The overall goal of my thesis has been to use these substrates to better understand the fundamental properties of bioluminescence, as well as to improve its practical applications and push the boundaries of what is possible.

My first goal was two-fold. First, I wanted to generally improve and expand bioluminescence imaging reagents by increasing the intensity of light that is emitted from luciferase with our synthetic luciferins. Second, I wanted to develop mutant luciferases that efficiently and selectively utilize specific synthetic luciferins in order to add a third reporter system for use with firefly luciferase and *Renilla* luciferase. In CHAPTER II, I report the synthesis and characterization of 10 additional synthetic luciferins based off of the structures of CycLuc1 and CycLuc2 (Reddy et al., 2010). Several of these new luciferin analogs improve the near-IR photon flux in live cells >10-fold with WT firefly luciferase. Additionally, we identify a triple mutant luciferase that 1) is almost completely inactive with D-luciferin in vitro and in live cells; and 2) selects for and improves the signal intensity of several synthetic luciferins to levels comparable to WT luciferase with D-luciferin. Therefore, we have improved upon what is achievable with WT luciferase and D-luciferin by increasing the light emitted in the near-IR and have

taken the first step toward developing a third bioluminescent reporter for use in conjunction with current technologies.

For my next thesis goal, I chose to investigate latent luciferase activity from fatty acyl-CoA synthetases using our synthetic luciferins. In CHAPTER III, I report on the identification and characterization of CG6178, an ACSL from *Drosophila melanogaster*. CG6178 is the first latent luciferase discovered, capable of emitting light with the synthetic luciferin CycLuc2 but not with D-luciferin. In CHAPTER IV, I continue that work with the expanded panel of synthetic luciferins from CHAPTER II and show: 1) CG6178 luciferase activity extends to synthetic luciferins other than CycLuc2; and 2) the ACSL AbLL from *Agrypnus binodulus* also possesses latent luciferase activity, but with altered substrate selectivity to CG6178. However, neither of these enzymes emit light with the intensity needed for use as a reporter. Therefore, in CHAPTER V, I evaluate luciferase/CG6178 and luciferase/AbLL chimeric enzymes for the improved substrate selectivity of the ACSLs but with the high photon flux of luciferase. Here we find that by exchanging the C-terminal domain of luciferase for that of an ACSL, we can select against D-luciferin, while improving signal intensity of and substrate selectivity for synthetic luciferins.

Finally, the third goal of my thesis research was to expand the bioluminescence toolkit and develop an assay for a specific enzyme. Luciferase has been shown to possess ACSL activity and we have also identified two ACSLs that possesses luciferase activity. Therefore, we hypothesized that the

luciferins were binding the active site by mimicking a fatty acid and would be ideally suited to probe the chemistry of enzymes that release a fatty acid. In CHAPTER VI, I show that by replacing the carboxylate of a luciferin substrate with an amide, the resulting pro-luciferin becomes a specific substrate for the drug target fatty acid amide hydrolase (FAAH). Since a luciferin amide is not a substrate for luciferase, only in the presence of FAAH activity will the amide be hydrolyzed and support light emission. These sensors readily translate from in vitro, to live luciferase-expressing cells, to live luciferase-expressing mice and are specific for FAAH in each case.

CHAPTER II:

Aminoluciferins Extend Firefly Luciferase Bioluminescence into the Near-Infrared and Can Be Preferred Substrates over D-Luciferin

Mofford, D.M. *et. al.* (2014) *JACS*, 136(38), 13277–13282.

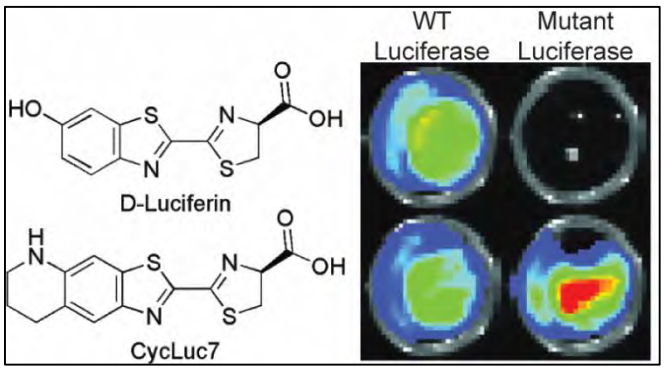

Summary

Firefly luciferase adenylates and oxidizes D-luciferin to chemically generate visible light and is widely used for biological assays and imaging. Here we show that both luciferase and luciferin can be reengineered to extend the scope of this light-emitting reaction. D-Luciferin can be replaced by synthetic luciferin analogs that increase near-infrared photon flux >10-fold over that of D-luciferin in live luciferase-expressing cells. Firefly luciferase can be mutated to accept and utilize rigid aminoluciferins with high activity in both live and lysed cells yet exhibit 10,000-fold selectivity over the natural luciferase substrate. These new luciferin analogs thus pave the way to an extended family of bioluminescent reporters.

Introduction

Fireflies are beetles that have evolved the remarkable ability to emit visible light based on a chemical reaction. Instead of a photon of light, firefly luciferase uses adenosine triphosphate and the chemical energy of oxygen to convert its substrate D-luciferin into an excited-state molecule of oxyluciferin (Fraga, 2008) (**Figure 2.1A**). This bioluminescent reaction has been widely used as a biological reporter both in vitro (Fan and Wood, 2007) and in vivo (Prescher and Contag, 2010). Although bioluminescence has much lower background than fluorescence and is more sensitive for in vivo imaging, it has been limited by the relative lack of luciferases and luciferins compared to the broad palette of fluorescent probes.

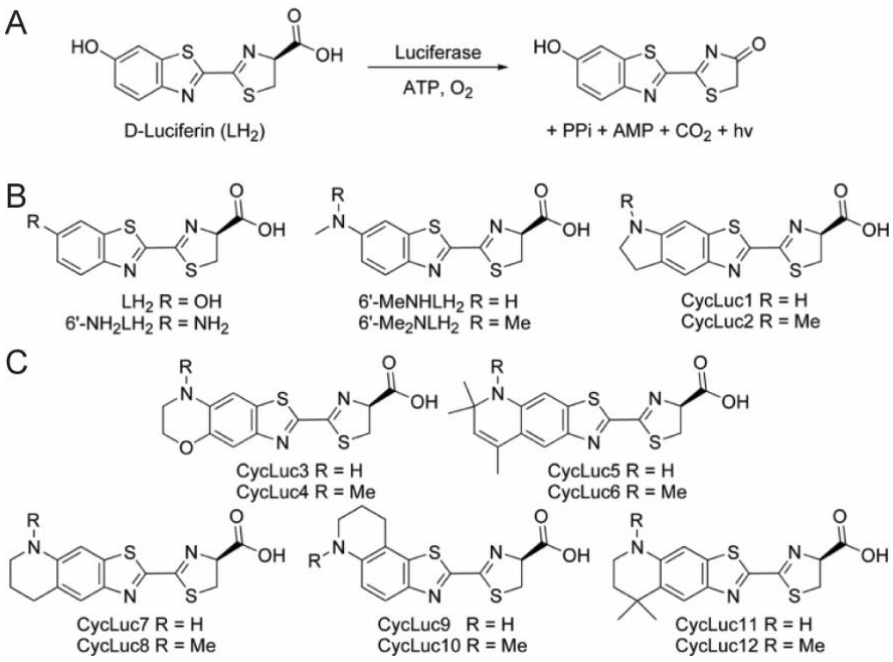

Figure 2.1. Luciferase mechanism and substrates. (A) Firefly luciferase catalyzes the adenylation and oxidation of its native substrate D-luciferin to emit a photon of light. (B) Previously synthesized aminoluciferin analogs. (C) New aminoluciferins from this work.

In nature, D-luciferin is the only luminogenic substrate for beetle luciferases. Over the past few years, many new luciferin analogs have been described, including several that yield peak light emission well into the red (Conley et al., 2012; Iwano et al., 2013; Kojima et al., 2013; Reddy et al., 2010; Takakura et al., 2010, 2011). Synthetic luciferins thus have the potential to extend bioluminescence imaging to wavelengths where tissue is more transparent to light. However, there is already a significant red and near-infrared component to luciferase emission with D-luciferin, and shifting the peak wavelength does not necessarily mean that the overall level of red light has actually increased (Branchini et al., 2005a; Kojima et al., 2013; Viviani et al., 1999). The synthetic luciferin CycLuc1 (**Figure 2.1**) performs better than D-luciferin for bioluminescence imaging in live mice, primarily due to its improved ability to access the luciferase rather than a red-shift in light emission (Evans et al., 2014). Therefore, substrates that combine this ready access to intracellular luciferase in live cells with a redshift in total emission are expected to be candidates to further improve in vivo performance (Adams and Miller, 2014).

Structural differences between luciferins could also potentially allow the creation of orthogonal luciferases. Although mutant firefly luciferases that exhibit luciferin selectivity have been reported, D-luciferin remains a light-emitting substrate (Harwood et al., 2011). Surprisingly, recent work has identified the *Drosophila* fatty acyl-CoA synthetase CG6178 as a latent luciferase that emits light with CycLuc2 but not D-luciferin (Mofford et al., 2014a). While this

demonstrates that it is possible to retain luciferase activity in beetle luciferase homologues that are unresponsive to D-luciferin, higher rates of photon emission are desirable for use as reporters.

With all of these considerations in mind, we synthesized compact, rigid aminoluciferins modeled after CycLuc1 and CycLuc2 (Harwood et al., 2011; Reddy et al., 2010) (**Figure 2.1**). We found that these new substrates could greatly increase the total photon flux of near-IR light from live luciferase-expressing cells over D-luciferin. Moreover, high photon flux was observed from a newly identified mutant luciferase that gave virtually no light emission with the natural substrate. Chemical modification of the luciferin substrate can thus extend the scope of bioluminescence beyond what is possible with D-luciferin (Adams and Miller, 2014).

Results and Discussion

Synthesis of new rigid aminoluciferins. The synthetic aminoluciferins CycLuc1 and CycLuc2 have 5',6'-fused five-membered indoline rings (**Figure 2.1B**). To evaluate the effect of this ring fusion on bioluminescence, we synthesized new luciferin analogs with fused six-membered rings of varying composition. Luciferin analogs CycLuc3 and CycLuc4, containing a six-membered oxazine ring, were readily accessed following a slight modification of the CycLuc1 synthesis paradigm (Reddy et al., 2010) (**Scheme 2.1**).

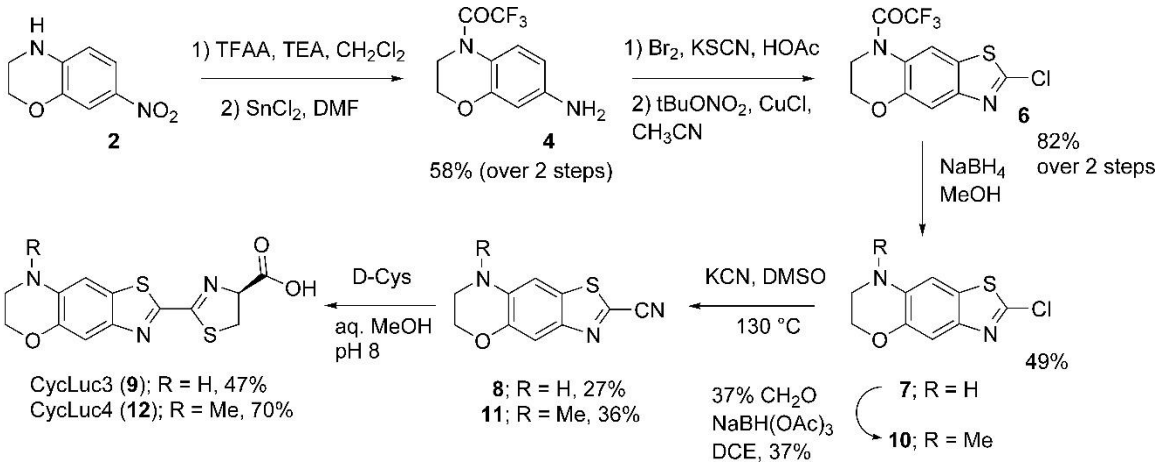

Scheme 2.1. Synthesis of CycLuc3 and CycLuc4

CycLuc5 and CycLuc6 were designed to emit light at longer wavelengths and to test the scope of substrates that could be accommodated by the luciferase (**Scheme 2.2**). These bulky, lipophilic analogs incorporate 2,2,4-trimethyl-dihydroquinoline, a scaffold that has been widely used to red-shift the emission of many classes of fluorophores, including coumarins (Panchuk-Voloshina et al., 1999), rhodamines (Belov et al., 2009; Panchuk-Voloshina et al., 1999), and oxazines (Pauff and Miller, 2011). Attempted synthesis of intermediate **16** by trifluoroacetylation of the corresponding nitroarene as in Scheme 2.1 failed, presumably due to a combination of steric hindrance and electronic deactivation (Williamson and Ward, 2005). We therefore synthesized the Boc-protected compound **14** (Bonger et al., 2009), which suffers the same steric hindrance but was anticipated to be less electronically deactivated. Gratifyingly, trifluoroacetylation of this intermediate was successful (Williamson and Ward, 2005), and subsequent TFA deprotection readily afforded **16**. Elaboration as

shown in Scheme 2.2 afforded the desired luciferin analogs CycLuc5 and CycLuc6.

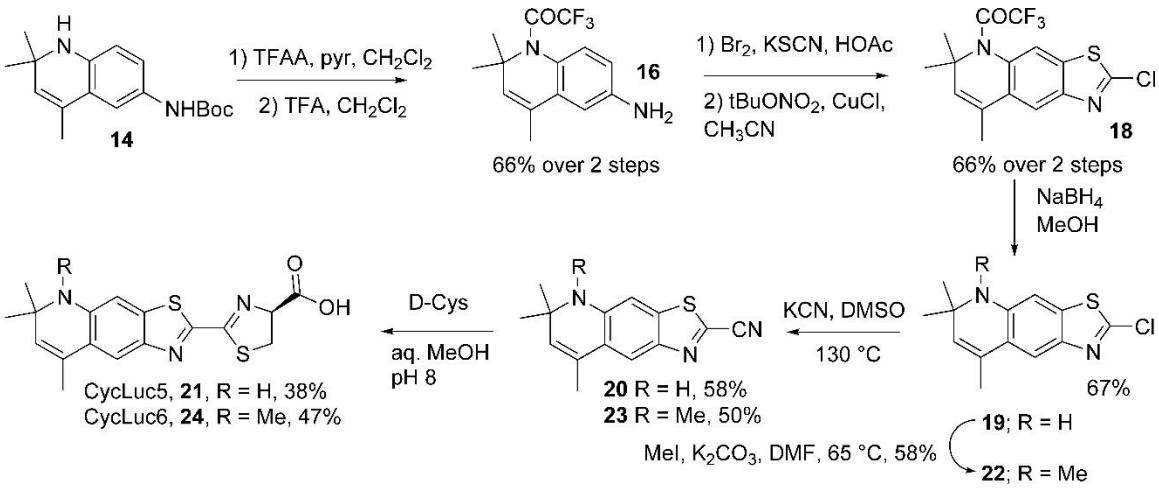

Scheme 2.2. Synthesis of CycLuc5 and CycLuc6

The corresponding saturated tetrahydroquinoline aminoluciferins analogs CycLuc7 and CycLuc8 were synthesized using the same general synthetic route as CycLuc1−CycLuc4 (**Figure 2.1C** and **Scheme 2.3**). Surprisingly, attempts to access the 5',6'-fused ring - differing from CycLuc1 by only a single methylene - primarily yielded the 6',7'-fused product in a >8:1 ratio. Nonetheless, elaboration of **32b** to the 5',6'-fused cyclic alkylaminoluciferins CycLuc7 and CycLuc8 proceeded uneventfully. The 6',7'-fused product **32a** was similarly converted into 6',7'-fused cyclic alkylaminoluciferins CycLuc9 and CycLuc10.

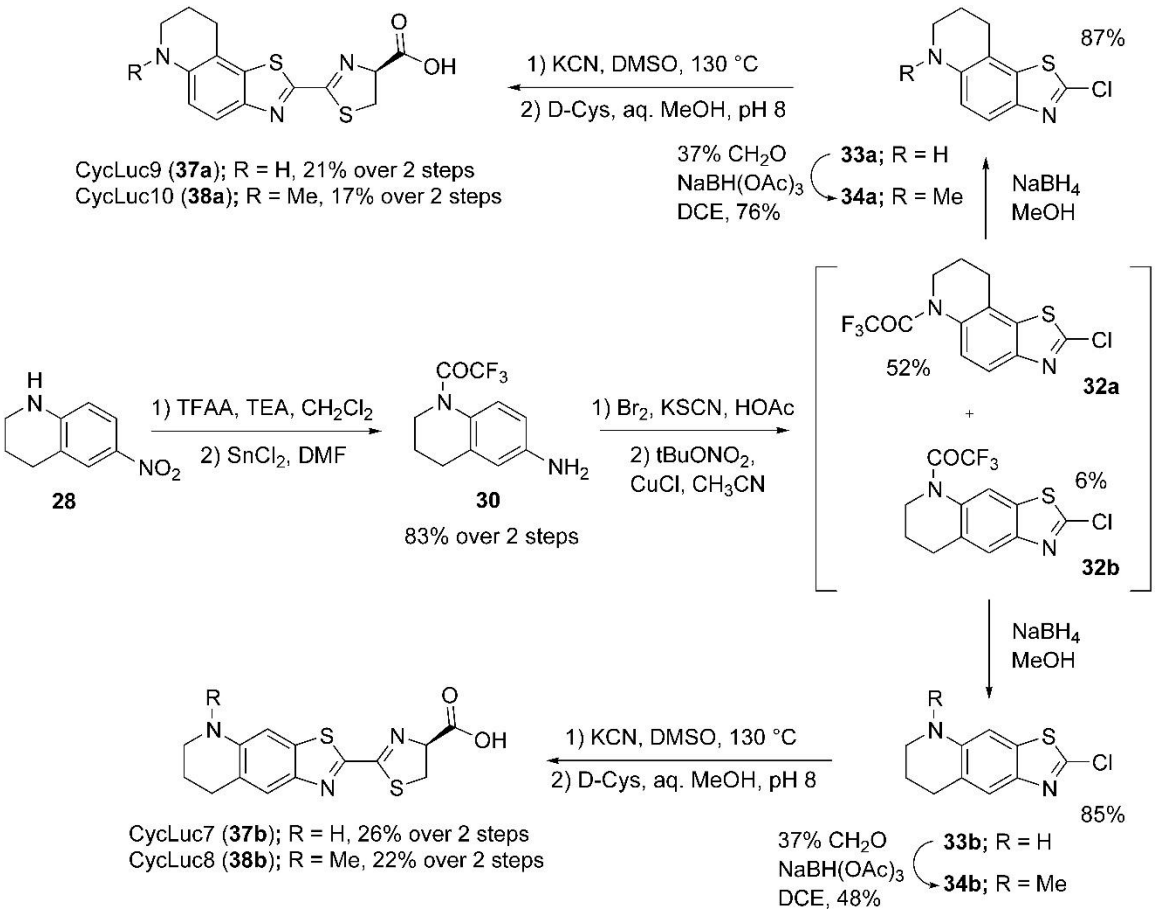

Scheme 2.3. Synthesis of CycLuc7−CycLuc10

Finally, 5',6'-fused cyclic aminoluciferins CycLuc11 and CycLuc12 were synthesized as bulkier and more lipophilic analogs of CycLuc7 and CycLuc8, where the gem-dimethyl substituents also direct exclusive formation of the 5',6'-fused isomers (**Figure 2.1C** and **Scheme 2.4**).

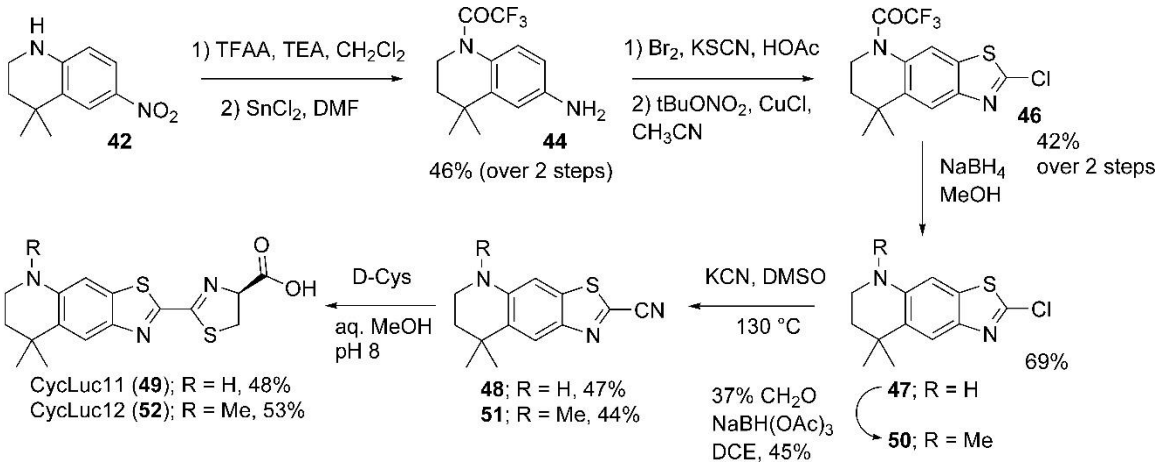

Scheme 2.4. Synthesis of CycLuc11 and CycLuc12

Luciferase activity in vitro. At the outset of this work, it was anticipated that some subset of the rigid luciferin analogs would not be well accommodated by the luciferase. However, all of the new aminoluciferin analogs are substrates, further underscoring the generality of the light emission chemistry and the tolerance of luciferase for modifications.

When purified firefly luciferase is treated with D-luciferin or an aminoluciferin, a high initial rate of light emission (burst) is observed in the first few seconds, which is then followed by a substantial decrease in the rate of sustained light output. This effect is more pronounced for high-affinity aminoluciferins than for D-luciferin itself, and all of the new substrates exhibited this same general behavior under saturating substrate conditions (**Figure 2.2** and **Figure 2.3**). Relative to D-luciferin with the wild-type (WT) luciferase, the initial rate of photon flux ranged from a high of 43% for CycLuc4 to a low of 2% for CycLuc11. This initial rate is high compared to luciferin analogs in which the

benzothiazole has been replaced (Iwano et al., 2013; McCutcheon et al., 2012; Woodroofe et al., 2012). However, aminoluciferins have reduced emission 1 min after substrate addition, consistent with product inhibition as the primary factor limiting the light emission in vitro (Reddy et al., 2010; Woodroofe et al., 2008) (**Figure 2.2** and **Figure 2.3**).

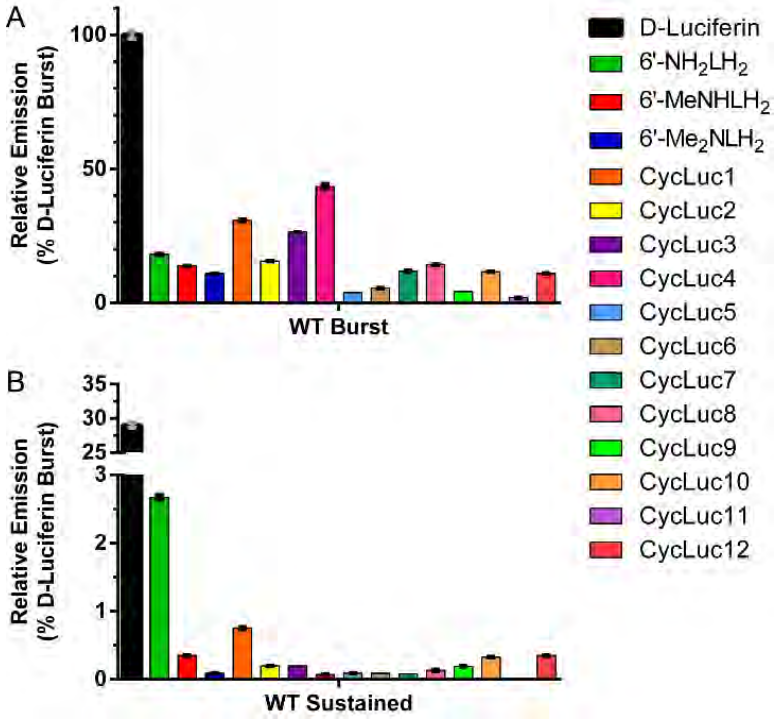

Figure 2.2. Initial and sustained bioluminescence intensity with purified WT luciferase. (A) Initial rates of emission from WT luciferase (0.2 nM) with each luciferin analog (250 μM) relative to D-luciferin. (B) Relative emission from A 1 min after substrate addition. The assays were performed in triplicate and are represented as the mean ± SEM.

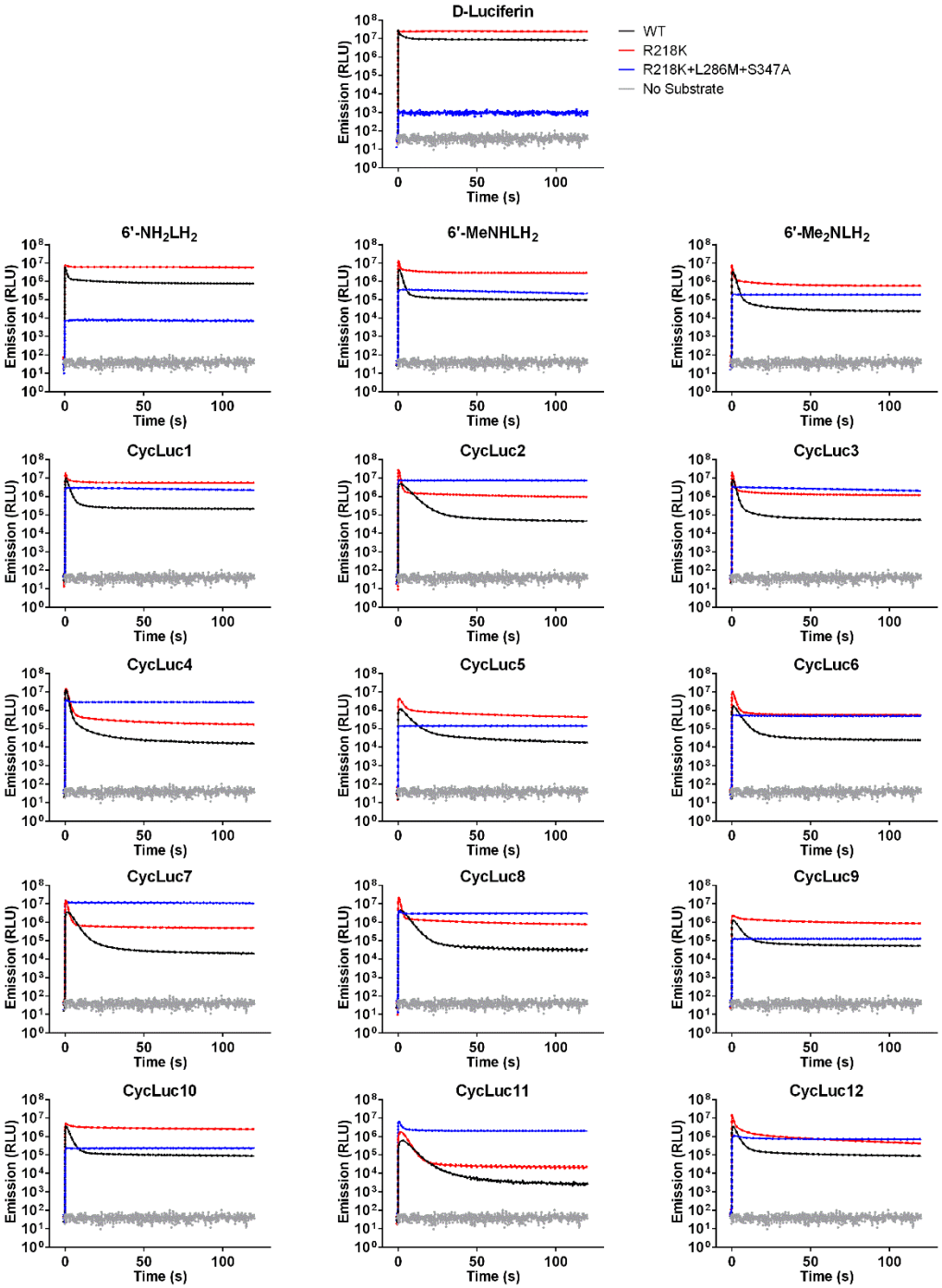

Figure 2.3. Burst kinetics profiles of all luciferins with each luciferase. Purified enzyme (0.2 nM final) was rapidly injected into substrate (250 μM final). Light emission was recorded every 0.2 s for 1 s pre-injection and 120 s post-injection. Background luminescent signal in the absence of substrate is shown for reference (in gray). The assays were performed in triplicate and are represented as the mean ± SEM and presented on the same log scale.

Bioluminescence emission wavelengths. Peak bioluminescence emission for the aminoluciferins ranged from 594 to 642 nm (**Figure 2.4**, **Figure 2.5**, and **Table 2.1**). As expected, CycLuc6 yielded strongly red-shifted bioluminescence (636 nm), exceeding that of red-emitting mutant firefly luciferases (Branchini et al., 2005a), railroad worm (beetle) luciferase (Viviani et al., 1999), and the red-shifted emission from 6'-Me_2NLH_2 (Reddy et al., 2010). However, we were surprised to find that CycLuc10 yielded an even more red-shifted peak (642 nm). To determine whether these differences are inherent to each luciferin, we measured the fluorescence emission wavelengths of the substrates. The fluorescence and bioluminescence emission wavelengths of aminoluciferins were found to be strongly correlated, suggesting that the bioluminescence wavelength is primarily dictated by the photophysical properties of the luciferin (**Figure 2.6**). Bioluminescence is red-shifted by 50−75 nm from the substrate fluorescence in phosphate-buffered saline, which is expected since the oxyluciferin emitter produced in the luciferase has increased conjugation with respect to the substrate.

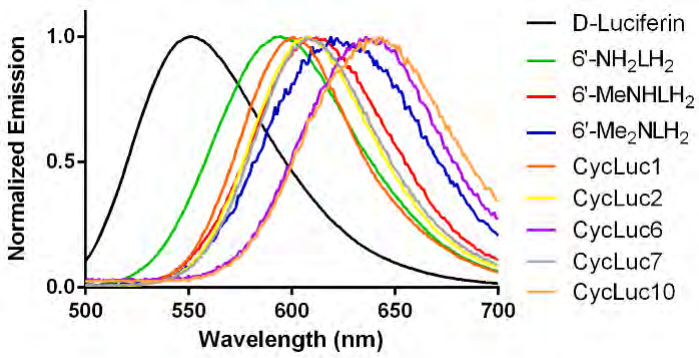

Figure 2.4. Bioluminescence emission spectra for WT luciferase with selected substrates.

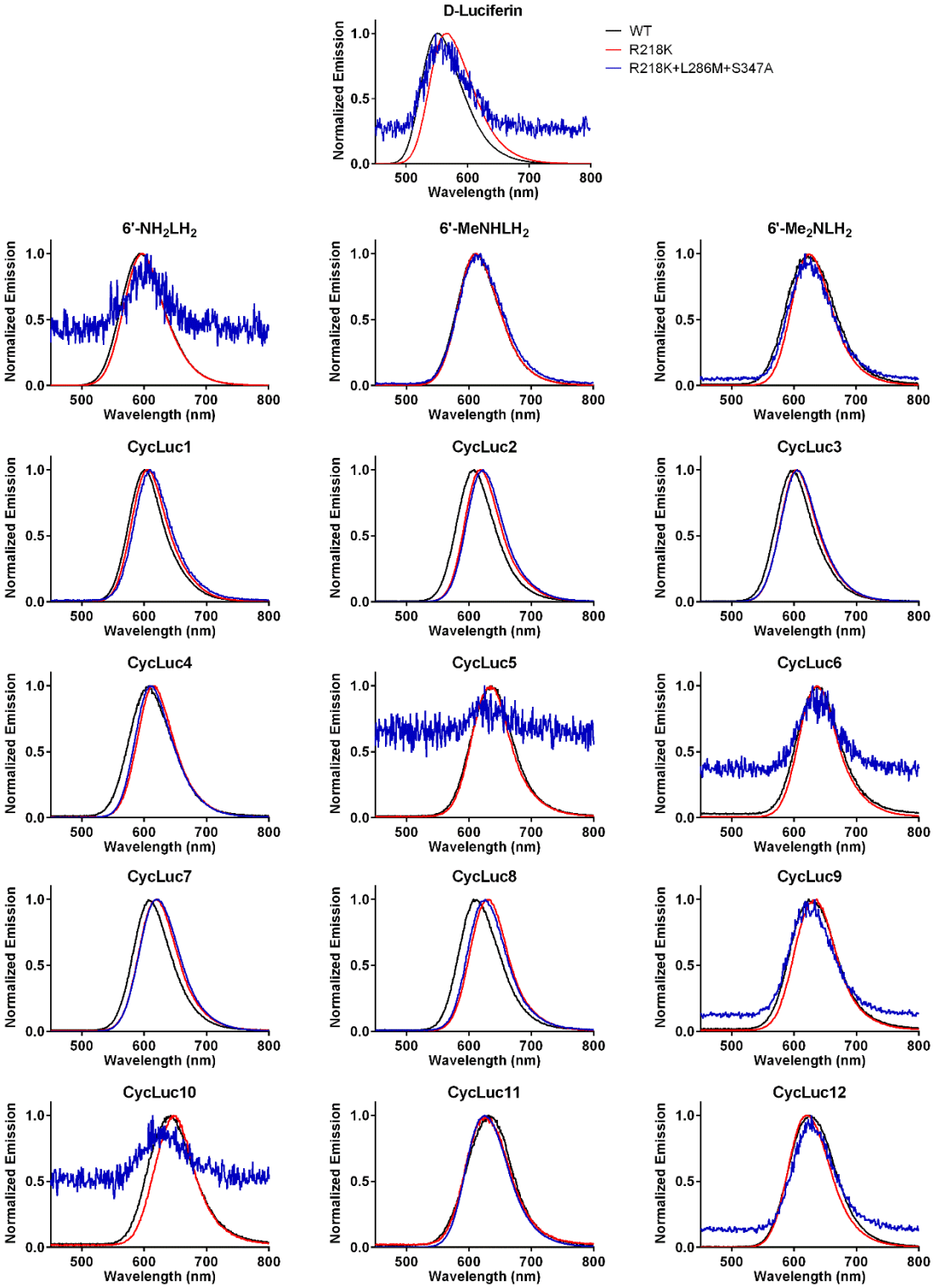

Figure 2.5. Normalized emission spectra of all luciferins with each luciferase.

Table 2.1. Fluorescence and bioluminescence emission wavelengths of all luciferins.

	Fluorescence (PBS)	WT	R/K	R/K+L/M+S/A
LH_2	528 nm	551 nm	566 nm	558 nm
6'-NH_2LH_2	517	594	599	605
6'-$MeNHLH_2$	532	610	610	618
6'-Me_2NLH_2	554	619	624	623
CycLuc1	540	601	605	608
CycLuc2	556	609	619	623
CycLuc3	531	598	605	605
CycLuc4	544	607	614	613
CycLuc5	559	635	635	625
CycLuc6	567	636	637	637
CycLuc7	548	607	620	623
CycLuc8	560	610	632	626
CycLuc9	554	627	636	628
CycLuc10	576	642	648	633
CycLuc11	551	631	626	625
CycLuc12	559	625	622	628

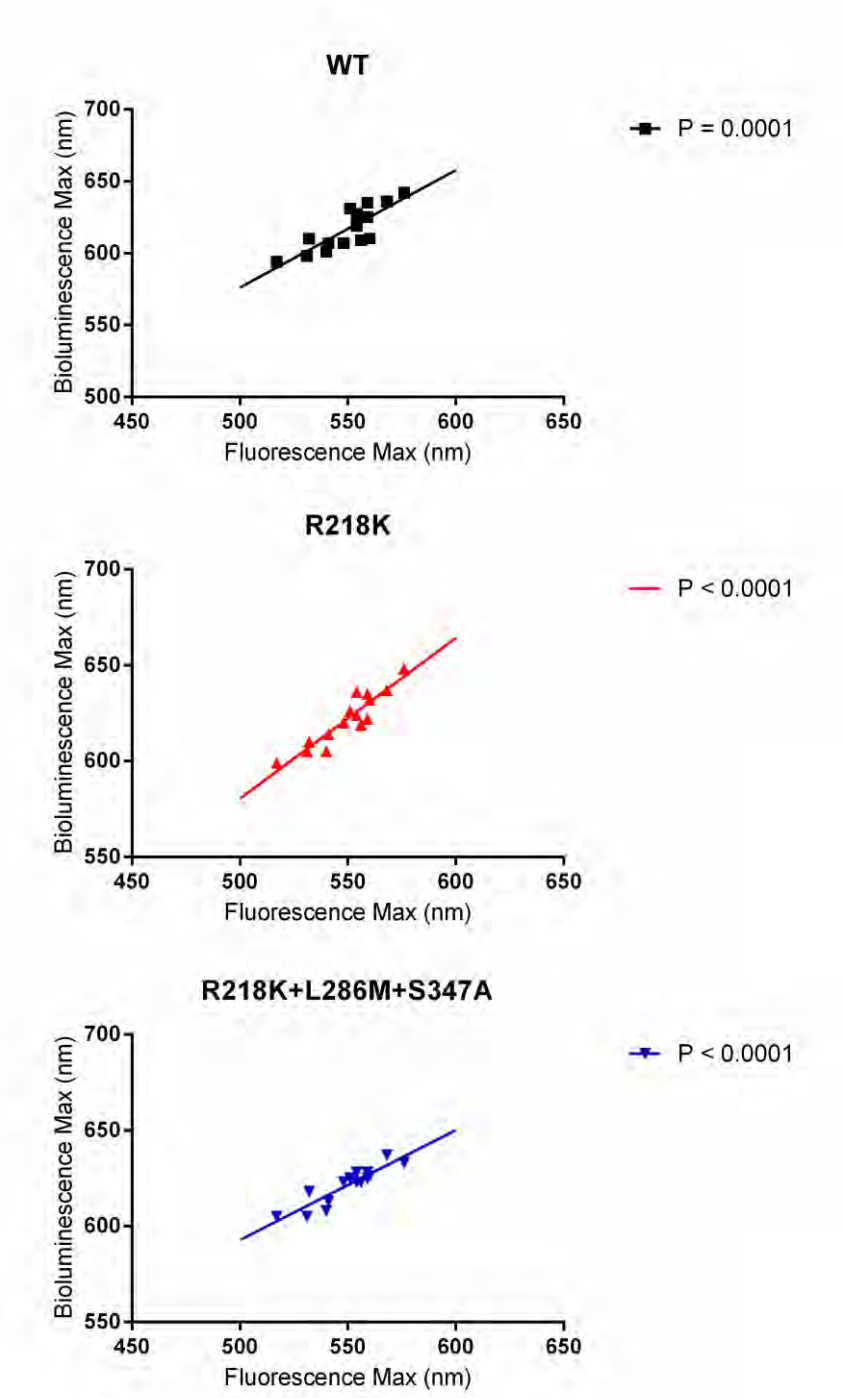

Figure 2.6. Fluorescence peak emission wavelength of each aminoluciferin correlates with the bioluminescence peak wavelength for each luciferase. Fluorescence vs bioluminescence values were fit by linear regression. Pearson correlation values are r = 0.83 (WT), r = 0.92 (R218K) and r = 0.91 (triple mutant).

The fluorescence emission of acyclic monoalkylated aminoluciferins generally ranges from 520 to 540 nm (Woodroofe et al., 2008), more red-shifted than that of 6'-aminoluciferin (517 nm) but less so than for dialkylated substrates such as 6'-Me_2NLH_2 (554 nm). CycLuc6 fluoresces at still longer wavelength (567 nm), while CycLuc10 is the most red-shifted of all the luciferin analogs (576 nm). While this was initially surprising, Atkins and Bliss have described similar behavior for aminocoumarin derivatives (Atkins and Bliss, 1978).

Mutation of luciferase modulates emission. We have previously found that the luciferase active-site mutant R218K increases the rate of light emission from CycLuc1, CycLuc2, 6'-$MeNHLH_2$, and 6'-Me_2NLH_2 (Harwood et al., 2011). This effect is not particularly selective, as it is observed with all of the aminoluciferins (**Figure 2.3**, **Figure 2.7**, and **Figure 2.8**). For instance, CycLuc7 exhibits higher initial and sustained emission rates with R218K compared to WT (**Figure 2.7**). The R218K mutant also resulted in a slight red-shift in bioluminescence for most substrates, pushing the maximal emission wavelength for CycLuc10 to 648 nm (**Figure 2.5** and **Table 2.1**).

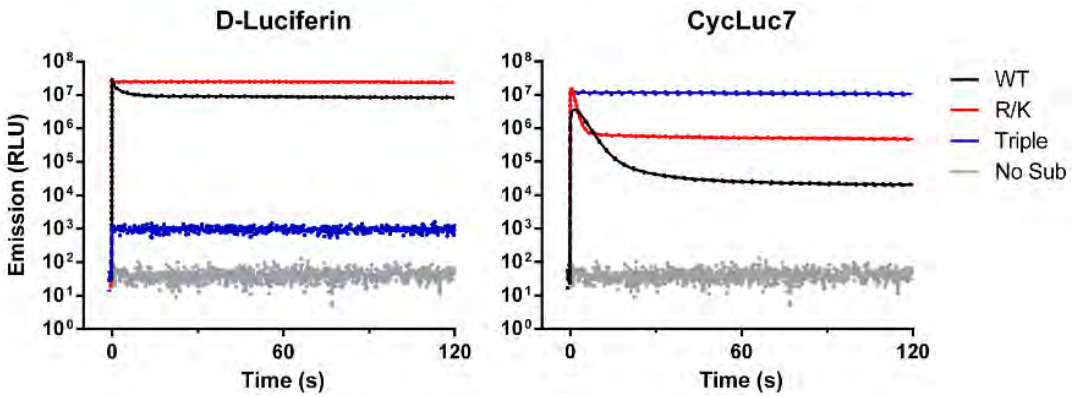

Figure 2.7. Burst kinetics profiles of D-luciferin and CycLuc7 treated with purified WT and mutant luciferases. Purified enzyme (0.2 nM final) was rapidly injected into substrate (250 μM final). Light emission was recorded every 0.2 s for 1 s pre-injection and 120 s post-injection. Background luminescent signal in the absence of substrate is shown for reference (in gray). The assays were performed in triplicate and are represented as the mean ± SEM and presented on the same log scale.

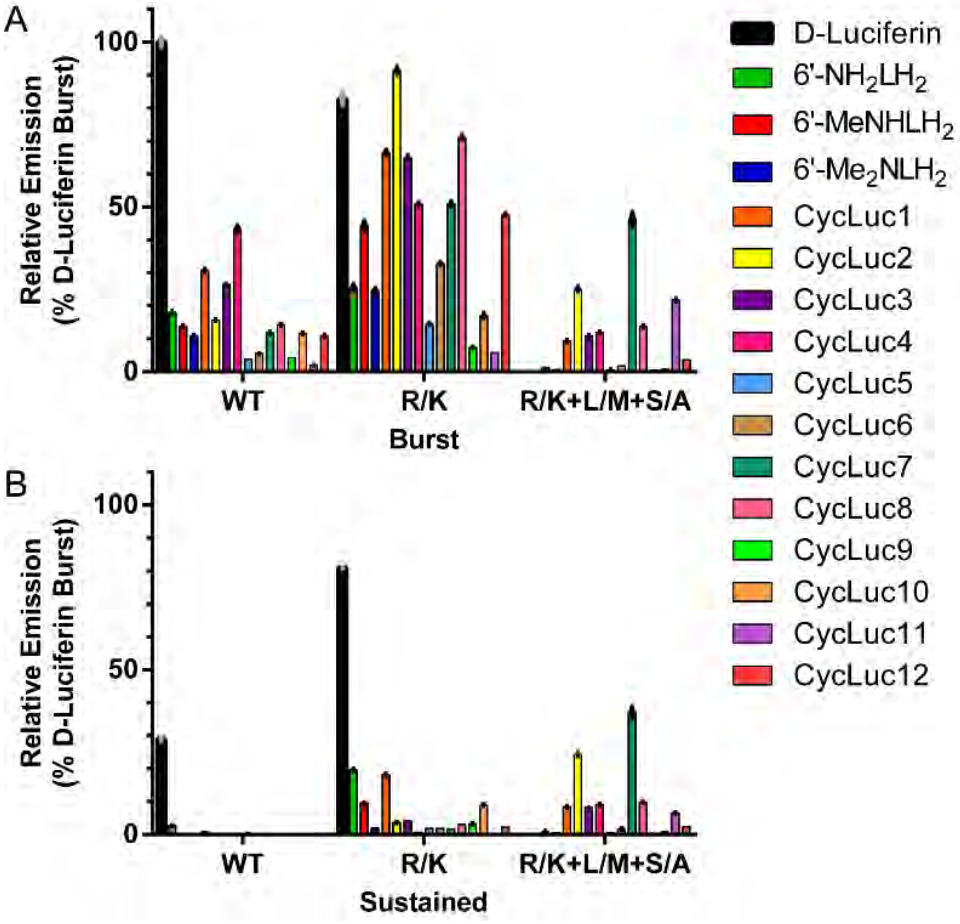

Figure 2.8. Initial and sustained bioluminescence intensity with purified WT and mutant luciferases. (A) Initial rates of emission within the first 2 s of substrate addition from the indicated luciferase (0.2 nM) with each luciferin analogs (250 μM) relative to WT with D-luciferin. (B) Relative emission from A 1 min after substrate addition. The assays were performed in triplicate and are represented as the mean ± SEM.

Toward orthogonal luciferases. In principle, chemical and structural differences in luciferin substrates could be exploited to create new orthogonal luciferases. However, active-site mutations such as R218K and L286M raise the K_m of D-luciferin but do not prevent its utilization as a substrate (Harwood et al., 2011). A more selective point mutant, S347A, raises the K_m and lowers the rate of emission from D-luciferin, possibly because it removes a hydrogen-bonding interaction with the benzothiazole nitrogen that may be more important for D-luciferin binding and orientation than for aminoluciferins (Branchini et al., 2003; Harwood et al., 2011). Yet D-luciferin remains a substrate for this mutant luciferase as well. Thus, previous work has not established whether high luciferase activity can be retained in luciferase mutants that do not yield light emission from D-luciferin.

Here we find that the combination of R218K, L286M, and S347A renders D-luciferin essentially inactive. The purified triple-mutant luciferase dramatically reduced both the initial and sustained rates of photon emission from D-luciferin by >10,000-fold (**Figure 2.3** and **Figure 2.7**). Gratifyingly, this is not due to a lack of luciferase activity, as the photon flux from CycLuc2, CycLuc7, and CycLuc11 actually increased compared to that of the WT enzyme (**Figure 2.3** and **Figure 2.8**). CycLuc7 is the optimal substrate for the triple-mutant luciferase in vitro, achieving 46% of the initial rate of D-luciferin with WT luciferase. This result demonstrates that high luciferase activity can be maintained in a luciferase mutant that is essentially unresponsive to the native substrate D-luciferin.

Furthermore, product inhibition has largely been eliminated, as there is little diminution in flux after the initial burst (**Figure 2.3**, **Figure 2.7**, and **Figure 2.8**).

Luciferin emission in live luciferase-expressing cells. We next compared the aminoluciferins to D-luciferin in live WT luciferase-expressing Chinese Hamster Ovary (CHO) cells. Under these conditions, the luciferin substrate must cross the cell membrane to access the luciferase. In marked contrast to what is observed in vitro, almost all of the alkylated aminoluciferins yield higher flux than D-luciferin when assayed at a concentration <30 μM (**Figure 2.9** and **Figure 2.10**). At high substrate concentration (250 μM), the relative emission from D-luciferin is still equaled or exceeded by those of CycLuc1, CycLuc10, and CycLuc12 (**Figure 2.9**). However, if the cell membrane is removed by cell lysis, D-luciferin is the superior substrate at both high and low doses, suggesting that substrate access is the primary factor limiting luciferins in live cells (**Figure 2.11**).

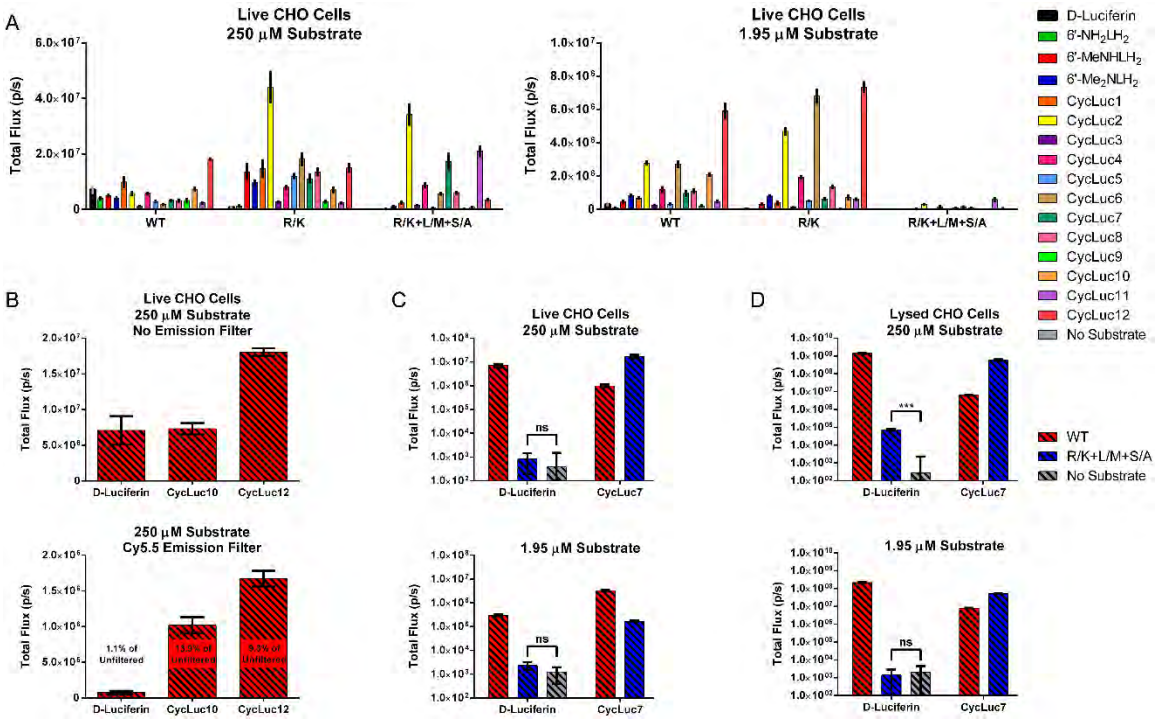

Figure 2.9. Photon flux from luciferase-expressing CHO cells. (A) Live cells expressing the indicated luciferase and treated with high or low doses of luciferin. (B) Comparison of total and near-IR photon flux from WT luciferase with the indicated luciferins. (C,D) Comparison of photon flux from WT and triple-mutant luciferase with D-luciferin or CycLuc7 in live cells (C) or lysed cells (D). All assays were performed in triplicate and are represented as the mean ± SEM.

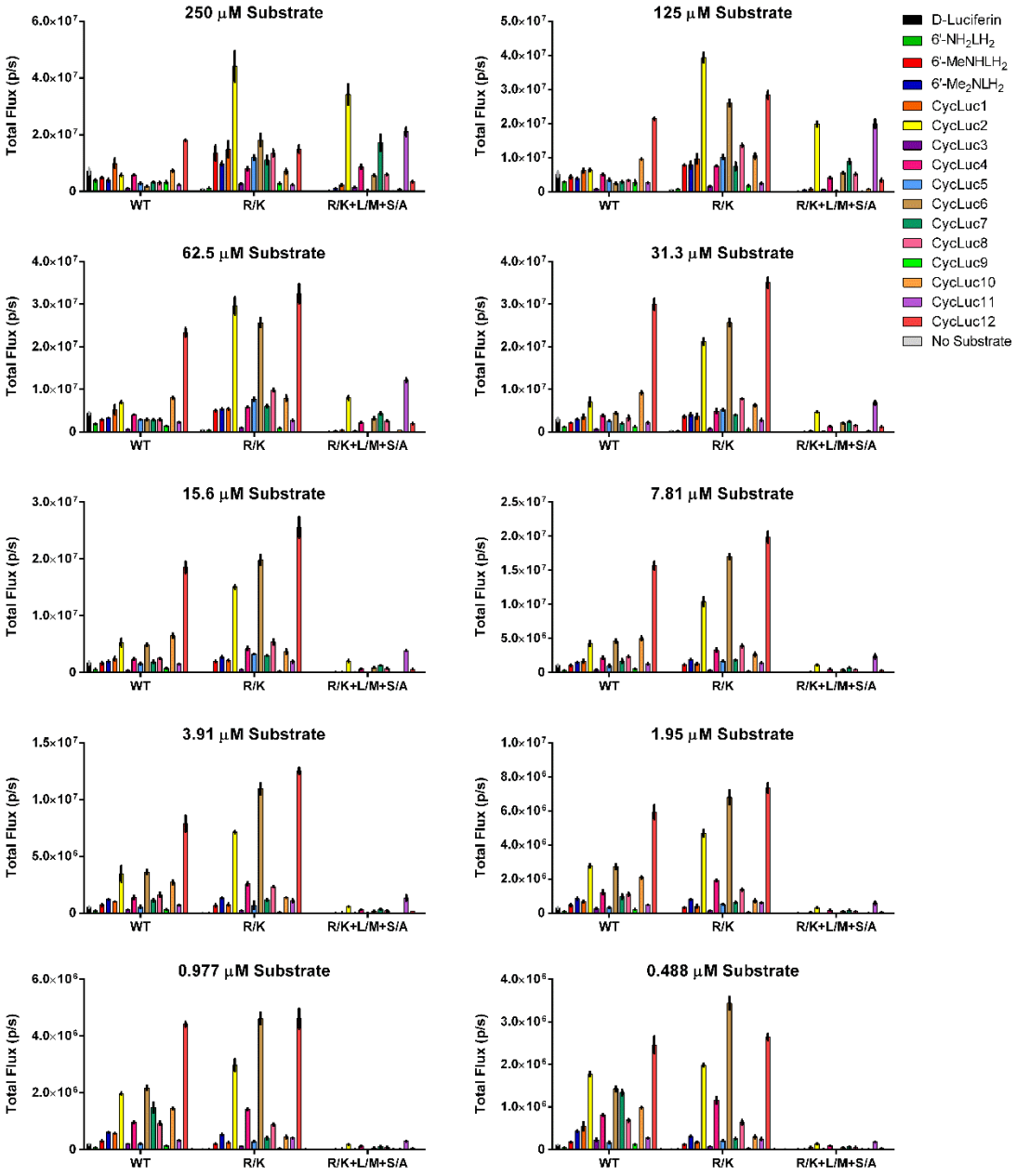

Figure 2.10. Photon flux from live luciferase-expressing CHO cells. Cells were incubated with the indicated concentration of each substrate. Note that the y-axis scale differs at different substrate concentrations. The assays were performed in triplicate and are represented as the mean ± SEM.

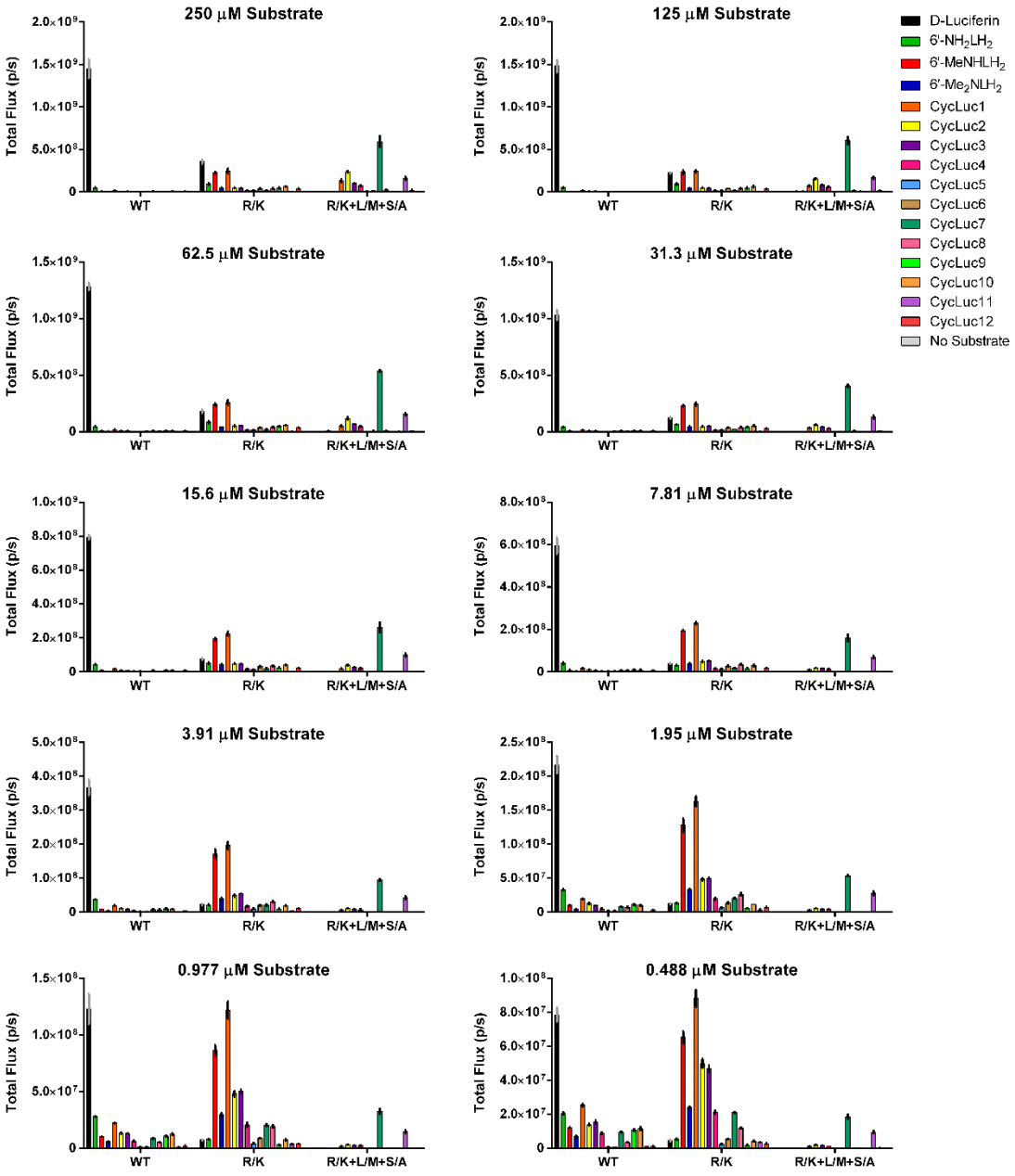

Figure 2.11. Total photon flux from lysed luciferase-expressing CHO cells. Lysate was treated with the indicated concentration of substrate. Note that the y-axis scale at different substrate concentrations differs. The assay was performed in triplicate and is represented as the mean ± SEM.

Near-IR photon flux in live cells. The peak emission wavelengths of aminoluciferins are red-shifted in vitro. To assess the near-IR emission from each luciferin in live cells, we measured the relative photon flux passing through a Cy5.5 filter (695−770 nm). All of the aminoluciferins exhibited greater relative photon flux in the near-IR than D-luciferin (**Figure 2.9B** and **Figure 2.12**). For every substrate except 6'-aminoluciferin and CycLuc3, this translated to a higher total near-IR photon flux from live cells than D-luciferin under both low-dose and high-dose conditions (**Figure 2.12**). CycLuc10 gave the greatest fraction of near-IR light emission: 13.9% of the total photon flux, >10-fold higher than that of D-luciferin (**Figure 2.9B**). However, total near-IR flux of CycLuc10 was slightly exceeded by that of CycLuc12. Thus, the substrate that yields the highest cellular near-IR light emission is a function of substrate access (affinity and cell permeability) as well as wavelength.

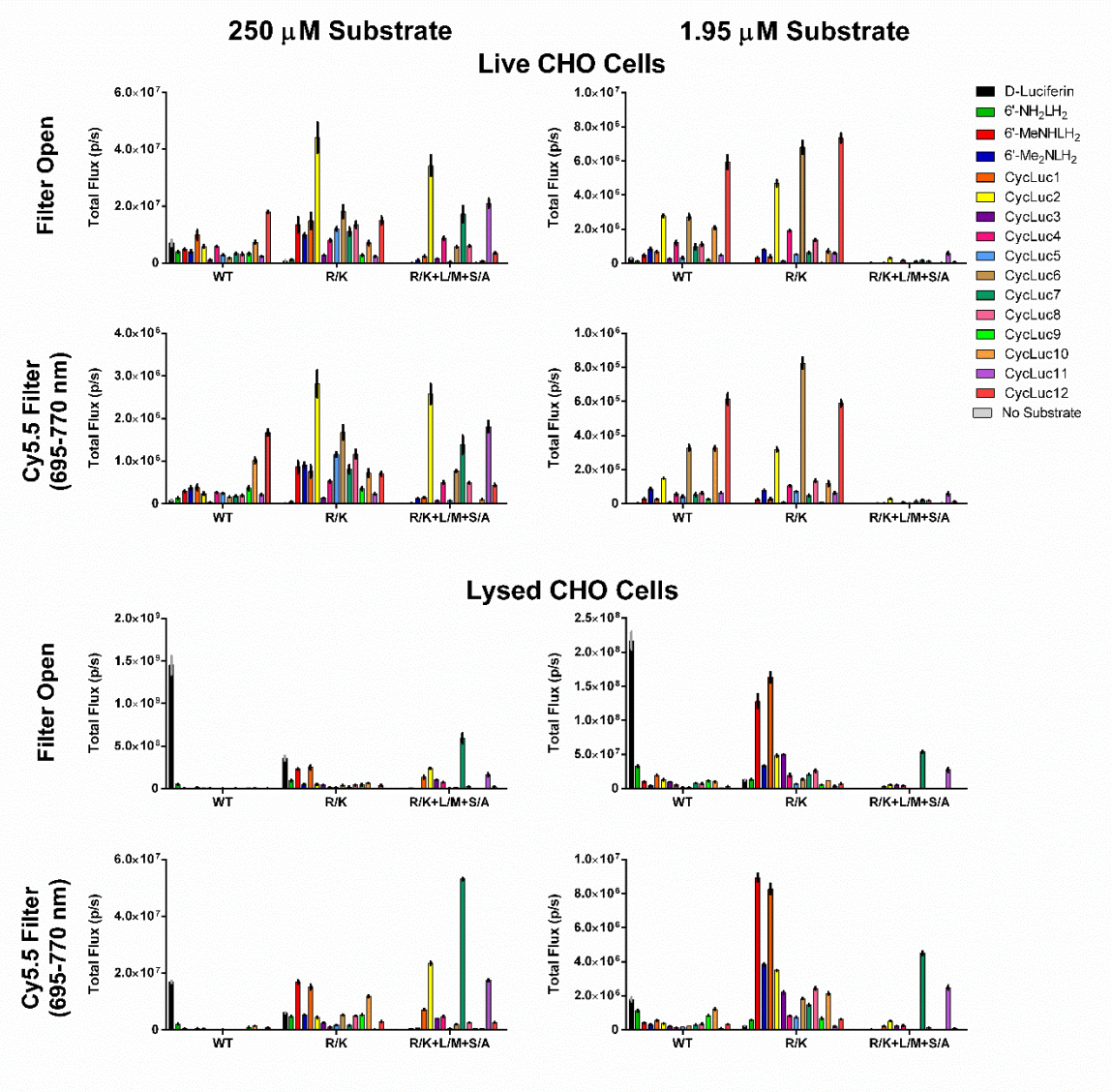

Figure 2.12. Total photon flux from live and lysed luciferase-expressing CHO cells with and without a Cy5.5 bandpass filter. Cells were treated with 250 μM or 1.95 μM luciferin and imaged with either no filter or through a Cy5.5 bandpass filter. The assay was performed in triplicate and is represented as the mean ± SEM.

Mutant luciferases in live and lysed cells. Transfection of CHO cells with R218K luciferase instead of WT luciferase improved relative photon flux from synthetic luciferins compared to D-luciferin (**Figure 2.9** and **Figure 2.10**). CycLuc2 yielded the highest signal in live cells, and most alkylated aminoluciferins were superior to D-luciferin at both low and high substrate concentrations (**Figure 2.9** and **Figure 2.10**). Further highlighting the importance of factors other than peak emission wavelength on the total emission of red-shifted photons in live cells, CycLuc2 yielded the highest Cy5.5-filtered signal at 250 μM, while CycLuc6 was best at low concentration (**Figure 2.9** and **Figure 2.12**). The longer emission wavelength of CycLuc6 (**Figure 2.4**) and its higher cell permeability likely lead to its superior flux at low concentrations, while the higher maximal rate of photon emission for CycLuc2 ultimately prevails at high substrate concentration (**Figure 2.8**). Thus, the best-performing substrates are context-dependent.

No signal above background could be measured from live cells expressing the triple-mutant luciferase after treatment with D-luciferin (**Figure 2.9C**). In contrast, CycLuc2, CycLuc7, and CycLuc11 achieve high photon flux (**Figure 2.9**). The triple mutant possesses lower affinity for its substrates compared to WT or R218K luciferase, yielding reduced photon flux at low substrate concentration (**Figure 2.9** and **Figure 2.10**). However, in lysed cells, the lower affinity of the triple mutant improved the signal from CycLuc7 and CycLuc11 due to its lessened product inhibition (**Figure 2.9D** and **Figure 2.11**). CycLuc7 is the best

substrate in cell lysates, achieving ~20% of the D-luciferin signal with the WT luciferase (**Figure 2.9** and **Figure 2.11**). Mutant and WT luciferase protein expression is equivalent in transfected cells by Western blot (**Figure 2.13**), and the differences between luciferases in cell lysates (**Figure 2.11**) generally mirrors what is observed with equal concentrations of purified proteins in vitro (**Figure 2.8**). The triple-mutant luciferase is thus a significant step toward orthogonal bioluminescent reporters of gene expression in both live and lysed cells, as it yields high light output with (alkylated) aminoluciferins but little to no signal with D-luciferin. We speculate that the triple mutant primarily discriminates between substrates by lowering substrate affinity and removing an interaction important for orienting the native substrate (S347). Luciferin analogs possessing high affinity for luciferase and an alternative “handle” for proper orientation remain effective substrates (Harwood et al., 2011; Mofford et al., 2014a). Given that the mutations that comprise the triple mutant were originally identified to individually improve luciferase activity with CycLuc1 (Harwood et al., 2011), it is likely that further improvements in selectivity and function are possible for this broadened palette of luciferins. Ironically, the identification of a luciferase that emits strongly with D-luciferin but does not respond to synthetic luciferins has been more elusive. The development of fully orthogonal luciferin−luciferase reporter pairs will therefore require further work, perhaps by eschewing D-luciferin altogether in favor of two or more synthetic substrates.

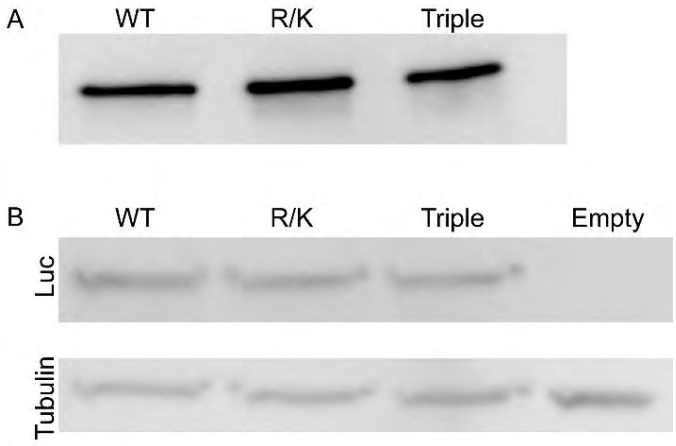

Figure 2.13. Western blot analysis of luciferase expression. (A) Purified recombinant luciferases are equally recognized by an anti-luciferase antibody. (B) CHO cell lysates transfected with WT or mutant luciferases yield equivalent expression. α-tubulin is shown as a loading control.

Conclusion

There is reason to expect that substrate performance in live cells, rather than with purified protein or cell lysates, is more predictive of in vivo behavior. In recent collaborative work we have found that CycLuc1 allows dramatically improved bioluminescence imaging in live mice compared to the standard imaging conditions with D-luciferin (Evans et al., 2014). Tumor cells can be imaged with 20−200-fold less substrate than D-luciferin, and luciferase expression deep in the brain that cannot be detected with D-luciferin is detectable with CycLuc1 (Evans et al., 2014). Many of the substrates described here provide higher total and red-shifted photon flux in live cells, suggesting that they may also have superior properties for in vivo imaging. Differences in substrate affinity, lipophilicity, and functionality are also anticipated to affect the pharmacokinetics of the luciferins in vivo, perhaps allowing tuning of

bioluminescent half-lives and/or tissue distribution. Moreover, we have found that mutation of luciferase can essentially eliminate light output from the native D-luciferin substrate while retaining or improving light emission from one or more aminoluciferin substrates to levels comparable to or, in live cells, superior to that of D-luciferin with the WT luciferase. Thus, these synthetic luciferins and mutant luciferases not only expand the palette of luminogenic molecules but transcend the emission properties of D-luciferin and firefly luciferase. They are therefore expected to have significant potential for bioluminescence imaging applications both in vitro and in vivo.

Materials and Methods

Collaborators

Gadarla Randheer Reddy of the Miller Lab:

Design and synthesis of all synthetic luciferins

General

Chemicals were purchased from Aldrich, TCI, Oakwood, or Matrix Scientific unless otherwise noted. Data were plotted with GraphPad Prism 6.0. Nuclear magnetic resonance (NMR) spectra were recorded on a Varian Mercury 400 MHz NMR spectrometer. Small molecule mass spectral data were recorded on a Waters QTOF Premier spectrometer. D-luciferin was obtained from Anaspec and 6'-aminoluciferin was obtained from Marker Gene Technologies

Inc. CycLuc1, CycLuc2, 6'-MeNHLH$_2$, and 6'-Me$_2$NLH$_2$ were synthesized as previously described (Reddy et al., 2010). Protein concentrations were determined using Coomassie Plus (Thermo Scientific). Immobilized glutathione (Thermo Scientific) was used for glutathione S-transferase (GST)-tagged protein purification.

Plasmid constructs

R218K luciferase was created as previously described (Harwood et al., 2011). The triple mutant R218K/L286M/S347A was generated by introducing L286M and S347A mutations identified in Harwood et al. into the R218K luciferase, using the Quickchange site-directed mutagenesis kit (Stratagene).

Luciferase expression and purification

Luciferases were expressed and purified as GST-fusion proteins from the vector pGEX6P-1 as previously described (Harwood et al., 2011). Briefly, JM109 cells were grown at 37 °C until the OD600 reached 0.5-1, induced with 0.1 mM IPTG, and incubated with shaking at 20 °C overnight. Cells were pelleted at 5000 RPM in a Sorvall 2C3C Plus centrifuge (H600A rotor) at 4 °C for 15 min, then flash frozen in liquid nitrogen and purified immediately or stored at -80 °C. The *E. coli* pellets from 1 L of culture were thawed on ice, resuspended in 25 mL lysis buffer (50 mM Tris [pH 7.4], 500 mM NaCl, and 0.5% Tween 20) containing 1 mM phenylmethylsulfonyl fluoride, and disrupted by sonification (Branson

Sonifier). Dithiothreitol (DTT) was added at 10 mM, and the resulting cell lysate was clarified by centrifugation at 35,000 rpm in a Beckman 50.2 Ti rotor for 60 min at 4 °C. The supernatant was batch-bound to immobilized glutathione for 1 hr at 4 °C, and the beads were washed with lysis buffer containing 10 mM DTT, followed by wash buffer (50 mM Tris [pH 8.1], 250 mM NaCl, and 10 mM DTT) and storage buffer (50 mM Tris [pH 7.4], 0.1 mM EDTA, 150 mM NaCl, 1 mM TCEP). Twenty units of PreScission Protease (GE Healthcare) were added, and incubation continued overnight at 4 °C to cleave the GST-fusion and elute the untagged luciferase protein.

Purified protein luminescence assays

Luminescence assays were initiated by adding 30 µL of purified luciferase in enzyme buffer (20 mM Tris [pH 7.4], 0.1 mM EDTA, 1 mM TCEP, and 0.8 mg/mL BSA) to 30 µL 2x substrate in substrate buffer (20 mM Tris [pH 7.4], 0.1 mM EDTA, 8 mM $MgSO_4$, and 4 mM ATP) in a black 96-well plate (Costar 3915). Imaging was performed one minute after enzyme addition using a Xenogen IVIS-100 at a final enzyme concentration of 10 nM and final substrate concentrations ranging from 0.122 to 250 µM. Data acquisition and analysis was performed with Living Image® software. Data are reported as total flux (p/s) for each ROI corresponding to each well of the 96-well plate.

Bioluminescence emission scans

Each purified luciferase in enzyme buffer was rapidly injected into a cuvette containing substrate in substrate buffer to a final enzyme concentration of 100 nM and a final substrate concentration of 10 μM. The emission from 400 to 800 nm was recorded in a SPEX FluoroMax-3 fluorimeter with closed excitation slits 10 s after injection.

Burst kinetics assays

Using a Turner Biosystems 20/20n luminometer, 40 μL of purified luciferase in enzyme injection buffer (20 mM Tris [pH 7.4], 0.1 mM EDTA, 0.625 mM TCEP, and 0.5 mg/mL BSA) was rapidly injected into a clear Eppendorf tube containing 10 μL of substrate in substrate injection buffer (20 mM Tris [pH 7.4], 0.1 mM EDTA, 20 mM $MgSO_4$, and 10 mM ATP) to a final enzyme concentration of 0.2 nM and a final luciferin substrate concentration of 250 μM. Measurements were taken every 0.2 s for 1 s pre-injection and 120 s post-injection. Data acquisition was performed with SIS for 2020n v1.9.0 software. Data are reported as Relative Light Units (RLU). To correct for the wavelength sensitivity of the PMT in the 20/20n, total flux was also measured using the IVIS-100 as described above with a final enzyme concentration of 10 nM and a final substrate concentration of 250 μM. Data from the IVIS and from the 20/20n at the 60 s time point were normalized to the WT + D-luciferin value. The correction factor of each enzyme/substrate pair was calculated by dividing the normalized IVIS data by the

normalized 20/20n data. All 20/20n data were then multiplied by their respective correction factors.

Cell culture

Chinese hamster ovary (CHO) cells were grown in a CO_2 incubator at 37°C with 5% CO_2 and were cultured in F-12K Nutrient Mixture (GIBCO) supplemented with 10% fetal bovine serum and 100 U/mL penicillin/streptomycin.

Transfections

The WT firefly luciferase luc2 gene (Promega) and codon optimized mutants were cloned into the BamHI and NotI sites of pcDNA 3.1 and transfected into CHO cells for live and lysed cell experiments. Transient transfections were performed at RT using Lipofectamine 2000 on cells plated at 60–75% confluency in 96-well black tissue culture-treated plates (Costar 3916) for live cell assays, or 6-well plates for lysed cell assays. For live cells, 0.075 µg DNA/well was transfected; for lysed cells, 2.25 µg DNA/well was transfected. Assays were performed in triplicate 24 hr after transfection.

Live and lysed CHO cell luminescence assays

Transfected CHO cells were washed with HBSS. For live cell imaging, the cells in 96-well plates were incubated with 60 µL of substrate in HBSS at final concentrations ranging from 0.122 to 1,000 µM. Imaging was performed using

the IVIS-100 with no emission filter, three minutes after addition of substrate. Additional images were taken through a Cy5.5 bandpass filter (695-770 nm) four minutes after substrate addition. Cells grown in 6-well plates were first lysed for 20 min at RT with Passive Lysis Buffer (1 mL per well). Luminescence assays were initiated by adding 30 µL of lysate to 30 µL of 2x substrate in lysed cell substrate buffer (20 mM Tris [pH 7.4], 0.1 mM EDTA, 8 mM $MgSO_4$, 4 mM ATP, 6 mg/mL BSA, 250 µM Coenzyme A, and 33 mM DTT) in a black 96-well plate (Costar 3915) with final substrate concentrations ranging from 0.122 to 250 µM. Imaging was performed with the emission filter open one minute after addition of substrate. Additional images were taken through the Cy5.5 filter two minutes after substrate addition.

Western blot

Transfected CHO cells in 6-well plates were washed with HBSS and lysed for 20 min at RT with Passive Lysis Buffer (250 µL per well). Cell debris was pelleted by centrifugation at 13,000 RPM at 4°C for 10 minutes. Total protein concentration of the supernatant was determined using Coomassie Plus Bradford Reagent and 18 µg total lysate protein was used for electrophoresis. Samples were prepared by adding 167 mM DTT and 1x SDS gel loading buffer to each lysate to a final volume of 27 µL. Samples were run on 10% SDS-PAGE, transferred to a nitrocellulose membrane, and incubated in blocking buffer (5% nonfat dry milk in western wash buffer [10 mM Tris (pH 7.4), 150 mM NaCl, 0.1%

Tween-20]) for 45 minutes. Luciferase primary antibody (Promega, Cat. # G7451) was diluted 1:1000 in blocking buffer to 6 mL final volume and incubated with the membranes at room temperature for 2 hours. Membranes were washed with Western wash buffer (4 x 6 mL) and incubated at room temperature with 6 mL secondary anti-goat antibody-HRP (Santa Cruz, Cat. # SC-2033) diluted 1:4000 in blocking buffer. The membranes were again washed (4 x 6 mL) and incubated with SuperSignal West Dura Extended Duration Substrate (Pierce) for 5 minutes. The chemiluminescence was imaged using an LAS-3000 CCD camera and quantified by Multi Gauge software (FujiFilm). Antibody was then stripped by washing the membranes with Stripping Buffer (100 mM glycine, 20 mM magnesium acetate, 50 mM potassium chloride, pH 2.2 [Bio-Rad]; 2 x 10 mL), and western wash buffer (3 x 6 mL). Membranes were then re-blocked and incubated overnight at 4 °C with 6 mL primary anti-α-tubulin antibody (Sigma Aldrich, Cat. # T9026) diluted 1:3000 in blocking buffer. Membranes were washed with western wash buffer (4 x 6 mL) and incubated at room temperature with 6 mL secondary anti-mouse antibody-HRP (GE Healthcare, Cat. # RPN4201) diluted 1:10000 in blocking buffer for 45 minutes. The membranes were again washed and incubated with SuperSignal West Dura Extended Duration Substrate for 5 minutes. The chemiluminescence was imaged using an LAS-3000 and quantified by Multi Gauge software. Purified recombinant enzymes were tested using the same procedure by loading 50 ng for electrophoresis and incubating with primary luciferase antibody overnight at 4 °C.

CHAPTER III:

Latent Luciferase Activity in the Fruit Fly Revealed by a Synthetic Luciferin

Mofford, D.M. *et. al.* (2014) *PNAS*, 111(12), 4443–4448.

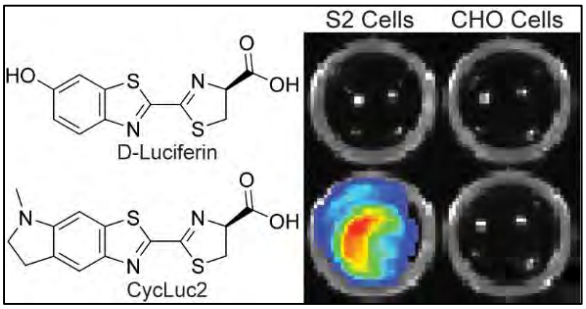

Summary

Beetle luciferases are thought to have evolved from fatty acyl-CoA synthetases present in all insects. Both classes of enzymes activate fatty acids with ATP to form acyl-adenylate intermediates, but only luciferases can activate and oxidize D-luciferin to emit light. Here we show that the *Drosophila* fatty acyl-CoA synthetase CG6178, which cannot use D-luciferin as a substrate, is able to catalyze light emission from the synthetic luciferin analog CycLuc2. Bioluminescence can be detected from the purified protein, live *Drosophila* Schneider 2 cells, and from mammalian cells transfected with CG6178. Thus, the non-luminescent fruit fly possesses an inherent capacity for bioluminescence that is only revealed upon treatment with a xenobiotic molecule. This result expands the scope of bioluminescence and demonstrates that the introduction of a new substrate can unmask latent enzymatic activity that differs significantly from an enzyme's normal function without requiring mutation.

Introduction

Bioluminescence in insects is almost exclusively confined to a small subset of beetles, including click beetles (Wood et al., 1989), railroad worm beetle larvae (Viviani et al., 1999), and perhaps the best known example, the firefly *Photinus pyralis* (Fraga, 2008). However, all insects express long-chain fatty acyl-CoA synthetases (ACSLs) that share high homology to beetle luciferases and are hypothesized to be their evolutionary antecedents (Day et al., 2009; McElroy et al., 1967; Viviani et al., 2013). These two classes of enzymes are both members of the adenylate-forming superfamily (Chang et al., 1997) and share the ability to make AMP esters of fatty acids as well as the ability to displace the AMP ester with CoASH (Oba et al., 2003) (**Figure 3.1**). Beetle luciferases differ from other insect ACSLs in their ability to chemically generate light by adenylating and oxidizing D-luciferin, a small molecule naturally found in bioluminescent beetles. How this additional activity developed is unknown, although weak bioluminescence has been reported by treating a beetle ACSL with D-luciferin (Prado et al., 2011; Viviani et al., 2013).

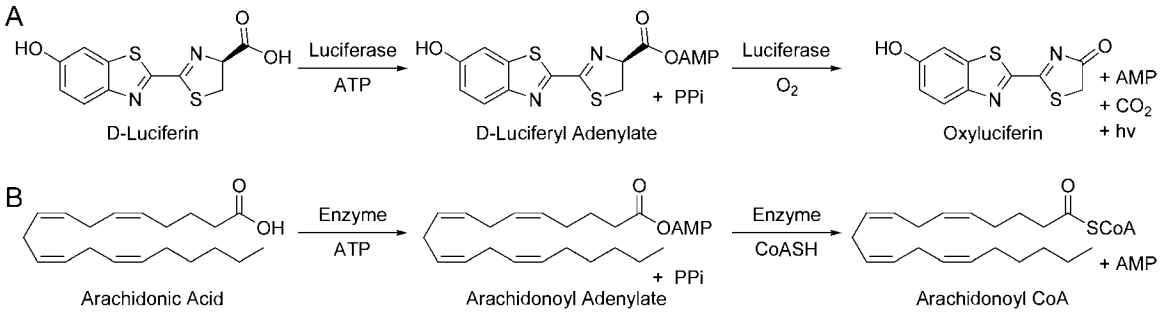

Figure 3.1. Firefly luciferase and long-chain fatty acyl-CoA synthetases catalyze similar two-step mechanisms. (A) Firefly luciferase catalyzes the formation of an activated AMP ester of its native substrate, D-luciferin. Subsequent oxidation within the luciferase binding pocket generates an excited-state oxyluciferin molecule that is responsible for light emission. (B) Long-chain fatty acyl-CoA synthetases catalyze the formation of activated AMP esters from long-chain fatty acids such as arachidonic acid. AMP is then displaced by CoASH to form the fatty acyl-CoA product.

We have previously found that mutation of firefly luciferase can improve light emission from synthetic luciferin substrates while concurrently reducing light emission from D-luciferin (Harwood et al., 2011). This suggested that the requirements for D-luciferin bioluminescence and for bioluminescence with synthetic luciferin substrates are not the same in mutant luciferases and, by extension, in luciferase homologs. Consequently, we reasoned that even though insect ACSLs from non-bioluminescent organisms outside the order of beetles fail to emit light with D-luciferin, this does not necessarily mean that they are incapable of luciferase activity. Clearly, the catalytic machinery needed to form AMP esters from carboxylic acids is present in ACSLs (**Figure 3.1**), potentially allowing access to an adenylate of a luciferin analog. Furthermore, oxygen has ready access to ligand binding sites in proteins (Baron et al., 2009), and luciferin

active esters in basic DMSO are known to be readily oxidized to generate an excited-state molecule that can emit light (Seliger and McElroy, 1962; White et al., 1971). We therefore speculated that ACSLs lack luciferase activity with D-luciferin because D-luciferin is a poor ligand for ACSLs and/or binds in a geometry that is not conducive to adenylation. If this hypothesis were true, treatment with a suitable synthetic luciferin substrate that possessed higher affinity and/or conformational rigidity could potentially reveal latent luciferase activity in an ACSL.

Results

To test the idea that ACSLs could have latent luciferase activity, we turned to the *Drosophila* fatty acyl-CoA synthetase CG6178 (Oba et al., 2004) (**Figure 3.2**). The fruit fly *Drosophila melanogaster* is a widely used insect model organism from the order Diptera. With the exception of fungus gnats from the Mycetophilidae family (Viviani et al., 2002), no members of this order of insects are bioluminescent. Furthermore, none of the Diptera expresses a beetle-like luciferase, and CG6178 has been shown to lack luciferase activity with D-luciferin (Oba et al., 2004). We therefore incubated purified CG6178 protein with a panel of synthetic luciferins that we previously designed to emit red light with firefly luciferase (Harwood et al., 2011; Reddy et al., 2010) (**Figure 3.3**). Strikingly, the rigid luciferin substrate CycLuc2 revealed latent luciferase activity in CG6178. The peak emission wavelength is in the red (610 nm), nearly identical to that of

CycLuc2 with firefly luciferase, and consistent with the predicted effect of the luciferin structure on its photophysical properties (Reddy et al., 2010) (**Figure 3.4**). By contrast, no light emission was observed after treatment of CG6178 with D-luciferin or 6'-aminoluciferin. CycLuc1 – differing by a single methyl group from CycLuc2 – is a much weaker light emitter with CG6178, as is the dialkylated but less rigid substrate 6'-Me_2NLH_2. Only the D-enantiomer of CycLuc2 results in bioluminescence (**Figure 3.5**), consistent with the stereoselective oxidation of D-luciferin observed with firefly luciferase (Nakamura et al., 2005), where oxygen has access to only one side of the binding pocket (Fraga, 2008; Sundlov et al., 2012). The addition of CoASH, frequently used as an additive in luciferase assays (Fraga, 2008), significantly reduces the light emission observed from CG6178 (**Figure 3.5**).

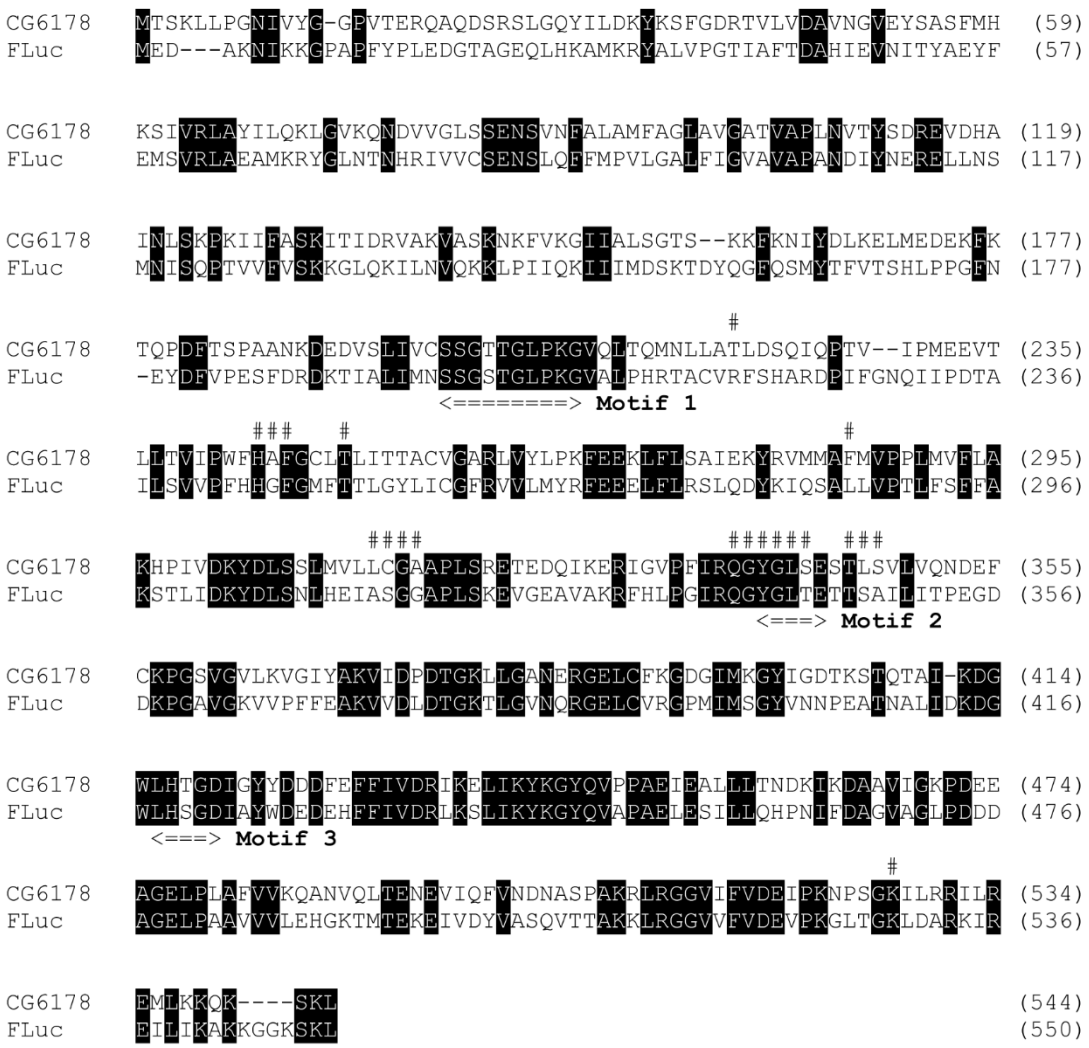

Figure 3.2. Amino acid alignment between CG6178 (*Drosophila melanogaster*) and FLuc (*Photinus pyralis*). Primary sequences of *D. melanogaster* CG6178 and *P. pyralis* luciferase were aligned with ClustalX (Larkin et al., 2007). The alignment was then displayed using Geneious version 6.1.6 software. CG6178 shows 38% identity to FLuc. Motifs 1, 2, and 3 are conserved among members of the acyl-adenylate superfamily (Chang et al., 1997). Residues within 5 Å of the dehydroluciferin portion of DSLA in the *P. pyralis* luciferase crystal structure (PDB ID code 4G36) were identified as forming the luciferin binding pocket and are marked with "#."

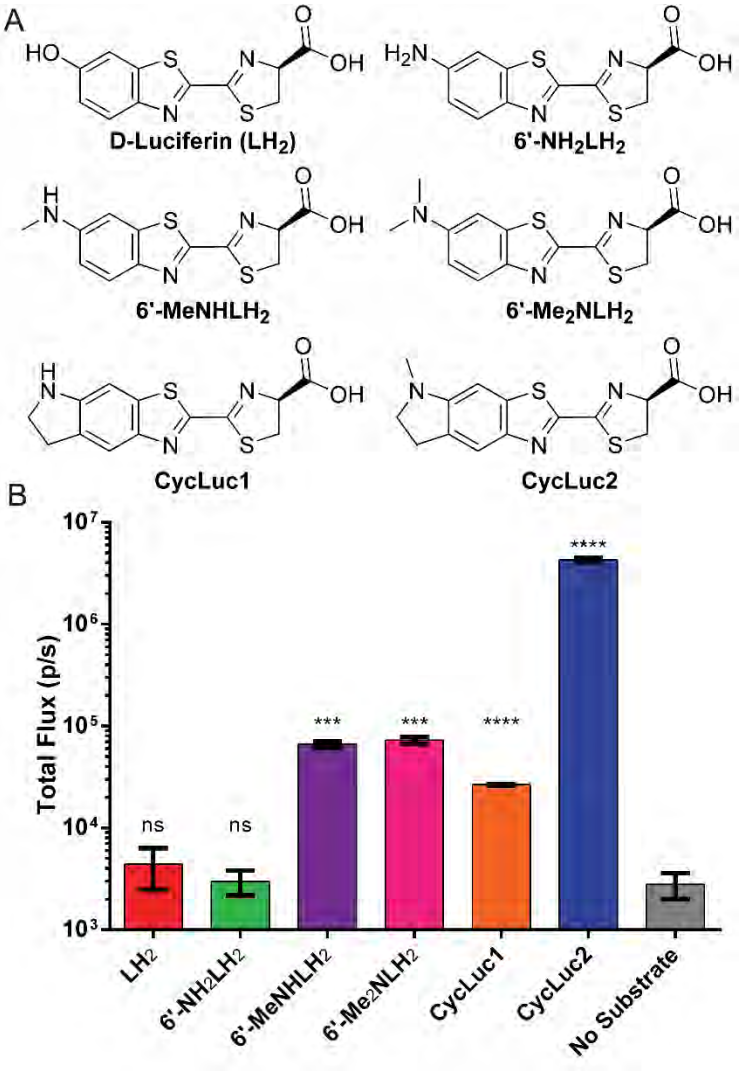

Figure 3.3. CG6178 is a latent luciferase when treated with the synthetic luciferin CycLuc2. (A) Chemical structures of D-luciferin and all synthetic luciferins. (B) Photon flux from CG6178 (20 nM) treated with the indicated substrate (125 μM). The assay was performed in triplicate and is represented on a log scale as the mean ± SEM and compared by t test to a no substrate control. ns, not statistically significant; *** $P < 0.001$, **** $P < 0.0001$.

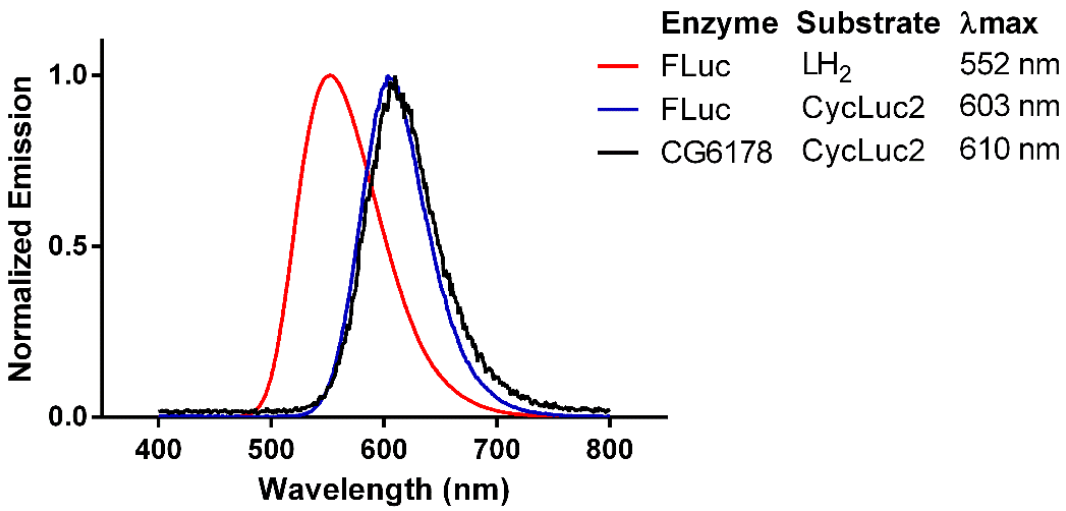

Figure 3.4. CycLuc2 emits red-shifted light compared with D-luciferin with both FLuc and CG6178. Emission profiles for purified FLuc and CG6178 were generated as described in Materials and Methods. CycLuc2 emits at a similar wavelength with both FLuc and CG6178.

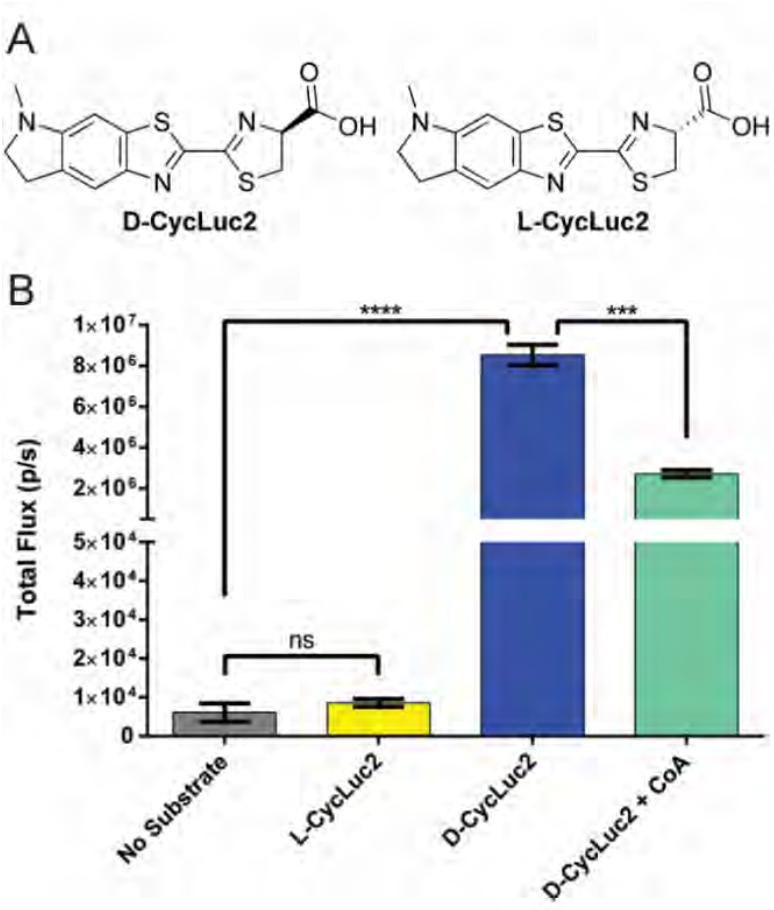

Figure 3.5. Effect of CycLuc2 chirality and CoA addition on CG6178 bioluminescence. (A) Chemical structures of D-CycLuc2 and L-CycLuc2. (B) CG6178 (20 nM) was treated with L-CycLuc2 (150 μM), D-CycLuc2 (125 μM), or D-CycLuc2 (125 μM) with CoA (125 μM). The assay was performed in triplicate and is represented as the mean ± SEM and compared using the unpaired t test to a no-substrate control. ns, not statistically significant; *** $P < 0.001$, **** $P < 0.0001$.

To emit light, the luciferin substrate must be converted to an active ester and then oxidized to the excited-state oxyluciferin. Using radiolabeled ATP, Oba et al. (Oba et al., 2004) found that CG6178 can adenylate fatty acids but fails to form the adenylate of D-luciferin. This could reflect a lack of binding by D-luciferin, or the inability of CG6178 to catalyze the formation of the respective AMP ester. To clarify the basis for this defect, we measured light emission from CycLuc2 in the presence of D-luciferin. We found that D-luciferin is a competitive inhibitor of CycLuc2-mediated light emission with a K_i value of 25.7 ± 4.5 μM (**Table 3.1**). Surprisingly, the K_m for CycLuc2 with CG6178 is 13.8 ± 1.9 μM, similar to that of D-luciferin, and much higher than the submicromolar K_m of CycLuc2 with firefly luciferase (Harwood et al., 2011). Thus, CG6178 binds both D-luciferin and CycLuc2 with similar midmicromolar affinity but is unable to subsequently adenylate D-luciferin to form LH_2-AMP. Consistent with the role of CG6178 as a long-chain fatty acyl-CoA synthetase, the long-chain fatty acids palmitic acid, oleic acid, and linolenic acid were all competitive inhibitors of light emission with K_i values of 2–4 μM (**Table 3.1**). The medium-chain caprylic (octanoic) acid was a weaker inhibitor (13 μM), and the short-chain acetic acid had a calculated K_i value of >1 mM (**Table 3.1**).

Table 3.1. D-luciferin and long-chain fatty acids competitively inhibit light output from CycLuc2-treated CG6178

Inhibitor	K_i (μM)	± SD (μM)
LH_2	25.7	4.5
Acetic Acid	1,411	1,007
Caprylic Acid	13.3	2.8
Palmitic Acid	2.0	1.2
Oleic Acid	4.1	2.6
Linolenic Acid	3.2	1.4

Purified CG6178 and CycLuc2 at concentrations ranging from 0.122 to 125 μM was treated with either no inhibitor; 25, 50, or 100 μM of D-luciferin or acetic acid; 15, 30, or 50 μM of caprylic acid; or 1, 5, or 15 μM of palmitic, oleic, or linolenic acids. The assays were performed in triplicate and each curve was fit to the Michaelis–Menten equation by nonlinear regression (GraphPad 6.0) to determine apparent K_m and V_{max} values. All K_i values were calculated using the equation $K_{m(app)} = K_m(1 + [I]/K_i)$ for each inhibitor concentration and are represented as the mean ± SD.

Light emission from firefly luciferase in vitro is typically characterized by a "burst" phase, where a high initial rate of photon emission is achieved in the first few seconds, followed by a reduction in the rate of photon flux in a subsequent "glow" phase of much longer duration (Fraga, 2008). The basis for this behavior has not been fully elucidated, but it is generally thought to be due to rapid formation of the excited-state oxyluciferin, followed by slow dissociation of the products after initial photon emission (Fraga, 2008). CG6178 lacks this characteristic burst phase but proceeds directly to the glow phase (**Figure 3.6**),

suggesting that the maximal rate of light emission is slower than the dissociation rate of the products and, unsurprisingly, slower than firefly luciferase. Light emission is dependent on the presence of ATP, because only a very weak signal is observed without it, probably owing to residual levels in the protein prep of CG6178 (**Figure 3.7**). Total integrated light output over two minutes for 100 μM CycLuc2 with CG6178 was 0.11% of 100 μM D-luciferin with firefly luciferase, and 2.5% of 100 μM CycLuc2 with firefly luciferase. When integrating the signal emitted during the second minute (e.g., after the luciferase burst), the relative emission from CycLuc2 with CG6178 increased to 0.14% of firefly luciferase with D-luciferin and only 6.7-fold less than luciferase with CycLuc2 (**Figure 3.6**).

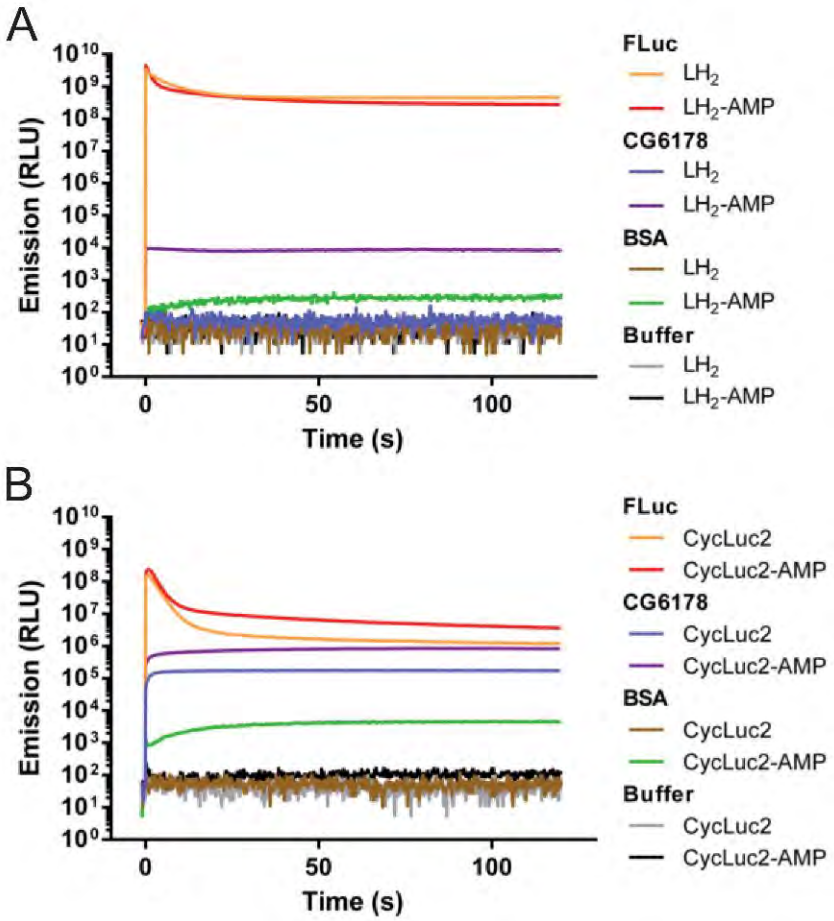

Figure 3.6. Burst kinetics profiles of D-luciferin, CycLuc2, and their respective adenylates. Purified FLuc, CG6178, or enzyme buffer with or without BSA was rapidly injected into (A) LH_2, LH_2-AMP or (B) CycLuc2, CycLuc2-AMP (100 μM final). Light emission was recorded every 0.2 s for 1 s pre-injection and 120 s post-injection.

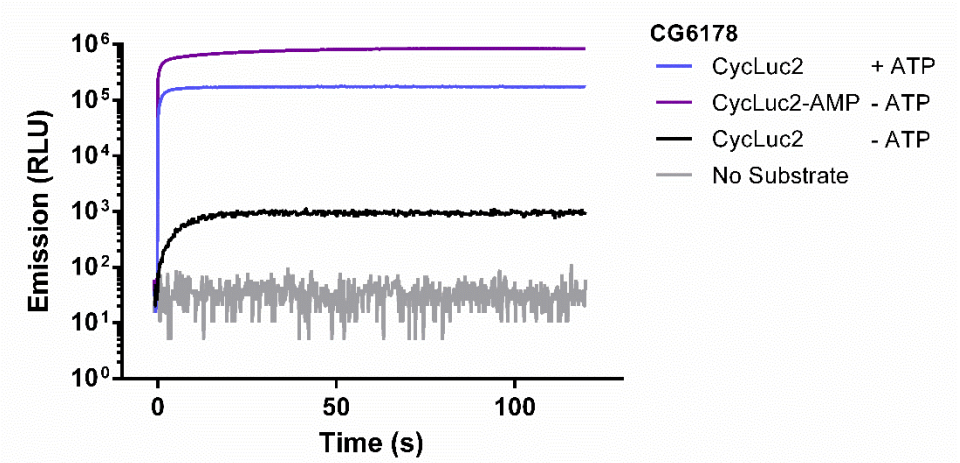

Figure 3.7. Burst kinetics profiles of CG6178 and CycLuc2 or CycLuc2-AMP with and without ATP. Purified CG6178 (40 nM final) was rapidly injected into CycLuc2, CycLuc2-AMP (100 µM final) with or without 2 mM ATP final added to the buffer. Light emission was recorded every 0.2 s for 1 s pre-injection and 120 s post-injection.

We next synthesized the adenylates of D-luciferin and CycLuc2 (LH_2-AMP and CycLuc2-AMP) to determine the effect of bypassing adenylation on the rate of photon flux from CG6178. Treatment of CG6178 with CycLuc2-AMP led to rapid and robust light emission at a rate that was 4.5-fold higher than CycLuc2 alone (**Figure 3.6**). This suggests that adenylation of CycLuc2 is the rate-limiting step in the formation of the excited-state oxyluciferin (Hastings et al., 1953). Consistent with this observation, bypassing the prohibitive adenylation step for D-luciferin by supplying LH_2-AMP also allowed measurable light emission, albeit at a slower rate than CycLuc2. Both adenylates also displayed weak but measurable background bioluminescence in the presence of a high concentration (7,500 nM) of BSA (Viviani and Ohmiya, 2006), but CycLuc2-AMP emission

increased 2,100-fold upon the addition of catalytic quantities of CG6178 (40 nM), whereas LH_2-AMP emission increased 40-fold (**Figure 3.6**).

In principle, the presence of a latent luciferase in fruit flies means that these insects could be rendered bioluminescent if treated with CycLuc2. However, we were unable to detect bioluminescence from fruit flies fed food containing 100 μM CycLuc2. We therefore asked whether bioluminescence could be detected from the endogenous expression of CG6178 in *Drosophila* Schneider 2 (S2) cells (Chintapalli et al., 2007), where compound access and cell number can both be readily controlled. Both live and lysed *Drosophila* S2 cells do, in fact, elicit a bioluminescent glow when treated with CycLuc2 (**Figure 3.8** and **Figure 3.9**). Photon flux was linear with S2 cell number down to a detection limit of 5,000 cells at an average of 0.3 photons per second per cell (**Figure 3.10**). No photon flux over background was observed when S2 cells were treated with D-luciferin (**Figure 3.8**).

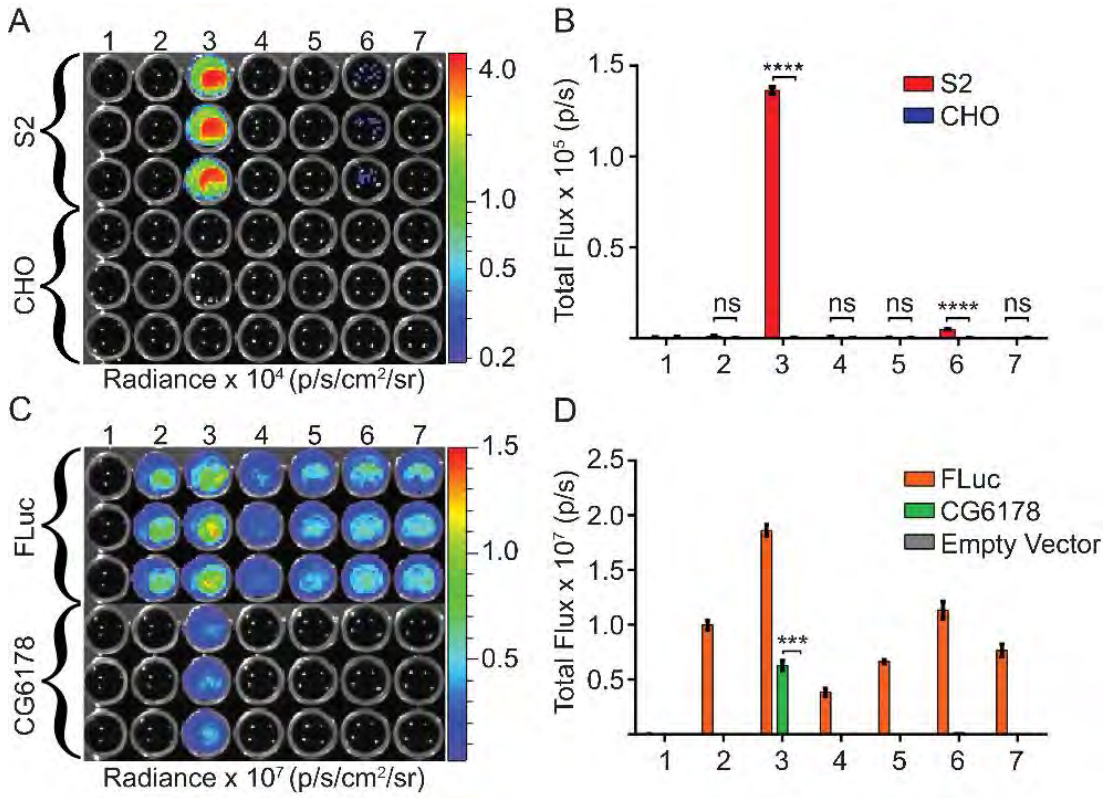

Figure 3.8. CG6178 bioluminescence is detected in both live S2 cells and live transfected CHO cells. (A) Plate image of 3.0 × 10^5 live S2 and CHO cells treated with (1) no substrate or with 100 μM of (2) D-luciferin, (3) CycLuc2, (4) 6'-NH_2LH_2, (5) 6'-$MeNHLH_2$, (6) 6'-Me_2NLH_2, or (7) CycLuc1. (B) Quantified flux from live S2 and CHO cells. (C) Plate images of ~8.0 × 10^3 live CHO cells transiently transfected with FLuc or CG6178 after treatment as above. (D) Quantified flux from transfected CHO cells. All assays were performed in triplicate, represented as the mean ± SEM, and compared by t test. ns, not statistically significant; *** P <0.001, **** P < 0.0001.

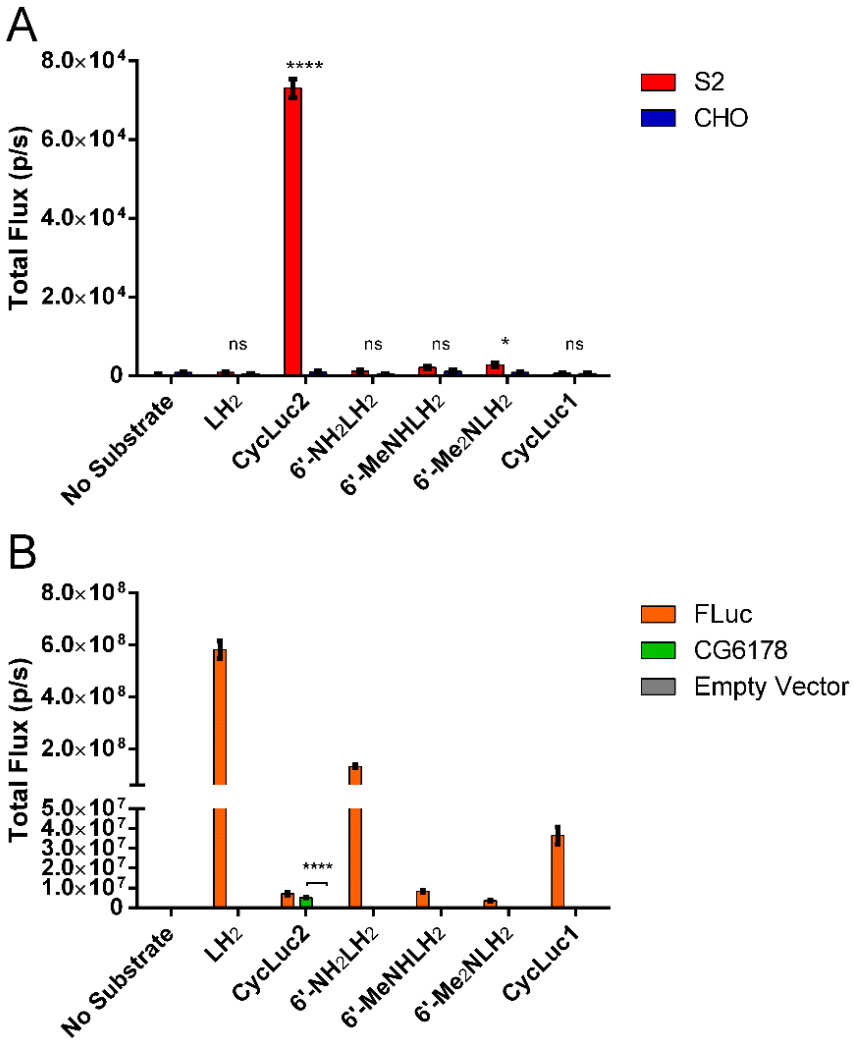

Figure 3.9. CG6178 light emission is detectable in both lysed Schneider 2 (S2) cells and lysed transiently transfected CHO cells. (A) Light emission from 3.0×10^5 lysed S2 or CHO cells. (B) Light emission from ~7.6×10^4 lysed transfected CHO cells. All assays were performed in triplicate, represented as the mean ± SEM, and compared using the unpaired t test. ns, not statistically significant; * $P < 0.05$, **** $P < 0.0001$.

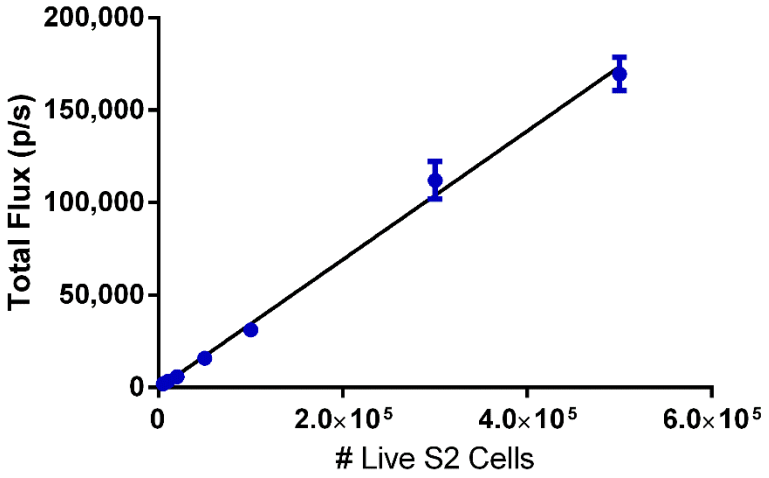

Figure 3.10. Bioluminescence from live *Drosophila* S2 cells treated with CycLuc2 correlates linearly with the number of cells present. Light emission from live S2 cells treated with 100 μM CycLuc2 shows a linear correlation between photon flux and cell number. The assay was performed in triplicate, is represented as the mean ± SEM, and was fit by linear regression (GraphPad 6.0) (R^2 = 0.9913).

Mammalian CHO cells did not emit light after treatment with any of the tested luciferins. However, transfection of CHO cells with CG6178 rendered them highly bioluminescent in the presence of CycLuc2. Overexpression from a CMV promoter rather than the endogenous *Drosophila* dHNF4 promoter (Palanker et al., 2009) yielded bioluminescence of much greater intensity (~800 photons per second per cell; **Figure 3.8** and **Figure 3.9**). The luciferase activity exhibited the same selectivity for CycLuc2 as purified CG6178 and live S2 cells, and treatment of transfected CHO cells with D-luciferin did not result in light emission (**Figure 3.8**). Photon flux from live CG6178-transfected CHO cells treated with 100 μM CycLuc2 was 63% of that from firefly luciferase-transfected CHO cells treated with 100 μM D-luciferin (**Figure 3.8**).

Discussion

It has long been surmised that beetle luciferases evolved from ACSLs. Here we have shown that an ACSL from a non-bioluminescent insect species outside the order of beetles is in fact a latent luciferase, capable of catalyzing light emission from a small molecule substrate. Bioluminescence can be selectively detected with the synthetic luciferin CycLuc2 in vitro and in live *Drosophila* S2 cells and CG6178-transfected mammalian CHO cells. D-luciferin is an inhibitor of CG6178 but is not a substrate for CG6178. Interestingly, both CG6178 and firefly luciferase are competitively inhibited by many medium- and long-chain fatty acids (C8–C20), but not all of these are good substrates for adenylation (e.g., palmitate) (Matsuki et al., 1999; Oba et al., 2005). This suggests that subtle conformational differences can affect whether or not the carboxylate is able to react with ATP in the binding pocket to form the AMP ester. We therefore postulate that the unique rigid and asymmetric ring structure of CycLuc2 acts as a handle to help properly align the substrate within the CG6178 pocket, allowing adenylation to occur where it fails with D-luciferin.

According to our model, CG6178 possesses latent luciferase activity because its natural substrate promiscuity (Glasner et al., 2006; Khersonsky and Tawfik, 2010; Oba et al., 2005; O'Brien and Herschlag, 1999) allows the adenylation of CycLuc2, thereby enabling the intrinsic chemistry accessible to this adenylated intermediate to proceed within the protected confines of the enzyme pocket. Unlike fatty acids, CycLuc2 possesses a chromophore, and once

activated to CycLuc2-AMP it can be oxidized to emit light. Although there is no known role for oxygen in the natural catalytic function of ACSLs, oxygen is ubiquitous and has ready access to hydrophobic pockets in proteins (Baron et al., 2009). Because of the spin-forbidden interaction of triplet oxygen with singlet-state molecules, oxygen is generally unreactive in the absence of an activating cofactor such as a transition metal or flavin, so its presence in protein active sites is usually unnoticed and inconsequential. One exception is the reduction of oxygen to superoxide by carbanions (Abell and Schloss, 1991; Fetzner and Steiner, 2010; Russell and Bemis, 1966). Although alternative explanations for the mechanism of firefly luciferase have been offered (Sundlov et al., 2012), we propose that formation of the luciferin-AMP ester within the enzyme allows access to a resonance-stabilized carbanion that can reduce molecular dioxygen to superoxide by single-electron transfer and then react by subsequent recombination of the radical pair after spin inversion to form a peroxide (**Figure 3.11**). The formation of a carbanion intermediate may be further facilitated in the enzyme by coordination of the substrate carbonyl oxygen to a conserved lysine residue (K443 in FLuc), which has been shown to be important for the oxidative reaction of LH_2-AMP with firefly luciferase (Branchini et al., 2005b; Sundlov et al., 2012) and is found in all beetle luciferases and many ACSLs, including CG6178 (**Figure 3.2**). Access to the luciferyl-AMP chemical intermediate thus opens up new chemical reactivity space that is directed by both the substrate and the enzyme.

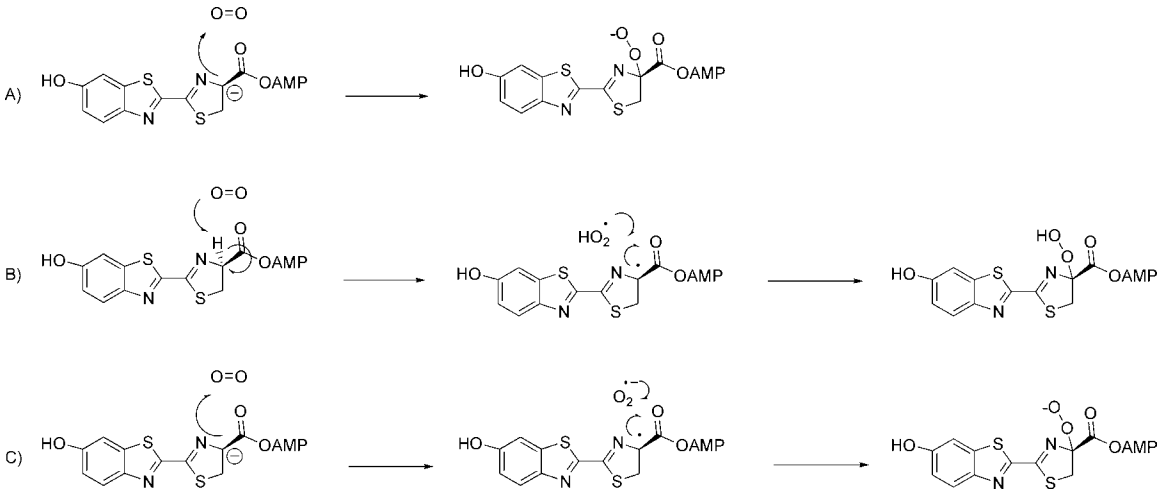

Figure 3.11. Proposed mechanisms of LH_2-AMP oxidation. (A) The classical mechanism (Fraga, 2008) proposes direct reaction of a carbanion with oxygen, which is spin-forbidden. (B) A recently proposed alternative (Sundlov et al., 2012) suggests that oxygen acts to abstract a hydrogen from the C4 of the luciferin substrate to form a radical, which then recombines with the hydroperoxy radical to form a peroxide. However, oxygen abstraction of a hydrogen is disfavored by 40–50 kcal/mol (Fossey et al., 1995). (C) We propose that a carbanion at C4 reduces triplet oxygen by single-electron transfer to form superoxide and a C4 radical, a mechanism with precedence in both chemistry (Russell and Bemis, 1966) and enzymology (Abell and Schloss, 1991; Fetzner and Steiner, 2010). Recombination of these radicals after spin-flip forms a peroxide that subsequently reacts by the canonical mechanism (Fraga, 2008).

The interplay between enzyme-directed substrate activation and the substrate-directed chemistry that ensues has significant implications for evolution and for the design of new enzymatic activities. In this case, a new overall catalytic function – light emission – is revealed simply upon the addition of a xenobiotic substrate. The selectivity of CG6178 for CycLuc2 over D-luciferin could potentially be exploited for the design of new substrate-selective luciferases (Harwood et al., 2011), perhaps by combining features of both beetle luciferases and ACSLs. Furthermore, although we did not observe

bioluminescence from the mammalian ACSLs in CHO cells, which have lower homology to firefly luciferase, mammalian ACS enzymes are known to adenylate xenobiotics such as ibuprofen (Tracy et al., 1993; Watkins and Ellis, 2012). We therefore expect that probing the intersection between the luminogenic chemistry of small-molecule luciferin analogs (Branchini et al., 1989; Conley et al., 2012; Iwano et al., 2013; McCutcheon et al., 2012; Reddy et al., 2010; Takakura et al., 2010; Woodroofe et al., 2008, 2012) and the activation chemistry of existing adenylating enzymes (Watkins and Ellis, 2012) will reveal that latent luciferase activity is more common than previously thought.

Materials and Methods

Collaborators

Gadarla Randheer Reddy of the Miller Lab: Synthesis of all synthetic luciferins

General

Chemicals for synthesis were obtained from Aldrich unless otherwise noted. D-luciferin was obtained from Anaspec and 6'-aminoluciferin was obtained from Marker Gene Technologies, Inc. CycLuc1, CycLuc2, 6'-$MeNHLH_2$, and 6'-Me_2NLH_2 were synthesized as previously described (Reddy et al., 2010). Protein concentrations were determined using Coomassie Plus (Thermo Scientific). Immobilized glutathione (Thermo Scientific) was used for GST-tagged protein

purification. Unless otherwise stated, all protein purification steps were performed at 4 °C. Data were plotted and analyzed with GraphPad Prism 6.0. High-resolution mass spectral data were recorded on a Waters QTOF Premier spectrometer (University of Massachusetts Medical School Proteomics and Mass Spectrometry Facility). Small molecule absorbance was measured using a Cary 50 Bio UV-Visible spectrophotometer. Burst kinetics assays were performed on a Turner Biosystems 20/20n luminometer and reported as relative light units (RLU). Unless otherwise noted, all other bioluminescence assays were performed on a Xenogen IVIS-100. Data acquisition and analysis were performed with Living Image software and reported as radiance [photons per second per square centimeter per steradian ($p/s/cm^2/sr$)] or total flux [photons per second (p/s)] for each region of interest corresponding to each well of the 96-well plate. All RP-HPLC was performed on an Agilent 1100 using a C18 column (Waters Atlantis 4.6 × 250 mm) at a flow rate of 1.0 mL/min using solvent A (0.1% formic acid in H_2O) and solvent B (0.1% formic acid in CH_3CN).

Protein expression and purification

The *Drosophila* protein CG6178 was PCR-amplified from the *Drosophila* Gene Collection cDNA library (GM05240) (Stapleton et al., 2002) and cloned into the BamHI–NotI sites of pGEX6P-1. CG6178 and firefly luciferase were expressed and purified as GST-fusion proteins from the vector pGEX6P-1 as previously described (Harwood et al., 2011). PreScission Protease (GE

Healthcare) cleavage of the GST-fusion was used to elute the untagged protein (Harwood et al., 2011).

Substrate dose–response assays with purified protein

Luminescence assays were initiated by adding 30 µL of 40 nM purified enzyme in enzyme buffer [20 mM Tris (pH 7.4), 0.1 mM EDTA, 1 mM (tris-(2-carboxyethyl) phosphine) (TCEP), and 0.8 mg/mL BSA] to 30 µL of 2x substrate in substrate buffer [20 mM Tris (pH 7.6), 0.1 mM EDTA, 8 mM $MgSO_4$, and 4 mM ATP] in a black 96-well plate (Costar 3915). Imaging was performed 1 min after enzyme addition, with final substrate concentrations ranging from 0.122 to 125 µM using the IVIS-100 as described above.

Bioluminescence emission scans

Each purified enzyme in enzyme buffer was rapidly injected into a cuvette containing substrate in substrate buffer to a final enzyme concentration of 100 nM for luciferase and 1,000 nM for CG6178 and a final substrate concentration of 200 µM. The emission from 400 to 800 nm was recorded in a SPEX FluoroMax-3 fluorimeter with closed excitation slits 10 s after injection. Data are normalized to the peak emission intensity and reported as normalized emission.

Burst kinetics assays

Using a Turner Biosystems 20/20n luminometer, 40 µL of purified enzyme in injection buffer [25 mM Tris (pH 7.7), 0.125 mM EDTA, 5mM $MgSO_4$, 2.5 mM ATP, 0.625 mg/mL BSA, and 0.625 mM TCEP] was rapidly injected into a clear Eppendorf tube containing 10 µL substrate in 10 mM sodium acetate (pH 4.5) to final enzyme concentrations of 0.4 nM for luciferase and 40 nM for CG6178, a final substrate concentration of 100 µM for all substrates, and a final pH of 7.4. Measurements were taken every 0.2 s for 1 s pre-injection and 120 s post-injection. Data acquisition was performed with SIS for 20/20n v1.9.0 software. Data are reported as RLU integrated for each 0.2 s interval. Because photon flux for luciferase is linear with luciferase concentration over the 0.4–40 nM range, data for luciferase were multiplied by 100 to correct for the concentration difference for comparison with CG6178. To correct for the wavelength sensitivity of the PMT in the 20/20n, the emission intensities were also measured using the IVIS-100 as described above. Data from the IVIS and from the 20/20n at the 60 second time point were normalized to the WT + LH_2 value. The correction factor of CycLuc2 was calculated by dividing the normalized IVIS data by the normalized 20/20n data. All 20/20n data were then multiplied by this correction factor (underreported by 3.6-fold).

Cell culture

Drosophila S2 cells were grown at ambient temperature and were cultured in Schneider's *Drosophila* Medium (Gibco) supplemented with 10% FBS and 100 U/mL penicillin/streptomycin (P/S). CHO-K1 cells were grown in a CO_2 incubator at 37 °C with 5% CO_2 and were cultured in F-12K Nutrient Mixture (Gibco) supplemented with 10% FBS and 100 U/mL P/S.

Live cell luminescence assays

S2 cells were washed with HBSS, scraped from the tissue culture dish, and suspended in Schneider's medium. CHO cells were washed with HBSS, trypsinized, and suspended in F-12K medium. Both were centrifuged at 25 x g for 10 min to pellet the cells. Each was suspended in HBSS at a concentration of 6,000 cells per microliter and 50 µL per well was plated in 96-well black tissue culture-treated plates (3916; Costar). Luminescence assays were initiated by adding 50 µL of 2x substrate in HBSS at a final concentration of 100 µM. Imaging was performed 1 min after addition of substrate using the IVIS-100 as described above.

Lysed cell luminescence assays

S2 cells were washed with HBSS, scraped from the tissue culture dish, and suspended in Schneider's medium. CHO cells were washed with HBSS, trypsinized, and suspended in F-12K medium. Both were centrifuged at 25 x g for

10 min to pellet the cells. Each was suspended in 1x Passive Lysis Buffer (Promega) at a concentration of 6,000 cells per microliter. Luminescence assays were initiated by adding 50 µL of 2x substrate in lysed cell substrate buffer [20 mM Tris (pH 7.4), 0.1 mM EDTA, 8 mM $MgSO_4$, 4mM ATP, 1 mg/mL BSA, and 1mM TCEP] to 50 µL of lysate in a black 96-well plate (3915; Costar) with a final substrate concentration of 100 µM. Imaging was performed 1 min after addition of substrate using the IVIS-100 as described above.

Transfections

CG6178 and firefly luciferase were cloned into the BamHI and NotI sites of pcDNA 3.1 and transfected into CHO-K1 cells for live and lysed cell experiments. Transient transfections were performed using Lipofectamine 2000 on cells plated at 60–75% confluency in 96-well black tissue culture treated plates (3916; Costar) for live cell assays or six-well plates for lysed cell assays. For live cells, 0.075 µg DNA per well was transfected; for lysed cells, 2.25 µg DNA per well was transfected. Assays were performed in triplicate 24 h after transfection.

Transfected CHO cell luminescence assays

Transfected CHO cells were washed with HBSS. For live cell imaging, the cells in 96-well plates were incubated with 60 µL of 100 µM substrate in HBSS and imaging was performed 3 min after addition of substrate. Cells grown in six-well plates were first lysed for 20 min at room temperature with Passive Lysis

Buffer (1 mL per well). Luminescence assays were initiated by adding 30 µL of lysate to 30 µL of 2x substrate in lysed cell substrate buffer in a black 96-well plate (3915; Costar). Imaging was performed 1 min after addition of lysate, at a final substrate concentration of 100 µM using the IVIS-100 as described above.

D-luciferyl-adenylate synthesis

The synthesis of D-LH_2-AMP was similar to a previously described method (Branchini et al., 2002). Under an argon atmosphere, a solution of 100 mg (0.49 mmol) of dicyclohexylcarbodiimide in 0.8 mL dry DMSO was added to a solution of D-LH_2 (4.5 mg, 0.16 mmol) and adenosine-5'-monophosphate (15 mg, 0.043 mmol) in dry DMSO. The reaction mixture was mixed at room temperature for 10 min and 5 mL acetone was added to quench the reaction. The resulting white precipitate was collected by centrifugation, washed twice with 3 mL cold acetone, and extracted into 10 mM sodium acetate, pH 4.5, containing 40 mM sodium chloride (2 x 0.75 mL). D-LH_2-AMP was isolated from the pooled extracts by RP-HPLC (0–5 min, 15% B; 5–40 min, linear gradient to 40% B). D-LH_2-AMP eluted at 14.8 min. The concentration in eluent was determined spectrophotometrically using D-LH_2 as a reference [UV LH_2 (H_2O:CH_3CN, 75:25, vol/vol) λ_{max} 330 nm (ε = 16,800)] and the product was aliquoted, lyophilized to a solid, and stored at −20 °C. High-resolution MS-electrospray ionization (HRMS-ESI) $[M-H]^-$ calculated for $C_{21}H_{19}N_7O_9PS_2$ was 608.0444; the value found was 608.0424.

CycLuc2-adenylate synthesis

Under an argon atmosphere, a solution of 59 mg (0.0.29 mmol) of dicyclohexylcarbodiimide in 0.47mL dry DMSO was added to a solution of CycLuc2 (3.0 mg, 0.009 mmol) and adenosine-5′-monophosphate (8.8 mg, 0.025 mmol) in dry DMSO. The reaction mixture was mixed at room temperature for 10 min and 3 mL acetone was added to quench the reaction. The resulting white precipitate was collected by centrifugation, washed twice with 2 mL cold acetone, and extracted into 10 mM sodium acetate, pH 4.5, containing 40 mM sodium chloride (2 × 0.45 mL). CycLuc2-AMP was isolated from the pooled extracts by RP-HPLC (0–5 min, 25% B; 5–40 min, linear gradient to 50% B). CycLuc2-AMP eluted at 11.8 min. The concentration in eluent was determined spectrophotometrically using CycLuc2 as a reference [UV CycLuc2 (H_2O:CH3CN, 70:30, vol/vol) λ_{max} 396 nm (ε = 8,600)] and the product was aliquoted and lyophilized to a solid and stored at −20 °C. HRMS-ESI [M-H]− calculated for $C_{24}H_{24}N_8O_8PS_2$ was 647.0899; the value found was 647.0896.

CHAPTER IV:

Insect fatty acyl-CoA synthetases exhibit unique latent luciferase activity with synthetic luciferin analogs

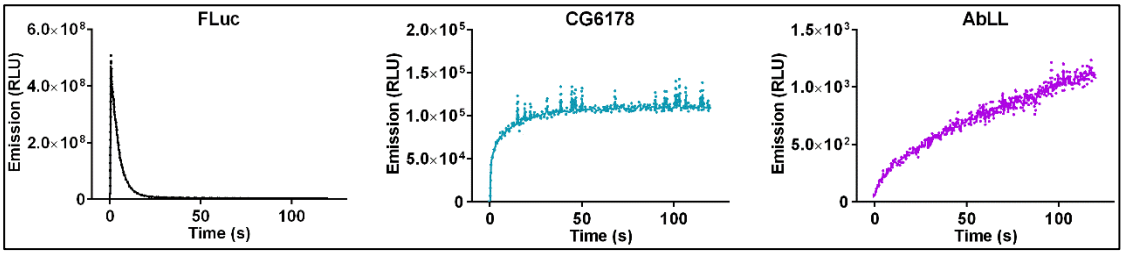

Summary

Long-chain fatty acyl-CoA synthetases (ACSLs) are homologs of firefly luciferase. Recently, we found that an ACSL from *Drosophila melanogaster*, CG6178, is a latent luciferase that emits light with the synthetic luciferin CycLuc2 but not with the natural beetle luciferase substrate D-luciferin. Here we examine firefly luciferase, CG6178, and two additional ACSLs with a substrate palette of 22 synthetic luciferins. We find that the latent luciferase activity of CG6178 extends beyond CycLuc2. Furthermore, an ACSL from the non-luminescent beetle *Agrypnus binodulus* is a second latent luciferase with different substrate specificity than CG6178, while an ACSL from the luminescent beetle *Pyrophorus angustus* lacks any luciferase activity despite a higher homology to luciferase.

Introduction

Firefly luciferase (from *Photinus pyralis*) and fatty acyl-CoA synthetases (ACSLs) are both members of the acyl-adenylate/thioester-forming enzyme superfamily (Chang et al., 1997). These enzymes share the ability to catalyze the formation of fatty acyl-CoA products from free fatty acids (Oba et al., 2003) (**Figure 4.1**). However, luciferase also has the ability to catalyze bioluminescent light emission from its native substrate D-luciferin (**Figure 4.1**). Very weak activity has been shown from an ACSL with D-luciferin (Viviani et al., 2013), but not from any ACSL outside the order of beetles. We recently reported that the ACSL CG6178 from *Drosophila melanogaster* is able to act on the synthetic luciferin analog CycLuc2 and catalyze light emission (Mofford et al., 2014a). Therefore, it is possible to reveal latent luciferase activity from an ACSL if supplied with an appropriate synthetic substrate.

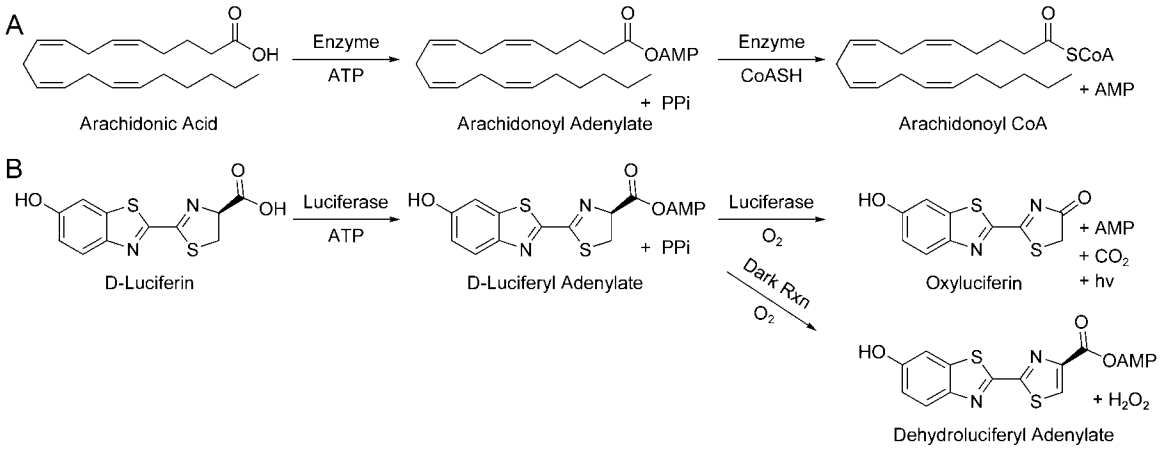

Figure 4.1. Fatty acyl-CoA synthetases and firefly luciferase catalyze similar, two-step reactions. (A) Fatty acyl-CoA synthetases catalyze the formation of an activated adenylate of a free fatty acid followed by displacement of the adenylate by CoASH to form the acyl-CoA product. (B) Firefly luciferase catalyzes the formation of an activated adenylate of D-luciferin followed by oxidation to an excited state oxyluciferin that is responsible for light emission. Oxidation can also produce the off-pathway “dark product” dehydroluciferyl adenylate that inhibits luciferase and does not emit light.

Oba et al. have characterized several luciferase-like enzymes from various insects, showing them to be ACSLs (Oba et al., 2004, 2008, 2010). The ***A****grypnus* ***b****inodulus* **L**uciferase **L**ike protein (AbLL) from a non-luminous Japanese click beetle, possesses high sequence identity to firefly luciferase (46%, **Figure 4.2**) and to other beetle luciferases (e.g. *Pyrophorus plagiophthalmus* luciferase, 55%) (Oba et al., 2008). However, no bioluminescent light is produced upon treatment with D-luciferin. The ***P****yrophorus* ***a****ngustus* **L**uciferase **L**ike protein (PaLL) from the luminous Panamanian click beetle also possesses high sequence identity to firefly luciferase (46%, **Figure 4.2**) and even higher identity to its own dorsal and ventral luciferases (dPaLuc and vPaLuc, 58% each) but does not emit light with D-luciferin (Oba et al., 2010). Both of these ACSLs possess higher identity to firefly luciferase than the latent luciferase CG6178 (39%) and the actual beetle luciferase from *P. plagiophthalmus* (48%). Due to their high homology to multiple luciferases and their fatty acyl-CoA synthetase activity, we hypothesized that these enzymes would also possess latent luciferase activity and tested both against our panel of synthetic luciferin analogs.

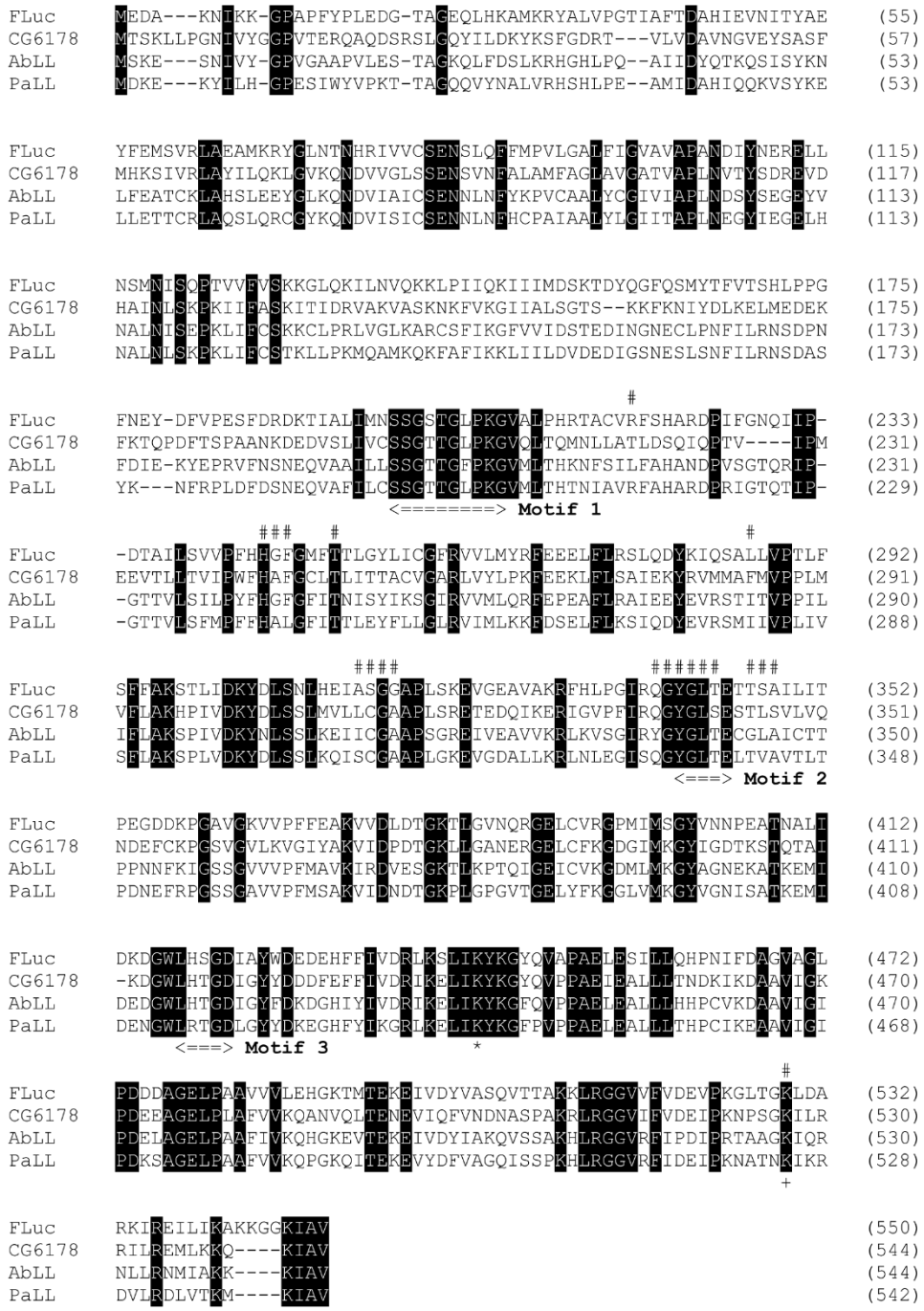

Figure 4.2. Primary sequence alignment of firefly luciferase and three fatty acyl-CoA synthetases. Primary sequences are displayed as a Clustal format alignment by Mafft (Katoh et al., 2002). Motifs 1-3 are conserved between members of the acyl-adenylate superfamily. Residues within 5 Å of the luciferin binding pocket are marked above with #. Luciferase K443 is involved in oxidation or thioesterification of the substrate and is marked below with *. Luciferase K529 is involved in adenylation of the substrate and is marked below with +.

Results

We have reported the synthesis and characterization of an expanded panel of synthetic luciferin analogs based on the general structure of CycLuc1 and CycLuc2 (Mofford et al., 2014b; Reddy et al., 2010) (**Figure 4.3**). Additionally, luciferins with a simplified aromatic core and extended π-conjugation have been reported (Iwano et al., 2013) and we have utilized a similar core structure to develop several additional π-conjugated substrates using our CycLuc modifications (**Figure 4.3**).

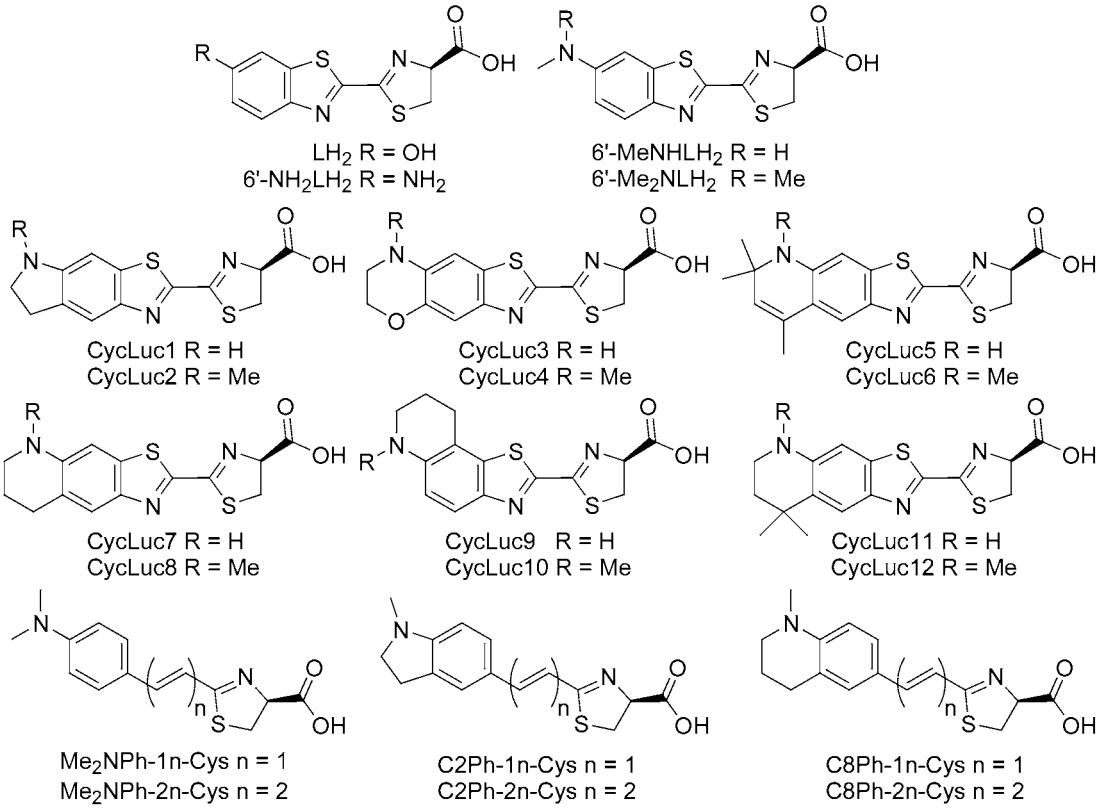

Figure 4.3. Chemical structures of luciferin substrates.

Upon screening CG6178 with our expanded panel of synthetic luciferins, we identified several additional substrates that support light emission (**Figure 4.4** and **Figure 4.5**). CycLuc2 remains the optimal substrate at high dosage (250 μM, **Figure 4.4**). Several other dialkylated luciferins (CycLuc4, 8, and 12) also support light emission. In fact, CycLuc12 produces the highest total flux under lower dose conditions (3.91 μM, **Figure 4.5**). While they are not dialkylated, CycLuc7 and 11 are also able to act as substrates. AbLL also possesses latent luciferase activity, but with a substrate selectivity that is markedly different than CG6178 (**Figure 4.4** and **Figure 4.5**). Like CG6178, AbLL is able to utilize CycLuc2, 7, 11 and 12, but prefers CycLuc7 over CycLuc2. AbLL also accepts the short cinnamyl-type substrates Me_2NPh-1n-Cys and C8Ph-1n-Cys that are inactive with CG6178. Curiously, AbLL is unable to use C2Ph-1n-Cys differing from C8Ph-1n-Cys by a single methylene. AbLL also emits weaker overall light compared to CG6178, even though it has increased sequence identity to firefly luciferase. PaLL has equal sequence identity to luciferase as AbLL, but was inactive with all tested substrates (**Figure 4.4** and **Figure 4.5**).

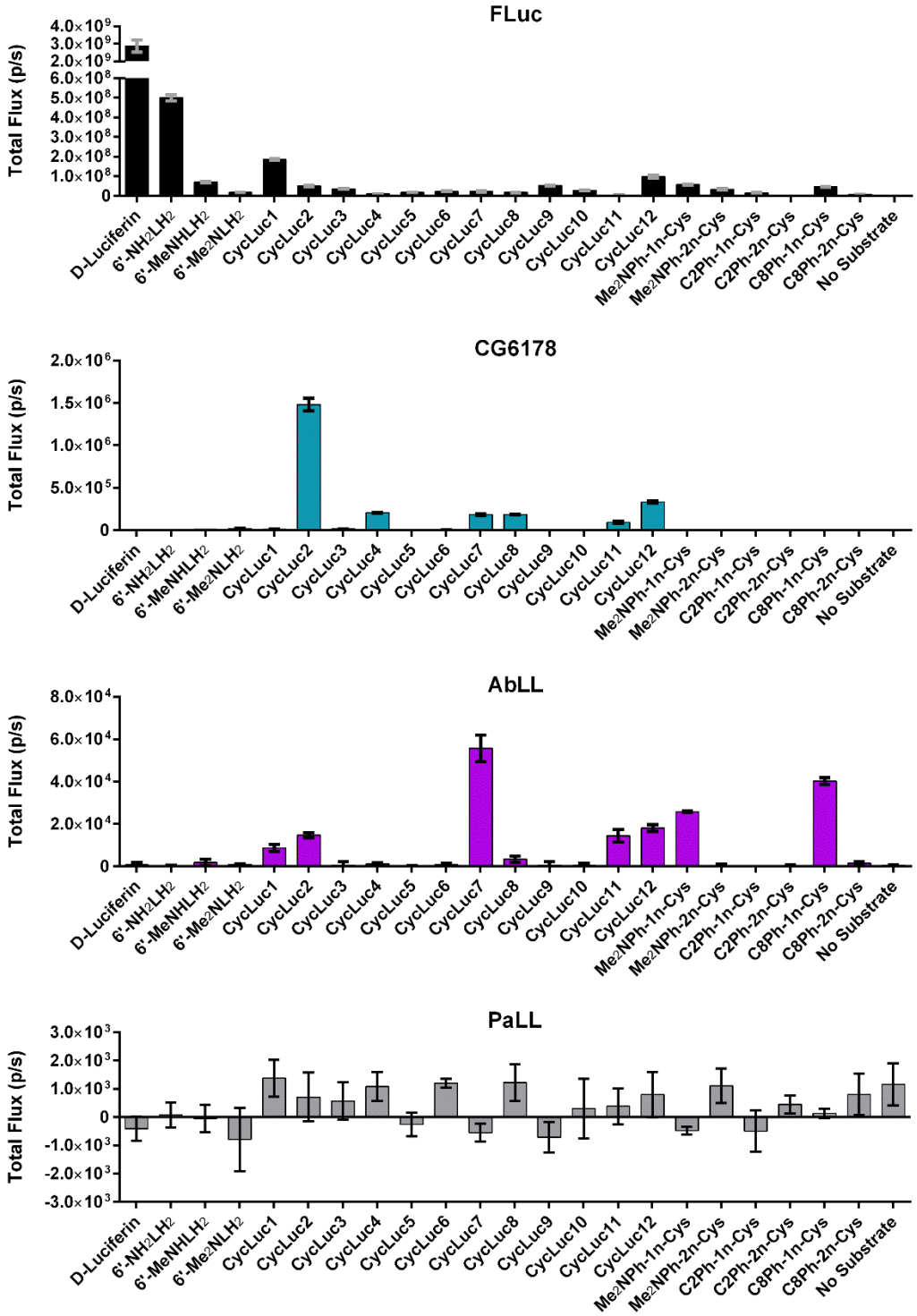

Figure 4.4. ACSL activity upon treatment with 250 μM of the indicated luciferin analog. The indicated ACSL (20nM final) was treated with the indicated luciferin analog (250 μM final). The assay was performed in triplicate and is represented as the mean ± SEM.

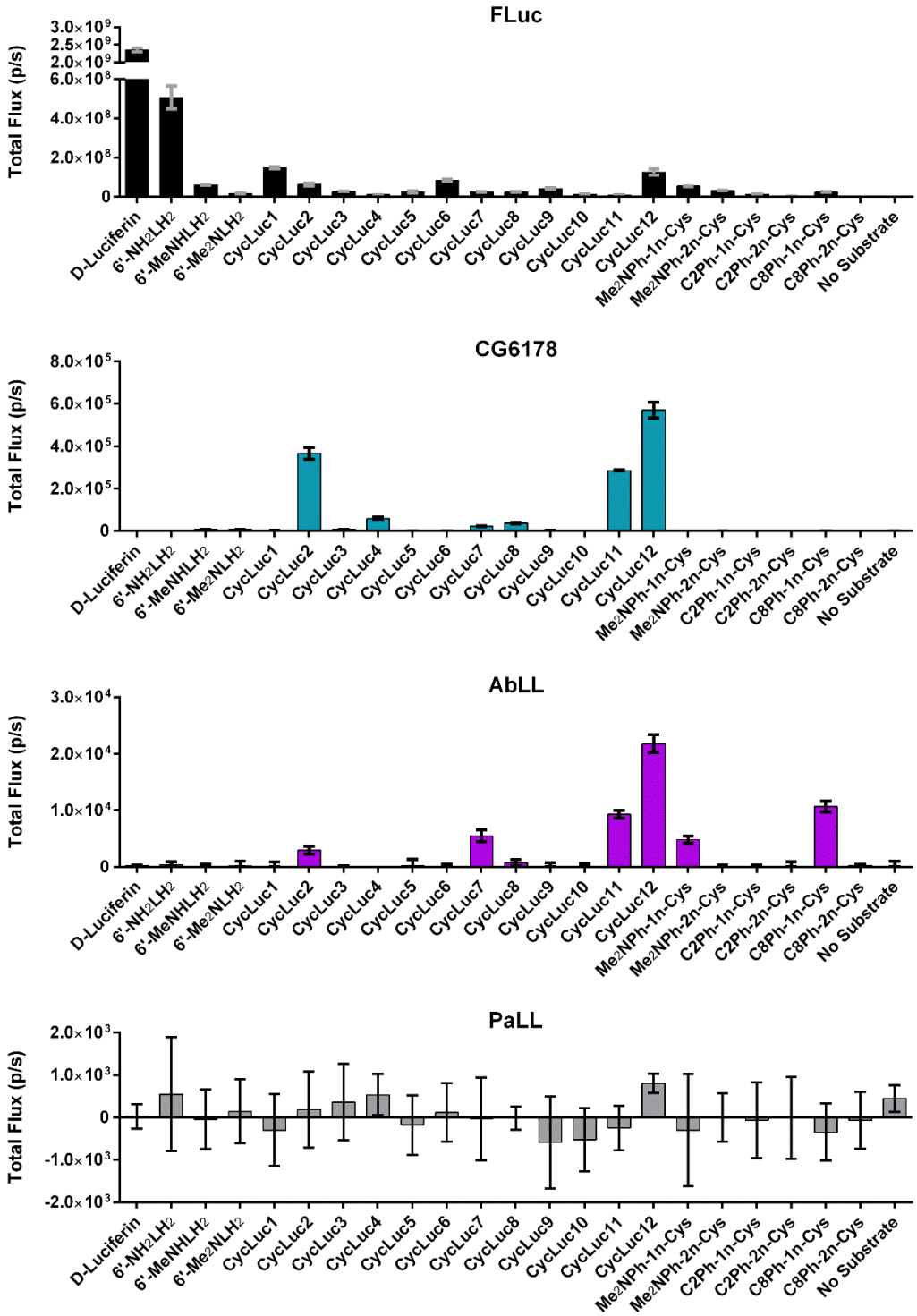

Figure 4.5. ACSL activity upon treatment with 3.91 μM of the indicated luciferin analog. The indicated ACSL (20nM final) was treated with the indicated luciferin analog (3.91 μM final). The assay was performed in triplicate and is represented as the mean ± SEM.

Since the first enzymatic step of catalysis is adenylation, we examined the effects of the ATP reagent on light emission, and found that ATP purity affects the maximal rate of flux from both CG6178 and AbLL. Enzymatic V_{max} using ATP from Sigma was reduced compared to using ATP from MP Biomedicals; CG6178 was particularly sensitive (ΔV_{max} = 13-fold reduction with CycLuc2) (**Figure 4.6**, **Figure 4.7**, and **Figure 4.8**). We hypothesize that there is a small amount of contaminating pyrophosphate present in the ATP from Sigma that is responsible for this reduction. Addition of pyrophosphate to MP Bio's ATP results in a similar level of light to Sigma's ATP (**Figure 4.9**). Moreover, pre-treatment of Sigma's ATP with pyrophosphatase produced an increase in signal similar to that achieved with MP Bio's ATP (**Figure 4.9**). The noncompetitive inhibition by pyrophosphate (K_i 0.87 μM ± 0.32 μM) lowers the effective enzyme concentration, while having no effect on the K_m of the luciferin substrate (**Figure 4.6** and **Figure 4.7**).

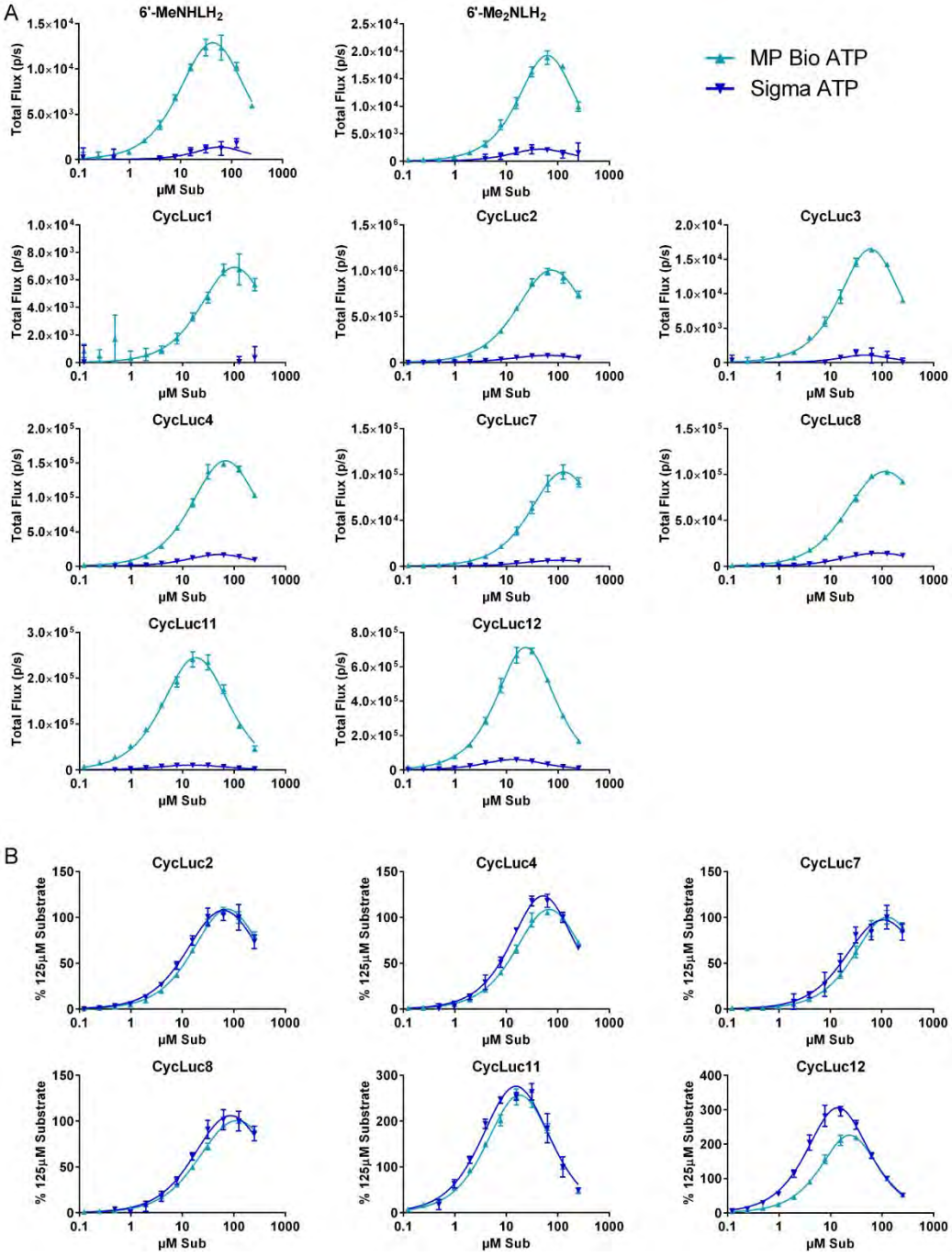

Figure 4.6. CG6178 activity is reduced by using impure ATP. (A) Dose-response curves of CG6178 and the indicated luciferin analog using ATP purchased from either Sigma or MP Biomedicals. (B) Dose-response curves from (A) normalized to total flux at 125 μM substrate. The assays were performed in triplicate and are represented as the mean ± SEM. Curves were fit to the Substrate Inhibition equation [$Y=V_{max}*X/(K_m + X*(1+X/K_i))$] by nonlinear regression.

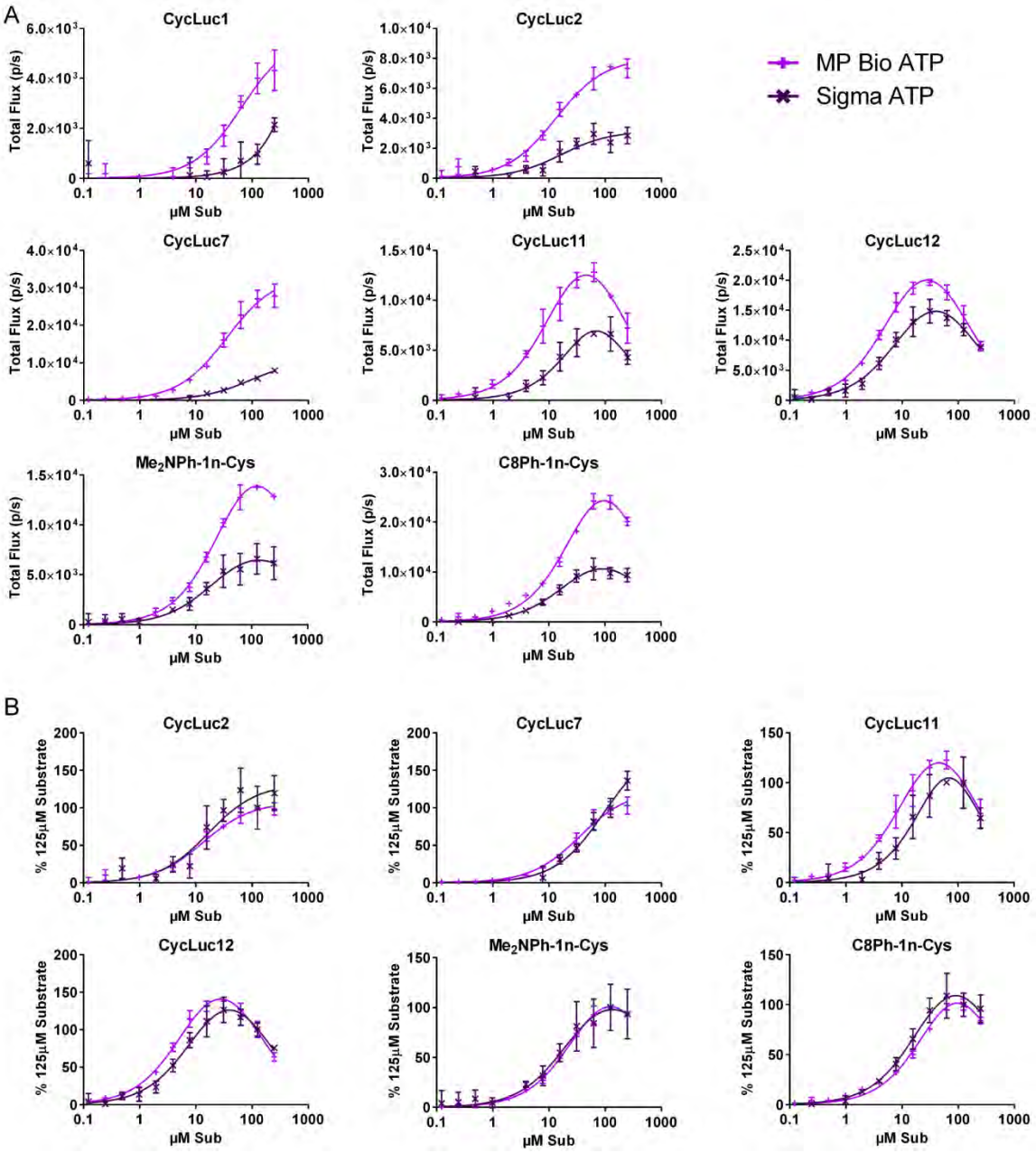

Figure 4.7. AbLL activity is reduced by using impure ATP. (A) Dose-response curves of AbLL and the indicated luciferin analog using ATP purchased from either Sigma or MP Biomedicals. (B) Dose-response curves from (A) normalized to total flux at 125 μM substrate. The assays were performed in triplicate and are represented as the mean ± SEM. CycLuc1, 2, and 7 curves were fit to the Michaelis–Menten equation by nonlinear regression. Other curves were fit to the Substrate Inhibition equation [$Y=V_{max}*X/(K_m + X*(1+X/K_i))$] by nonlinear regression.

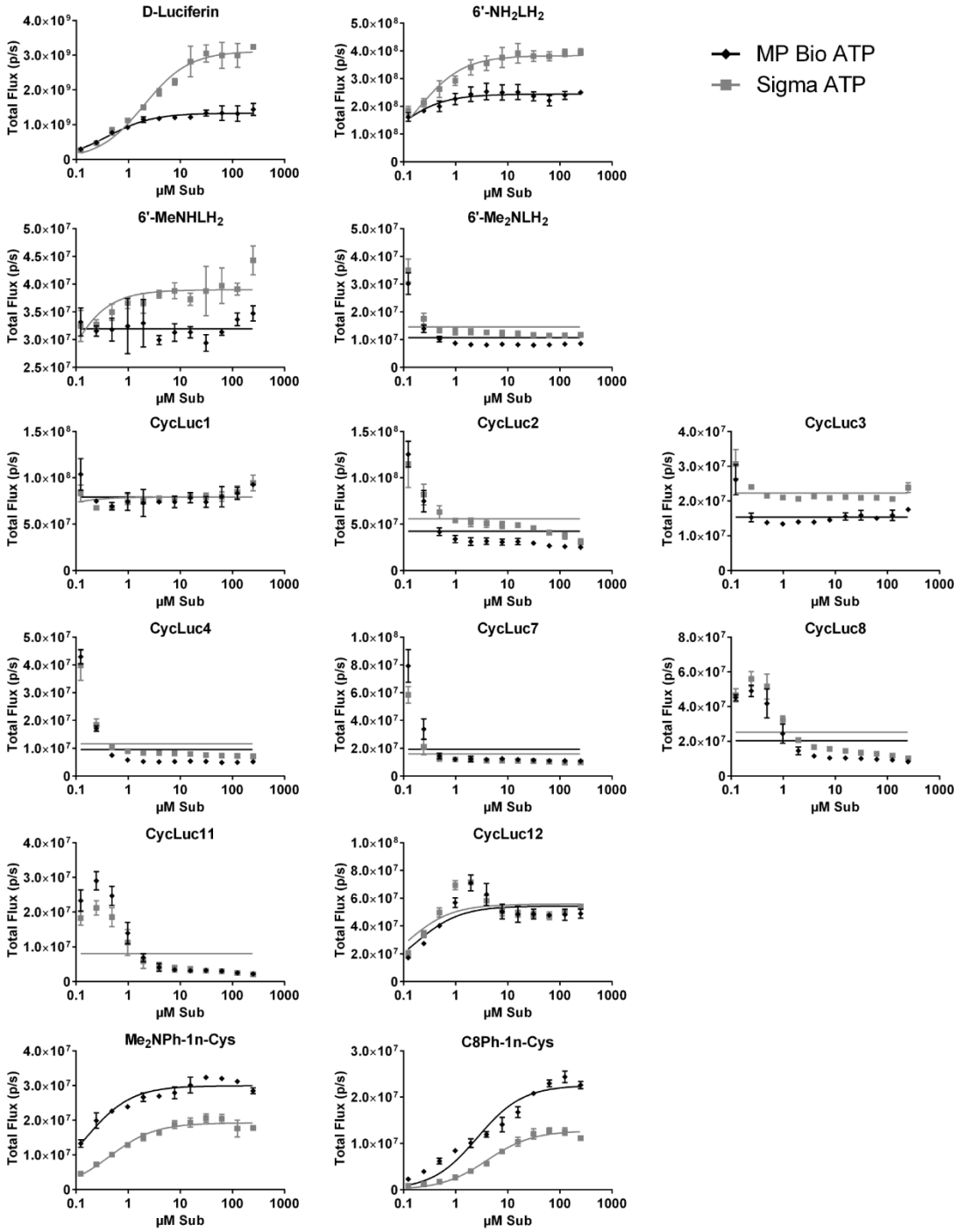

Figure 4.8. Firefly luciferase activity is minimally affected by ATP purity. Dose-response curves of FLuc and the indicated luciferin analog using ATP purchased from either Sigma or MP Biomedicals. The assays were performed in triplicate and are represented as the mean ± SEM. Curves were fit to the Michaelis–Menten equation by nonlinear regression.

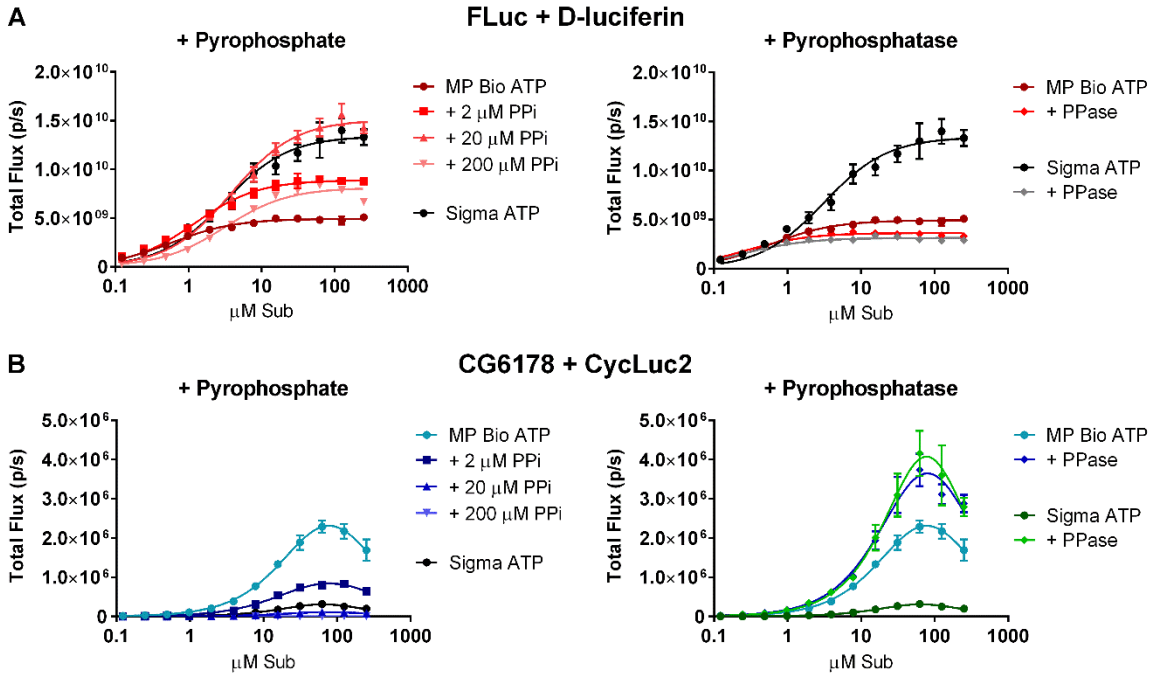

Figure 4.9. PPi Affects Light Emission from FLuc and CG6178. (A) Dose-response curves of FLuc light emission with D-luciferin using ATP purchased from either MP Biomedicals or Sigma. Left Panel: MP Bio ATP is supplemented with increasing concentrations of pyrophosphate (PPi). Right Panel: Each ATP with or without pre-treatment with pyrophosphatase (PPase). (B) Dose-response curves of CG6178 light emission with CycLuc2 using ATP purchased from either MP Biomedicals or Sigma. Left Panel: MP Bio ATP is supplemented with increasing concentrations of pyrophosphate (PPi). Right Panel: Each ATP with or without pre-treatment with pyrophosphatase (PPase). The assays were performed in triplicate and are represented as the mean ± SEM. FLuc curves were fit to the Michaelis–Menten equation by nonlinear regression. CG6178 curves were fit to the Substrate Inhibition equation [$Y=V_{max}*X/(K_m + X*(1+X/K_i))$] by nonlinear regression. Note: Assays were performed with 2 mM ATP final.

Interestingly, the contaminating pyrophosphate has a very different effect on firefly luciferase (**Figure 4.8**). It slightly increases the V_{max} of firefly luciferase with D-luciferin, likely because it can react with the enzyme-bound potent inhibitor dehydroluciferyl adenylate (**Figure 4.1**) to release dehydroluciferin and ATP. A similar effect has been observed upon the addition of CoASH, which is hypothesized to release the dehydroluciferyl adenylate inhibitor as the CoA ester (Fraga et al., 2005). However, upon treatment with high pyrophosphate dose (200 μM, 10% ATP concentration), luciferase light emission is inhibited as well (**Figure 4.9**).

Reactions between the synthetic luciferins and firefly luciferase were less sensitive to ATP purity (**Figure 4.8**). Previous work in the lab has also established that the addition of CoASH has little effect on aminoluciferins (Reddy et al., 2010). The chemical structures of these substrates may make them less likely to form the dehydroluciferyl adenylate, so the addition of pyrophosphate or CoASH has no discernible effect. Alternatively, the high-affinity synthetic luciferins may be capable of forming dehydroluciferin inhibitors that are so potent that pyrophosphate-mediated conversion of dehydroluciferyl adenylates to dehydroluciferin and ATP does not meaningfully reduce inhibition. Another possibility is that pyrophosphate cannot form dehydroluciferins and ATP from the dehydroluciferyl adenylates of the aminoluciferins considered here.

Additionally, neither CG6178 nor AbLL behave as expected with traditional Michaelis-Menten kinetics (**Figure 4.6** and **Figure 4.7**). Both display the

predicted increase in emission with increasing dosage at low substrate concentrations. However, both then show a decrease in total flux at or near the highest substrate concentrations tested. We hypothesize that the decrease is due to substrate inhibition, where the enzyme is actually inhibited by its own substrate (Reed et al., 2010). Accounting for substrate inhibition by fitting the data with the equation $Y=V_{max}*X/(K_m + X*(1+X/K_i))$ still results in a good fit. We propose that there could be a secondary allosteric binding site for the luciferin, where at high concentration the luciferin also acts as a noncompetitive inhibitor, forcing the enzyme into a conformation that is unable to catalyze light emission. Indeed, it is the more hydrophobic substrates such as CycLuc11 and 12 where this effect is most pronounced and these substrates would be most apt to bind a small hydrophobic pocket and disrupt catalysis.

Upon rapid injection of enzyme to substrate, firefly luciferase produces a burst of light followed by an immediate decay to a lower level steady state (Fraga, 2008). These are known as the “burst phase” and “glow phase” respectively. This decay is thought to be a result of product inhibition by either the light-emitting oxyluciferin and AMP products, or the “dark” dehydroluciferyl adenylate side-product. The decay is more pronounced with the tighter binding synthetic luciferins than with D-luciferin (**Figure 4.10**).

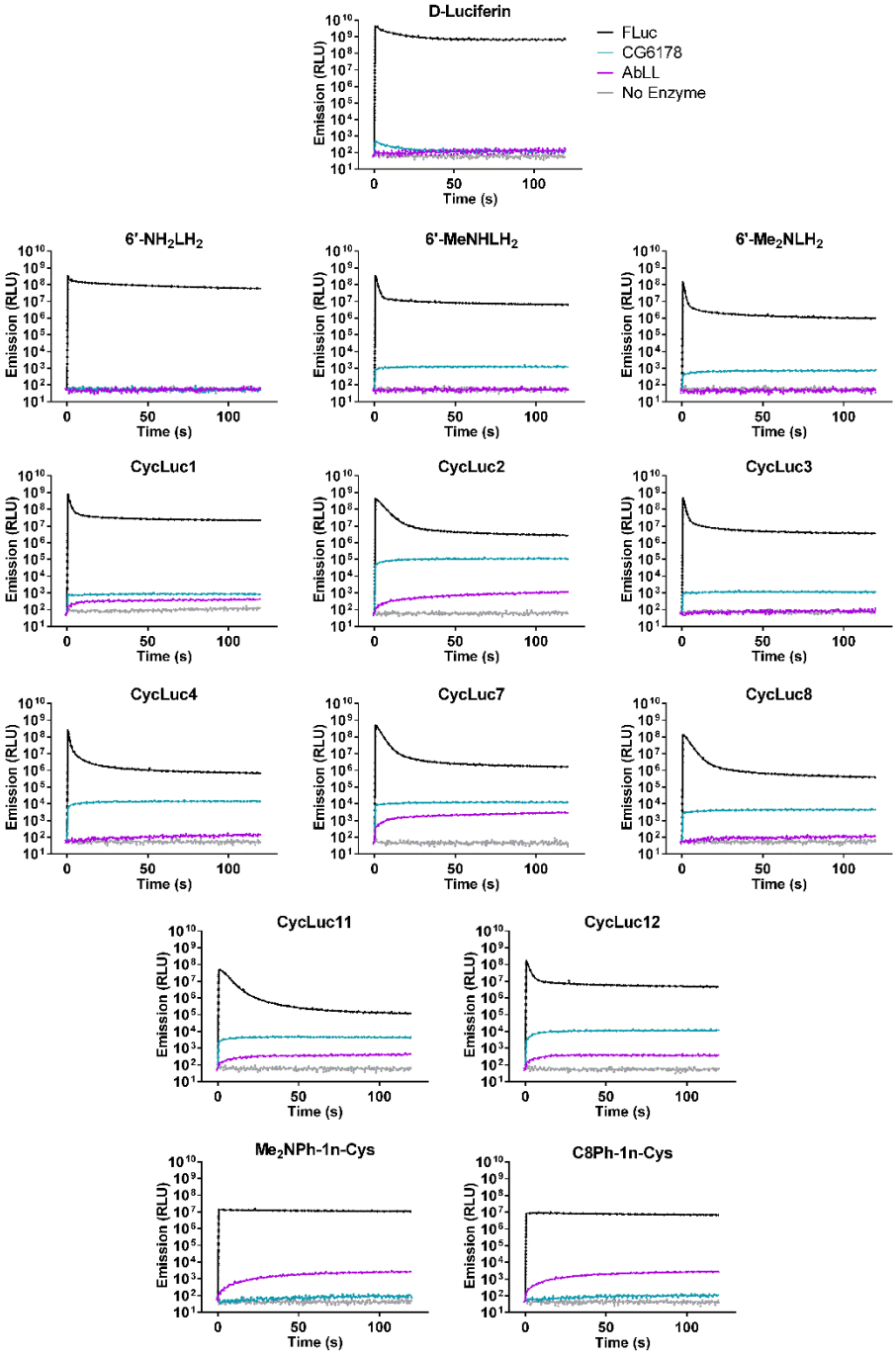

Figure 4.10. Burst kinetics of each ACSL with the indicated luciferin analog. Purified enzyme (100 nM final) was rapidly injected into substrate (250 μM final). Light emission was recorded every 0.5 s for 1 s pre-injection and 120 s post-injection. Background luminescent signal in the absence of enzyme is shown for reference (in gray). The assays were performed in triplicate, are represented as the mean ± SEM, and are presented on the same log scale.

CG6178 and AbLL each display distinct and alternative profiles to luciferase. For example, CG6178 does not exhibit a burst phase, proceeding directly to the glow phase within the first few seconds post-injection (**Figure 4.10** and **Figure 4.11**). AbLL does not reach a steady state level of light emission, continuing to increase even two minutes after injection (**Figure 4.10** and **Figure 4.11**). These distinct profiles suggest that there are altered mechanisms of catalysis between the three enzymes.

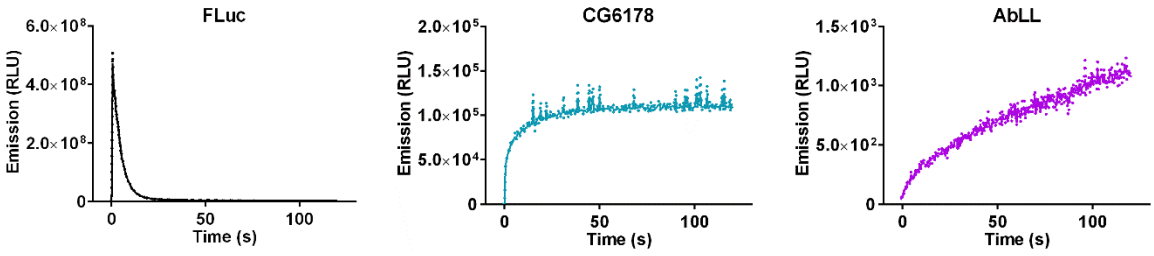

Figure 4.11. CycLuc2 burst kinetics with ACSLs. Purified enzyme (100 nM final) was rapidly injected into substrate (250 μM final). Light emission was recorded every 0.5 s for 1 s pre-injection and 120 s post-injection. The assays were performed in triplicate, are represented as the mean ± SEM, and are presented on an appropriate linear scale.

Discussion

CG6178 is an ACSL from the fruit fly and the first latent luciferase described. Although CycLuc2 remains the best substrate identified at high substrate concentration, other rigid aminoluciferins can also serve as light-emitting substrates (e.g. CycLuc4, 8, and 12). AbLL is another latent luciferase that exhibits different substrate specificity, and even emitting light with luciferin analogs that are inactive with CG6178 (i.e. Me_2NPh-1n-Cys and C8Ph-1n-Cys). On the other hand, PaLL has no luciferase activity with any of the tested luciferin analogs. These results stand in stark contrast to firefly luciferase, which is remarkably tolerant to substrate modification and will emit light with D-luciferin and all 21 synthetic luciferin analogs.

Unexpectedly, homology to a beetle luciferase was not a good predictor of latent luciferase activity among the three ACSLs tested. PaLL is an ACSL from the luminous beetle *P. angustus* that is 58% identical to its own luciferases, vPaLuc and dPaLuc, and 46% identical to firefly luciferase; yet it exhibited no luciferase activity with any of the tested substrates. AbLL, an ACSL from the non-luminous beetle *A. binodulus*, is 55% identical to *P. plagiophthalmus* click beetle luciferase and shares higher identity to firefly luciferase than CG6178 (46% vs. 39%), yet is a weaker latent luciferase. These results then beg the question: what are the defining features that can predict latent luciferase activity?

In order for luciferase to catalyze light emission, it must be able to efficiently couple the adenylation and oxidation of each luciferin substrate.

Luciferase possesses two conserved lysine residues (K529 and K443) that are responsible for adenylation and oxidation respectively (Branchini et al., 2005b). Both are conserved in the three ACSLs, as they are necessary for adenylation and thioesterification of their natural fatty acid substrates (**Figure 4.2**). Luciferase undergoes a conformational change between the two catalytic steps in order to position the correct lysine in the active site (Sundlov et al., 2012). Therefore, the position of each lysine during catalysis and the ability of luciferase to undergo the conformational changes between catalytic steps all connect to finally catalyze light emission.

CG6178 fails to emit light with D-luciferin because it is unable to form its adenylate (Oba et al., 2004). Although, D-luciferin can bind in the active site of CG6178 and act as an inhibitor of CycLuc2-mediated light emission (Mofford et al., 2014a). Ergo, D-luciferin is probably not positioned properly relative to the first lysine (K527, CG6178 numbering) and/or ATP for that catalytic step. However, if supplied with pre-adenylated D-luciferin, CG6178 is able to oxidize that intermediate and emit light, meaning K441 is aligned correctly (Mofford et al., 2014a). The cyclic dialkylated modifications of CycLuc2, 4, 8, and 12 must alter the binding orientation relative to K527 (and/or ATP) to allow adenylation to occur. Additionally, CG6178 does not display the typical burst phase of firefly luciferase, but proceeds directly to the glow phase. This shows the absence of product inhibition and suggests that product dissociation is not the rate limiting step in catalysis. CG6178 may undergo a slower conformational change between

catalytic steps relative to firefly luciferase. Moreover, the presence of contaminating pyrophosphate from the Sigma ATP results in a significant decrease in the maximal rate of light emitted. Perhaps the excess pyrophosphate is forcing the luciferyl adenylate to undergo the reverse reaction and release the luciferin and ATP, instead of proceeding to the oxidation step. If the conformational change between steps is slower, that may give pyrophosphate enough time to react before oxidation can occur.

AbLL displays weaker total photon flux relative to CG6178, with notably different substrate selectivity. The differences in substrate preference are likely caused by variations in the substrate binding pocket. Changes in the residues that line the pocket will alter the binding orientations of each luciferin relative to the two catalytic lysines and the ATP co-substrate, allowing AbLL to only utilize a subset of the panel. By studying the shape of the AbLL (and CG6178) binding pocket, it may be possible to engineer a luciferase to adopt the same substrate specificity while exhibiting the higher total photon flux of firefly luciferase.

The weaker level of light emission from AbLL may be explained by the slow burst kinetics observed. AbLL may not couple the adenylation and oxidation steps of catalysis as efficiently as the other enzymes so it may take longer for the total population of enzyme to reach a steady state. Using pre-adenylated luciferin it should be possible to determine which catalytic steps are responsible for the decrease. For example, if the slow burst is due to a slow adenylation rate, using pre-adenylated luciferin will compensate and increase the burst rate. If the slow

burst is due to oxidation, using pre-adenylated luciferin will have no effect. If the slow burst is due to a combination of both steps, using pre-adenylated luciferin should slightly increase the burst rate. Then, once we determine which catalytic step(s) are less efficient, we can compare AbLL to CG6178 and luciferase, using both sequence alignment and structural studies. Hopefully the differences and similarities between the enzymes will link back to the differences in catalysis, and the characteristics of a luciferase will start to take shape.

Finally, PaLL does not support light emission from any of the tested luciferin analogs, despite having 58% sequence identity to the two luciferases found in *P. angustus* and 46% identity to firefly luciferase. This enzyme may be the best ACSL we have tested to determine the features necessary for latent luciferase activity. First, we can test luciferin binding by screening for inhibition of fatty acyl-CoA synthesis. If the luciferin is able to bind to the active site, then it should also be a competitive inhibitor of the enzyme's native function. Second, if the luciferin can bind, we can bypass the adenylation step using pre-adenylated luciferin. As with determining the slow burst of AbLL, using pre-adenylated luciferin can dissect which catalytic step(s) are deficient with PaLL. Then, once we have determined where PaLL falls short, we can compare it to the other ACSLs to identify the differences and map them back to those defects.

So what are the defining features of a beetle luciferase? The enzyme must: 1) bind a luciferin in an orientation conducive to adenylation; 2) adenylate the carboxylate; 3) undergo a conformational change to align the second lysine in

the active site, and 4) oxidize the luciferyl adenylate to an excited-state oxyluciferin. As for how to predict which ACSLs will have luciferase activity, that remains unclear. Structural studies of these ACSLs may aid in dissecting the differences in emission efficiency (e.g., by comparing PaLL to the others). Additionally, many of the residues that line the luciferin binding pocket of firefly luciferase are not well conserved amongst ACSLs. Some of these residues have already been identified as important for emission with D-luciferin. For example, S347 in firefly luciferase is critical for catalysis with D-luciferin, as the S347A mutation has detrimental effects on both K_m and V_{max}. Perhaps testing more ACSLs will allow for recognition of conserved residues that are critical for light emission with all luciferins and will help to identify other ACSLs with latent luciferase activity.

In summary, we have identified a second latent luciferase (AbLL) among insect ACSLs with a different substrate fingerprint than CG6178. This demonstrates that nascent luciferase activity in an ACSL is not limited to the fruit fly. However, we see that luciferase activity is also not universal to all insect ACSLs (e.g. PaLL). These results suggest that ACSLs can be a source of genetic diversity and structural insights for the construction of substrate-selective luciferases, especially if the defining characteristics of latent luciferase activity can be unveiled.

Materials and Methods

Collaborators

Gadarla Randheer Reddy of the Miller Lab:

Synthesis of all benzothiazole core synthetic luciferins

Kiran Reddy of the Miller Lab:

Synthesis of all phenyl core extended-conjugation synthetic luciferins

General

Chemicals were purchased from Aldrich, Matrix Scientific, Oakwood, or TCI. ATP was purchased from both MP Biomedicals and Sigma. D-luciferin was obtained from Anaspec and 6'-NH_2LH_2 was obtained from Marker Gene Technologies Inc. CycLuc1, CycLuc2, 6'-$MeNHLH_2$, and 6'-Me_2NLH_2 were synthesized as previously described (Reddy et al., 2010). CycLuc3-12 were synthesized as previously described (Mofford et al., 2014b). Other luciferins were prepared within the Miller lab. Data were plotted with GraphPad Prism 6.0.

Plasmid constructs

The DNA sequences for long-chain fatty acyl-CoA synthetases CG6178, AbLL, and PaLL were codon optimized for mammalian expression, synthesized by GenScript, and cloned into the BamHI–NotI sites of pGEX6P-1. WT luc2 luciferase was used in pGEX6P-1 as previously described (Mofford et al., 2014b).

Enzyme expression and purification

Luciferases, fatty acyl-CoA synthetases, and chimeras were expressed and purified as GST-fusion proteins from the pGEX6P-1 vector as previously described (Mofford et al., 2014b). Briefly, JM109 cells were grown at 37 °C until the OD600 reached 0.5-1, induced with 0.1 mM IPTG, and incubated with shaking at 20 °C overnight. Cells were pelleted at 5000 RPM, then flash frozen in liquid nitrogen. The *E. coli* pellets from 1 L of culture were thawed on ice, resuspended in 25 mL lysis buffer (50 mM Tris [pH 7.4], 500 mM NaCl, and 0.5% Tween 20) containing 1 mM phenylmethylsulfonyl fluoride, and disrupted by sonification (Branson Sonifier). Dithiothreitol (DTT) was added at 10 mM, and the resulting cell lysate was clarified by centrifugation at 35,000 RPM for 60 min at 4 °C. The supernatant was batch-bound to immobilized glutathione (Thermo Scientific) for 1 hr at 4 °C, and the beads were washed with lysis buffer containing 10 mM DTT, followed by wash buffer (50 mM Tris [pH 8.1], 250 mM NaCl, and 10 mM DTT) and storage buffer (50 mM Tris [pH 7.4], 0.1 mM EDTA, 150 mM NaCl, 1 mM TCEP). Twenty units of PreScission Protease (GE Healthcare) were added, and incubation continued overnight at 4 °C to cleave the GST-fusion and elute the untagged enzyme. Protein concentrations were determined using Coomassie Plus (Thermo Scientific).

Purified protein luminescence assays

Luminescence assays were initiated by adding 30 µL of purified luciferase in enzyme buffer (20 mM Tris [pH 7.4], 0.1 mM EDTA, 1 mM TCEP, and 0.8 mg/mL BSA) to 30 µL 2x substrate in substrate buffer (20 mM Tris [pH 7.4], 0.1 mM EDTA, 8 mM $MgSO_4$, and 4 mM ATP) in a black 96-well plate (Costar 3915). Imaging was performed one minute after enzyme addition using a Xenogen IVIS-100 at a final enzyme concentration of 20 nM and final substrate concentrations ranging from 0.122 to 250 µM. Data acquisition and analysis was performed with Living Image® software. Data are reported as total flux (p/s) for each ROI corresponding to each well of the 96-well plate.

ATP evaluation assays using pyrophosphate and pyrophosphatase

D-Luciferin and CycLuc2 were prepared at concentrations from 1,000 µM to 0.488 µM in evaluation buffer (20 mM Tris [pH 7.4] and 0.1 mM EDTA). ATP from either MP Biomedicals or Sigma was prepared at 16 mM in evaluation buffer with 32 mM $MgSO_4$. Pyrophosphate was prepared at 1.6 mM, 160 µM, and 16 µM in evaluation buffer. Pyrophosphatase (NEB) was prepared at 4 units/mL in enzyme buffer. Luciferase and CG6178 were prepared at 80 nM in enzyme buffer. In a black 96-well plate (Costar 3915), 25 µL luciferin, 12.5 µL ATP, and 12.5 µL pyrophosphate or evaluation buffer were added. Enzyme buffer (25 µL) was added, proceeding directly to luminescence, or pyrophosphatase (25 µL) was added and held at ambient temperature for 45 minutes. Luminescence was

then initiated by adding 25 µL of luciferase or CG6178. Imaging was performed one minute after luciferase/CG6178 addition at a final concentrations of 250 µM to 0.122 µM luciferin; 2 mM ATP; 0 µM, 2 µM, 20 µM, or 200 µM pyrophosphate; 0 or 0.1 units/well pyrophosphatase; and 20 nM luciferase/CG6178.

Burst kinetics assays

Using a Promega GloMax-Multi Detection System, 50 µL of purified enzyme in enzyme buffer was rapidly injected into a white 96-well plate (Costar 3912) containing 50 µL of 2x substrate in substrate buffer to a final enzyme concentration of 100 nM and a final luciferin substrate concentration of 250 µM. Measurements were taken every 0.5 s for 1 s pre-injection and 120 s post-injection. Data are reported as Relative Light Units (RLU).

CHAPTER V:

Chimeric Firefly Luciferase / Fatty Acyl-CoA Synthetase Enzymes Improve Substrate Selectivity

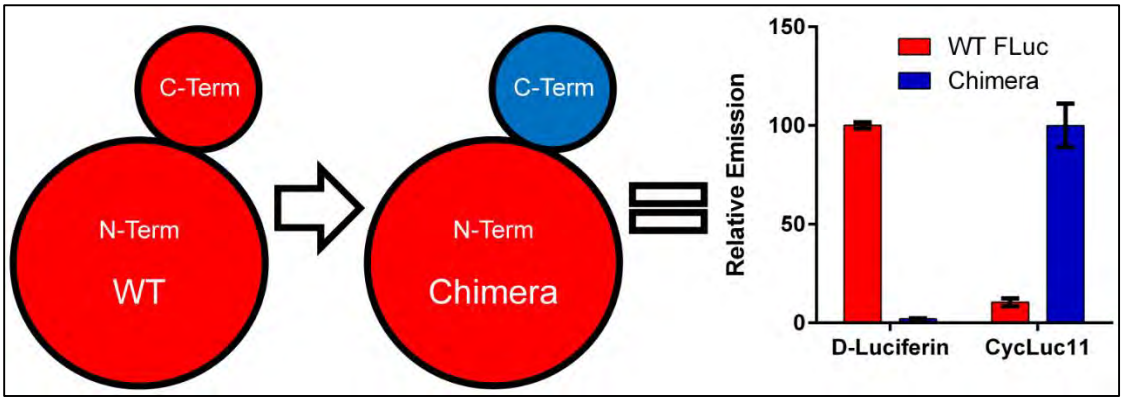

Summary

Firefly luciferase and its homologs, the long-chain fatty acyl-CoA synthetases (ACSLs), are each comprised of two domains: a substrate binding N-terminal domain and a catalytic C-terminal domain. Here we show that swapping the C-terminal domain of an ACSL onto the N-terminal domain of luciferase is tolerated and can confer selectivity toward synthetic luciferin substrates. Thus, the development of luciferase/ACSL chimeric enzymes represents an alternative strategy to modulate luciferase function and increase the utility of bioluminescence based imaging reagents.

Introduction

Firefly luciferase is the enzyme responsible for the brilliant light emitted by the firefly *Photinus pyralis*. Luciferase catalyzes a two-step reaction consisting of adenylation and oxidation of its native substrate D-luciferin (Fraga, 2008) (**Figure 5.1**). Luciferase is comprised of a large N-terminal domain (residues 1-436) and a small C-terminal domain (residues 440-550) joined by a short hinge region of ^{437}ArgLeuLys^{439} (Sundlov et al., 2012). D-Luciferin and ATP both bind in the N-terminal domain. However, the C-terminal domain contains two catalytic lysine residues (K443 and K529) responsible for facilitating the oxidation and adenylation of D-luciferin, respectively (**Figure 5.2**) (Branchini et al., 2005b; Sundlov et al., 2012). At rest, luciferase is in a conformation conducive to adenylation, with K529 positioned in the active site. After adenylation, the C-terminal domain undergoes a ~140° rotation to align K443 in the active site for subsequent oxidation (Sundlov et al., 2012).

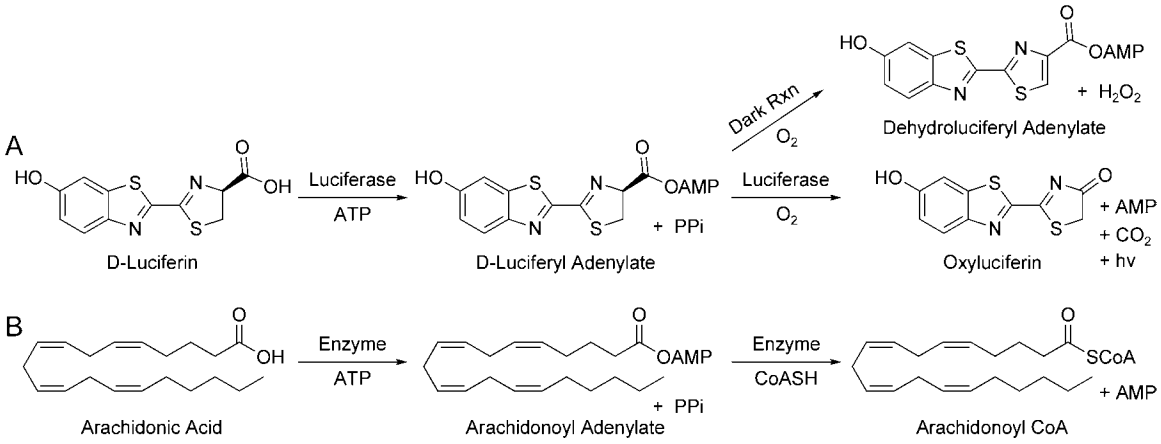

Figure 5.1. Parallels between luciferase and fatty acyl-CoA synthetase mechanisms. (A) Firefly luciferase catalyzes adenylation and subsequent oxidation of its native substrate, D-luciferin, to form an excited state oxyluciferin molecule that is responsible for light emission. Oxidation can also produce the off-pathway "dark product" dehydroluciferyl adenylate that does not emit light. (B) Long-chain fatty acyl-CoA synthetases catalyze adenylation and subsequent thioesterification of long-chain fatty acids, such as arachidonic acid, to form the fatty acyl-CoA product.

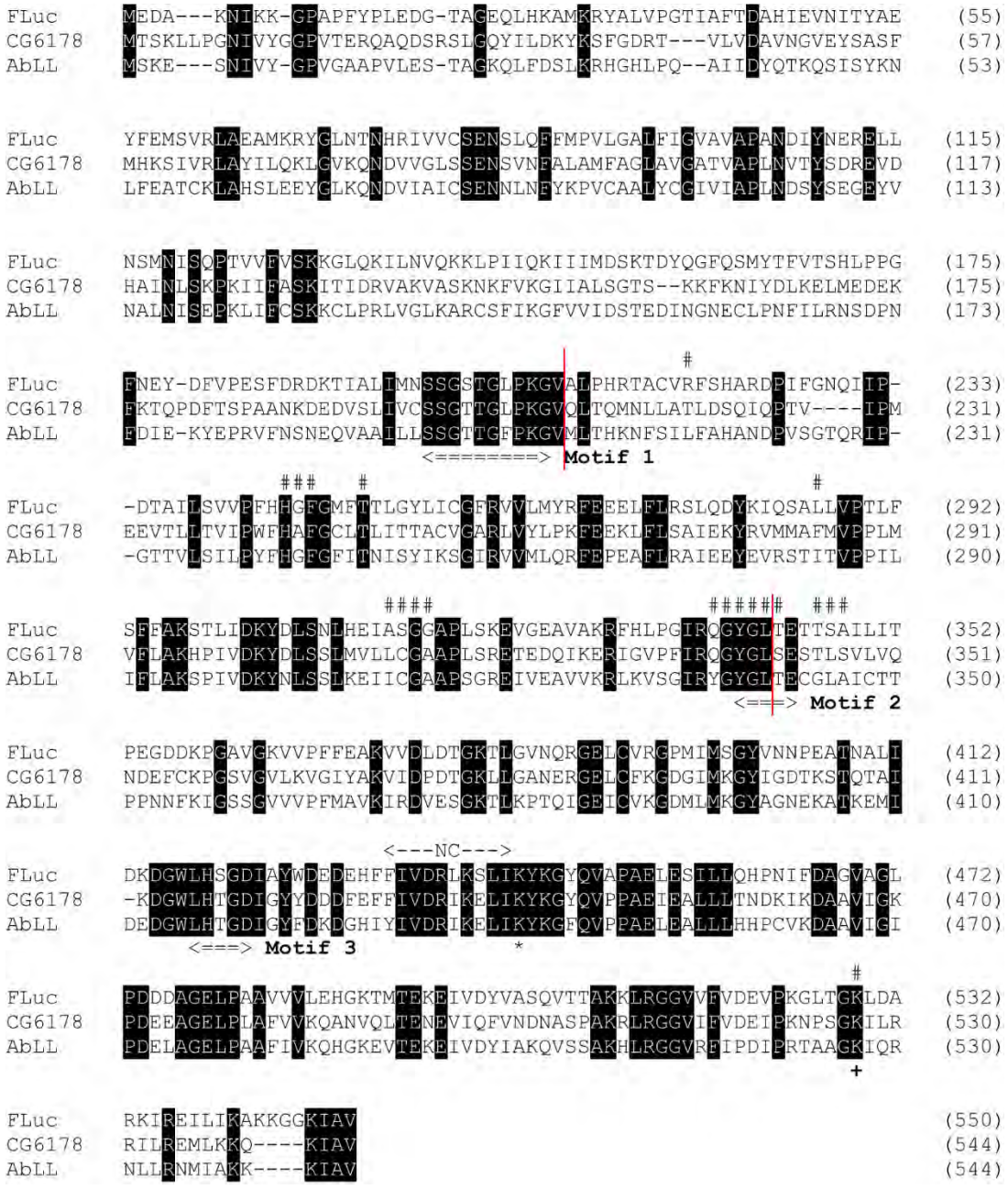

Figure 5.2. Amino acid alignment of firefly luciferase and two fatty acyl-CoA synthetases, CG6178 and AbLL. Primary sequences are displayed as a Clustal format alignment by Mafft (Katoh et al., 2002). Motifs 1-3 are conserved between members of the acyl-adenylate superfamily. Residues within 5 Å of the luciferin binding pocket are marked above with #. K443, marked below with *, is involved in oxidation or thioesterification of the substrate. K529, marked below with +, is involved in adenylation of the substrate. <---NC---> marks the interface between the N- and C-termini. Red bars mark the splice sites for the active site chimeras.

In addition to catalyzing light emission, luciferase has also been shown to act as a long-chain fatty acyl-CoA synthetase (ACSL) and catalyze the synthesis of fatty acyl-CoAs from free fatty acids (Oba et al., 2003) (**Figure 5.1**). Fatty acyl-CoA synthesis involves a two-step mechanism beginning with the adenylation of the fatty acid, followed by thioesterification to form the final acyl-CoA product. This second step is in contrast to the oxidation of D-luciferyl adenylate during light emission. Dedicated ACSLs share high homology to luciferase and are hypothesized to be luciferase's evolutionary predecessor (McElroy et al., 1967; Oba et al., 2006a; Viviani et al., 2013). Like luciferase, ACSLs are comprised of two domains: a large N-terminal and a small C-terminal domain (Gulick et al., 2003; Reger et al., 2008). Similarly, fatty acid and ATP binding occur in the N-terminal domain, while the C-terminal domain provides the two conserved lysine residues for adenylation, followed by thioesterification (**Figure 5.2**).

Our lab has developed a panel of synthetic luciferin analogs (Mofford et al., 2014b; Reddy et al., 2010) (**Figure 5.3**) and recently reported that the ACSL CG6178 from *Drosophila melanogaster* possesses latent luciferase activity when supplied with a suitable synthetic substrate (Mofford et al., 2014a). We have since identified a second ACSL, AbLL, from a non-luminous click beetle *Agrypnus binodulus* (Oba et al., 2008) that also possesses luciferase activity but with different substrate specificity than CG6178. Both of these ACSLs share high sequence identity to firefly luciferase (**Figure 5.2**), yet neither emit light upon treatment with D-luciferin (Mofford et al., 2014a; Oba et al., 2008).

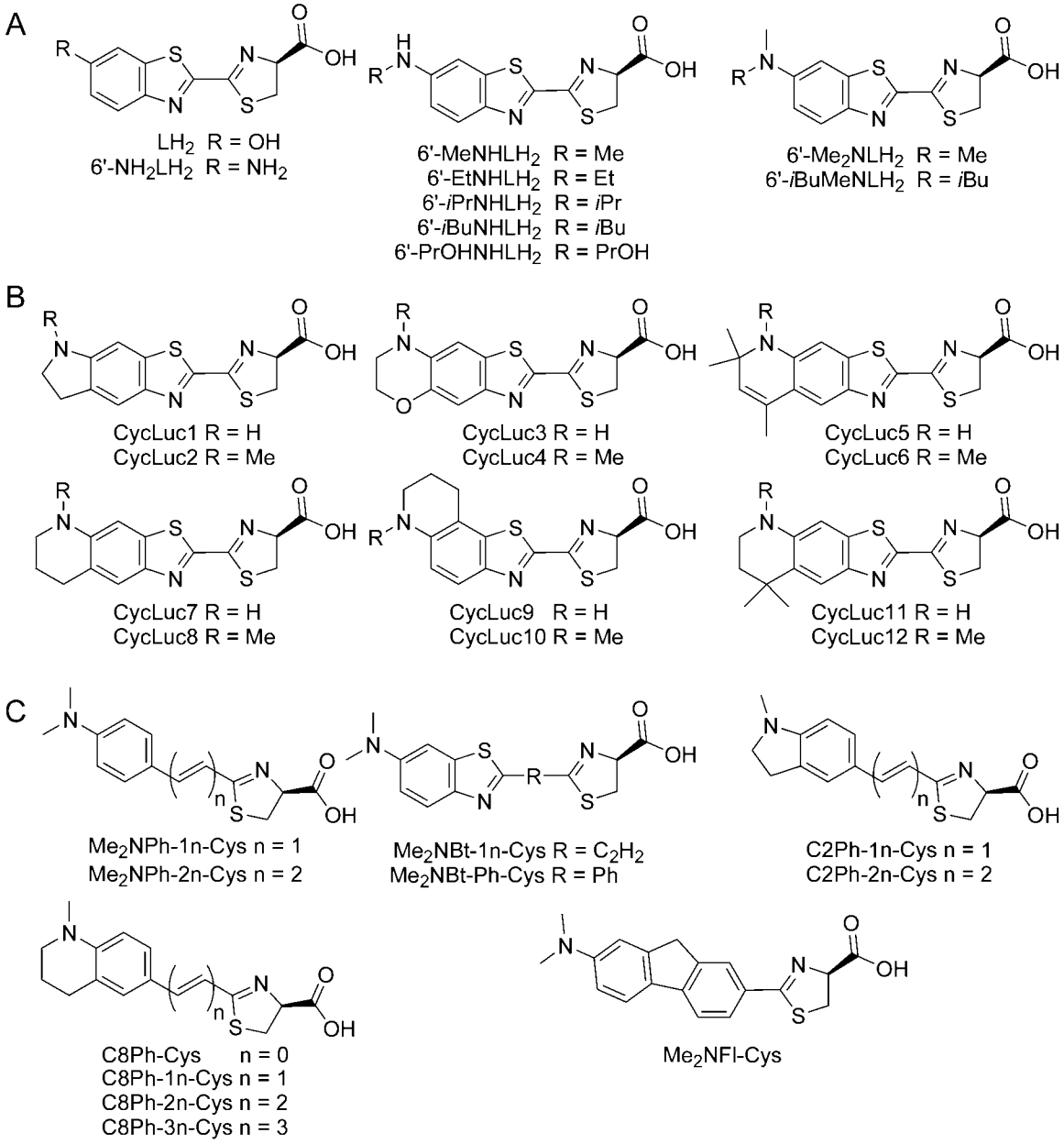

Figure 5.3. Chemical structures of all luciferin analogs. (A) Acyclic and (B) Cyclic luciferin analogs use the traditional benzothiazole-thiazoline core of D-luciferin with either acyclic or cyclic modifications at the 6' position respectively (Mofford et al., 2014b; Reddy et al., 2010). (C) “Non-traditional core” luciferin analogs use chromophores not limited to the benzothiazole-thiazoline core of D-luciferin. Me_2NPh-1n-Cys and Me_2NPh-2n-Cys were originally reported by Iwano et al. (Iwano et al., 2013).

While these findings show luciferase homologs possess latent luciferase activity, both CG6178 and AbLL lack the signal intensity needed for practical bioluminescent sensors. We therefore hypothesized that chimeric enzymes between luciferase and an ACSL would provide the substrate selectivity of the ACSL, but generate higher rates of light emission that are desirable for use as a reporter. Here we evaluate the bioluminescent activity and substrate selectivity of chimeric luciferase/ACSL enzymes.

Results

In order to generate a luciferase with improved selectivity, we first sought to create chimeras of luciferase and CG6178 that swap the residues predicted to line the luciferin binding pocket. We chose our initial splice sites at highly conserved areas in the primary sequence (**Figure 5.2 red bars**) based on the hypothesis that the secondary and tertiary enzyme folds would also be conserved in those areas and the chimeras would still fold correctly. Using Gibson Assembly (Gibson et al., 2009), we generated the FLuc/CG/FLuc chimera containing residues 1-208 of luciferase, 210-341 of CG6178 and 343-550 of luciferase. For comparison, we also made the reverse CG/FLuc/CG chimera. Unfortunately, our design hypothesis was incorrect and these enzymes were inactive as luciferases (**Figure 5.4**). Moreover, both were poorly expressed and impure, probably reflecting stability issues due to poor conservation of inter-domain contacts (**Figure 5.4**). Potentially, a better choice of splice sites and/or

compensatory mutation to conserve inter-domain contacts could allow for successful application of this strategy.

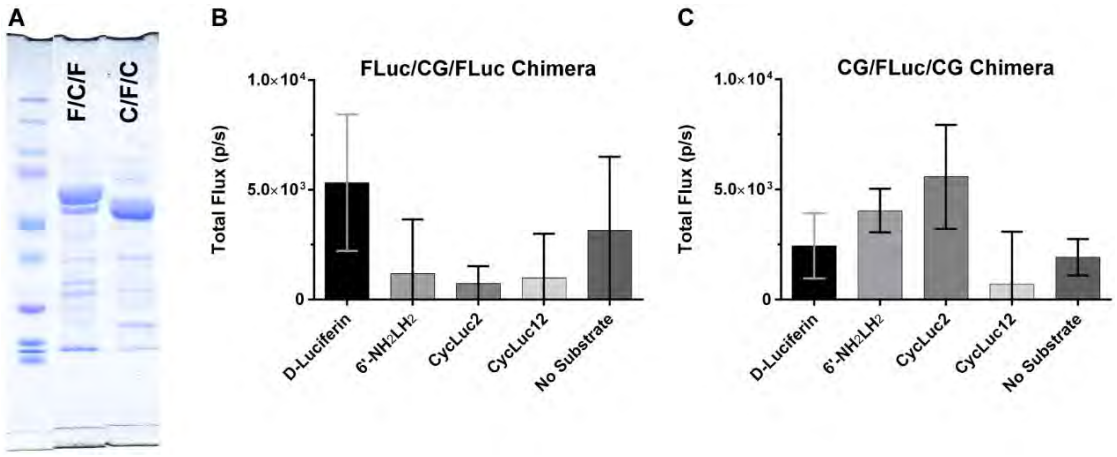

Figure 5.4. Luciferase/CG6178 active site chimeras are non-functional luciferases. (A) SDS-PAGE gel of FLuc/CG/FLuc and CG/FLuc/CG chimeras. (B) FLuc/CG/FLuc and (C) CG/FLuc/CG (20 nM final) treated with 250 μM of the indicated luciferin analog. The assay was performed in triplicate and is represented as the mean ± SEM.

Alternatively, instead of generating chimeras within the N-terminal domain of luciferase and disturbing any inter-domain contacts, we chose to exploit the two-domain architecture of these enzymes. Since the N-terminal and C-terminal domains are separate, they should be able to fold independently and result in a functional enzyme. By placing our splice site at the junction of the two domains (R437 luciferase numbering, **Figure 5.2**), we created the luciferase/CG6178 and luciferase/AbLL chimeras: FLuc/CG, FLuc/Ab, CG/FLuc, and Ab/FLuc. Gratifyingly, all four of these enzymes expressed cleanly and at normal yields (**Figure 5.5**).

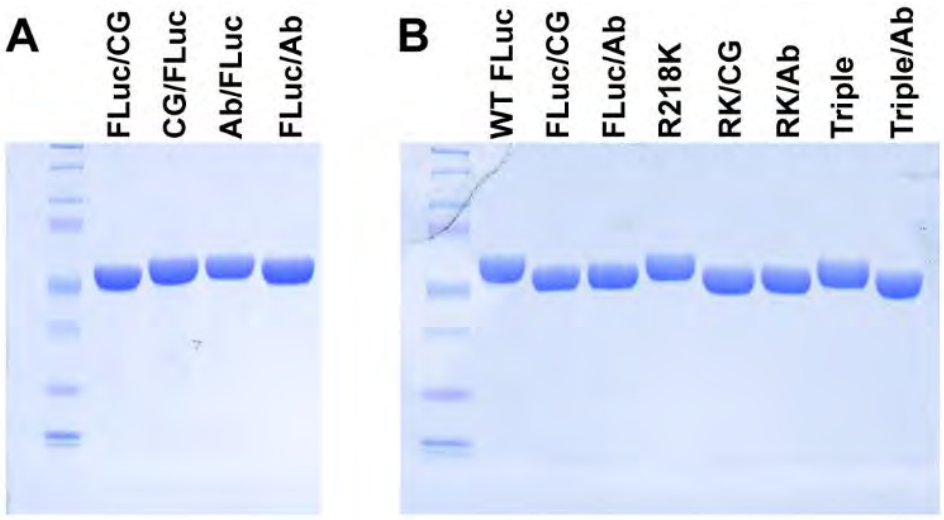

Figure 5.5. Luciferase/ACSL C-terminal chimeras are well expressed. (A) SDS-PAGE gel of luciferase/CG6178 and luciferase/AbLL C-terminal fusions. (B) SDS-PAGE gel of WT and mutant luciferase C-terminal fusions.

Although the CG/FLuc and Ab/FLuc C-terminal fusions did function as luciferases, they lowered the already weak light emitted from WT CG6178 and AbLL and were thus not investigated further (**Figure 5.6**). However, FLuc/CG and FLuc/Ab did retain high luciferase activity. As reported by Oba et al. (Oba et al., 2006b), we found that the FLuc/CG fusion is less active toward D-luciferin than WT luciferase (**Figure 5.7** and **Figure 5.8**). Nonetheless, the maximal sustained photon flux one minute after substrate introduction was equivalent or even exceeding WT with many of the synthetic luciferins, especially those that are not limited to the traditional benzothiazole-thiazoline core structure of D-luciferin (**Figure 5.7**, **Figure 5.8**, **Figure 5.9**, and **Figure 5.10**). Even more surprisingly, the C-terminal fusion with AbLL (FLuc/Ab) drastically lowered activity with D-luciferin but greatly improved maximum activity with several

synthetic luciferins (e.g., 6'-*i*BuMeNLH$_2$, CycLuc4, and CycLuc11) (**Figure 5.7**, **Figure 5.8**, **Figure 5.9**, and **Figure 5.10**). Many synthetic luciferins display high affinity for WT luciferase and the C-terminal fusions, and their corresponding oxyluciferin products become potent inhibitors of subsequent rounds of catalysis. Since these data are acquired one minute after introduction of substrate to enzyme, there is substantial product inhibition observed. Therefore, the measured photon flux does not always obey Michaelis-Menten kinetics (**Figure 5.8**, **Figure 5.9**, and **Figure 5.10**). Interestingly, the chimeras improve the photon flux from these substrates without sacrificing their high affinity. For example, CycLuc4 appears to have reached V_{max} at all concentrations tested, and with all three enzymes (**Figure 5.9**). However, FLuc/Ab displays increased photon flux relative to the other two. Other luciferase mutants we have observed typically increase the maximal rate of light emitted with a given substrate by lowering the affinity and reducing product inhibition (Harwood et al., 2011; Mofford et al., 2014b). This does not appear to be the case with the C-terminal fusions.

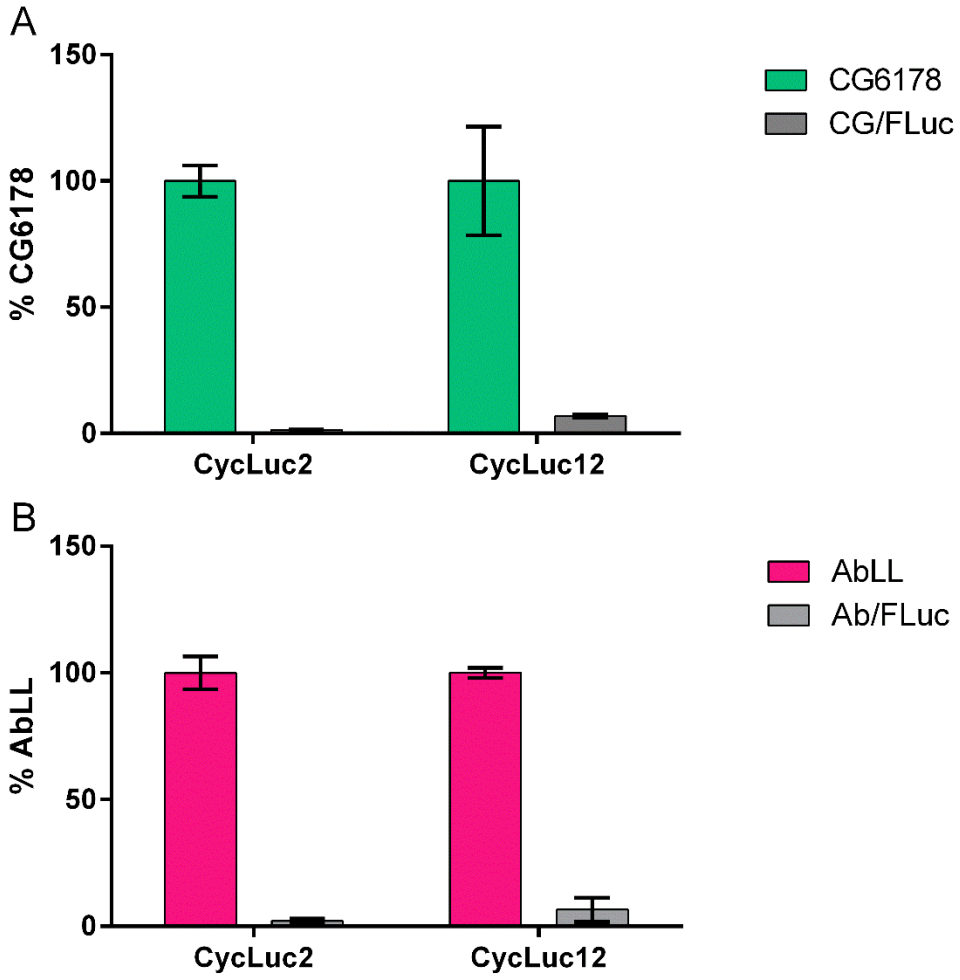

Figure 5.6. CG6178/Luciferase and AbLL/Luciferase C-Terminal Chimeras have lower photon flux compared to their WT counterparts. (A) WT CG6178 vs. CG6178/FLuc and (B) WT AbLL vs. AbLL/FLuc treated with 250 μM of the indicated luciferin analog. Data are normalized to the parent enzyme signal. The assay was performed in triplicate and is represented as the mean ± SEM.

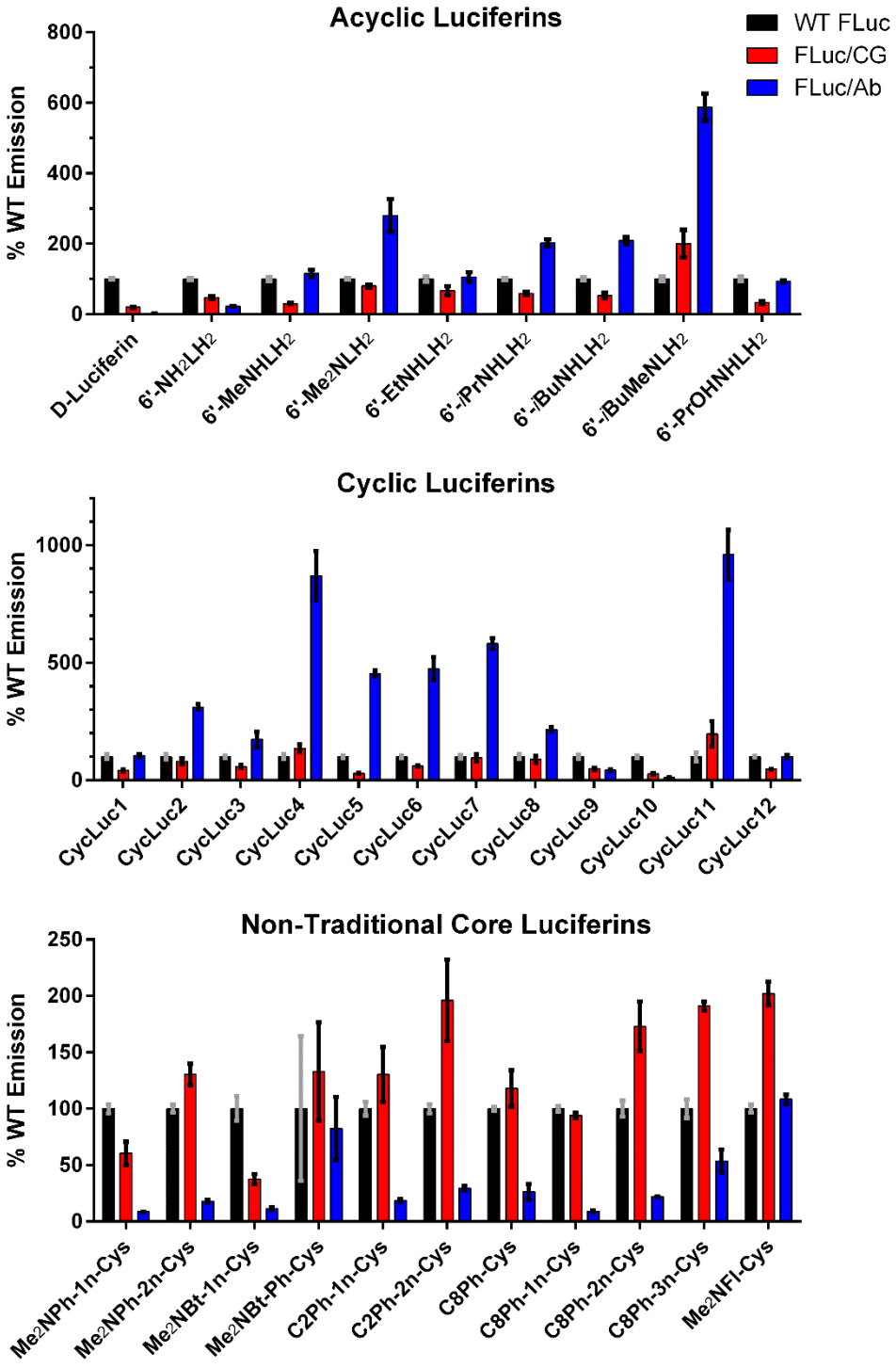

Figure 5.7. Normalized photon flux from WT luciferase and each WT chimera. Purified luciferase (10 nM) was treated with 250 μM of the indicated luciferin analog. Data are normalized to the signal from WT luciferase. The assay was performed in triplicate and is represented as the mean ± SEM.

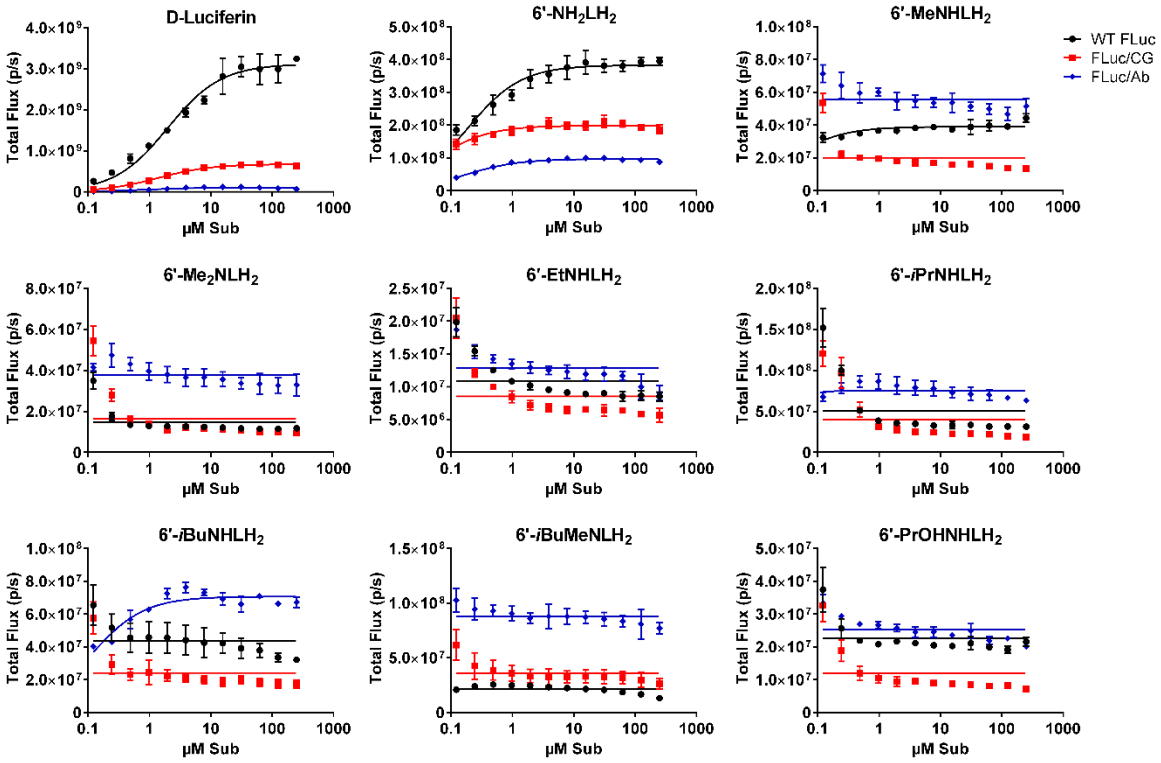

Figure 5.8. Dose-response curves of WT luciferase and WT chimeras with acyclic luciferins. Purified luciferase (10 nM) was treated with 0.122 to 250 μM of the indicated luciferin analog. The assay was performed in triplicate and is represented as the mean ± SEM. Data were fit to the Michaelis-Menten equation by nonlinear regression, though many high affinity substrates do not fit this analysis well.

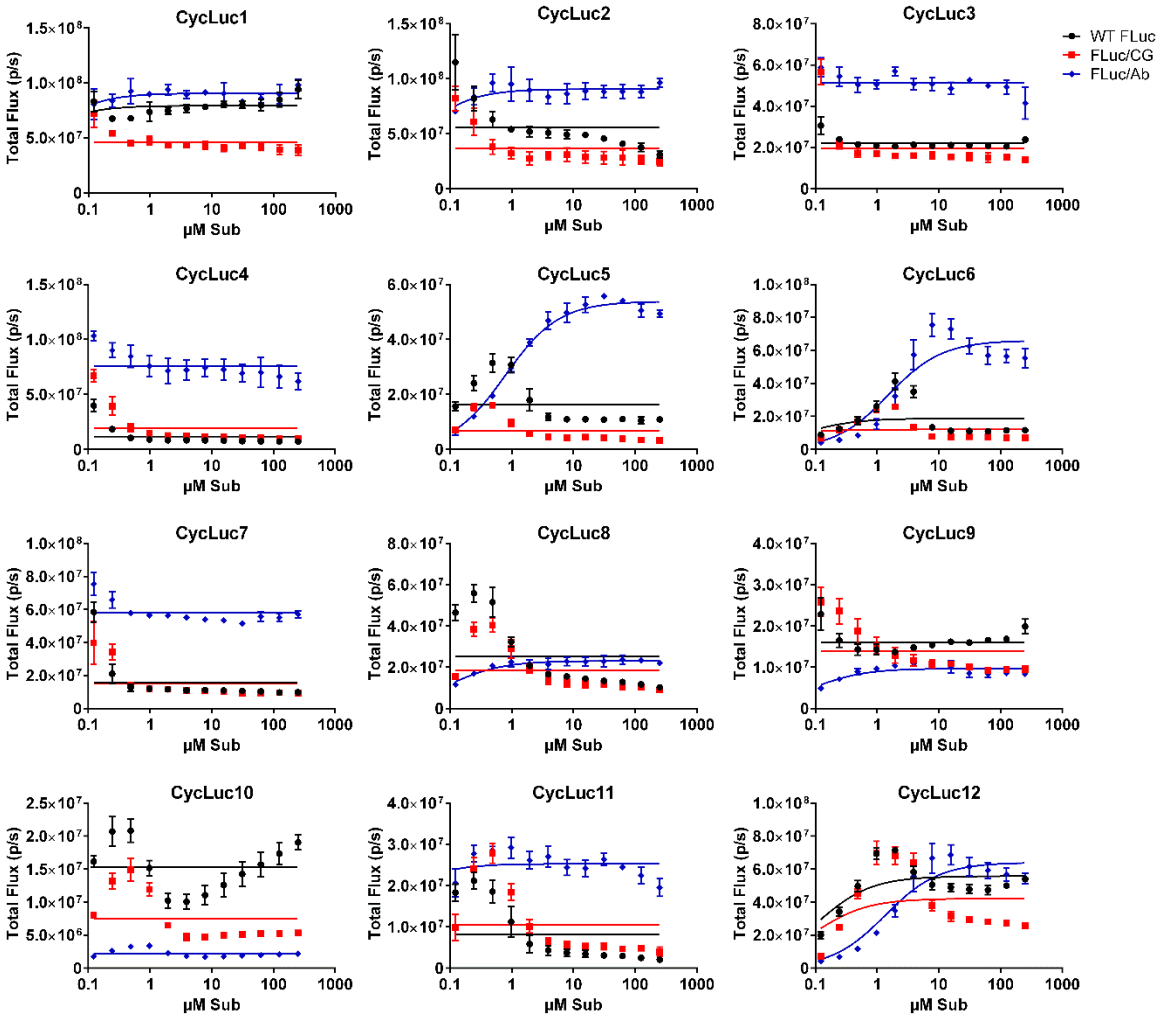

Figure 5.9. Dose-response curves of WT luciferase and WT chimeras with cyclic luciferins. Purified luciferase (10 nM) was treated with 0.122 to 250 μM of the indicated luciferin analog. The assay was performed in triplicate and is represented as the mean ± SEM. Data were fit to the Michaelis-Menten equation by nonlinear regression, though many high affinity substrates do not fit this analysis well.

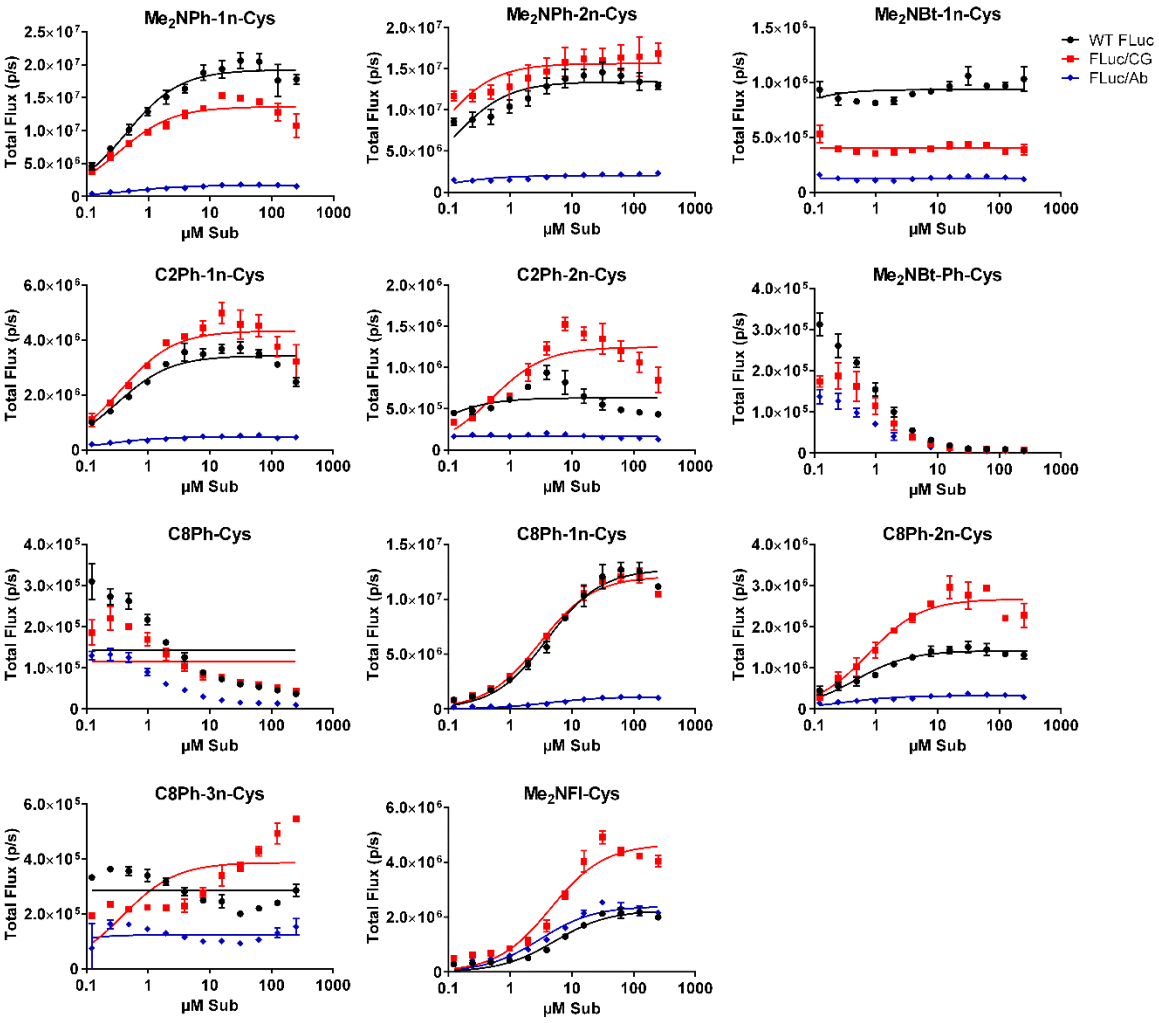

Figure 5.10. Dose-response curves of WT luciferase and WT chimeras with non-traditional core luciferins. Purified luciferase (10 nM) was treated with 0.122 to 250 μM of the indicated luciferin analog. The assay was performed in triplicate and is represented as the mean ± SEM. Data were fit to the Michaelis-Menten equation by nonlinear regression, though many high affinity substrates do not fit this analysis well.

Following our success with the WT luciferase fusions, we generated C-terminal fusions with the N-terminal domains of the luciferase mutants R218K and R218K+L286M+S347A (RK/CG, RK/Ab, and Triple/Ab). Both of these mutant luciferases have been shown to increase the maximal rate of photon flux for many high-affinity synthetic substrates, albeit with a decreased substrate affinity compared to WT (Mofford et al., 2014b). Moreover, both mutant luciferases can achieve a higher maximal photon flux with synthetic luciferins than either WT luciferase or the ACSL C-terminal fusions described above (Mofford et al., 2014b), making their respective chimeras interesting targets for synergistic improvement.

For the most part, the beneficial effect of C-terminal fusions did not readily translate to the mutant luciferases. The R218K fusions did show improved light emission with a small subset of the synthetic substrates. For example, RK/Ab showed improved flux with 6'-*i*BuMeNLH$_2$ and CycLuc11 (**Figure 5.11**). However, this did not extend to the other substrates, nor was the effect as substantial as that observed with the FLuc/Ab fusion. The RK/CG fusion was able to improve flux from the “non-traditional core” luciferins, but was markedly worse than R218K with almost all of the traditional core substrates. The triple mutant-AbLL fusion (Triple/Ab) was worse with every substrate compared to the parent luciferase (**Figure 5.12**). The triple mutant-CG6178 fusion was not evaluated.

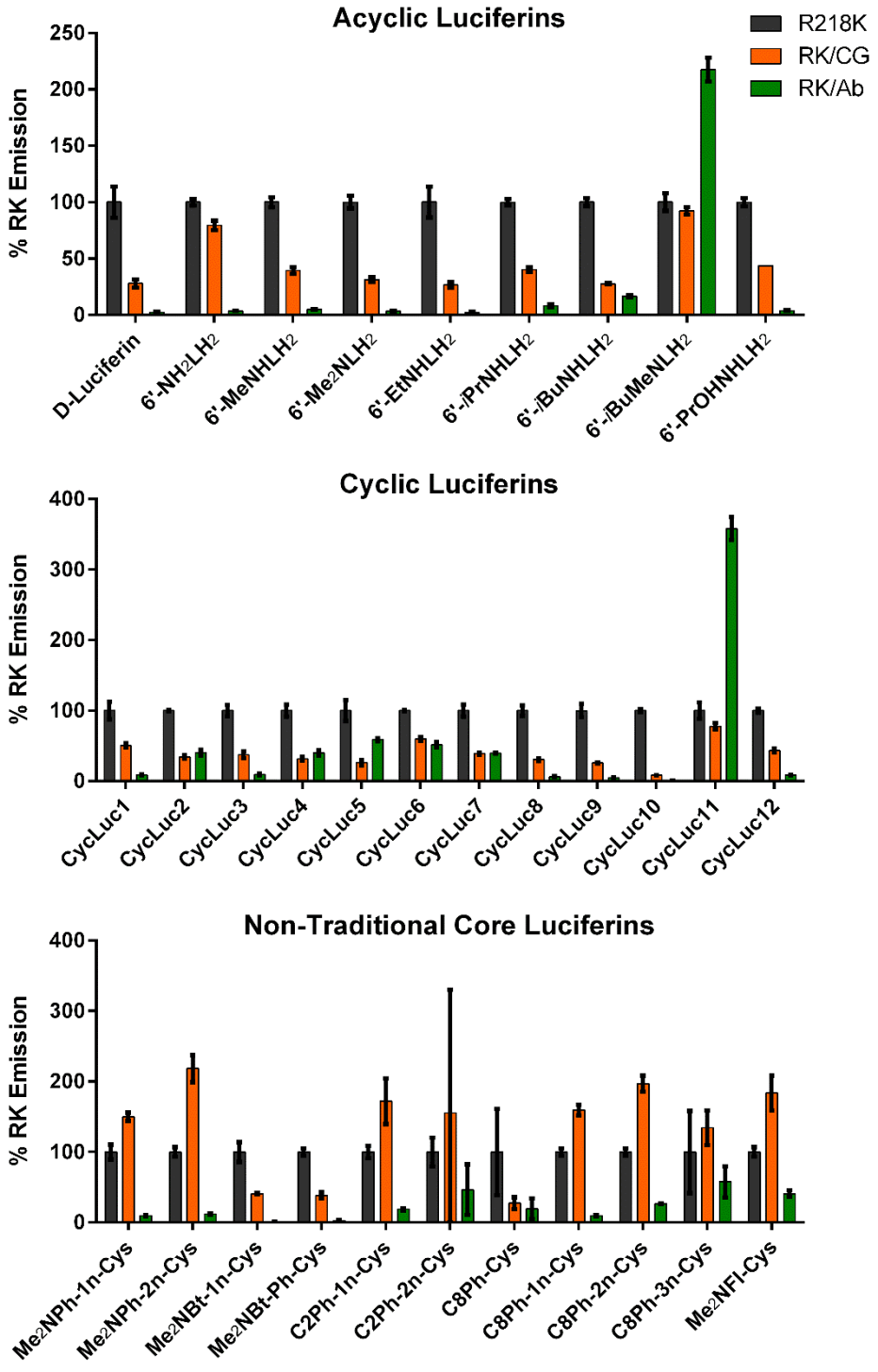

Figure 5.11. Normalized photon flux from R218K luciferase and each R218K chimera. Purified luciferase (10 nM) was treated with 250 μM of the indicated luciferin analog. Data are normalized to the signal from WT luciferase. The assay was performed in triplicate and is represented as the mean ± SEM.

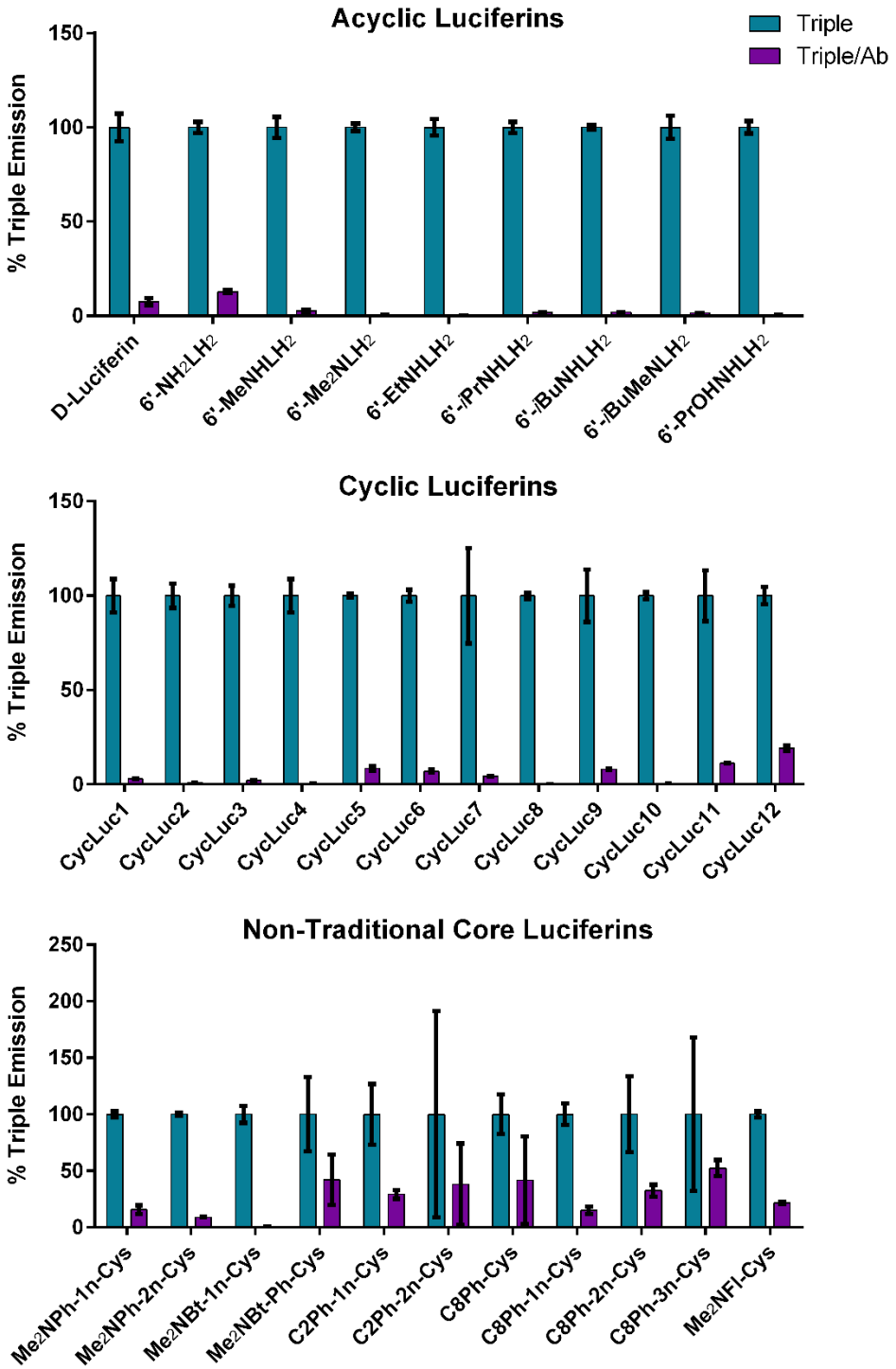

Figure 5.12. Normalized photon flux from R218K+L286M+S347A luciferase and each triple mutant chimera. Purified luciferase (10 nM) was treated with 250 μM of the indicated luciferin analog. Data are normalized to the signal from WT luciferase. The assay was performed in triplicate and is represented as the mean ± SEM.

To better determine the reason for the change in light emission with the chimeras, we measured the burst kinetics of each enzyme/substrate pair. Upon rapid injection of enzyme to substrate, luciferase displays an almost immediate burst of light during a “burst phase” (Fraga, 2008), followed by a decrease in total flux to a lower level during the subsequent “glow phase”. The decrease is caused by slow dissociation of either the oxyluciferin and AMP light-emitting products, or the “dark” dehydroluciferyl adenylate side-product (**Figure 5.1**). This product inhibition limits the subsequent rounds of catalysis. The burst phase peak at saturating substrate concentration represents the maximal rate of light emission that the luciferase can achieve (Branchini et al., 2014). Therefore, we can use each burst profile to compare the relative maximal rates and levels of product inhibition between the parent luciferase and each chimera.

The FLuc/CG fusion results in little change in the peak emission rate during the burst phase compared to WT luciferase (**Figure 5.13**, **Figure 5.14**, and **Figure 5.15**). However, several traditional core substrates show increased product inhibition resulting in a lower level of sustained light emission during the glow phase (e.g. 6'-NH_2LH_2, 6'-$MeNHLH_2$, CycLuc2, and CycLuc10). Conversely, many of the “non-traditional core” substrates actually displayed less product inhibition, resulting in improved flux during the glow phase (e.g. Me_2NPh-2n-Cys and C2Ph-1n-Cys).

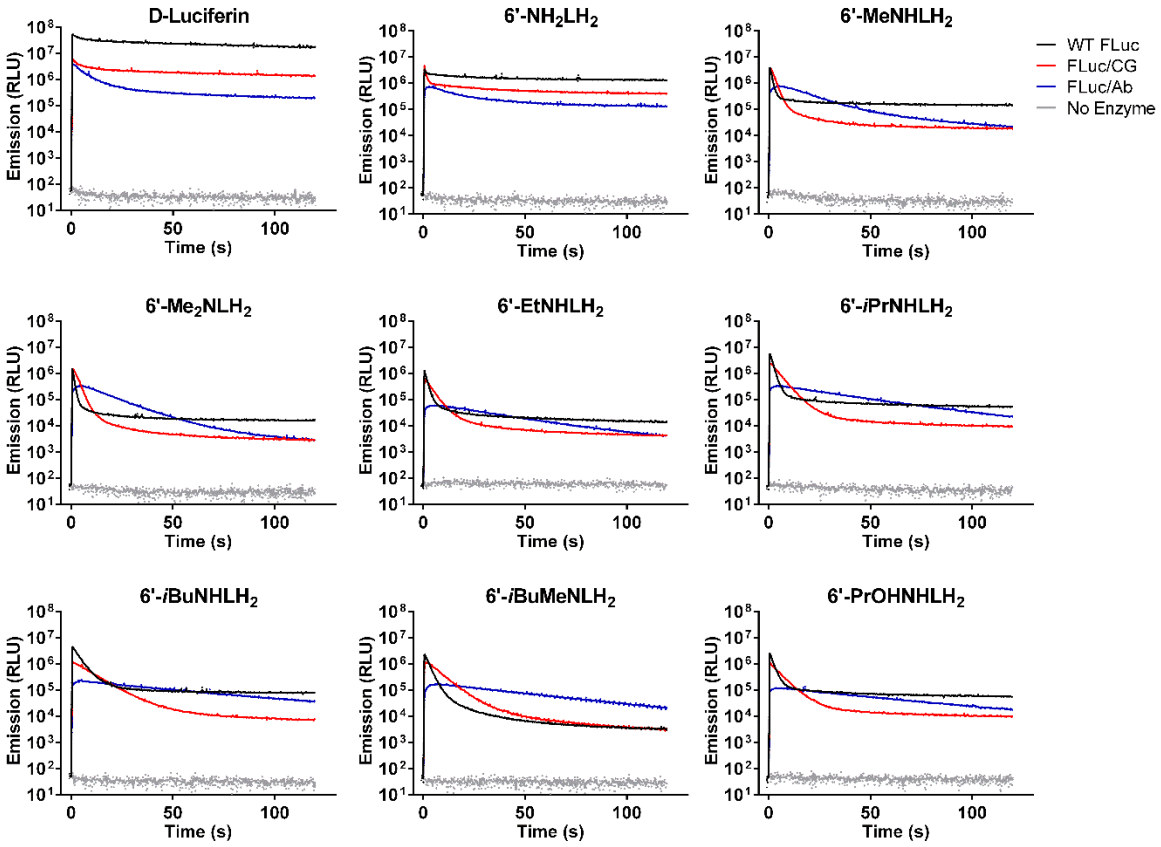

Figure 5.13. Burst kinetics profiles of WT luciferase and WT chimeras with acyclic luciferins. Purified luciferase (100 nM final) was rapidly injected into the indicated luciferin analog (250 μM final). Light emission was recorded every 0.5 s for 1 s pre-injection and 120 s post-injection. The assay was performed in triplicate and is represented as the mean ± SEM.

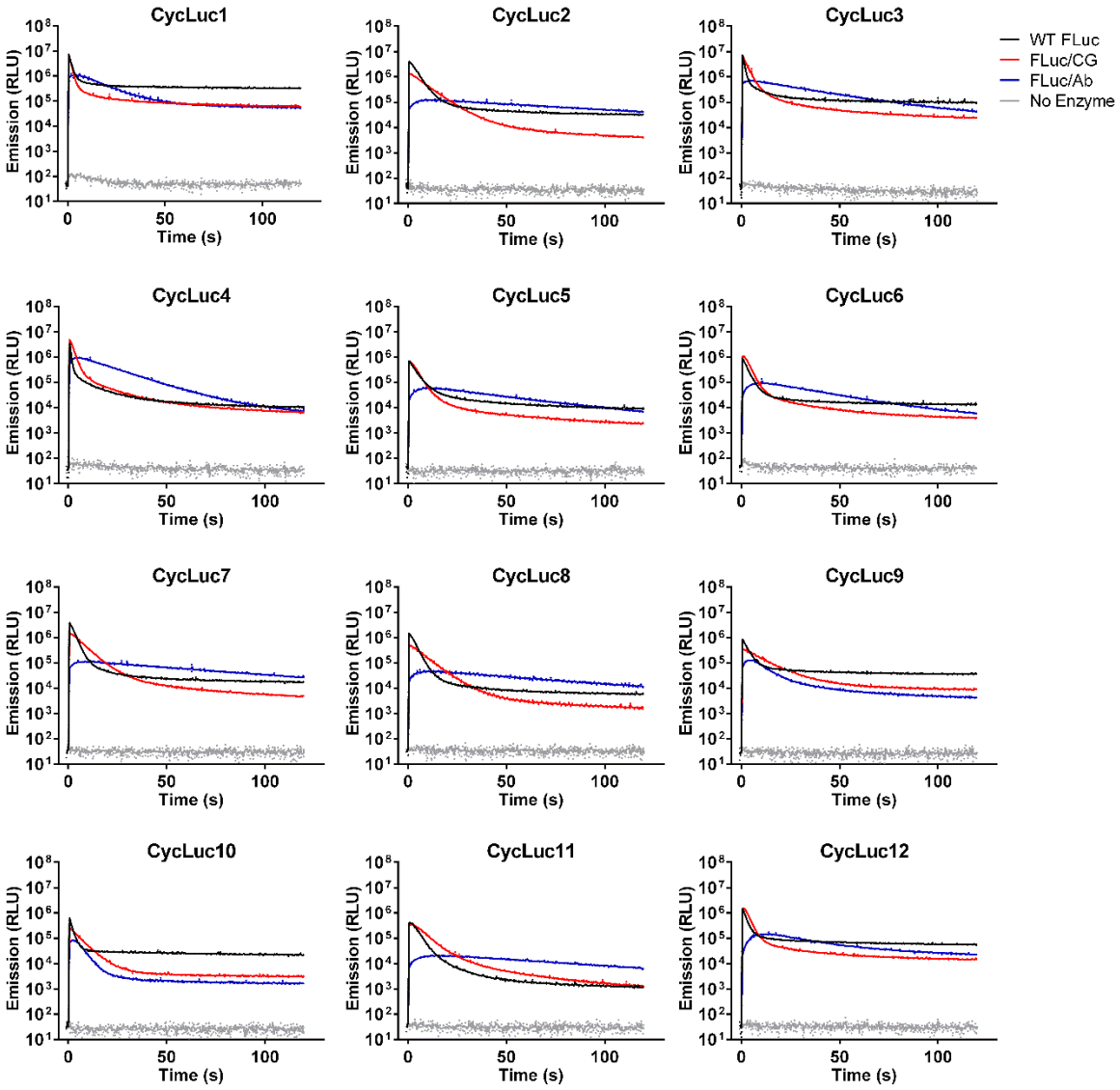

Figure 5.14. Burst kinetics profiles of WT luciferase and WT chimeras with cyclic luciferins. Purified luciferase (100 nM final) was rapidly injected into the indicated luciferin analog (250 μM final). Light emission was recorded every 0.5 s for 1 s pre-injection and 120 s post-injection. The assay was performed in triplicate and is represented as the mean ± SEM.

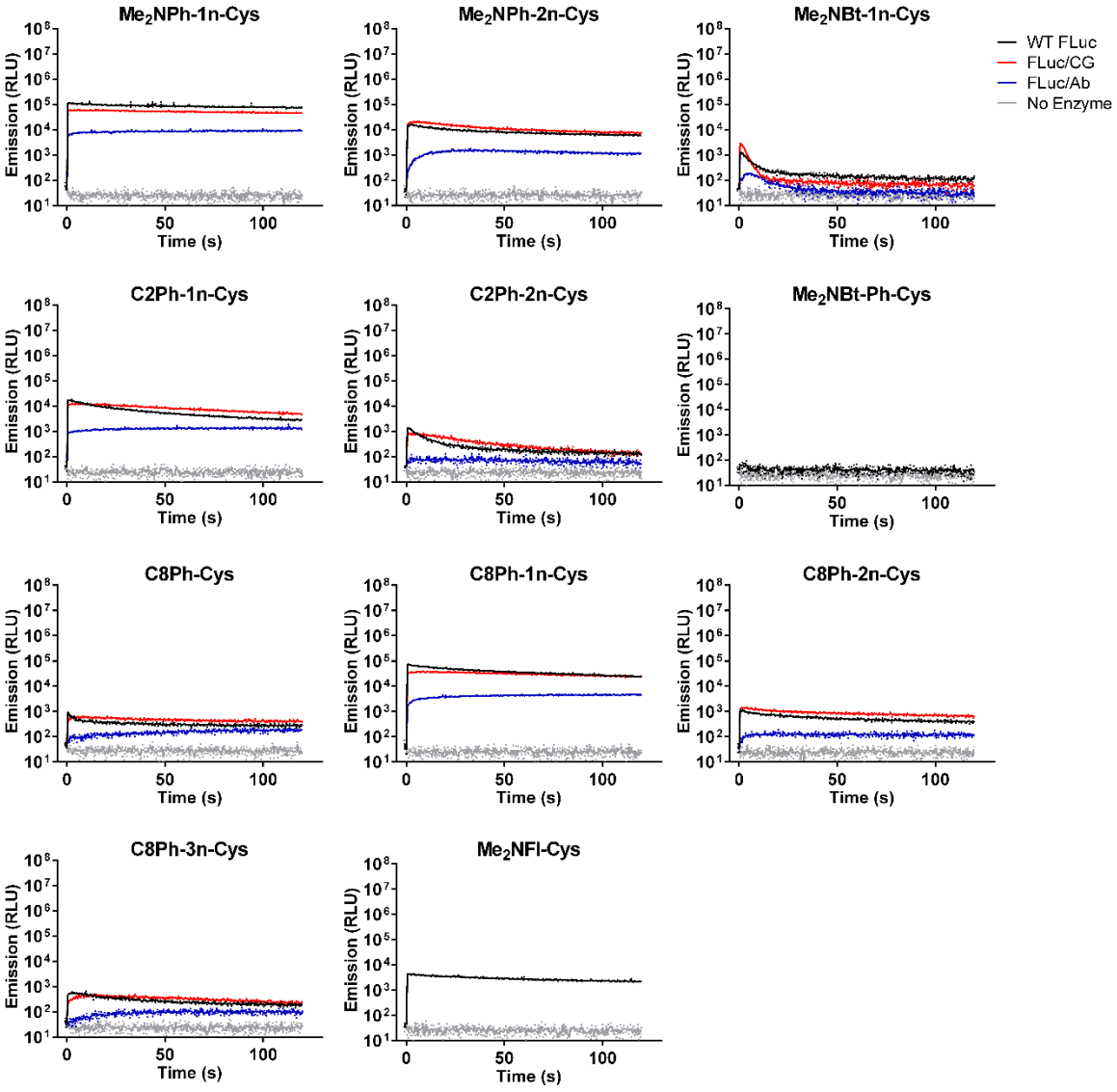

Figure 5.15. Burst kinetics profiles of WT luciferase and WT chimeras with non-traditional core luciferins. Purified luciferase (100 nM final) was rapidly injected into the indicated luciferin analog (250 μM final). Light emission was recorded every 0.5 s for 1 s pre-injection and 120 s post-injection. The assay was performed in triplicate and is represented as the mean ± SEM.

Like FLuc/CG, the RK/CG chimera produced similar peak burst rates relative to the parent R218K luciferase, but also displays increased product inhibition (**Figure 5.16**). This translates to almost all of the traditional core luciferins producing weaker total flux with the chimera than with R218K. However, as with FLuc/CG, product inhibition with RK/CG is lessened with the “non-traditional core” luciferins, resulting in an increase in sustained light output during the glow phase (e.g. Me_2NPh-2n-Cys).

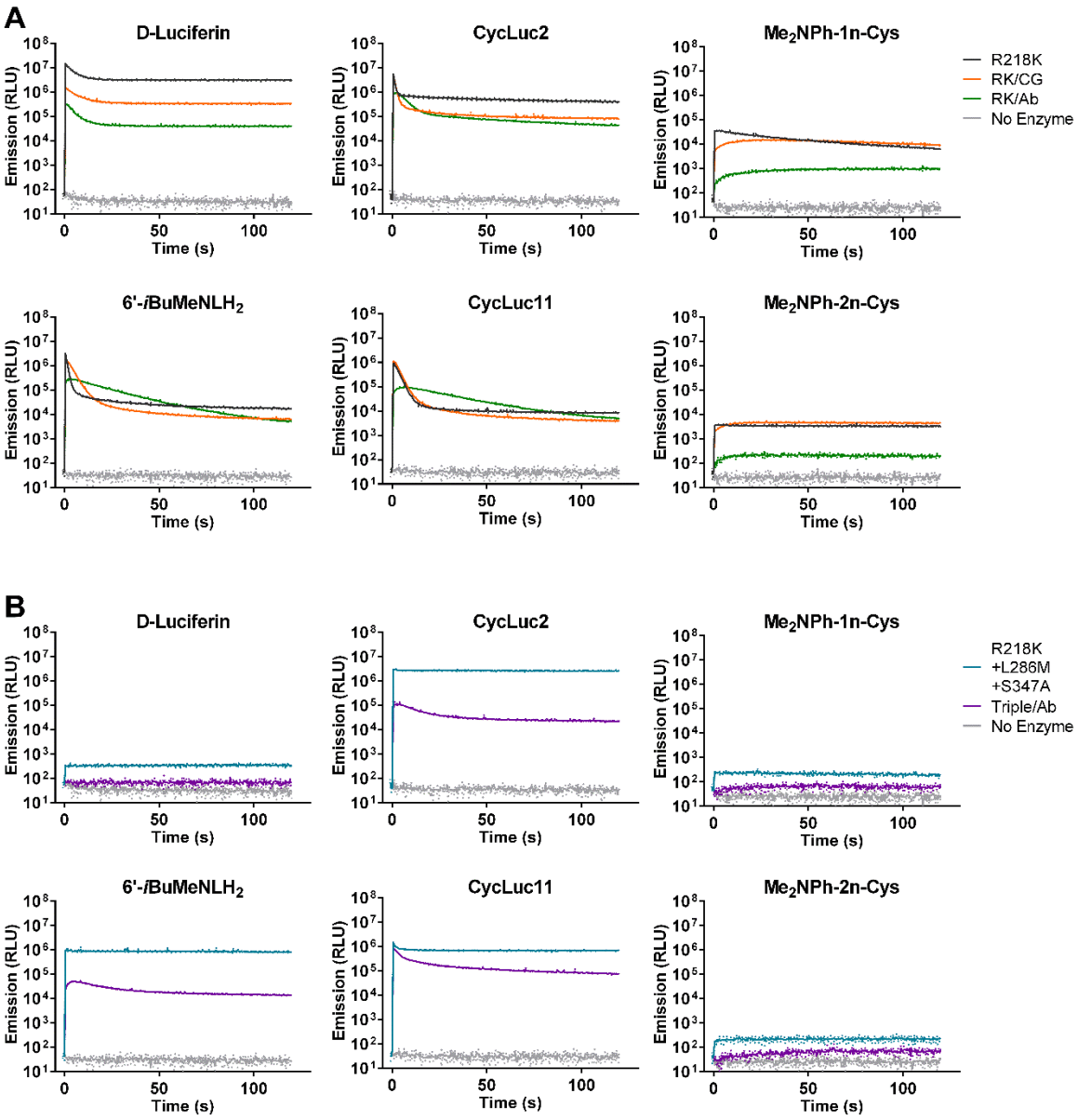

Figure 5.16. Burst kinetics profiles of R218K and triple mutant luciferases and their chimeras with select luciferins. Purified R218K luciferase or chimera (A) or R218K+L286M+S347A luciferase or chimera (B) [100 nM final] was rapidly injected into the indicated luciferin analog (250 μM final). Light emission was recorded every 0.5 s for 1 s pre-injection and 120 s post-injection. The assay was performed in triplicate and is represented as the mean ± SEM.

In contrast to the CG6178 fusions, all three AbLL chimeras displayed a drastic reduction in the peak rate of light emission. Interestingly, FLuc/Ab follows the decreased burst with almost no product inhibition, resulting in an increase in sustained light emitted during the glow phase, especially with 6'-*i*BuMeNLH$_2$, CycLuc4, and CycLuc11 (**Figure 5.13**, **Figure 5.14**, and **Figure 5.15**). On the other hand, RK/Ab and Triple/Ab both follow the decrease in the peak burst rate with equivalent or even increased product inhibition compared to their respective parent luciferases. Thus, RK/Ab produces weaker sustained light emission with all substrates except 6'-*i*BuMeNLH$_2$ and CycLuc11 and Triple/Ab emits weaker sustained light emission with all substrates. (**Figure 5.16**).

Discussion

The C-terminal domain of firefly luciferase provides two catalytic residues into the active site: lysine 529 is essential for AMP-ester formation, and after domain rotation, lysine 443 plays a critical role in the subsequent thioesterification or oxidation. Replacement of the C-terminal domain of firefly luciferase with that of CG6178 or AbLL is well tolerated. Despite the lack of direct interaction between the C-terminal domain and the substrate bound to the N-terminal domain, we find that C-terminal domain swapping can have profound effects on substrate utilization. These results complement Branchini et al.'s recent finding that a C-terminal chimera of two luciferases can improve the overall activity of firefly luciferase toward D-luciferin (Branchini et al., 2014).

The observed differences to light emission by the chimeras may reflect changes in any or all of the key phases of catalysis. First, subtle differences in the alignment of the two lysines with respect to the luciferin substrate at either or both catalytic steps can manifest as changes in the rate of adenylation and/or oxidation. Next, the ability of the chimeric enzymes to undergo the necessary conformational change between the catalytic steps or the ability of the oxyluciferin, AMP, or dehydroluciferyl adenylate products to dissociate can impact the overall rate of light emission. Finally, changes to the quantum yield, the ability of the luciferin to access an excited-state oxyluciferin, or the ratio of oxyluciferin to dehydroluciferyl adenylate could be responsible for changes in the amount of light observed.

The FLuc/CG and RK/CG chimeras generally result in comparable peak emission rate during the burst phase of catalysis compared to WT and R218K luciferases respectively. This suggests that the orientation of the two lysines is well conserved, the first conformational change of the C-terminal domain is unaffected, and the quantum yield is maintained. The variation in light emitted appears to be caused by an increase in product inhibition. A minor allosteric contact of the new domain could disrupt the second conformational change back to the adenylation state, causing the products to bind more tightly and stay bound longer than in the parent luciferases. Alternatively, a small increase in the formation of dehydroluciferyl adenylate could cause increased product inhibition. The dehydroluciferyl adenylate of D-luciferin is a more potent inhibitor of

luciferase (K_i = 3.8 ± 0.7 nM) than its oxyluciferin (K_i = 0.50 ± 0.03 μM) (Ribeiro and Esteves da Silva, 2008), a feature that most likely translates to each synthetic luciferin. Therefore a small increase in dehydroluciferyl adenylate that does not significantly impact the burst height may still accumulate over time to lower the observed level of light during the glow phase. Interestingly, the domain swap has the opposite effect on the "non-traditional core" luciferins than on the traditional substrates. The extended conjugation in these substrates may push the more bulky aromatic rings away from their normal contacts and shift their binding orientations, removing the potential for increased product affinity. The alternative core structures may also favor a reduction in dehydroluciferyl adenylate formation. Thus, the potentially subtle differences the luciferin orientation within the binding pocket can have a profound effect on the total light observed.

Conversely, all three AbLL fusions result in a dramatic decrease in the peak emission rate during the burst phase compared to their respective parent luciferases. The FLuc/Ab chimera displays little to no product inhibition, resulting in significantly increased total flux during the glow phase with several luciferin analogs (e.g., 6'-*i*BuMeNLH_2, CycLuc4, CycLuc11). However, the burst height is so reduced with the "non-traditional core" luciferins that all of these substrates produce a lower level of light during the glow phase. Both the RK/Ab and Triple/Ab chimeras retain equal or even increased product inhibition compared to their respective parent luciferases, resulting in an even lower level of sustained

light during the glow phase. The RK/Ab fusion produced lower sustained light from all substrates except 6'-*i*BuMeNLH$_2$ and CycLuc11, while the Triple/Ab fusion produced lower sustained light from all substrates. Thus, swapping the C-terminus combined with the changes brought on by these mutations are neither additive nor synergistic.

The decrease in burst intensity from the AbLL fusions is indicative of a decrease in the overall catalytic rate of the enzymes. The effects of FLuc/Ab and RK/Ab are not as consistent between substrates as those of FLuc/CG and RK/CG, suggesting that the orientation of one or both lysines within the active site has been affected. The varying luciferin structures likely result in alterations to their respective orientations in the binding pocket and some are more apt to tolerate the new positions of these lysines than others. Also, the rate of each conformational change between the two domains after each catalytic step may have been impacted/slowed down. A slower first conformational change would result in a slower substrate oxidation rate, and may translate to a slower reversion back to the resting state, thus lowering the overall rate of catalysis and decreasing product inhibition by providing the products more time to dissociate. Alternatively, the quantum yield and/or ability of the luciferin to access the excited state may be affected.

It should be possible to determine which of these parameters have impacted the photon flux from the AbLL fusions. First, using pre-adenylated luciferin, we can evaluate whether the lower burst rate is due to one or both of

the catalytic steps. For example, if the decreased burst is due to a slower adenylation rate, using pre-adenylated luciferin will compensate and the chimera should burst like WT. If the decrease is due to a slower oxidation rate, then using pre-adenylated luciferin will result in no change to the burst profile. If the decreased burst is due to a defect in both catalytic steps, using pre-adenylated luciferin will result in a partial increase in the burst rate. Second, we can determine the relative quantum yields of the light emitting reaction for each enzyme/substrate pair using the method described by Branchini et al (Branchini et al., 2014). Finally, we can directly measure the ratio of the oxyluciferin and dehydroluciferyl adenylate products by HPLC. By running all of these experiments, we can narrow down the causes of the changes in light emission by the chimera. However, at this time, we have not investigated the effects of pre-adenylated luciferin or relative quantum yield using the chimeric luciferases.

Conclusion

Here we demonstrate that C-terminal fusions between firefly luciferase and ACSLs are well tolerated and result in functional luciferases. Remarkably, despite the lack of direct interactions between the substrates and the C-terminal domain, these chimeras improve photon flux with multiple synthetic luciferins and increase substrate specificity compared to WT luciferase. While both ACSLs (CG6178 and AbLL) used here possess latent luciferase activity, the substrate specificity engendered by their respective C-terminal domains in the chimeras

differs from that of the full ACSL. Neither of the WT luciferase fusions result in as dramatic of an effect as the active site mutations R218K or R218K+L286M+S347A. However, the chimeras do not lower the affinity of the substrates as severely as these mutants do. Thus, C-terminal fusions between luciferase and ACSLs represent an alternative strategy to direct mutation that can modulate luciferase function and develop new and improved bioluminescent reporters.

Materials and Methods

Collaborators

Gadarla Randheer Reddy of the Miller Lab:

Synthesis of all benzothiazole core synthetic luciferins

Kiran Reddy of the Miller Lab:

Synthesis of all “non-traditional core” synthetic luciferins

General

Chemicals were purchased from Aldrich, Matrix Scientific, Oakwood, or TCI. D-luciferin was obtained from Anaspec and 6'-NH_2LH_2 was obtained from Marker Gene Technologies Inc. CycLuc1, CycLuc2, 6'-$MeNHLH_2$, and 6'-Me_2NLH_2 were synthesized as previously described (Reddy et al., 2010). CycLuc3-12 were synthesized as previously described (Mofford et al., 2014b).

Other acyclic luciferins and “non-traditional core” luciferins were prepared within the Miller lab. Data were plotted with GraphPad Prism 6.0.

Plasmid constructs

The DNA sequences for long-chain fatty acyl-CoA synthetases CG6178 (**Figure 5.17**) and AbLL (**Figure 5.18**) were codon optimized for mammalian expression, synthesized by GenScript, and cloned into the BamHI–NotI sites of pGEX6P-1. WT luc2 luciferase (**Figure 5.19**) and codon optimized R218K and triple mutant R218K/L286M/S347A were used as previously described (Mofford et al., 2014b). Plasmid constructs containing the chimeric enzymes were generated using Gibson Assembly (NEB). Fragments of each cDNA corresponding to the desired region of each enzyme were PCR amplified and purified via agarose gel purification. PCR primers were designed to give overlapping ends of complementary DNA with the adjacent fragment of DNA for that chimera, per Gibson Assembly instructions (**Figure 5.20**). Each DNA fragment and pGEX6P-1 plasmid digested with BamHI and NotI were incubated with Gibson Assembly master mix per the manufacturer’s instructions to generate the final combined constructs (**Figure 5.21** and **Figure 5.22**).

Codon Optimized CG6178

Primary Amino Acid Sequence:

MTSKLLPGNIVYGGPVTERQAQDSRSLGQYILDKYKSFGDRTVLVDAVNG
VEYSASFMHKSIVRLAYILQKLGVKQNDVVGLSSENSVNFALAMFAGLAV
GATVAPLNVTYSDREVDHAINLSKPKIIFASKITIDRVAKVASKNKFVKG
IIALSGTSKKFKNIYDLKELMEDEKFKTQPDFTSPAANKDEDVSLIVCSS
GTTGLPKGVQLTQMNLLATLDSQIQPTVIPMEEVTLLTVIPWFHAFGCLT
LITTACVGARLVYLPKFEEKLFLSAIEKYRVMMAFMVPPLMVFLAKHPIV
DKYDLSSLMVLLCGAAPLSRETEDQIKERIGVPFIRQGYGLSESTLSVLV
QNDEFCKPGSVGVLKVGIYAKVIDPDTGKLLGANERGELCFKGDGIMKGY
IGDTKSTQTAIKDGWLHTGDIGYYDDDFEFFIVDRIKELIKYKGYQVPPA
EIEALLLTNDKIKDAAVIGKPDEEAGELPLAFVVKQANVQLTENEVIQFV
NDNASPAKRLRGGVIFVDEIPKNPSGKILRRILREMLKKQKIAV-

Codon Sequence:

ATGACTTCAAAGCTGCTGCCAGGAAACATCGTGTATGGAGGACCCGTCAC
AGAGAGACAGGCTCAGGACTCAAGATCACTGGGACAGTACATCCTGGATA
AGTATAAAAGCTTTGGCGATCGCACCGTGCTGGTGGACGCAGTGAACGGG
GTCGAGTACTCCGCCTCTTTCATGCACAAGTCCATTGTGCGACTGGCTTA
TATCCTGCAGAAGCTGGGGGTGAAACAGAATGACGTGGTCGGACTGAGCT
CCGAGAACTCTGTGAATTTCGCCCTGGCTATGTTTGCAGGACTGGCCGTG
GGCGCTACAGTCGCACCTCTGAACGTGACTTACAGTGATAGAGAAGTGGA
CCATGCCATCAATCTGTCTAAGCCAAAGATCATCTTCGCTAGTAAGATCA
CAATTGACCGCGTGGCCAAAGTCGCTTCTAAGAACAAATTCGTGAAGGGC
ATCATTGCCCTGAGCGGGACTAGCAAGAAGTTCAAGAATATCTACGATCT
GAAAGAGCTGATGGAGGACGAAAAGTTCAAAACTCAGCCAGATTTTACCT
CACCCGCCGCTAACAAGGATGAAGACGTGAGCCTGATCGTCTGCTCTAGT
GGCACCACAGGGCTGCCAAAAGGCGTGCAGCTGACCCAGATGAATCTGCT
GGCTACACTGGACAGCCAGATTCAGCCCACCGTGATCCCTATGGAGGAAG
TGACCCTGCTGACAGTCATTCCCTGGTTCCACGCCTTTGGATGCCTGACA
CTGATCACTACCGCTTGTGTGGGCGCAAGACTGGTCTACCTGCCTAAGTT
CGAGGAAAAACTGTTTCTGAGCGCTATTGAGAAGTATAGAGTGATGATGG
CATTCATGGTGCCCCCTCTGATGGTCTTTCTGGCCAAGCATCCCATCGTG
GATAAATACGACCTGTCAAGCCTGATGGTGCTGCTGTGTGGAGCAGCACC
ACTGTCCAGGGAGACTGAAGATCAGATCAAGGAGCGAATTGGAGTGCCTT
TTATCCGGCAGGGATACGGCCTGAGTGAGTCAACCCTGTCCGTGCTGGTC
CAGAACGACGAGTTCTGCAAGCCAGGATCTGTGGGCGTCCTGAAGGTCGG
CATCTACGCAAAAGTCATCGATCCCGACACAGGGAAACTGCTGGGAGCCA
ATGAGCGGGGGGAACTGTGTTTTAAGGGGGATGGAATTATGAAAGGGTAC
ATCGGAGACACTAAGTCCACACAGACTGCCATCAAGGATGGCTGGCTGCA
CACCGGCGACATCGGGTACTATGACGATGACTT**CGAGTTCTTTATCGTGG**
ATAGAATTAAGGAACTGATCAAGTACAAAGGCTATCAGGTGCCACCCGCC
GAGATTGAAGCTCTGCTGCTGACAAACGATAAGATCAAGGACGCTGCAGT
GATCGGAAAGCCTGACGAGGAAGCAGGCGAGCTGCCACTGGCCTTCGTGG
TCAAACAGGCTAACGTGCAGCTGACTGAGAATGAAGTGATCCAGTTTGTC
AACGATAATGCAAGTCCTGCAAAGAGGCTGCGAGGAGGCGTGATCTTCGT
GGACGAGATCCCTAAGAATCCATCAGGCAAAATTCTGCGGAGAATCCTGC
GGGAAATGCTGAA**GAAACAGAAGATCGCCGTGTAA**

Figure 5.17. Codon optimized CG6178 amino acid and codon sequence. Forward PCR primer sequences for the N- and C-terminal domains are highlighted in yellow. Reverse primer sequences are highlighted in purple.

Codon Optimized AbLL

Primary Amino Acid Sequence:

MSKESNIVYGPVGAAPVLESTAGKQLFDSLKRHGHLPQAIIDYQTKQSIS
YKNLFEATCKLAHSLEEYGLKQNDVIAICSENNLNFYKPVCAALYCGIVI
APLNDSYSEGEYVNALNISEPKLIFCSKKCLPRLVGLKARCSFIKGFVVI
DSTEDINGNECLPNFILRNSDPNFDIEKYEPRVFNSNEQVAAILLSSGTT
GFPKGVMLTHKNFSILFAHANDPVSGTQRIPGTTVLSILPYFHGFGFITN
ISYIKSGIRVVMLQRFEPEAFLRAIEEYEVRSTITVPPILIFLAKSPIVD
KYNLSSLKEIICGAAPSGREIVEAVVKRLKVSGIRYGYGLTECGLAICTT
PPNNFKIGSSGVVVPFMAVKIRDVESGKTLKPTQIGEICVKGDMLMKGYA
GNEKATKEMIDEDGWLHTGDIGYFDKDGHIYIVDRIKELIKYKGFQVPPA
ELEALLLHHPCVKDAAVIGIPDELAGELPAAFIVKQHGKEVTEKEIVDYI
AKQVSSAKHLRGGVRFIPDIPRTAAGKIQRNLLRNMIAKKKIAV-

Codon Sequence:

ATGTCCAAGGAGAGTAATATCGTCTATGGTCCAGTCGGCGCAGCCCCCGT
CCTCGAAAGTACAGCAGGGAAACAGCTCTTTGATTCTCTGAAGAGACACG
GCCATCTCCCTCAGGCTATCATTGACTACCAGACCAAGCAGAGTATCTCA
TATAAAAACCTGTTCGAGGCCACATGCAAGCTGGCTCACAGCCTCGAGGA
ATACGGACTGAAACAGAACGACGTGATCGCCATCTGTTCCGAAAACAATC
TGAACTTCTACAAGCCAGTCTGCGCCGCTCTGTATTGTGGGATCGTGATT
GCCCCCCTCAATGATAGCTACTCCGAGGGTGAATATGTGAACGCTCTGAA
TATTTCAGAGCCCAAGCTCATCTTCTGCAGCAAGAAATGTCTCCCTCGAC
TGGTGGGGCTCAAGGCCAGGTGCAGCTTCATCAAGGGTTTTGTGGTCATC
GACTCTACCGAGGATATTAACGGCAATGAATGTCTGCCCAACTTCATCCT
CAGGAACTCTGACCCTAACTTCGATATCGAGAAGTACGAACCAAGAGTCT
TCAACAGCAATGAGCAGGTGGCAGCCATCCTGCTCAGCTCCGGGACCACA
GGTTTTCCAAAGGGCGTGATGCTGACTCACAAAAACTTCAGTATCCTCTT
TGCCCATGCTAATGACCCAGTCTCAGGCACCCAGAGAATCCCCGGAACTA
CCGTGCTGAGCATTCTCCCATACTTCCACGGGTTCGGTTTTATCACCAAC
ATCTCTTACATCAAGAGTGGCATCCGGGTGGTCATGCTGCAGCGCTTCGA
GCCCGAAGCATTTCTGCGCGCCATCGAGGAATACGAGGTCCGAAGCACCA
TTACAGTGCCCCCTATCCTGATTTTCCTCGCCAAGTCCCCCATCGTGGAT
AAGTACAATCTGTCTAGTCTCAAGGAAATCATTTGCGGGGCTGCACCTTC
TGGTCGGGAGATCGTCGAAGCAGTGGTCAAGAGACTGAAAGTGAGTGGCA
TCCGGTACGGCTATGGACTGACAGAGTGCGGACTCGCTATCTGTACAACT
CCACCCAACAATTTCAAGATTGGCTCAAGCGGAGTGGTCGTGCCTTTTAT
GGCCGTCAAAATCCGCGACGTGGAGTCCGGCAAGACTCTGAAACCAACCC
AGATTGGGGAAATCTGCGTGAAGGGCGACATGCTGATGAAAGGGTACGCC
GGTAACGAGAAGGCCACAAAAGAGATGATCGACGAAGATGGATGGCTGCA
CACTGGCGACATTGGATACTTCGACAAGGATG**GGCATATCTATATTGTGG**
ATAGG**ATCAAGGAGCTGATCAAGTATAA**AGGGTTTCAGGTGCCTCCAGCT
GAGCTGGAAGCACTGCTCCTGCACCATCCTTGTGTCAAGGACGCCGCTGT
GATCGGCATTCCTGATGAGCTGGCCGGAGAACTCCCAGCAGCCTTCATCG
TGAAGCAGCACGGAAAAGAGGTCACAGAGAAGGAAATTGTGGACTACATC
GCTAAGCAGGTCTCCTCTGCAAAACATCTGAGGGGCGGCGTGAGGTTCAT
CCCCGATATCCCTCGCACTGCTGCAGGGAAGATTCAGCGAAACCTCCTCC
GAAACATGATTG**CTAAAAAGAAGATCGCCGTGTGA**

Figure 5.18. Codon optimized AbLL amino acid and codon sequence. Forward PCR primer sequences for the N- and C-terminal domains are bold. Reverse primer sequences are highlighted in green.

WT luc2 Luciferase

Primary Amino Acid Sequence:

MEDAKNIKKGPAPFYPLEDGTAGEQLHKAMKRYALVPGTIAFTDAHIEVD
ITYAEYFEMSVRLAEAMKRYGLNTNHRIVVCSENSLQFFMPVLGALFIGV
AVAPANDIYNERELLNSMGISQPTVVFVSKKGLQKILNVQKKLPIIQKII
IMDSKTDYQGFQSMYTFVTSHLPPGFNEYDFVPESFDRDKTIALIMNSSG
STGLPKGVALPHRTACVRFSHARDPIFGNQIIPDTAILSVVPFHHGFGMF
TTLGYLICGFRVVLMYRFEEELFLRSLQDYKIQSALLVPTLFSFFAKSTL
IDKYDLSNLHEIASGGAPLSKEVGEAVAKRFHLPGIRQGYGLTETTSAIL
ITPEGDDKPGAVGKVVPFFEAKVVDLDTGKTLGVNQRGELCVRGPMIMSG
YVNNPEATNALIDKDGWLHSGDIAYWDEDEHFFIVDRLKSLIKYKGYQVA
PAELESILLQHPNIFDAGVAGLPDDDAGELPAAVVVLEHGKTMTEKEIVD
YVASQVTTAKKLRGGVVFVDEVPKGLTGKLDARKIREILIKAKKGGKIAV-

Codon Sequence:

ATGGAAGATGCCAAAAACATTAAGAAGGGCCCAGCGCCATTCTACCCACT
CGAAGACGGGACCGCCGGCGAGCAGCTGCACAAAGCCATGAAGCGCTACG
CCCTGGTGCCCGGCACCATCGCCTTTACCGACGCACATATCGAGGTGGAC
ATTACCTACGCCGAGTACTTCGAGATGAGCGTTCGGCTGGCAGAAGCTAT
GAAGCGCTATGGGCTGAATACAAACCATCGGATCGTGGTGTGCAGCGAGA
ATAGCTTGCAGTTCTTCATGCCCGTGTTGGGTGCCCTGTTCATCGGTGTG
GCTGTGGCCCCAGCTAACGACATCTACAACGAGCGCGAGCTGCTGAACAG
CATGGGCATCAGCCAGCCCACCGTCGTATTCGTGAGCAAGAAAGGGCTGC
AAAAGATCCTCAACGTGCAAAAGAAGCTACCGATCATACAAAAGATCATC
ATCATGGATAGCAAGACCGACTACCAGGGCTTCCAAAGCATGTACACCTT
CGTGACTTCCCATTTGCCACCCGGCTTCAACGAGTACGACTTCGTGCCCG
AGAGCTTCGACCGGGACAAAACCATCGCCCTGATCATGAACAGTAGTGGC
AGTACCGGATTGCCCAAGGGCGTAGCCCTACCGCACCGCACCGCTTGTGT
CCGATTCAGTCATGCCCGCGACCCCATCTTCGGCAACCAGATCATCCCCG
ACACCGCTATCCTCAGCGTGGTGCCATTTCACCACGGCTTCGGCATGTTC
ACCACGCTGGGCTACTTGATCTGCGGCTTTCGGGTCGTGCTCATGTACCG
CTTCGAGGAGGAGCTATTCTTGCGCAGCTTGCAAGACTATAAGATTCAAT
CTGCCCTGCTGGTGCCCACACTATTTAGCTTCTTCGCTAAGAGCACTCTC
ATCGACAAGTACGACCTAAGCAACTTGCACGAGATCGCCAGCGGCGGGGC
GCCGCTCAGCAAGGAGGTAGGTGAGGCCGTGGCCAAACGCTTCCACCTAC
CAGGCATCCGCCAGGGCTACGGCCTGACAGAAACAACCAGCGCCATTCTG
ATCACCCCCGAAGGGGACGACAAGCCTGGCGCAGTAGGCAAGGTGGTGCC
CTTCTTCGAGGCTAAGGTGGTGGACTTGGACACCGGTAAGACACTGGGTG
TGAACCAGCGCGGCGAGCTGTGCGTCCGTGGCCCCATGATCATGAGCGGC
TACGTTAACAACCCCGAGGCTACAAACGCTCTCATCGACAAGGACGGCTG
GCTGCACAGCGGCGACATCGCCTACTGGGACGAGGACGAGC**ACTTCTTCA**
TCGTGGACCGGCTGAAGAGCCTGATCAAATACAAGGGCTACCAGGTAGCC
CCAGCCGAACTGGAGAGCATCCTGCTGCAACACCCCAACATCTTCGACGC
CGGGGTCGCCGGCCTGCCCGACGACGATGCCGGCGAGCTGCCCGCCGCAG
TCGTCGTGCTGGAACACGGTAAAACCATGACCGAGAAGGAGATCGTGGAC
TATGTGGCCAGCCAGGTTACAACCGCCAAGAAGCTGCGCGGTGGTGTTGT
GTTCGTGGACGAGGTGCCTAAAGGACTGACCGGCAAGTTGGACGCCCGCA
AGATCCGCGAGATTCTCATTAAGGCCAAGAAGG**GCGGCAAGATCGCCGTGTAA**

Figure 5.19. WT luc2 luciferase amino acid and codon sequence. Forward PCR primer sequences for the N- and C-terminal domains are highlighted in blue. Reverse primer sequences are highlighted in red.

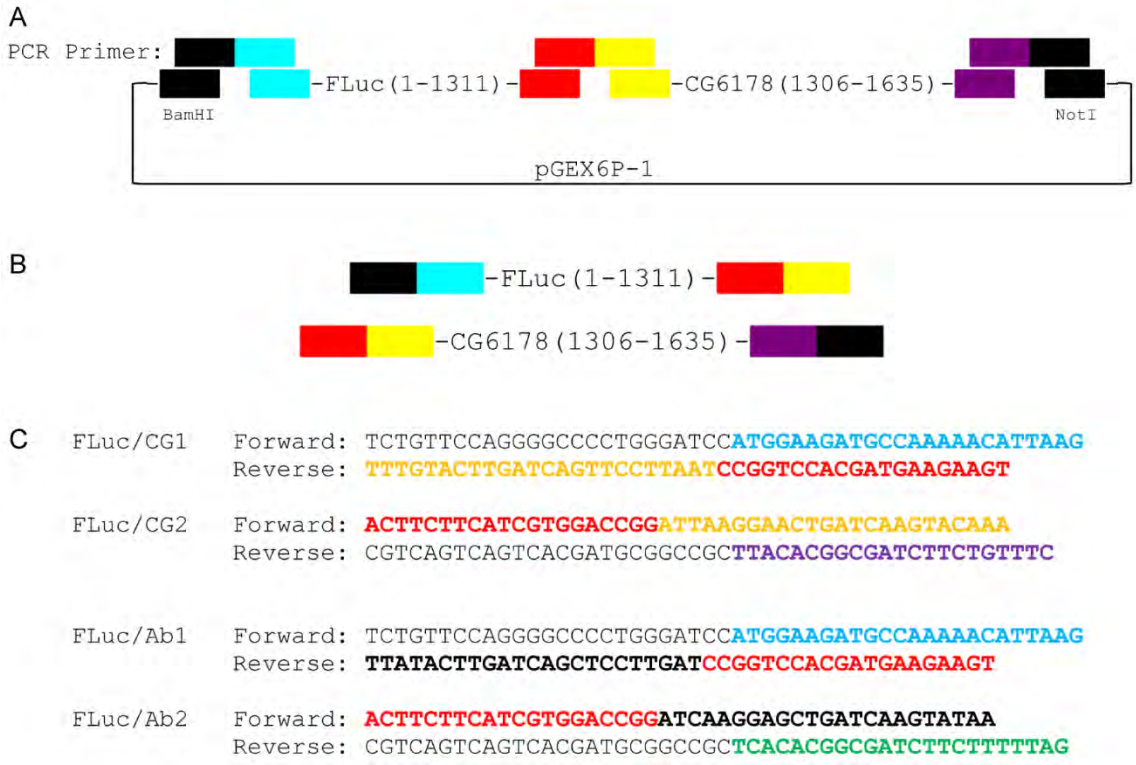

Figure 5.20. PCR primer design for chimeric constructs. (A) Representative construct for FLuc/CG chimera in pGEX6P-1 expression plasmid. PCR primers contain overlapping regions of the desired cDNA and the adjacent DNA. (B) PCR products of the representative FLuc/CG chimera. Note: The 3' end of the luciferase fragment is identical to the 5' end of the CG6178 fragment (marked by red-box/yellow-box). The 5' end of the luciferase fragment is identical to the pGEX6P-1 BamHI cut site and the 3' end is identical to the pGEX6P-1 NotI cut site (marked by black boxes). These overlapping identical areas are required for Gibson Assembly. (C) FLuc/CG and FLuc/Ab chimera PCR primers. Primer set 1 is for the N-terminal domain and primer set 2 is for the C-terminal domain.

FLuc/CG Chimera Final Sequence

Primary Amino Acid Sequence:

MEDAKNIKKGPAPFYPLEDGTAGEQLHKAMKRYALVPGTIAFTDAHIEVD
ITYAEYFEMSVRLAEAMKRYGLNTNHRIVVCSENSLQFFMPVLGALFIGV
AVAPANDIYNERELLNSMGISQPTVVFVSKKGLQKILNVQKKLPIIQKII
IMDSKTDYQGFQSMYTFVTSHLPPGFNEYDFVPESFDRDKTIALIMNSSG
STGLPKGVALPHRTACVRFSHARDPIFGNQIIPDTAILSVVPFHHGFGMF
TTLGYLICGFRVVLMYRFEEELFLRSLQDYKIQSALLVPTLFSFFAKSTL
IDKYDLSNLHEIASGGAPLSKEVGEAVAKRFHLPGIRQGYGLTETTSAIL
ITPEGDDKPGAVGKVVPFFEAKVVDLDTGKTLGVNQRGELCVRGPMIMSG
YVNNPEATNALIDKDGWLHSGDIAYWDEDEHFFIVDRIKELIKYKGYQVP
PAEIEALLLTNDKIKDAAVIGKPDEEAGELPLAFVVKQANVQLTENEVIQ
FVNDNASPAKRLRGGVIFVDEIPKNPSGKILRRILREMLKKQKIAV-

Codon Sequence:

ATGGAAGATGCCAAAAACATTAAGAAGGGCCCAGCGCCATTCTACCCACT
CGAAGACGGGACCGCCGGCGAGCAGCTGCACAAAGCCATGAAGCGCTACG
CCCTGGTGCCCGGCACCATCGCCTTTACCGACGCACATATCGAGGTGGAC
ATTACCTACGCCGAGTACTTCGAGATGAGCGTTCGGCTGGCAGAAGCTAT
GAAGCGCTATGGGCTGAATACAAACCATCGGATCGTGGTGTGCAGCGAGA
ATAGCTTGCAGTTCTTCATGCCCGTGTTGGGTGCCCTGTTCATCGGTGTG
GCTGTGGCCCCAGCTAACGACATCTACAACGAGCGCGAGCTGCTGAACAG
CATGGGCATCAGCCAGCCCACCGTCGTATTCGTGAGCAAGAAAGGGCTGC
AAAAGATCCTCAACGTGCAAAAGAAGCTACCGATCATACAAAAGATCATC
ATCATGGATAGCAAGACCGACTACCAGGGCTTCCAAAGCATGTACACCTT
CGTGACTTCCCATTTGCCACCCGGCTTCAACGAGTACGACTTCGTGCCCG
AGAGCTTCGACCGGGACAAAACCATCGCCCTGATCATGAACAGTAGTGGC
AGTACCGGATTGCCCAAGGGCGTAGCCCTACCGCACCGCACCGCTTGTGT
CCGATTCAGTCATGCCCGCGACCCCATCTTCGGCAACCAGATCATCCCCG
ACACCGCTATCCTCAGCGTGGTGCCATTTCACCACGGCTTCGGCATGTTC
ACCACGCTGGGCTACTTGATCTGCGGCTTTCGGGTCGTGCTCATGTACCG
CTTCGAGGAGGAGCTATTCTTGCGCAGCTTGCAAGACTATAAGATTCAAT
CTGCCCTGCTGGTGCCCACACTATTTAGCTTCTTCGCTAAGAGCACTCTC
ATCGACAAGTACGACCTAAGCAACTTGCACGAGATCGCCAGCGGCGGGGC
GCCGCTCAGCAAGGAGGTAGGTGAGGCCGTGGCCAAACGCTTCCACCTAC
CAGGCATCCGCCAGGGCTACGGCCTGACAGAAACAACCAGCGCCATTCTG
ATCACCCCCGAAGGGGACGACAAGCCTGGCGCAGTAGGCAAGGTGGTGCC
CTTCTTCGAGGCTAAGGTGGTGGACTTGGACACCGGTAAGACACTGGGTG
TGAACCAGCGCGGCGAGCTGTGCGTCCGTGGCCCCATGATCATGAGCGGC
TACGTTAACAACCCCGAGGCTACAAACGCTCTCATCGACAAGGACGGCTG
GCTGCACAGCGGCGACATCGCCTACTGGGACGAGGACGAGC**ACTTCTTCA**
TCGTGGACCGGATTAAGGAACTGATCAAGTACAAAGGCTATCAGGTGCCA
CCCGCCGAGATTGAAGCTCTGCTGCTGACAAACGATAAGATCAAGGACGC
TGCAGTGATCGGAAAGCCTGACGAGGAAGCAGGCGAGCTGCCACTGGCCT
TCGTGGTCAAACAGGCTAACGTGCAGCTGACTGAGAATGAAGTGATCCAG
TTTGTCAACGATAATGCAAGTCCTGCAAAGAGGCTGCGAGGAGGCGTGAT
CTTCGTGGACGAGATCCCTAAGAATCCATCAGGCAAAATTCTGCGGAGAA
TCCTGCGGGAAATGCTGAA**GAAACAGAAGATCGCCGTGTAA**

Figure 5.21. FLuc/CG chimera amino acid and codon sequence. The CG6178 C-terminal domain is highlighted in blue. Colored sequences reflect the Gibson Assembly primers from above.

FLuc/Ab Chimera Final Sequence

Primary Amino Acid Sequence:

MEDAKNIKKGPAPFYPLEDGTAGEQLHKAMKRYALVPGTIAFTDAHIEVD
ITYAEYFEMSVRLAEAMKRYGLNTNHRIVVCSENSLQFFMPVLGALFIGV
AVAPANDIYNERELLNSMGISQPTVVFVSKKGLQKILNVQKKLPIIQKII
IMDSKTDYQGFQSMYTFVTSHLPPGFNEYDFVPESFDRDKTIALIMNSSG
STGLPKGVALPHRTACVRFSHARDPIFGNQIIPDTAILSVVPFHHGFGMF
TTLGYLICGFRVVLMYRFEEELFLRSLQDYKIQSALLVPTLFSFFAKSTL
IDKYDLSNLHEIASGGAPLSKEVGEAVAKRFHLPGIRQGYGLTETTSAIL
ITPEGDDKPGAVGKVVPFFEAKVVDLDTGKTLGVNQRGELCVRGPMIMSG
YVNNPEATNALIDKDGWLHSGDIAYWDEDEHFFIVDRIKELIKYKGFQVP
PAELEALLLHHPCVKDAAVIGIPDELAGELPAAFIVKQHGKEVTEKEIVD
YIAKQVSSAKHLRGGVRFIPDIPRTAAGKIQRNLLRNMIAKKKIAV-

Codon Sequence:

ATGGAAGATGCCAAAAACATTAAGAAGGGCCCAGCGCCATTCTACCCACT
CGAAGACGGGACCGCCGGCGAGCAGCTGCACAAAGCCATGAAGCGCTACG
CCCTGGTGCCCGGCACCATCGCCTTTACCGACGCACATATCGAGGTGGAC
ATTACCTACGCCGAGTACTTCGAGATGAGCGTTCGGCTGGCAGAAGCTAT
GAAGCGCTATGGGCTGAATACAAACCATCGGATCGTGGTGTGCAGCGAGA
ATAGCTTGCAGTTCTTCATGCCCGTGTTGGGTGCCCTGTTCATCGGTGTG
GCTGTGGCCCCAGCTAACGACATCTACAACGAGCGCGAGCTGCTGAACAG
CATGGGCATCAGCCAGCCCACCGTCGTATTCGTGAGCAAGAAAGGGCTGC
AAAAGATCCTCAACGTGCAAAAGAAGCTACCGATCATACAAAAGATCATC
ATCATGGATAGCAAGACCGACTACCAGGGCTTCCAAAGCATGTACACCTT
CGTGACTTCCCATTTGCCACCCGGCTTCAACGAGTACGACTTCGTGCCCG
AGAGCTTCGACCGGGACAAAACCATCGCCCTGATCATGAACAGTAGTGGC
AGTACCGGATTGCCCAAGGGCGTAGCCCTACCGCACCGCACCGCTTGTGT
CCGATTCAGTCATGCCCGCGACCCCATCTTCGGCAACCAGATCATCCCCG
ACACCGCTATCCTCAGCGTGGTGCCATTTCACCACGGCTTCGGCATGTTC
ACCACGCTGGGCTACTTGATCTGCGGCTTTCGGGTCGTGCTCATGTACCG
CTTCGAGGAGGAGCTATTCTTGCGCAGCTTGCAAGACTATAAGATTCAAT
CTGCCCTGCTGGTGCCCACACTATTTAGCTTCTTCGCTAAGAGCACTCTC
ATCGACAAGTACGACCTAAGCAACTTGCACGAGATCGCCAGCGGCGGGGC
GCCGCTCAGCAAGGAGGTAGGTGAGGCCGTGGCCAAACGCTTCCACCTAC
CAGGCATCCGCCAGGGCTACGGCCTGACAGAAACAACCAGCGCCATTCTG
ATCACCCCCGAAGGGGACGACAAGCCTGGCGCAGTAGGCAAGGTGGTGCC
CTTCTTCGAGGCTAAGGTGGTGGACTTGGACACCGGTAAGACACTGGGTG
TGAACCAGCGCGGCGAGCTGTGCGTCCGTGGCCCCATGATCATGAGCGGC
TACGTTAACAACCCCGAGGCTACAAACGCTCTCATCGACAAGGACGGCTG
GCTGCACAGCGGCGACATCGCCTACTGGGACGAGGACGAGC**ACTTCTTCA**
TCGTGGACCGG**ATCAAGGAGCTGATCAAGTATAA**AGGGTTTCAGGTGCCT
CCAGCTGAGCTGGAAGCACTGCTCCTGCACCATCCTTGTGTCAAGGACGC
CGCTGTGATCGGCATTCCTGATGAGCTGGCCGGAGAACTCCCAGCAGCCT
TCATCGTGAAGCAGCACGGAAAAGAGGTCACAGAGAAGGAAATTGTGGAC
TACATCGCTAAGCAGGTCTCCTCTGCAAAACATCTGAGGGGCGGCGTGAG
GTTCATCCCCGATATCCCTCGCACTGCTGCAGGGAAGATTCAGCGAAACC
TCCTCCAAACATGATTG**CTAAAAAGAAGATCGCCGTGTGA**

Figure 5.22. FLuc/Ab chimera amino acid and codon sequence. The AbLL C-terminal domain is highlighted in green. Colored sequences reflect the Gibson Assembly primers from above.

Enzyme expression and purification

Luciferases, fatty acyl-CoA synthetases, and chimeras were expressed and purified as GST-fusion proteins from the pGEX6P-1 vector as previously described (Mofford et al., 2014b). Briefly, JM109 cells were grown at 37 °C until the OD600 reached 0.5-1, induced with 0.1 mM IPTG, and incubated with shaking at 20 °C overnight. Cells were pelleted at 5000 RPM, then flash frozen in liquid nitrogen. The *E. coli* pellets from 1 L of culture were thawed on ice, resuspended in 25 mL lysis buffer (50 mM Tris [pH 7.4], 500 mM NaCl, and 0.5% Tween 20) containing 1 mM phenylmethylsulfonyl fluoride, and disrupted by sonification (Branson Sonifier). Dithiothreitol (DTT) was added at 10 mM, and the resulting cell lysate was clarified by centrifugation at 35,000 RPM for 60 min at 4 °C. The supernatant was batch-bound to immobilized glutathione (Thermo Scientific) for 1 hr at 4 °C, and the beads were washed with lysis buffer containing 10 mM DTT, followed by wash buffer (50 mM Tris [pH 8.1], 250 mM NaCl, and 10 mM DTT) and storage buffer (50 mM Tris [pH 7.4], 0.1 mM EDTA, 150 mM NaCl, 1 mM TCEP). Twenty units of PreScission Protease (GE Healthcare) were added, and incubation continued overnight at 4 °C to cleave the GST-fusion and elute the untagged enzyme. Protein concentrations were determined using Coomassie Plus (Thermo Scientific).

Purified protein luminescence assays

Luminescence assays were initiated by adding 30 µL of purified luciferase in enzyme buffer (20 mM Tris [pH 7.4], 0.1 mM EDTA, 1 mM TCEP, and 0.8 mg/mL BSA) to 30 µL 2x substrate in substrate buffer (20 mM Tris [pH 7.4], 0.1 mM EDTA, 8 mM $MgSO_4$, and 4 mM ATP) in a black 96-well plate (Costar 3915). Imaging was performed one minute after enzyme addition using a Xenogen IVIS-100 at a final enzyme concentration of 10 nM and final substrate concentrations ranging from 0.122 to 250 µM. Data acquisition and analysis was performed with Living Image® software. Data are reported as total flux (p/s) for each ROI corresponding to each well of the 96-well plate.

Burst kinetics assays

Using a Promega GloMax-Multi Detection System, 50 µL of purified enzyme in enzyme buffer was rapidly injected into a white 96-well plate (Costar 3912) containing 50 µL of 2x substrate in substrate buffer to a final enzyme concentration of 100 nM and a final luciferin substrate concentration of 250 µM. Measurements were taken every 0.5 s for 1 s pre-injection and 120 s post-injection. Data are reported as Relative Light Units (RLU).

CHAPTER VI:

Luciferin Amides Enable in Vivo Bioluminescence Detection of Endogenous Fatty Acid Amide Hydrolase Activity

Mofford, D.M. *et. al*. (2015) *JACS.* 137(27), 8684–8687.

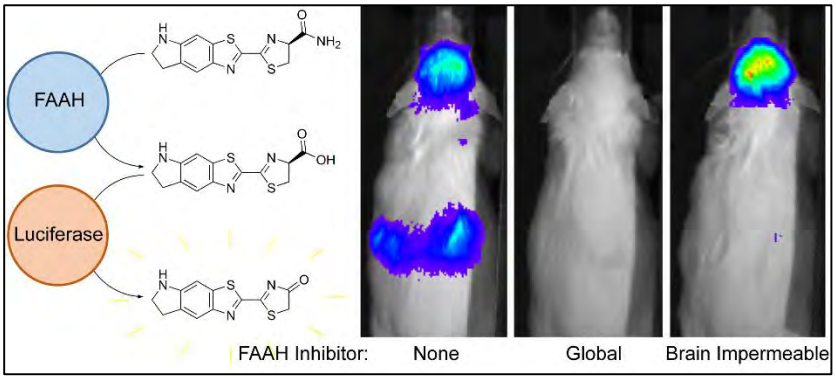

Summary

Firefly luciferase is homologous to fatty acyl-CoA synthetases. We hypothesized that the firefly luciferase substrate D-luciferin and its analogs are fatty acid mimics that are ideally suited to probe the chemistry of enzymes that release fatty acid products. Here, we synthesized luciferin amides and found that these molecules are hydrolyzed to substrates for firefly luciferase by the enzyme fatty acid amide hydrolase (FAAH). In the presence of luciferase, these molecules enable highly sensitive and selective bioluminescent detection of FAAH activity in vitro, in live cells, and in vivo. The potency and tissue distribution of FAAH inhibitors can be imaged in live mice, and luciferin amides serve as exemplary reagents for greatly improved bioluminescence imaging in FAAH-expressing tissues such as the brain.

Introduction

Firefly luciferase is best known for its light emission chemistry with D-luciferin, but it is also a long-chain fatty acyl-CoA synthetase (ACSL) that can bind fatty acid substrates such as arachidonic acid (Oba et al., 2003) (**Figure 6.1**). Conversely, we have recently shown that an ACSL from the fruit fly *Drosophila melanogaster* is a latent luciferase that can emit light with a synthetic luciferin (Mofford et al., 2014a). In both cases, adenylation of a carboxylic acid is the first step in catalysis. Furthermore, both enzymes can bind fatty acids ranging from octanoic acid to arachidonic acid, suggesting that D-luciferin and aminoluciferin analogs (Adams and Miller, 2014; Mofford et al., 2014b; Reddy et al., 2010) are acting as fatty acid mimics. Based in part on this observation, we hypothesized that luciferins are ideally suited to probe the chemistry of enzymes that release fatty acid products.

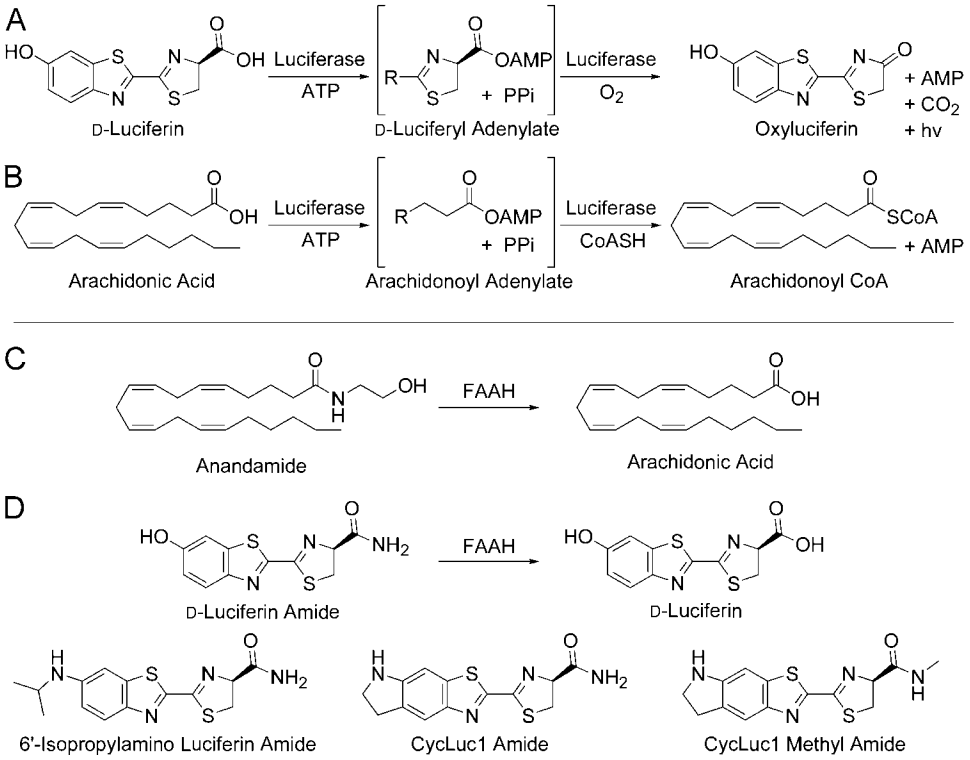

Figure 6.1. Enzyme mechanisms and luciferin structures. (A) Firefly luciferase catalyzes light emission from D-luciferin. (B) Firefly luciferase is also a fatty acyl-CoA synthetase. (C) FAAH cleaves anandamide to arachidonic acid. (D) Luciferin amides could allow bioluminescence imaging of FAAH activity.

Fatty acid amide hydrolase (FAAH) is a serine hydrolase that limits the lifetime and sphere of action of fatty acid amide second messengers by hydrolysis to their corresponding fatty acids (Blankman and Cravatt, 2013; Cravatt et al., 1996) (**Figure 6.1**). Most notably, arachidonoyl ethanolamine (anandamide) is a locally generated agonist for the cannabinoid receptor CB1. Inhibition of FAAH prolongs the action of anandamide and is therefore an attractive drug target for the treatment of pain, anxiety, and cannabinoid dependence (Blankman and Cravatt, 2013). Many FAAH inhibitors are being

developed as potential therapeutics, and there is great interest in detecting FAAH activity in vivo (Shoup et al., 2014). Current techniques to assay FAAH inhibitors in mice primarily require sacrificing the mouse, homogenizing the tissues, adding radioactive lipid substrates, and HPLC analysis of the products (Long et al., 2011). This places large demands on time and quantities of mice required to evaluate inhibitors and furthermore cannot give longitudinal data from the same animal. Some inroads have been made with PET imaging probes for FAAH, but these are specialized and expensive tools with low throughput and signal-to-noise that lack the specificity for whole-body imaging (Shoup et al., 2014).

FAAH readily accepts a wide range of saturated and unsaturated fatty acid amides in addition to anandamide (Boger et al., 2000; Cravatt et al., 1996) and has been shown to hydrolyze ethanolamides, primary amides, and methyl amides (Boger et al., 2000; Cravatt et al., 1996; Patricelli and Cravatt, 1999). We therefore hypothesized that FAAH could hydrolyze luciferin amides to their respective carboxylates, resulting in the formation of a luminogenic luciferase substrate (**Figure 6.1**). Here we show that luciferin amides allow exquisitely selective and sensitive imaging of endogenous FAAH activity in live cells and in live mice. FAAH is both necessary and sufficient for bioluminescence to occur and is the only enzyme activating these probes. The performance of FAAH inhibitors can be imaged in live mice, and inhibitors that cross the blood-brain barrier can be readily distinguished from those that cannot. Moreover, the amount of luciferin amide probe needed to perform this imaging is >1,000-fold

lower than typical D-luciferin imaging conditions but nonetheless improves overall signal from the brain. Thus, luciferin amides also excel at delivering luciferins into FAAH-expressing cells and tissues.

Results and Discussion

To test our initial hypothesis, we synthesized four luciferin amides (**Figure 6.1**) by the condensation of electrophilic nitriles (Mofford et al., 2014b; Reddy et al., 2010) with a D-cysteine amide (see Supporting Information). Without a free carboxylate, these luciferin analogs are not light-emitting substrates for purified firefly luciferase (**Figure 6.2** and **Figure 6.3**). Pretreatment of the luciferin amides with recombinant rat FAAH (Mileni et al., 2008) restores luminescent activity and could be specifically blocked by incubation with FAAH inhibitors such as PF3845 (Ahn et al., 2009) (**Figure 6.2** and **Figure 6.3**). The presence of FAAH or FAAH inhibitors has no effect on light emitted from the parent luciferins (**Figure 6.2** and **Figure 6.3**). Thus, luciferin amides can be used to detect FAAH activity and inhibition in vitro.

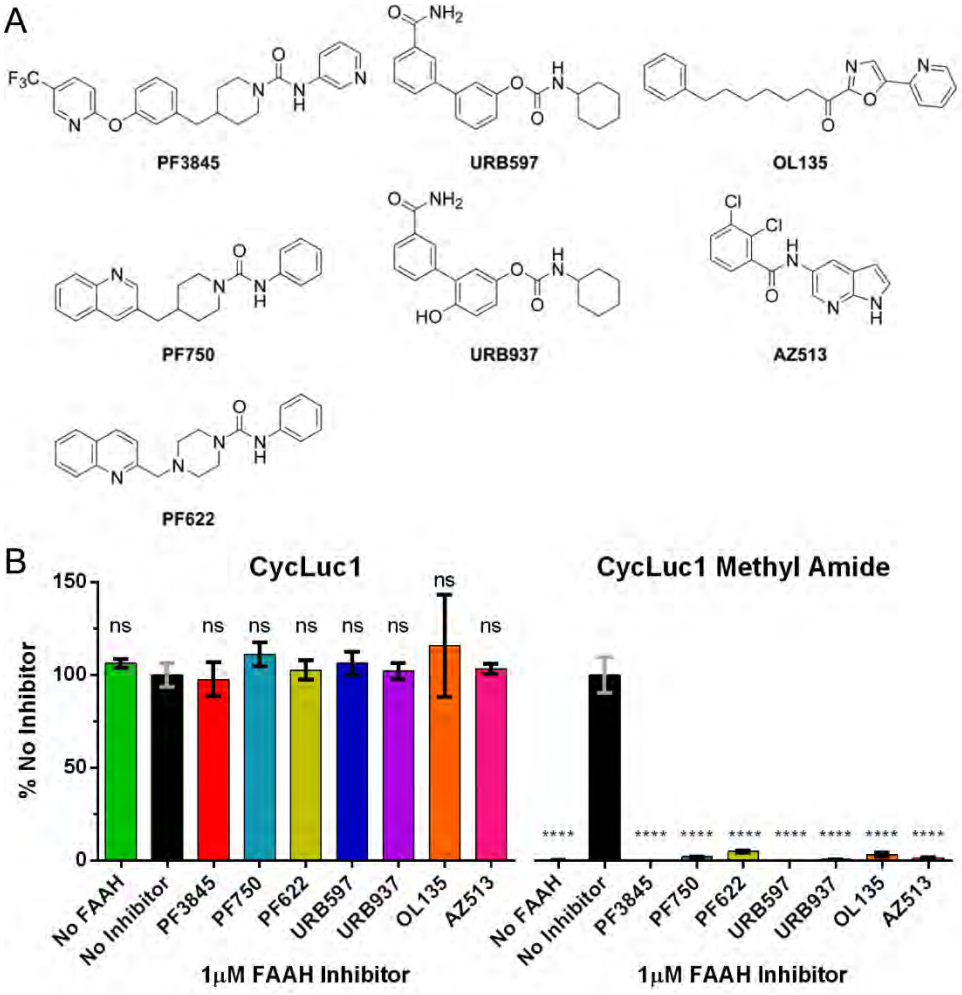

Figure 6.2. FAAH inhibitor structures and in vitro FAAH inhibitor screen. (A) FAAH inhibitor structures. (B) Photon flux from the indicated luciferin analog (10 μM) normalized to emission in the presence of FAAH with no FAAH inhibitor. The assay was performed in triplicate and is represented as the mean ± SEM.

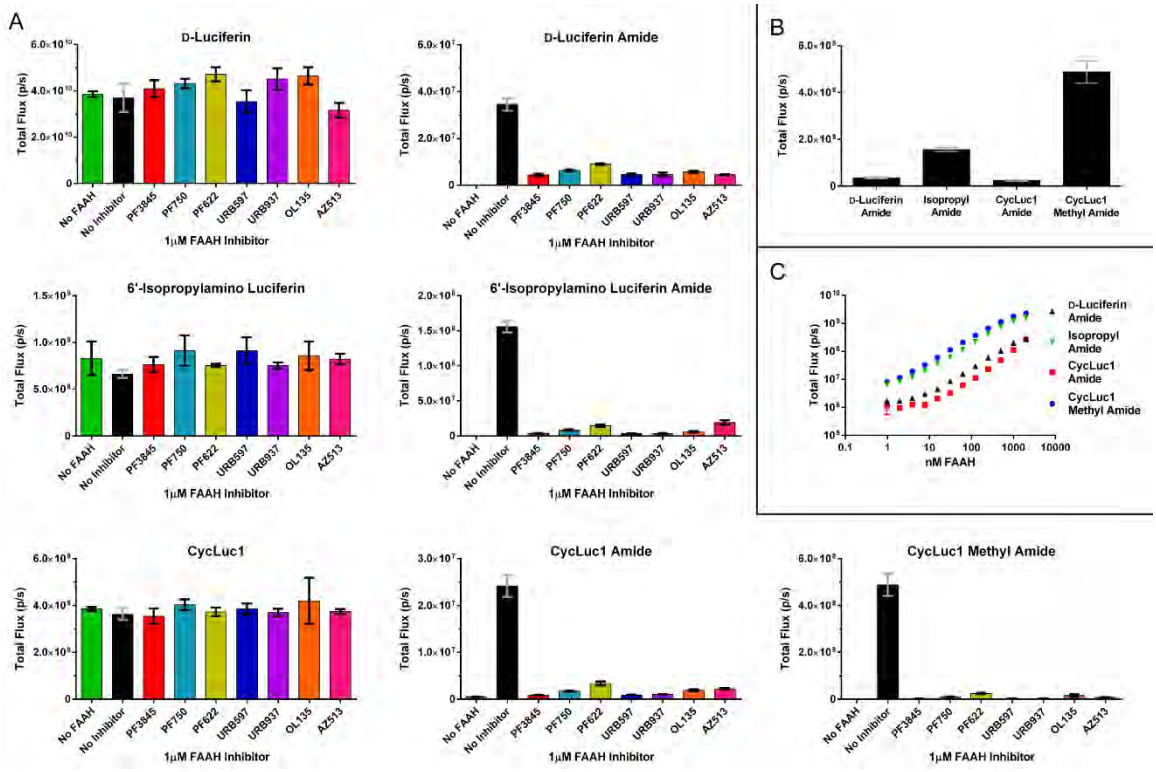

Figure 6.3. Luciferin amides report on rat FAAH activity in vitro. (A) Photon flux from the indicated luciferin analog (10 μM) in the absence of FAAH or presence of FAAH with and without a FAAH inhibitor. (B) Direct comparison of each luciferin amide after treatment with rFAAH without inhibitor from (A). (C) Dependence of photon flux on the concentration of rFAAH after 30 min incubation with the indicated luciferin amide at pH 7.4, ambient temperature. All assays were performed in triplicate and are represented as the mean ± SEM.

We next sought to determine whether luciferin amides were specific to FAAH and sensitive enough to enable the detection of FAAH activity in live cells. Chinese hamster ovary (CHO) cells are known to express FAAH (Okamoto et al., 2005), an integral membrane protein (Blankman and Cravatt, 2013), but at levels insufficient to detect with fluorescence-based assays (Ramarao et al., 2005). In contrast, treatment of luciferase-expressing CHO cells with luciferin amides

resulted in robust bioluminescence (**Figure 6.4A** and **Figure 6.5**). Potentially, in the complex environment of the cell, luciferin amides could be cleaved by proteases or other serine hydrolases. However, treatment with PF3845, which specifically inhibits FAAH but no other serine hydrolases (Ahn et al., 2009), blocked emission from luciferin amides but had no effect on luciferase activity in the presence of the parent luciferin (**Figure 6.4A**). Furthermore, inhibitors of other serine hydrolases had no effect, and we evaluated the potency of a wide range of FAAH inhibitors in the natural context of live cell membranes (**Figure 6.6** and **Figure 6.7**). Lacking an ionized carboxylate, the luciferin amides also served as excellent luciferin delivery vehicles in these FAAH expressing cells, yielding higher bioluminescence signals than their parent luciferins at concentrations <100 μM (**Figure 6.5**). CycLuc1 methyl amide achieved higher maximal photon flux than CycLuc1 amide, presumably because uncleaved CycLuc1 amide can ultimately inhibit luciferase, while CycLuc1 methyl amide cannot (**Figure 6.5** and **Figure 6.8**).

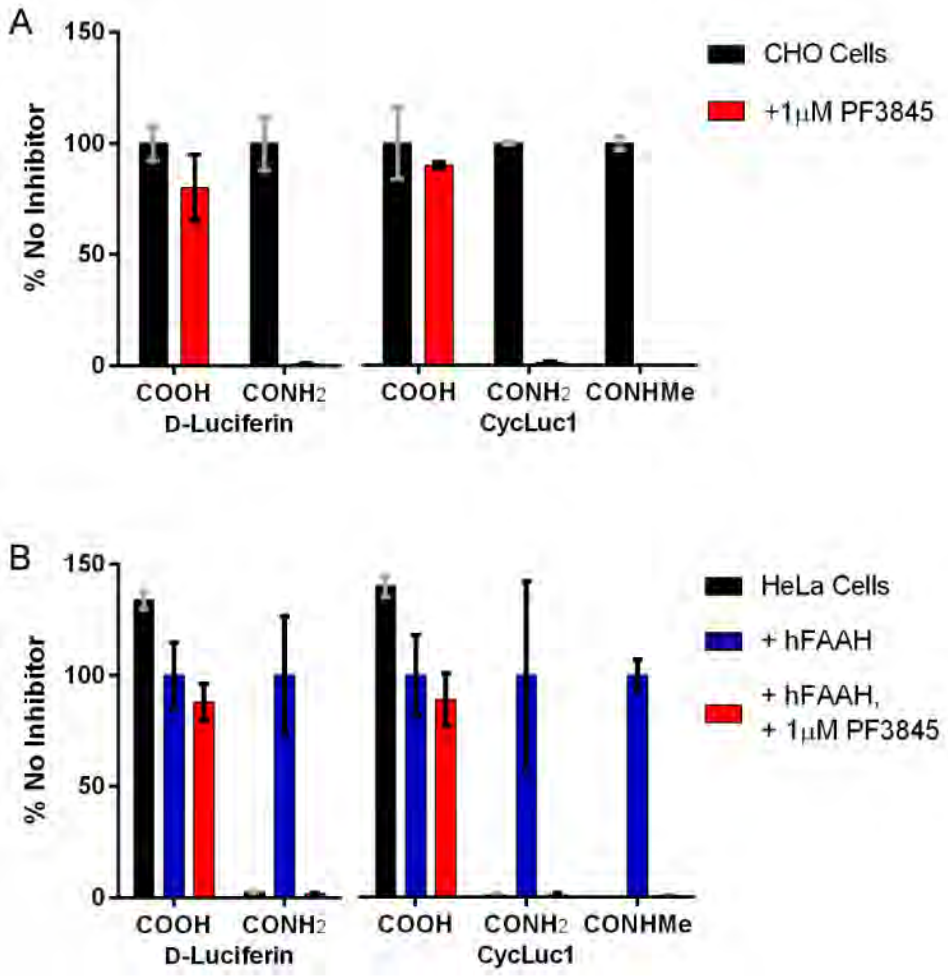

Figure 6.4. Luciferin amides report on FAAH activity in live mammalian cells. (A) Relative photon flux from live luciferase-expressing CHO cells treated with the indicated luciferins and luciferin amides (125 μM) in the absence (black bars) or presence (red bars) of the FAAH inhibitor PF3845. The data are normalized to the uninhibited sample for each luciferin (black bars). (B) Relative flux from live luciferase-expressing HeLa cells treated with the same set of substrates after transfection with empty pcDNA3.1 vector (black bars), pcDNA3.1-hFAAH (blue bars), or pcDNA3.1-hFAAH and treatment with the FAAH inhibitor PF3845 (red bars). The data are normalized to the uninhibited hFAAH transfected sample for each luciferin (blue bars). All assays were performed in triplicate and are represented as the mean ± SEM.

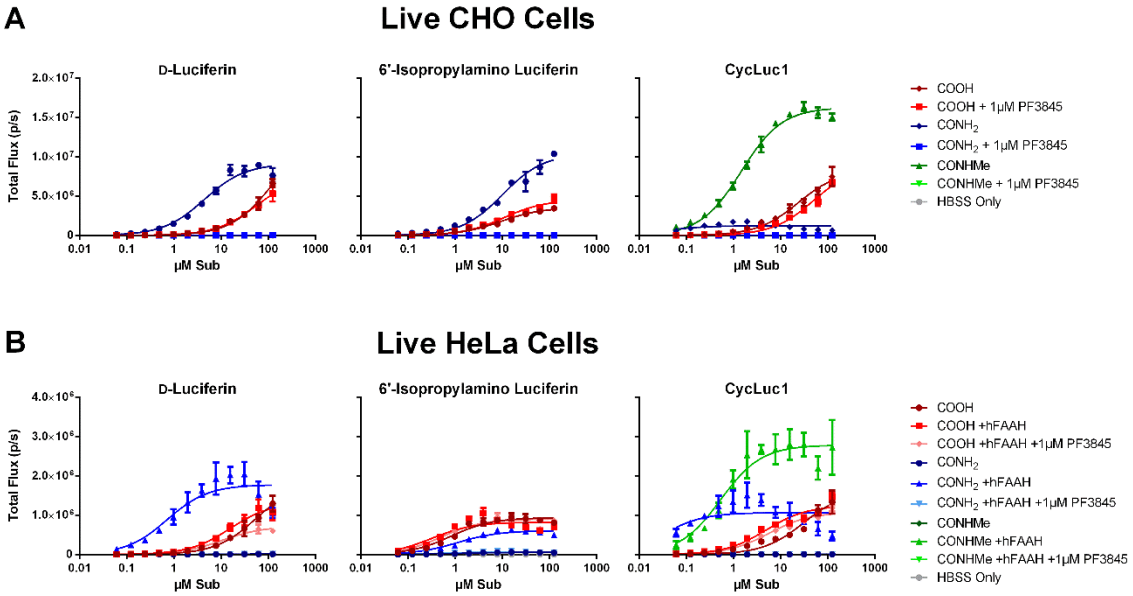

Figure 6.5. Luciferin amides report on FAAH activity in live cells and improve signal over parent luciferins. (A) Live CHO cells transfected with luciferase were incubated with 1 μM PF3845 for five minutes and then imaged with varying concentrations of the indicated luciferin analog. (B) Live HeLa cells co-transfected with either luciferase and human FAAH or luciferase and empty vector were incubated with 1 μM PF3845 for five minutes and then imaged with varying concentrations of the indicated luciferin analog. The assay was performed in triplicate and is represented as the mean ± SEM. Curves were fit to the Michaelis–Menten equation by nonlinear regression.

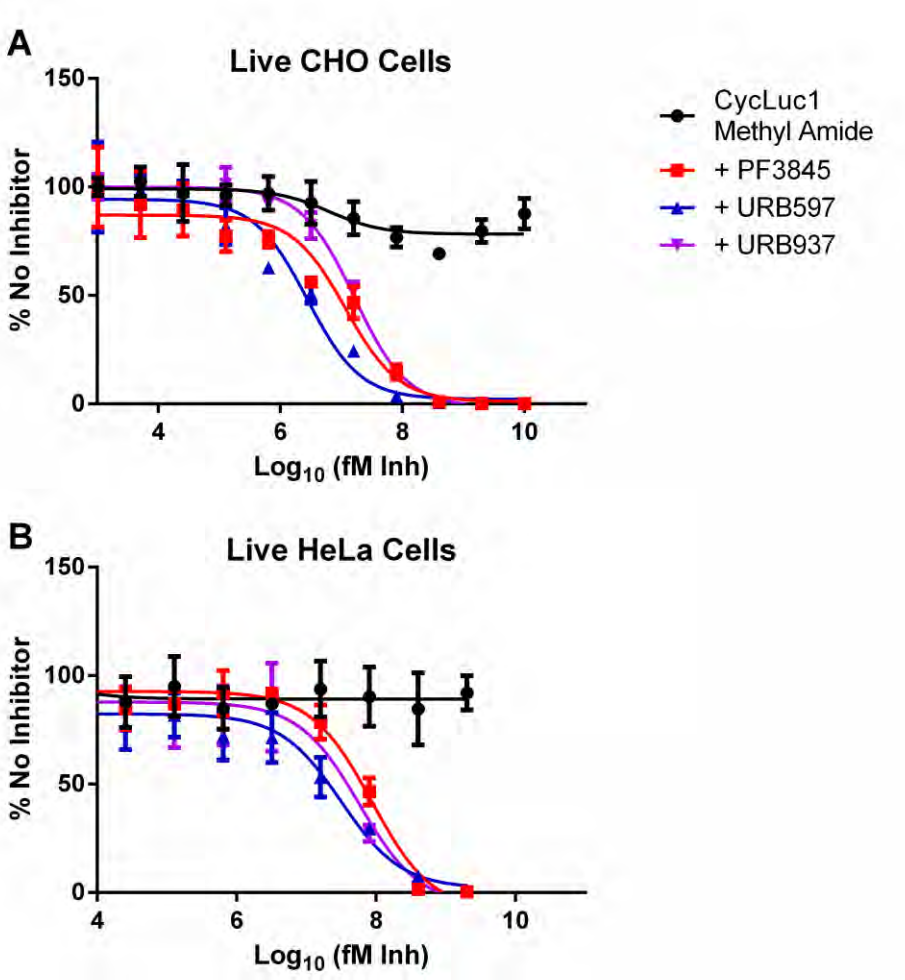

Figure 6.6. Luciferin amides report on inhibitor potency in live cells. (A) Live CHO cells transfected with luciferase were incubated with varying concentrations of FAAH inhibitor for five minutes and then imaged with CycLuc1 methyl amide (10 μM). (B) Live HeLa cells co-transfected with luciferase and human FAAH were incubated with varying concentrations of FAAH inhibitor for five minutes and then imaged with CycLuc1 methyl amide (10 μM). The assays were performed in triplicate and are represented as the mean ± SEM. Data was fit by nonlinear regression to log(inhibitor) vs. response (three parameters) to determine relative IC_{50} values. CHO cell IC_{50} values: PF3845, 12 nM; URB597, 2.7 nM; URB937, 16 nM. HeLa cell IC_{50} values: PF3845, 86 nM; URB597, 31 nM; URB937, 57 nM.

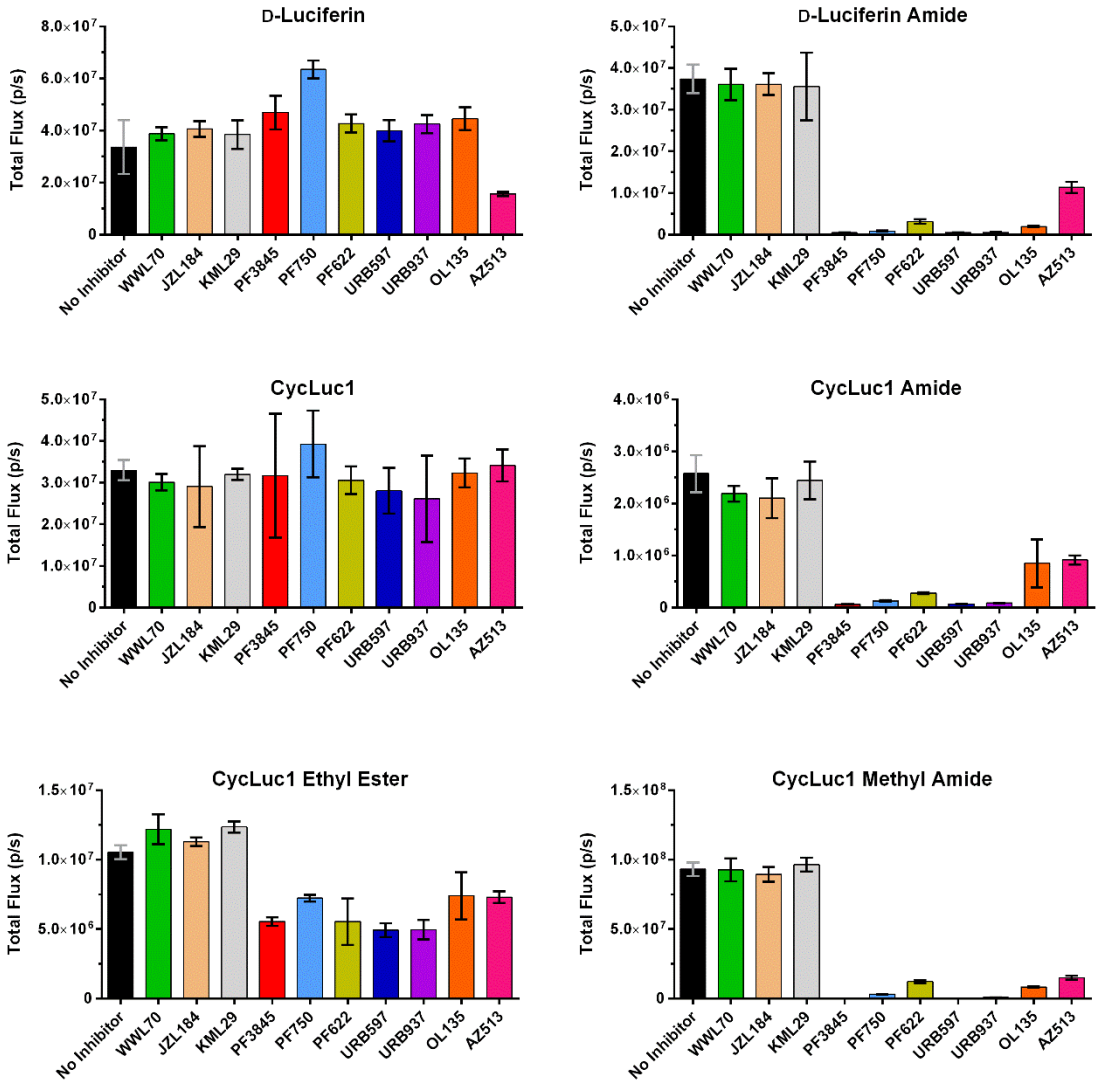

Figure 6.7. Luciferin amides report on FAAH activity in live CHO cells. Live CHO cells transfected with luciferase were incubated with 1 μM of the indicated serine hydrolase inhibitor for five minutes and then imaged with the indicated luciferin analog (10 μM). All assays were performed in triplicate and are represented as the mean ± SEM. FAAH inhibitors: PF3845, PF750, PF622, URB597, URB937, OL135, and AZ513; MAGL inhibitors: JZL184 and KML29; ABHD6 inhibitor: WWL70 (Bandiera et al., 2014).

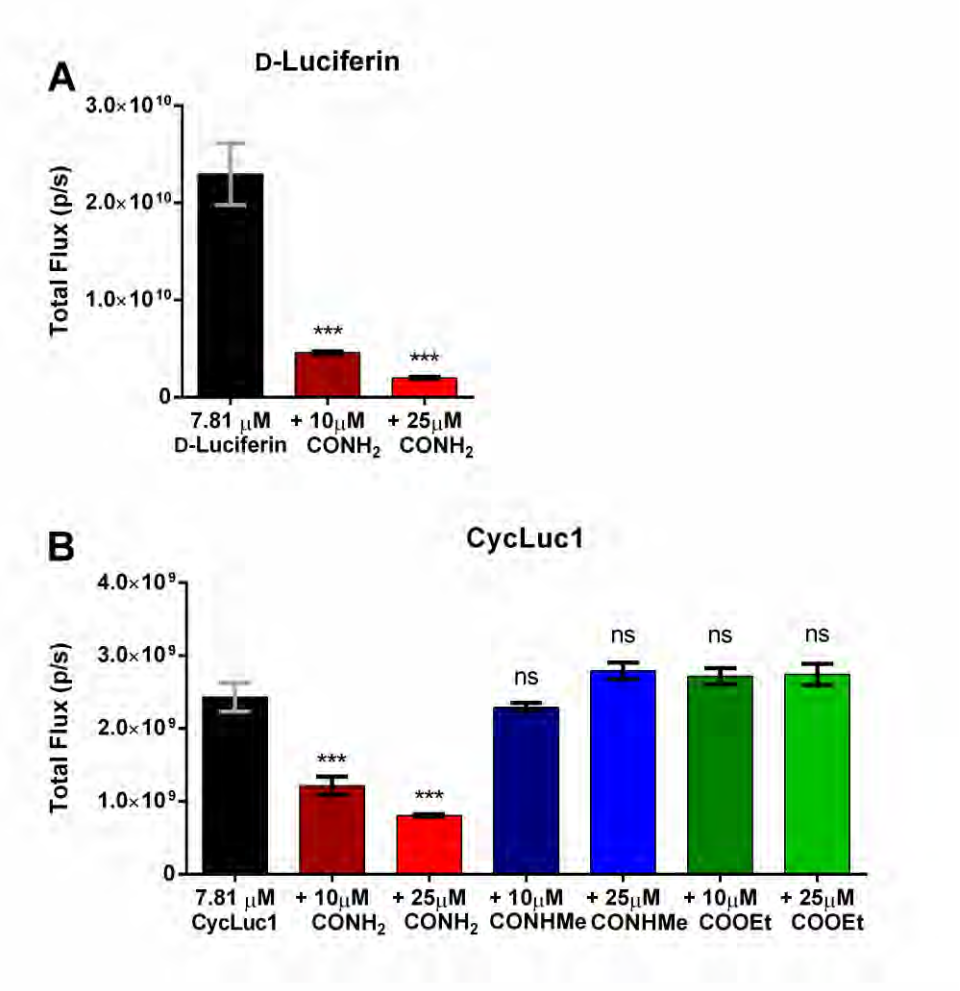

Figure 6.8. Luciferin primary amides can inhibit luciferase in vitro. (A) Purified firefly luciferase treated with 7.81 μM D-luciferin alone or in the presence of 10 μM or 25 μM D-luciferin amide. (B) Purified luciferase treated with 7.81 μM CycLuc1 alone or in the presence of 10 μM or 25 μM of CycLuc1 amide, CycLuc1 methyl amide, or CycLuc1 ethyl ester. The assay was performed in triplicate and is represented as the mean ± SEM. Each amide was compared to luciferin only by t-test. ns: not statistically significant; *** P <0.001.

HeLa cells do not express FAAH (Day et al., 2001; Dickason-Chesterfield et al., 2006), and luciferin amides do not yield bioluminescence in luciferase-expressing HeLa cells (**Figure 6.4B**). Transfection of HeLa cells with human FAAH enabled bioluminescence with luciferin amides (**Figure 6.4B** and **Figure 6.5**). Specific inhibition of the transfected FAAH with PF3845 blocked bioluminescence (**Figure 6.4B**) and the potency of FAAH inhibitors could be evaluated in these FAAH-transfected live cells (**Figure 6.6**). FAAH has been shown to cleave some fatty acid esters (Patricelli and Cravatt, 1999), and we find that it indeed also contributes to the cleavage of CycLuc1 ethyl ester (**Figure 6.9**). However, unlike CycLuc1 amides, the ethyl ester of CycLuc1 is not exclusively cleaved by FAAH and is hydrolyzed to CycLuc1 in both CHO and HeLa cells (**Figure 6.9**).

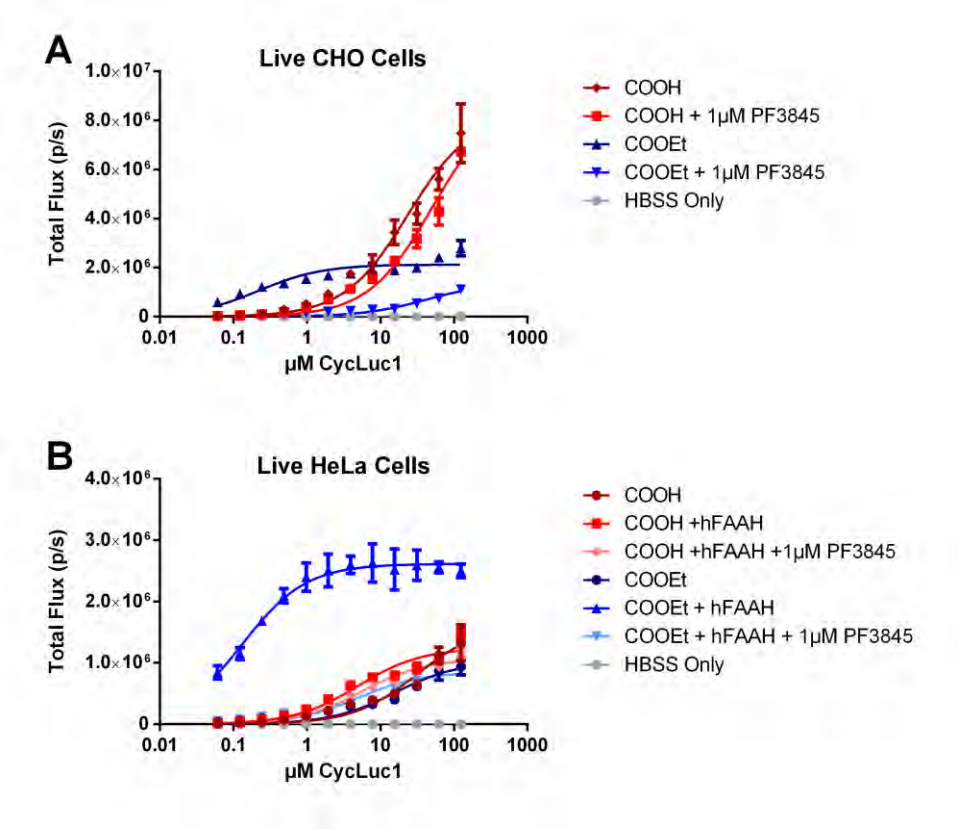

Figure 6.9. CycLuc1 ethyl ester supports bioluminescence from both live CHO and HeLa cells. (A) Live CHO cells transfected with luciferase were incubated with 1 μM PF3845 for five minutes and then imaged with varying concentrations of either CycLuc1 or CycLuc1 ethyl ester. (B) Live HeLa cells co-transfected with either luciferase and human FAAH or luciferase and empty vector were incubated with 1 μM PF3845 for five minutes and then imaged with varying concentrations of either CycLuc1 or CycLuc1 ethyl ester. The assay was performed in triplicate and is represented as the mean ± SEM. Curves were fit to the Michaelis–Menten equation by nonlinear regression.

In mice, FAAH is highly expressed in the brain (Long et al., 2011). We thus expected that luciferin amides would result in strong brain bioluminescence in luciferase-expressing mice if able to access this tissue. We used adeno-associated virus 9 (AAV9) to express luciferase only in the brain striatum (Evans et al., 2014). The amides are less water-soluble than the parent carboxylates,

necessitating a lower imaging dose. Nonetheless, CycLuc1 amide yielded dramatically higher photon flux in these mice than the parent luciferin CycLuc1 or the conventional substrate D-luciferin (**Figure 6.10**). A 400-fold lower dose of CycLuc1 amide was markedly superior to the standard imaging dose of D-luciferin (**Figure 6.10**). Even 1,000-fold lower doses yielded higher brain bioluminescence than D-luciferin (**Figure 6.11**).

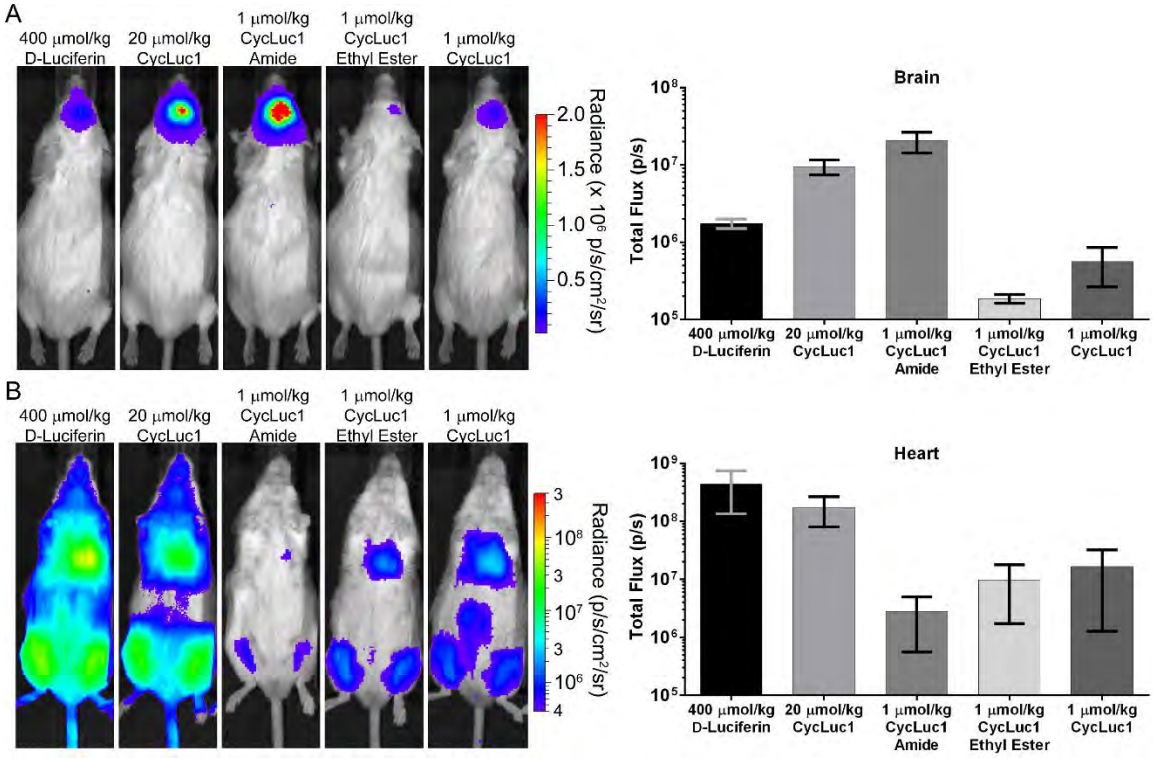

Figure 6.10. Bioluminescence from mice that express luciferase in specific tissues after treatment with luciferins and luciferin amides. CycLuc1 amide compared to D-Luciferin for bioluminescence imaging in live mice expressing luciferase in (A) the brain or (B) the heart and leg muscles. Quantification is represented as the mean ± SEM for n = 3 mice.

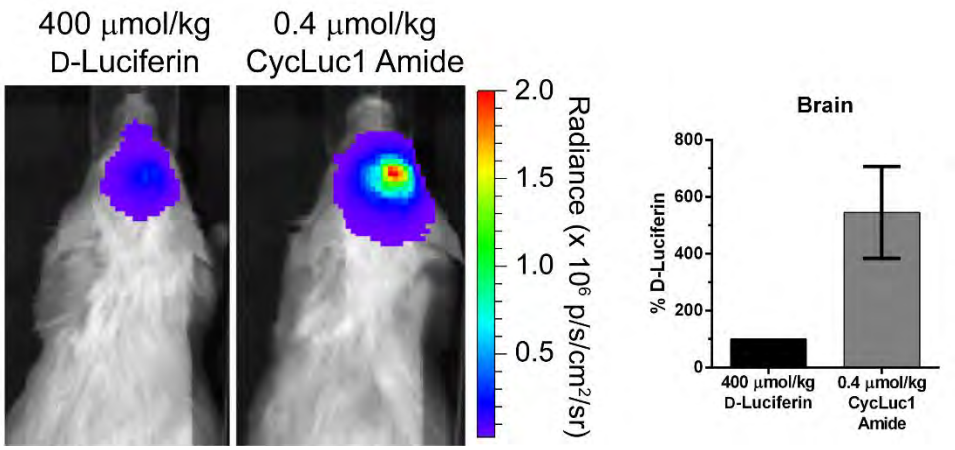

Figure 6.11. CycLuc1 amide increases total photon flux from the brain at 1,000-fold lower dose than D-luciferin. Mice striatally injected with AAV9-CMV-luc2 were treated with 0.4 μmol/kg CycLuc1 amide or 400 μmol/kg D-luciferin. Quantification was normalized to D-luciferin signal for each mouse and is represented as the mean ± SEM for n=3 mice.

Pretreatment with PF3845 (**Figure 6.2**), which has been demonstrated to inhibit only FAAH in mice (Ahn et al., 2009), completely blocked brain bioluminescence when using luciferin amides (**Figure 6.12**). Tail-vein injection of AAV9-CMV-luc2 primarily transduces heart (Inagaki et al., 2006) and leg muscles (**Figure 6.10**), tissues where FAAH activity has been reported to be absent (Long et al., 2011). In these mice, luciferin amides yielded dramatically lower photon flux than could be achieved with their parent luciferins (**Figure 6.10**). By contrast, CycLuc1 ethyl ester was on par with equal doses of the parent luciferin in the heart and leg muscles, but ineffective in the brain (**Figure 6.10**). These differences likely reflect the location of the liberating enzymatic activity and biodistribution of the more hydrophobic ester.

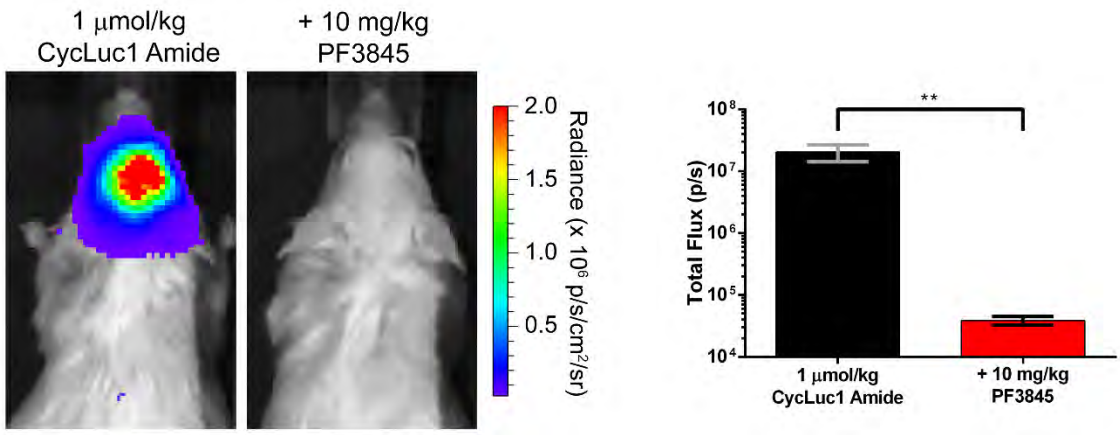

Figure 6.12. Inhibition of FAAH by PF3845 results in loss of signal from CycLuc1 amide in the brain. Mice striatally injected with AAV9-CMV-luc2 were imaged with CycLuc1 amide alone or after pre-treatment with 10 mg/kg PF3845. Quantification is represented as the mean ± SEM for n=3 mice and was compared by t-test. ** P <0.01.

To visualize FAAH activity throughout the mouse, we next turned to transgenic mice that express luciferase in all tissues (Cao et al., 2004). When D-luciferin or CycLuc1 is introduced into these mice, the weakest light emission is from the head, and bioluminescence is dominated by superficial tissues (**Figure 6.13** and **Figure 6.14**). In marked contrast, injection of CycLuc1 amide revealed the strongest bioluminescence signals from the brain and kidneys (**Figure 6.13**), tissues known to have high FAAH activity (Long et al., 2011). Ventral bioluminescence was less well-defined, which may reflect rapid transit of released luciferin out of FAAH-expressing tissues such as the liver (**Figure 6.14**). Pretreatment of mice with PF3845 completely blocked bioluminescence from luciferin amides in the brain and in all peripheral tissues (**Figure 6.13**, **Figure 6.15**, and **Figure 6.16**) but had no effect on bioluminescence from the parent

luciferins (**Figure 6.17**). The aminoluciferin amides (**Figure 6.1**) readily sense FAAH activity in vivo (**Figure 6.14**), and can be imaged at extremely low doses (as low as 8 nmol/kg; **Figure 6.18**). Although D-luciferin amide senses FAAH activity in vitro and in live cells, it works poorly in live mice and cannot sense FAAH activity in the brain (**Figure 6.14**). This is consistent with our contention that the improved biodistribution properties of aminoluciferins and low K_m values render them superior for use as luminogenic sensors in vivo (Adams and Miller, 2014). Interestingly, CycLuc1 methyl amide did not exhibit an advantage over CycLuc1 amide in the mouse (**Figure 6.14**). Presumably, inhibition of luciferase by uncleaved luciferin primary amides is not an issue at the substrate concentrations achieved in vivo.

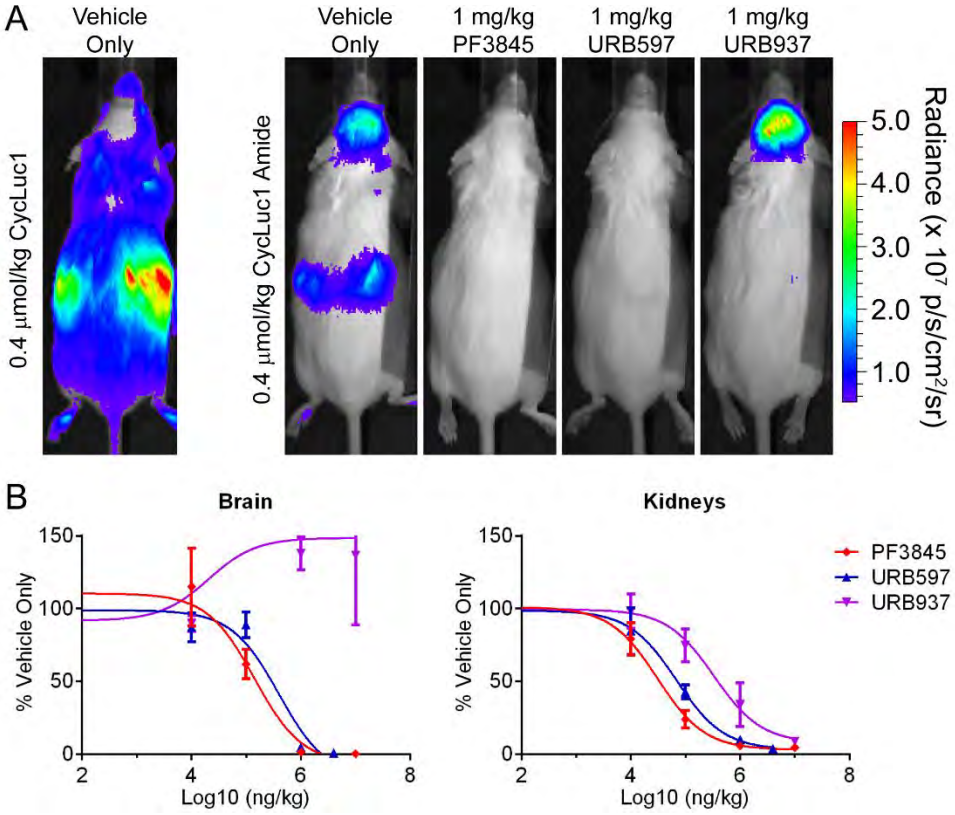

Figure 6.13. Luciferin amides report on FAAH activity in live mice that ubiquitously express luciferase. (A) Bioluminescence imaging with CycLuc1 or CycLuc1 amide in ubiquitously expressing transgenic luciferase mice treated with vehicle only or the indicated FAAH inhibitor. (B) Total flux from the brain and kidneys quantitated as a function of inhibitor concentration and normalized to the vehicle-only signal, represented as the mean ± SEM for n = 3 mice. Data were fit by nonlinear regression to determine relative IC_{50} values in the brain (PF3845, 0.14 mg/kg; URB597, 0.40 mg/kg; URB937, ND) and kidneys (PF3845, 0.03 mg/kg; URB597, 0.07 mg/kg; URB937, 0.33 mg/kg).

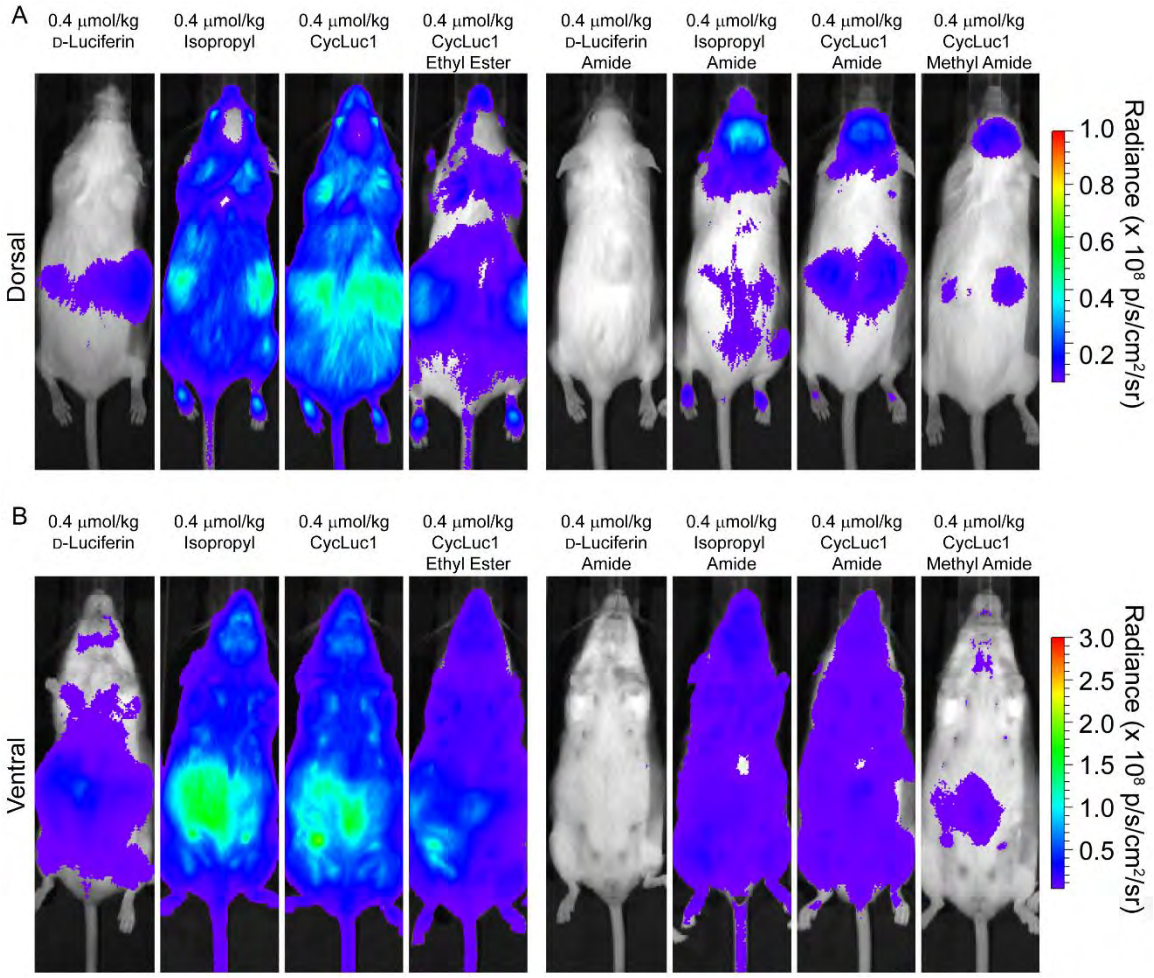

Figure 6.14. Bioluminescence from mice that ubiquitously express luciferase after treatment with luciferins and luciferin amides. (A) Dorsal view of FVB-Tg(CAG-luc) mice injected with the indicated substrate. (B) Ventral view of mice in (A).

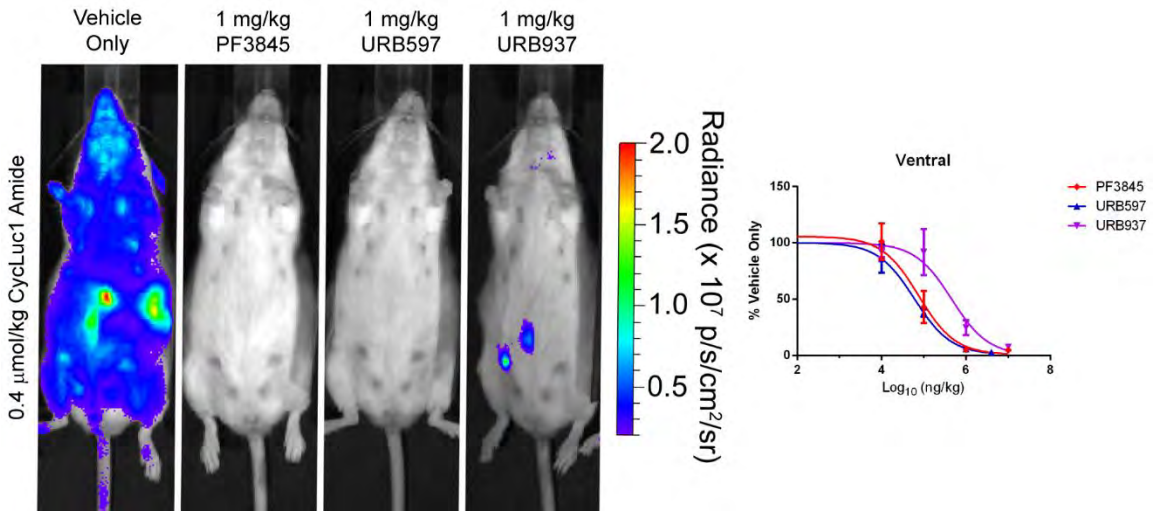

Figure 6.15. Ventral view of ubiquitously-expressing luciferase mice treated with CycLuc1 amide. Mice were pre-treated with vehicle only (18:1:1 PBS:Kolliphor:ethanol), or the indicated FAAH inhibitors. Quantification was normalized to the average vehicle-only signal and is represented as the mean ± SEM for n=3 mice. Data was fit by nonlinear regression to determine relative ventral IC_{50} values (PF3845: 0.08 mg/kg, URB597: 0.06 mg/kg, URB937: 0.46 mg/kg).

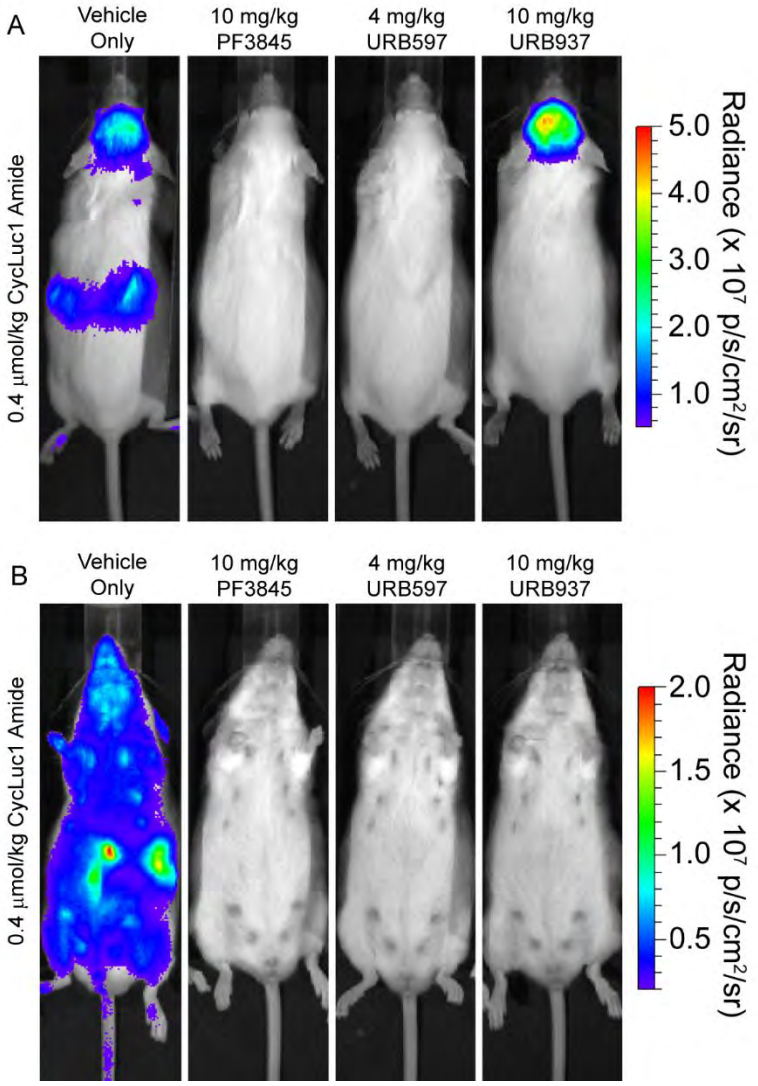

Figure 6.16. Mice ubiquitously-expressing luciferase treated with high inhibitor dose. Mice were pre-treated with vehicle only (18:1:1 PBS:Kolliphor:ethanol), or the indicated FAAH inhibitors and imaged with CycLuc1 amide.

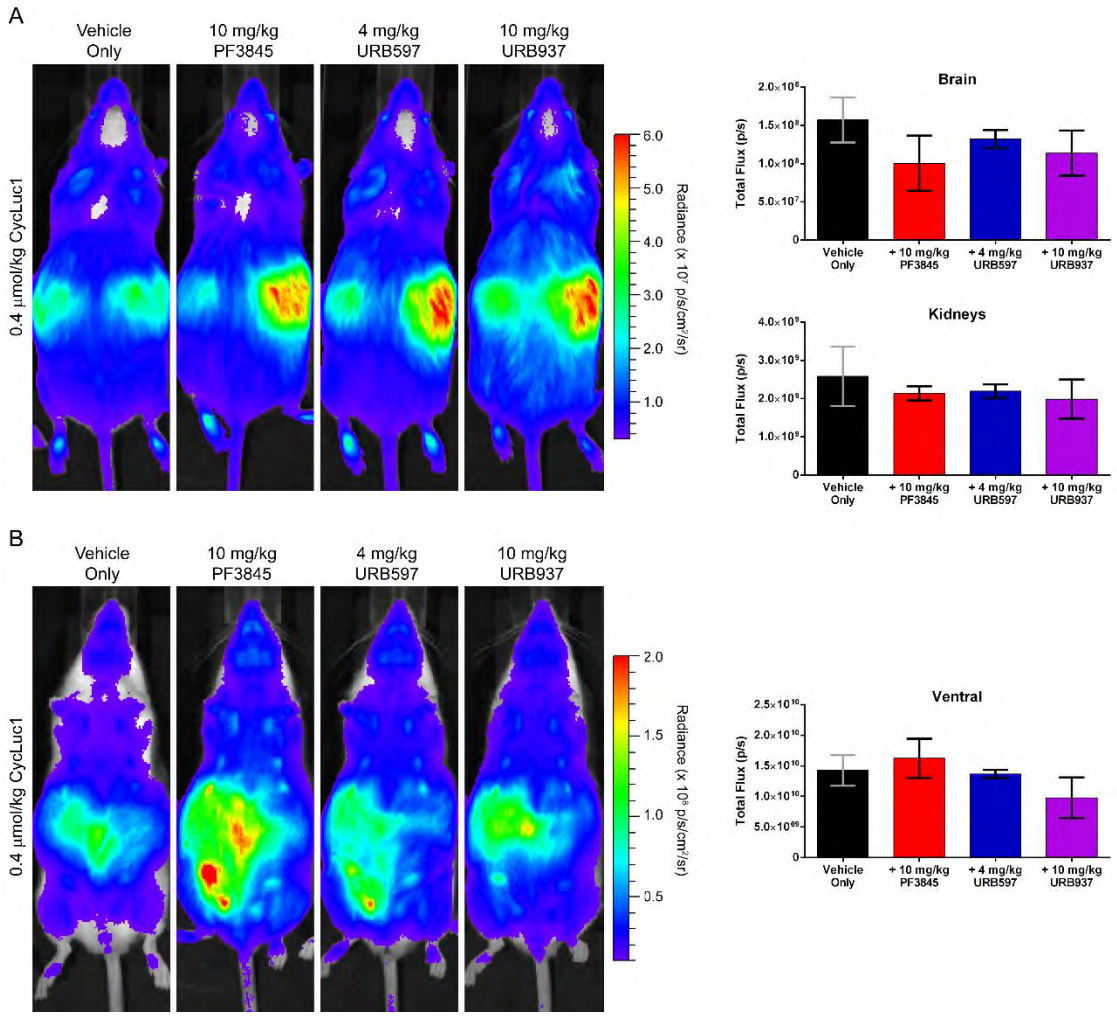

Figure 6.17. FAAH inhibitors do not affect parent luciferins. (A) Dorsal view of live FVB-Tg(CAG-luc) mice, injected with the indicated inhibitor and treated with CycLuc1. (B) Ventral view of mice in (A). Quantification is represented as the mean ± SEM for n=3 mice. Each inhibitor was compared to vehicle only by t-test. No statistically significant difference was found for any inhibitor.

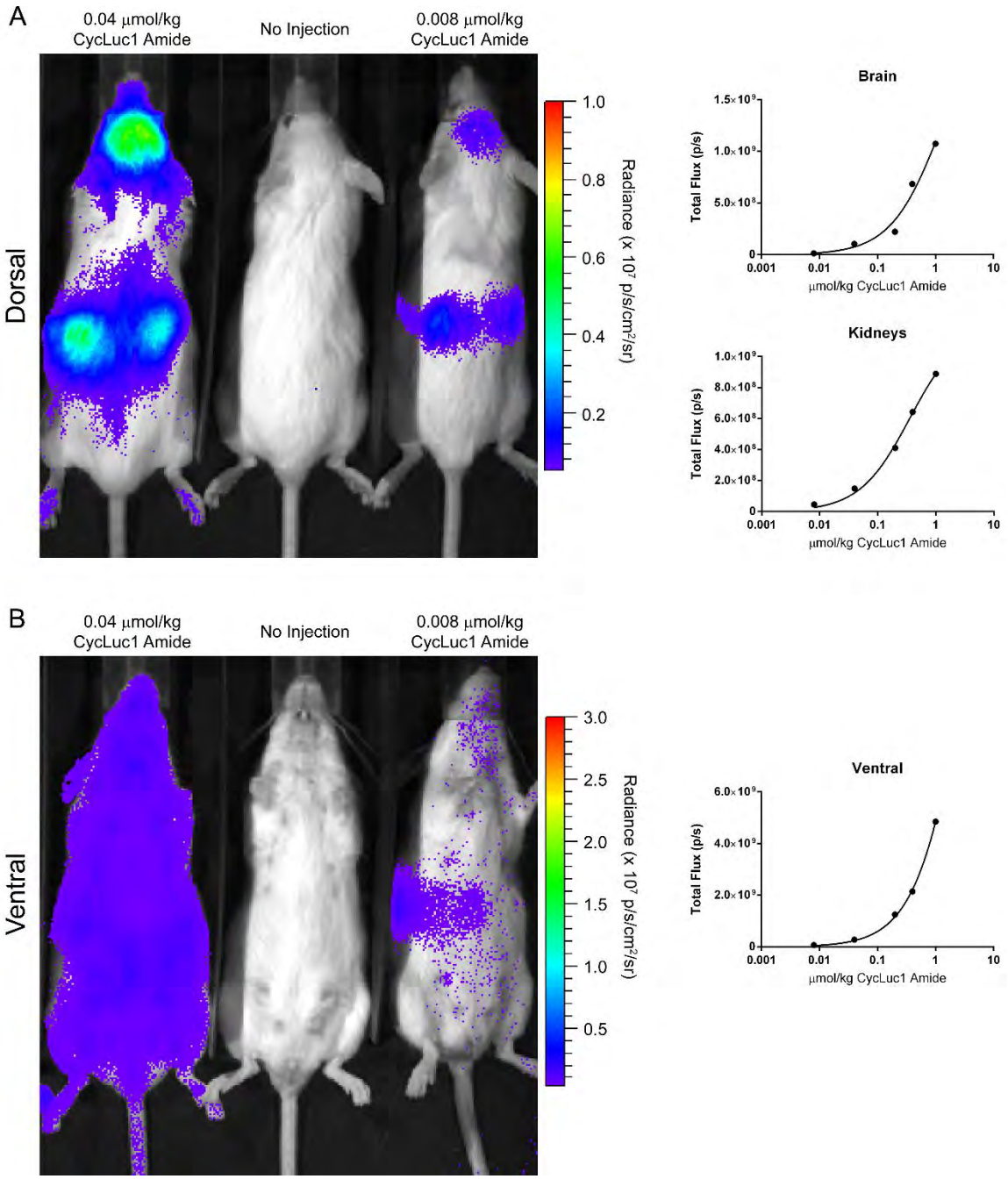

Figure 6.18. CycLuc1 amide can be imaged at doses as low as 8 nmol/kg and signal is not saturated at 1 µmol/kg. (A) Dorsal view of FVB-Tg(CAG-luc) mice injected with the indicated concentration of CycLuc1 amide. (B) Ventral view of mice in (A). Quantification is represented as n=1 mouse per substrate dose.

Finally, we sought to determine whether luciferin amides could be used to evaluate the tissue distribution of prospective FAAH inhibitors, which can have important effects on their efficacy (Clapper et al., 2010). URB937 is a brain-impermeable FAAH inhibitor that differs from the global FAAH inhibitor URB597 by a single hydroxyl group (Clapper et al., 2010) (**Figure 6.2**). Bioluminescence imaging with CycLuc1 amide confirmed that URB597 inhibits FAAH activity in both peripheral and brain tissues (**Figure 6.13**, **Figure 6.15**, and **Figure 6.16**), whereas no inhibition of FAAH activity is detected in the brains of URB937-treated mice (**Figure 6.13**).

Many bioluminescent sensors have been described based on “caged” pro-luciferins that can release a luciferin upon the action of an enzyme or reactive small molecule (Adams and Miller, 2014; Van de Bittner et al., 2013). The labile moiety is distinct from the luciferin and often separated by a self-immolative linker (Carl et al., 1981). A limitation of this approach is that the luciferin itself is not contributing to specific recognition or selectivity; the best one can hope for is that its presence is innocuous. Our approach embraces the inherent fatty acid mimetic properties of luciferin analogs to create sensors for enzymes that release fatty acids. The power of this approach is borne out in the exquisite specificity and sensitivity of luciferin amides for FAAH even in vivo, simply by replacing an oxygen atom with nitrogen (**Figure 6.1**). Furthermore, we find that luminogenic sensors based on high-affinity, cell-permeable aminoluciferins perform better in mice than those based on D-luciferin. As the number of structurally distinct

luciferin analogs grows (Adams and Miller, 2014; Mofford et al., 2014b), we anticipate there will be additional opportunities to build sensors based on the inherent properties of the luciferin itself.

In summary, we have found that luciferin amides are highly sensitive and selective reporters of FAAH activity. These sensors readily translate from in vitro assays to live cells to in vivo imaging to report on the activity of a single enzyme in its natural context. The bioluminescence approach described herein reveals otherwise invisible endogenous enzymatic activity in live cells and mice and more broadly allows imaging of the biodistribution consequences of subtle modifications to a prospective therapeutic inhibitor in vivo (e.g., ability to cross the blood-brain barrier). Further refinement and modification of the structure of the luciferin (Adams and Miller, 2014; Mofford et al., 2014b) and the scissile bond could potentially allow extension of this bioluminescence detection approach to other enzymes (Bandiera et al., 2014; Long and Cravatt, 2011). Finally, luciferin amides are excellent reagents for increasing the sensitivity of bioluminescence imaging in FAAH-expressing cells and tissues, such as the brain, and allow orders of magnitude lower imaging doses than the natural luciferase substrate.

Materials and Methods

Collaborators

Gadarla Randheer Reddy of the Miller Lab: Synthesis of all synthetic luciferins

Kiran Reddy of the Miller Lab: Synthesis of all luciferin amides

Spencer Adams of the Miller Lab:

Training and assistance with mouse imaging. Tail-vein injection of AAV.

General

Chemicals for synthesis were obtained from Aldrich. D-luciferin was obtained from Anaspec for in vitro work and from Gold Bio for mouse work. Serine hydrolase inhibitors were purchased from Cayman. CycLuc1 was synthesized as previously described (Reddy et al., 2010). Protein concentrations were determined using Coomassie Plus (Thermo Scientific). Immobilized glutathione (Thermo Scientific) was used for glutathione S-transferase (GST)-tagged protein purification. Kolliphor® EL was obtained from Sigma Life Sciences (Stock # C5135) Data were plotted and analyzed with GraphPad Prism 6.0. High resolution mass spectral data were recorded on a Waters QTOF Premier spectrometer (University of Massachusetts Medical School Proteomics and Mass Spectrometry Facility). Bioluminescence assays were performed on a Xenogen IVIS-100 system in the Small Animal Imaging facility. Data acquisition and analysis were performed with Living Image® software. Data are reported as total flux (p/s) for each region of interest (ROI). For in vitro and cellular assays, the

ROIs correspond to each well of a 96-well plate. For in vivo assays, the ROIs correspond to the indicated region of a mouse.

Plasmid constructs

Human and rat FAAH genes (hFAAH and rFAAH) were purchased from the Mammalian Gene Collection of Thermo Fisher Scientific (clone IDs: hFAAH 5728192, rFAAH 7370226). Residues 30-579 of the rFAAH gene were PCR-amplified and cloned into the EcoRI and NotI sites of pGEX6P-1, resulting in removal of the N-terminal transmembrane domain (Mileni et al., 2008). Full length hFAAH was PCR-amplified and cloned into the KpnI and NotI sites of pcDNA3.1 to yield pcDNA3.1-hFAAH.

Protein expression and purification

Rat FAAH (30-579) and firefly luciferase were expressed as GST-fusion proteins using the pGEX6P-1 vector in the *E. coli* strain JM109. Cells were grown at 37 °C until the OD600 reached 0.5-1, induced with 0.1 mM IPTG, and incubated at 20°C overnight. Cells were pelleted at 5,000 RPM in a Sorvall 2C3C Plus centrifuge (H600A rotor) at 4 °C for 15 min, then flash frozen in liquid nitrogen. *E. coli* pellets from 1 L of culture were thawed on ice, resuspended in 25 mL lysis buffer (50 mM Tris [pH 7.4], 500 mM NaCl, and 0.5% Tween 20) containing 1 mM phenylmethylsulfonyl fluoride, and disrupted by sonification (Branson Sonifier). Dithiothreitol (DTT) was added at 10 mM, and the resulting

cell lysate was clarified by centrifugation at 35,000 RPM in a Beckman 50.2 Ti rotor for 60 min at 4 °C. The supernatant was batch-bound to immobilized glutathione for 1 hr at 4 °C, and the beads were washed with lysis buffer containing 10 mM DTT, followed by wash buffer (50 mM Tris [pH 8.1], 250 mM NaCl, and 10 mM DTT) and storage buffer (50 mM Tris [pH 7.4], 0.1 mM EDTA, 150 mM NaCl, 1 mM TCEP). Twenty units of PreScission Protease (GE Healthcare) were added, and incubated overnight at 4 °C to cleave the GST-fusion and elute the untagged protein into storage buffer.

Purified protein rFAAH activity assays

FAAH inhibitors were prepared at 4 μM in substrate buffer (20 mM Tris [pH 7.4], 0.1 mM EDTA, 8 mM $MgSO_4$, and 4 mM ATP). Luciferins and luciferin amides were prepared at 40 μM in substrate buffer. Luciferase and rFAAH were prepared at 400 nM in enzyme buffer (20 mM Tris [pH 7.4], 0.1 mM EDTA, 1 mM TCEP, and 0.8 mg/mL BSA). In a black 96-well plate (Costar 3915), 25 μL FAAH inhibitor or substrate buffer was added to three wells each. rFAAH (25 μL) or enzyme buffer was added to the inhibitor and incubated at ambient temperature for 5 minutes. Luciferin or luciferin amide (25 μL) was then added to each well and incubated at ambient temperature for 20 minutes. Luminescence was then initiated by adding 25 μL of luciferase. Imaging was performed one minute after luciferase addition and integrated for 2-20s at a final concentration of 1 μM FAAH inhibitor, 10 μM luciferin, 100 nM rFAAH, and 100 nM luciferase.

Purified rFAAH dose-response assays

Purified rFAAH was prepared at concentrations ranging from 8 μM to 3.91 nM in enzyme buffer. Luciferin amides were prepared at 20 μM in substrate buffer. Luciferase was prepared at 400 nM in enzyme buffer. In a black 96-well plate (Costar 3915), 50 μL of each luciferin amide was added per well. rFAAH (25 μL) was then added to the amide and incubated at ambient temperature for 30 minutes. Luminescence was then initiated by adding 25 μL of luciferase. Imaging was performed one minute after luciferase addition for 2-20s at a final concentration of 2,000 nM to 0.977 nM rFAAH, 10 μM luciferin amide, and 100 nM luciferase.

Luciferin amide inhibitor assays with purified luciferase

Luciferin amides were prepared at 40 μM or 100 μM in substrate buffer. Luciferins were prepared at concentrations from 1,000 μM to 0.488 μM in substrate buffer. Luciferase was prepared at 200 nM in enzyme buffer. In a black 96-well plate (Costar 3915), 25 μL luciferin amide or substrate buffer was added to three rows each. Luciferin (25 μL) was added to the luciferin amide. Luminescence was then initiated by adding 50 μL of luciferase. Imaging was performed one minute after luciferase addition for 2-20s at a final concentration of 0 μM, 10 μM, or 25 μM luciferin amide, 250 μM to 0.122 μM luciferin, and 100 nM luciferase.

Cell culture

Chinese hamster ovary (CHO) cells and HeLa cells were grown in a CO_2 incubator at 37°C with 5% CO_2 and were cultured in F-12K Nutrient Mixture (GIBCO) and Dulbecco's Modified Eagle's Medium (DMEM) (GIBCO), respectively. Both media were supplemented with 10% fetal bovine serum and 100 U/mL penicillin/streptomycin.

Transfections

CHO cells were transfected with codon-optimized firefly luciferase (luc2) as previously described (Mofford et al., 2014b). HeLa cells were transfected with pcDNA3.1-luc2 plasmid (Mofford et al., 2014b) and either pcDNA3.1- hFAAH or empty pcDNA3.1 vector. Transient transfections were performed at RT using Lipofectamine 2000 on cells plated at 60%–75% confluency in 96-well black tissue culture treated plates (Costar 3916). For CHO cells, 0.075 µg DNA/well of pcDNA3.1-luc2 was transfected; for HeLa cells, 0.0375 µg DNA/well each of pcDNA3.1-luc2 and either pcDNA3.1- hFAAH or empty pcDNA3.1 was transfected. Assays were performed in triplicate 24 hrs after transfection.

Live cell FAAH activity assays

Transfected cells were washed with HBSS. For substrate dose-response curves, the cells in 96-well plates were incubated with 50 µL of 2 µM FAAH inhibitor in HBSS or HBSS only at ambient temperature for 5 minutes. Then, 50 µL of 2x substrate was added to each well to achieve final substrate

concentrations ranging from 125 μM to 0.061 μM. For inhibitor dose-response curves, the cells in 96-well plates were incubated with 50 μL of 2x FAAH inhibitor in HBSS at ambient temperature for 5 minutes (final inhibitor concentrations ranging from 10 μM to 0.21 pM). Then, 50 μL of 2x substrate was added to each well to a final luciferin concentration of 10 μM. Imaging was performed three minutes after addition of substrate.

Mice

All of the experiments involving mice were conducted in accordance with the Institutional Animal Care and Use Committee of The University of Massachusetts Medical School (docket #A-2474-14). Female FVB mice and luciferase-expressing transgenic mice (FVB-Tg(*CAG-luc,-GFP*)L2G85Chco/FathJ) were purchased from Jackson Laboratories (Bar Harbor, ME). Striatal injection of AAV9-CMV-luc2 into FVB mice was performed as previously described (Evans et al., 2014).

Tail-vein injection of AAV

FVB mice were injected in the lateral tail vein with $1x10^{11}$ particles of AAV9-CMV-luc2 luciferase (Evans et al., 2014) suspended in sterile filtered PBS at a final volume of 200 μL. The mice were held under a heat lamp to warm the tail for better visualization of the lateral tail vein due to vasodilation and then placed into a Tailveiner (Braintree Scientific, Braintree, MA). The tails were

cleaned with a 70% isopropyl alcohol wipe and injection was performed using a 27.5 gauge needle. Once the needle was withdrawn, the tail was compressed with sterile gauze to ensure complete homeostasis. The mice were monitored afterwards for recovery of normal behavior before returning to their colony. Imaging was performed weeks to months after AAV injection.

Substrate and FAAH inhibitor preparation for mouse injection

All FAAH inhibitors were prepared by direct dissolution into 18:1:1 PBS:Kolliphor:ethanol and sterile filtering through a 0.22 μm syringe filter. Each inhibitor was injected intraperitoneally (i.p.) at 5 μL/g mouse. Inhibitors were prepared at 2 mg/mL, 0.2 mg/mL, 0.02 mg/mL, and 0.002 mg/mL to achieve final concentrations of 10 mg/kg, 1 mg/kg, 0.1 mg/kg, and 0.01 mg/kg respectively. Due to limited solubility, URB597 was prepared at 0.4 mg/mL and injected at 10 μL/g to achieve a dose of 4 mg/kg. D-luciferin (100 mM) and CycLuc1 (5 mM) were prepared by direct dissolution into PBS and were sterile filtered through a 0.22 μm syringe filter. All other luciferins were prepared by diluting a 50 mM DMSO stock into PBS and sterile filtering through a 0.22 μm syringe filter. CycLuc1 ethyl ester was not soluble in PBS and was therefore prepared by diluting the 50 mM DMSO stock into 18:1:1 PBS:Kolliphor:ethanol. Each substrate was injected i.p. at 4 μL/g mouse. Substrates were prepared at 100 mM (D-Luciferin), 5 mM (CycLuc1), 250 μM (substrates for AAV mice), and 100

μM (substrates for FVB-Tg[CAG-luc] mice) to achieve final concentrations of 400 μmol/kg, 20 μmol/kg, 1 μmol/kg, and 0.4 μmol/kg respectively.

Bioluminescence imaging of mice

Each mouse was weighed to determine substrate and/or FAAH inhibitor dosing and anesthetized using 2.5% isoflurane in 1 L/min oxygen. FAAH inhibitors were injected i.p. at 5 μL/g mouse 30 minutes prior to luciferin injection. Luciferin substrate was injected i.p. at 4 μL/g mouse and mice were imaged dorsally at 10 minutes and ventrally at 13 minutes.

CHAPTER VII:

Luciferin Amides and Imaging in the Brain Discussion

AKA: “Luciferins Behave Like Drugs”

Mofford, D.M., and Miller, S.C. (2015). *ACS Chem. Neurosci.* 6(8), 1273–1275.

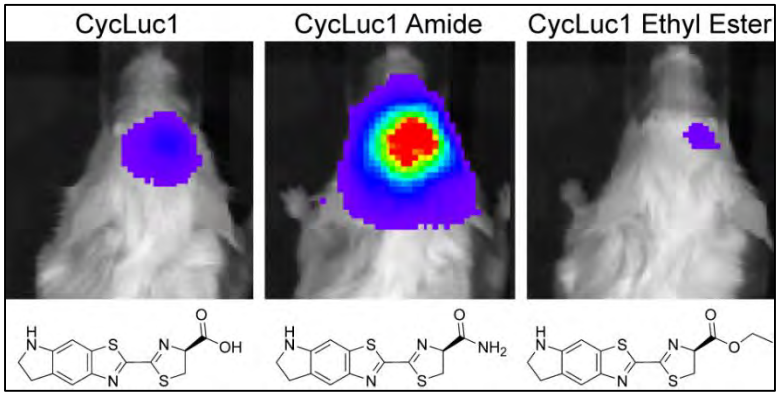

Summary

The light emission chemistry of firefly luciferase can be harnessed to reveal otherwise invisible biological processes occurring in the brains of live animals. Though powerful, the need for the luciferase substrate D-luciferin to traverse the blood-brain barrier poses limitations on the sensitivity and interpretation of these experiments. In this Viewpoint, we discuss bioluminescent imaging probes for the enzyme fatty acid amide hydrolase (FAAH) and the broader implications for optical imaging and drug delivery in the brain.

Viewpoint

Luciferins do not treat disease, but in many ways these exogenous molecules act like drugs. Instead of a eliciting a therapeutic response, luciferins emit light when they encounter their target (luciferase). If you want to light up the brain in a luciferase-expressing mouse, you essentially have a drug delivery problem: how to get across the blood-brain barrier. Generally, this means you want a molecule that is small (<500 MW), lipophilic enough to readily diffuse across cell membranes, and preferably not a substrate for the armada of efflux pumps poised at the border, ready to send your molecule packing. D-Luciferin, the substrate for firefly luciferase, gets a gold star for small size, but everything else has room for improvement.

Fireflies produce light by the oxidation of D-luciferin to an excited-state molecule (**Figure 7.1**). Recent work has shown that the enzyme firefly luciferase will accept many substrate analogues, allowing tuning of the molecular properties of the luciferin (Adams and Miller, 2014; Mofford et al., 2015). These synthetic luciferins are not necessarily “better” than the natural substrate. Indeed, if firefly luciferase is provided with a saturating concentration of luciferin in a test tube, the rate of photon emission is higher with the natural substrate D-luciferin than with any synthetic luciferin analogue yet made (Adams and Miller, 2014). However, in vivo, and particularly in the brain, the access of D-luciferin is limited. Saturating levels of D-luciferin are not achieved after intraperitoneal (IP) injection into live mice (Aswendt et al., 2013). Under these conditions, luciferin analogues

with higher cell permeability and lower K_m values for luciferase can perform better than the natural substrate, and do so at substantially lower imaging doses (Adams and Miller, 2014; Mofford et al., 2015).

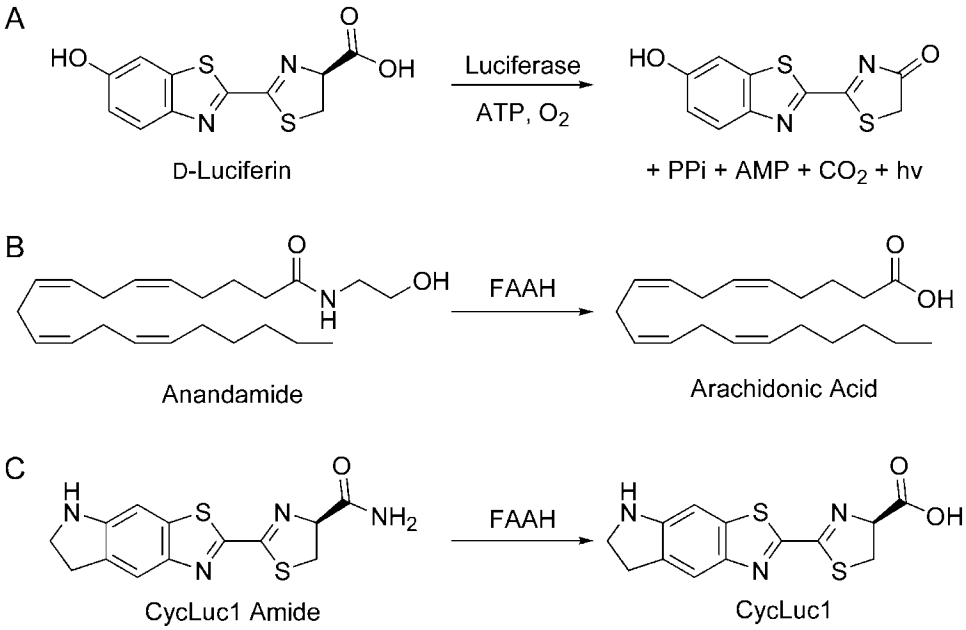

Figure 7.1. Enzyme catalyzed reactions. (A) Firefly luciferase oxidizes its substrate D-luciferin to emit light. This chemistry requires a free carboxylate. (B) FAAH hydrolyzes anandamide and many other fatty acid amides. (C) Luciferin amides can be hydrolyzed by FAAH to unmask substrates for luciferase (Mofford et al., 2015).

A complete picture of all the factors that restrict D-luciferin access to the brain has not yet emerged. In general, small lipophilic compounds can penetrate the blood-brain barrier (BBB), while large and/or hydrophilic compounds are excluded. D-Luciferin is small (<300 MW), but relatively polar. Its ability to access

the brain by simple diffusion is therefore expected to be modest. Furthermore, there are many efflux pumps (aka “drug resistance pumps”) that actively remove molecules from the brain. These include ABCG2, Pgp (ABCB1), MRP1 (ABCC1), and MRP4 (ABCC4) (Adams and Miller, 2014; Cheung et al., 2015). D-Luciferin was thought to be a substrate only for ABCG2 (Adams and Miller, 2014; Cheung et al., 2015). However, it has recently been reported to be a substrate for MRP4 as well (Cheung et al., 2015). The relevance of this finding for access to the brain has not yet been established.

It is important to be mindful of the role that the blood-brain barrier plays in restricting the access of the luciferin substrate. Some experimental techniques or disease states can disrupt the BBB. For example, injection of luciferase-expressing cells into the brain will disrupt the BBB, and immediate imaging of those injected cells is therefore unlikely to reflect an intact BBB. (Aswendt et al., 2013) And as recently demonstrated by Ayzenberg et al., (Ayzenberg et al., 2015) neuro-inflammation also has the potential to disrupt the BBB. The bioluminescent signal from D-luciferin may increase simply due to improved substrate access to brain tissue, and be confused with an increase in gene expression (Ayzenberg et al., 2015). Similarly, the growth of brain tumors that disrupt the BBB may also affect the interpretation of the resulting imaging data. Potentially, the use of luciferins that are less sensitive to BBB disruption could help avoid these issues.

Synthetic luciferin substrates with higher lipophilicity and lower K_m values for luciferase can improve imaging in the brain (Adams and Miller, 2014; Mofford et al., 2015) (**Figure 7.2**). These substrates are expected to more readily diffuse across cell membranes, and due to their lower K_m values less substrate is needed to saturate the luciferase. Changes to the luciferin structure may also affect efflux pump activity, but itis not yet clear if or how the efflux of synthetic luciferins from the brain differs from D-luciferin. All substrates for firefly luciferase require a free carboxylate. At physiological pH, the presence of an ionized carboxylate on the luciferin is thus another factor that limits its cell permeability and ability to cross the blood-brain barrier. This is where things get really interesting. Fatty acid amide hydrolase (FAAH) is the enzyme responsible for the hydrolysis of anandamide, an endogenous ligand for the cannabinoid receptor CB1 (**Figure 7.1**). We synthesized luciferin amides designed to be substrates for FAAH, a promising drug target for the treatment of pain and anxiety (Mofford et al., 2015). Cleavage of luciferin amides by FAAH liberates a luciferin substrate, allowing sensitive and specific bioluminescence detection of FAAH activity in the brain and periphery (Mofford et al., 2015). This was all by design- but what was surprising was that luciferin amides improve brain bioluminescence in live mice over both D-luciferin and their parent luciferins (Mofford et al., 2015) (**Figure 7.2**). Far less substrate is needed for imaging, and the photon flux is increased. Luciferin amides are acting as luciferin “pro-drugs”.

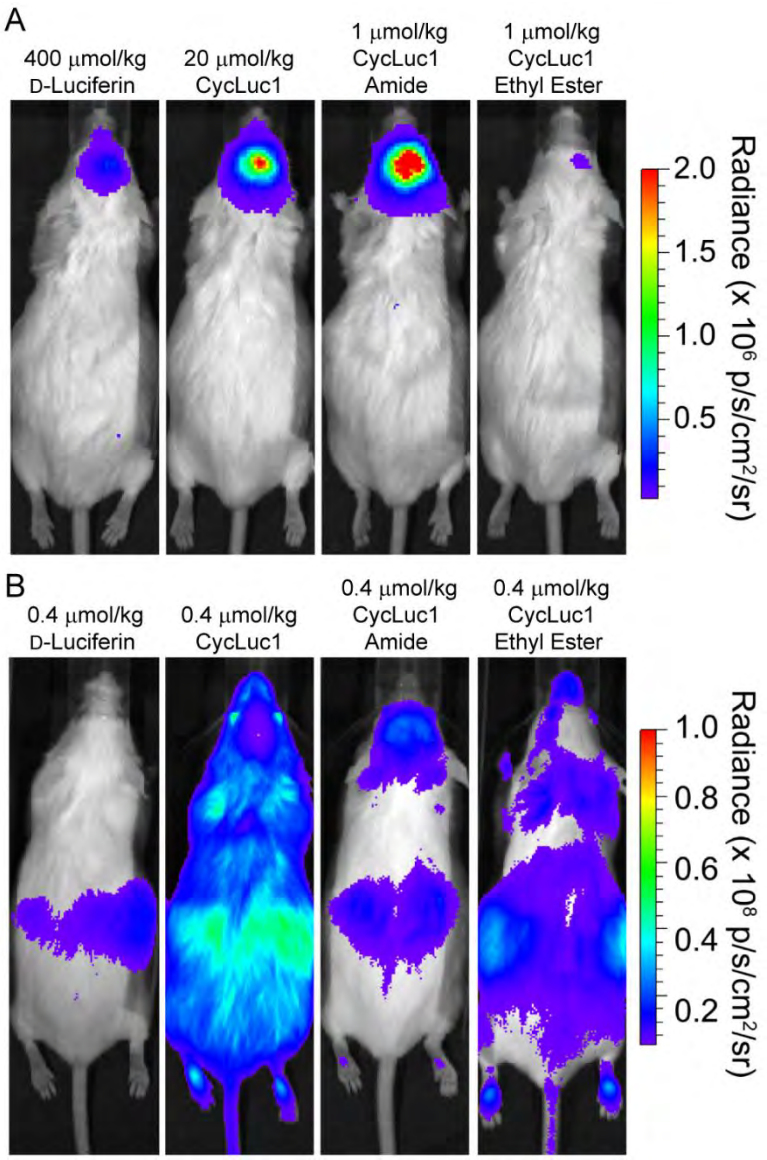

Figure 7.2. Bioluminescence imaging in luciferase-expressing mice. (A) Adeno-associated virus (AAV)9 was used to express luciferase only in the striatum of the brain. Photon flux from the same mouse was compared using the indicated luciferin analogue and dose (i.p. injection). (B) The same set of luciferin analogues was compared at equal dose in a transgenic mouse that ubiquitously expresses luciferase.

When imaging in mice that express luciferase in all tissues, bioluminescence is dominated by superficial tissues- wherever the luciferin goes, you will see light. A caveat of imaging in these mice is that emission from deep tissues that are harder to access is often obscured. This is particularly true in the head, where photon flux from the nose, eyes, ears, and tissue overlying the brain overshadows emission from the brain itself (**Figure 7.2**). Remarkably, it is the brain that yields the highest bioluminescence signal when these same mice are treated with luciferin amides (Mofford et al., 2015) (**Figure 7.2**). This reflects both the ability of luciferin amides to traverse the blood-brain barrier, and the high selectivity for cleavage to the light-emitting luciferin by FAAH.

Ask your average medicinal chemist how to improve the cellular delivery of a carboxylic acid, and they will say: make an ester. Esters are more lipophilic, and upon entry into cells are anticipated to be hydrolyzed to the carboxylic acid by “esterase activity” (where the specific enzyme or enzymes performing this activity are often unknown). Although luciferin esters can be hydrolyzed to their respective luciferins in cells and in mice, they have not been very effective at delivering luciferins into the brain (Mofford et al., 2015) (**Figure 7.2**). In part, this may be because “esterase activity” is everywhere. On the other hand, luciferin amides are exemplary at delivering synthetic luciferins into the brain, where endogenous FAAH activity liberates the parent luciferin (Mofford et al., 2015). Potentially, FAAH could be more generally exploited in a “pro-drug” strategy to specifically unmask a broader range of carboxylic acids in the brain. Somewhat

ironically, we find that FAAH is also responsible for some of the generic “esterase activity” toward luciferin esters, at least in tissue culture cells (Mofford et al., 2015).

Many optical imaging probes are too large or polar to efficiently enter the brain. Excitingly, bioluminescence imaging combines the specificity of a genetically encoded luciferase reporter with the versatility of a small yet highly tunable “drug-like” luciferin emitter, offering a wealth of opportunities to shed light on the inner workings of the brain, and also show how to get there.

CHAPTER VIII:

Discussion

Animals capable of glowing in the dark have fascinated people throughout history (Harvey, 1957). There are fish that make the oceans shimmer (Haddock et al., 2010), fungi that make the forests glow (Purtov et al., 2015), and beetles that light up the sky (Viviani, 2002). Our fascination with this phenomenon has led scientists on a long journey to determine why and how these creatures glow. The study of how an organism can emit light by bioluminescence is not only intriguing from an academic perspective, it has proven to be a useful tool to study numerous biological processes.

Bioluminescence imaging has become an invaluable resource for non-invasively reporting on biological functions, with the North American firefly, *Photinus pyralis*, providing the preferred reporter system (Welsh and Noguchi, 2012). The firefly luciferase enzyme is genetically encodable, stable in live cells and organisms (Welsh and Noguchi, 2012), and catalyzes light emission with a high quantum yield (Ando et al., 2008). Its substrate, D-luciferin, is small, stable, and easily synthesized (McCutcheon et al., 2015). Together, they can report on otherwise invisible events such as gene expression, enzyme activity, or protein/protein interactions by production of a readily detected photon of light (Badr and Tannous, 2011; Fan and Wood, 2007; Prescher and Contag, 2010).

Despite its numerous advantages, firefly bioluminescence is fundamentally limited by the photophysical properties of its substrate, D-luciferin. This molecule is relatively polar, has a modest affinity for firefly luciferase, and emits yellow-green light after catalysis by firefly luciferase (Fraga, 2008). All of these are areas that are less than optimal, especially for in vivo imaging. To overcome these shortcomings, in CHAPTER II, I discuss the development of synthetic luciferin analogs based on the core structure of D-luciferin (Mofford et al., 2014b; Reddy et al., 2010). These luciferins were designed to display red-shifted light emission, bringing the wavelength to a region where light is more able to penetrate through tissue (Mobley and Vo-Dinh, 2003; Weissleder and Ntziachristos, 2003). They also have increased affinity for luciferase (Harwood et al., 2011; Mofford et al., 2014b), so less substrate is required to saturate the enzyme; a particularly beneficial feature for use in live cells or animals where the cell membrane will limit access to the luciferase. Moreover, our modifications to the luciferin structure increase their hydrophobicity and lipophilicity, which should increase their cell permeability. Finally, D-luciferin is the only naturally occurring substrate for firefly luciferase and all other beetle luciferases. We hypothesized that structural differences between the synthetic luciferins described here could potentially be exploited to create selective luciferases, enabling discrimination between substrates for use without interference between signals.

Although the synthetic luciferins discussed in CHAPTER II may sound like the solution to all of the limitations of firefly bioluminescence, they are not without

their own flaws. The increased affinity for luciferase translates to an increase in product inhibition, and a decrease in the intensity of sustained light emitted in vitro (Harwood et al., 2011; Mofford et al., 2014b; Reddy et al., 2010). To date, no example of a synthetic substrate has actually improved on what is achievable with firefly luciferase and saturating conditions of D-luciferin (**Table 8.1**).

Table 8.1. Optimal enzyme/substrate pairs under various conditions.

Conditions	Enzyme	Substrate	Short Protocol	Other Considerations
in vitro	Wild-Type	D-luciferin	Add enzyme to 250 μM substrate. Measure light emitted after 1 minute.	Use at pH 7.4 with saturating Mg-ATP (2 mM).
Live Cells	R218K	CycLuc2	Overlay cells with 250 μM substrate. Measure light emitted after 3 minutes.	R218K + CycLuc12 gives highest flux at low substrate dose. May be more predictive of in vivo activity.
Cell Lysate	Wild-Type	D-luciferin	Add lysate to 250 μM substrate. Measure light emitted after 1 minute.	Use at pH 7.4 with saturating Mg-ATP (2 mM).
Dual Reporter	Wild-Type	D-luciferin	Add 250 μM D-luciferin. Measure light emitted after 1 minute from WT luciferase. Add 250 μM CycLuc7. Measure light emitted after 1 minute from Triple mutant. CycLuc7 product inhibition will inhibit WT signal.	Use Triple mutant to report on higher expression enzyme since WT + CycLuc7 gives higher background. Insufficient signal-to-noise for use in live cells. Use only in vitro or in lysate.
	R218K+L286M +S347A	CycLuc7		
Live Cells Near-IR	R218K	CycLuc2	Overlay cells with 250 μM substrate. Measure light emitted after 3 minutes.	R218K + CycLuc6 gives highest near-IR flux at low substrate dose. May be more predictive of in vivo activity.
FAAH Activity Assays				
in vitro	Wild-Type	CycLuc1 Methyl Amide	Add purified FAAH to 10 μM substrate. Incubate 30 minutes. Add luciferase. Measure light emitted after 1 minute.	Use at pH 7.4 with saturating Mg-ATP (2 mM).
Live Cells	Wild-Type	CycLuc1 Methyl Amide	Overlay cells with 10 μM substrate. Measure light emitted after 3 minutes.	Cells must express FAAH.
Live Mice	Wild-Type	CycLuc1 Amide	Inject mice intraperitoneally with 0.4 μmol/kg substrate. Measure light emitted after 10 minutes.	Mice must express luciferase in desired tissues.

Previous work in the lab identified several point mutations as beneficial for use with aminoluciferins (Harwood et al., 2011). For example, the R218K mutation generally improves the maximal photon flux from all of the aminoluciferins described in this chapter by reducing their affinity and limiting product inhibition. However, since all of the synthetic luciferins show increased photon flux, and D-luciferin remains a substrate with R218K, this single mutation is not sufficient to discriminate between substrates. We therefore combined R218K with the L286M and S347A mutations to create a triple mutant luciferase that not only increases the maximal rate of sustained light emission from several synthetic substrates, but displays unprecedented selectivity for our substrates over D-luciferin (**Table 8.1**). Photon flux from D-luciferin is reduced by 10,000-fold compared to WT, while photon flux from the preferred substrate, CycLuc7, increases 450-fold. We hypothesize that the combination of these three mutations functions in part by lowering the affinity of all luciferins, shifting the affinity for the synthetic substrates to the mid-micromolar range, while shifting the affinity for D-luciferin into the millimolar range.

Both mutant luciferases lower the binding affinity of each substrate and help relieve product inhibition, resulting in an increased rate of photon emission in vitro. However, if the reduction in substrate affinity is too great and the luciferase is used under limiting substrate conditions (i.e., in live cells and organisms), the amount of substrate required for effective catalysis may not be attainable. The R218K mutant does not appear to have this problem, producing

the highest photon flux of any luciferase/luciferin combination tested here from cells overlaid with high substrate dose (250 μM with CycLuc2), or low dose (1.95 μM with CycLuc12) (**Table 8.1**). Conversely, while the triple mutant luciferase exceeds the photon flux of WT with any luciferin upon treatment with high dose of CycLuc2, CycLuc7, and CycLuc11, the loss of affinity by the combination of all three mutations results in all substrates emitting lower photon flux than WT and D-luciferin at low substrate dose. Therefore, it is unlikely that the concentration of substrate needed for efficient catalysis will be achievable in live mice. For use under the limiting substrate conditions of live cells and organisms, I propose that there is a "Goldilocks zone" of substrate affinity, where the luciferin does not bind too tightly, reducing the photon flux via product inhibition, but also does not bind too weakly, necessitating the need for high substrate concentration for light emission. A K_m of approximately 1 μM seems to be optimal, especially when paired with the increased cell permeability of the synthetic luciferins (e.g., CycLuc12 is preferred in live cells at low substrate dose with both WT [K_m = 0.3 μM] and R218K [K_m = 1.7 μM]).

While the development of the triple mutant luciferase provides a proof-of-concept towards new, orthogonal bioluminescent systems, additional optimization is still required. As discussed in CHAPTER I, WT luciferase is remarkably promiscuous and functions with all of the synthetic substrates that we (and others) have developed. Although the triple mutant luciferase is inactive toward D-luciferin, CycLuc7 still emits with the WT luciferase. Moreover, the loss

of affinity of the triple mutant toward its substrates limits its usefulness in vivo. However, there are continually new luciferin analogs being produced bearing increasingly varied chemical structures (Branchini et al., 1989; Conley et al., 2012; Iwano et al., 2013; McCutcheon et al., 2012; Woodroofe et al., 2012). As the number of structurally distinct synthetic luciferins grows, there will be increased opportunity to exploit those differences in the development of orthogonal bioluminescent enzyme/substrate pairs.

The identification of a mutant luciferase that was more active toward substrates other than D-luciferin prompted us to look for other “luciferase-like” enzymes that do not emit light with D-luciferin. Long-chain fatty acyl-CoA synthetases (ACSLs) have been characterized based on their similarities to luciferase in an effort to identify additional bioluminescent enzymes (Oba et al., 2004, 2006a, 2008, 2010), but only very weak light emission has ever been observed with D-luciferin (Viviani et al., 2013). We hypothesized that bioluminescence is possible with these enzymes, but that D-luciferin is either unable to bind, or is binding in an orientation not conducive to catalysis. Perhaps, if supplied with an appropriate synthetic substrate, an ACSL could exhibit luciferase activity.

In CHAPTER III, I discuss the identification and characterization of the first latent luciferase discovered: CG6178 from *Drosophila melanogaster* (Mofford et al., 2014a). Furthermore, in CHAPTER IV, I report that another ACSL, AbLL from the non-luminous click beetle *Agrypnus binodulus*, also possesses luciferase

activity. Neither CG6178 nor AbLL display the same level of substrate promiscuity as firefly luciferase, only recognizing a subset of the synthetic luciferins tested. Interestingly, while neither enzyme catalyzes light emission with D-luciferin, their respective substrate specificities are distinct. For example, CG6178 catalyzes light emission within a similar class of substrates (i.e., cyclic dialkylated aminoluciferins similar to CycLuc2). Conversely, AbLL accepts substrates of varying structure and discriminates between substrates with relatively minor structural differences. AbLL recognizes two short cinnamyl-type substrates: the acyclic dimethylamine Me_2NPh-1n-Cys and the dialkylated tetrahydroquinoline C8Ph-1n-Cys, but is inactive toward the dialkylated indoline C2Ph-1n-Cys. Structural analysis of the AbLL binding pocket may determine how this level of recognition is accomplished. Moreover, structural studies of both latent luciferases may aid in the development of luciferases with improved substrate selectivity as discussed above. Neither CG6178 nor AbLL display the necessary photon flux for use as a bioluminescent reporter. However, we predict that structural analysis will make it possible to uncouple substrate specificity from signal intensity, allowing for the development of additional orthogonal luciferase reporters.

We were quite surprised to find that homology to luciferase is a poor predictor of luciferase activity. CG6178 possesses 39% identity to firefly luciferase, while AbLL possesses 46% identity; yet, AbLL emits weaker photon flux than CG6178. A third ACSL, PaLL from the luminous Panamanian click

beetle *Pyrophorus angustus*, also possesses 46% identity to luciferase, yet does not exhibit luciferase activity with any luciferin analog (CHAPTER IV). Perhaps conservation of primary amino acid sequence does not translate to conserved tertiary structure. There could be slight differences in each enzyme's final fold that dictate the presence or absence of luciferase activity. Conversely, there could be residues that are necessary for catalysis that have not become apparent from the limited number of ACSLs screened. For example, a putative binding site for oxygen has not been identified in luciferase (Branchini et al., 1998). If such a site exists, it may not be present in PaLL. However, we are still in the early stages of investigating luciferase activity in ACSLs. As more enzymes are screened, and as detailed structural studies are performed, patterns that can predict luciferase activity may still emerge.

Mammalian ACSLs are less homologous to firefly luciferase than insect ACSLs. In fact, it is thought that mammalian and insect ACSLs evolved independently (Oba et al., 2005). Therefore, while endogenous expression of CG6178 was sufficient to support light emission from live *Drosophila* S2 cells treated with CycLuc2, it was not surprising to find that CHO cells did not emit light when treated with any luciferin analog (CHAPTER III). Still, I predict that a suitable synthetic luciferin will elicit bioluminescence from a mammalian enzyme as well. Mammalian-specific luciferins may be quite distinct from our current analogs. As long as that luciferin contains a chromophore and a free carboxylate, binds to the enzyme in the correct orientation for adenylation and oxidation, and

oxygen can access the active site, bioluminescence should occur. If this can be achieved, it will not only show further commonality to light emission by bioluminescence, it would also present a useful source of diversity for the generation of new orthogonal pairs, as discussed above.

The identification of multiple ACSLs with latent luciferase activity prompted us to look more closely at the light emitting chemistry (CHAPTER III). The canonical mechanism is for oxygen to react with the intermediate luciferyl adenylate. However, since oxygen exists in a triplet-state, with two unpaired electrons occupying degenerate orbitals, it is “spin-forbidden” to react with singlet-state molecules such as the luciferyl adenylate (Min et al., 2011). We therefore proposed that the formation of a resonance stabilized carbanion at the C4 position of the luciferyl adenylate reduces molecular dioxygen by single electron transfer to form superoxide and a C4 radical (Fetzner and Steiner, 2010; Russell and Bemis, 1966). Reaction between those two radicals is no longer forbidden and they can recombine after a spin-flip to form a peroxide that can react via the canonical mechanism. This seemed to us to be the only thermodynamically-viable model. In fact, since we proposed this route, Branchini et al. have shown experimental support for reduction of molecular dioxygen by single electron transfer in a luciferin model system (Branchini et al., 2015). They report the formation of a superoxide anion, a feature consistent with our model but not the classical model. Thus, the oxidation chemistry did not need to evolve from an ACSL; the inherent reactivity of a carbanion with oxygen is sufficient. In

order for an enzyme to catalyze light emission, it must adenylate the luciferin, promote formation of the intermediate carbanion, and allow oxygen into the active site. The inherent carbanion reactivity, combined with the properties of the luciferin, will result in photon emission. Therefore, nascent enzymatic activity can be as much dependent on the properties of the substrate as on the actual enzyme.

In an effort to harness the substrate specificity of ACSLs with latent luciferase activity, while improving the photon intensity, in CHAPTER V I develop and characterize luciferase/ACSL chimeric enzymes. Firefly luciferase and ACSLs are divided into two domains: a large N-terminal substrate-binding domain, and a small C-terminal catalytic domain containing two lysine residues responsible for adenylation and oxidation/thioesterification. Here we find that replacing the C-terminal domain of firefly luciferase with that of either CG6178 or AbLL is not only permitted, but results in improved selectivity for synthetic luciferins over D-luciferin. While the luciferin binding pocket within the N-terminal domain should remain mostly unchanged in the C-terminal fusions, the orientation of those two lysines from each C-terminal domain may vary and thus impact overall catalysis. For example, the FLuc/CG fusion behaves very similarly to WT luciferase, while the FLuc/Ab fusion does not. Firefly luciferase displays burst kinetics as discussed in CHAPTER I, while AbLL slowly increases its photon flux even after two minutes, as shown in CHAPTER IV. The FLuc/Ab chimera displays an intermediate profile with a peak rate of light emission after

several seconds and little to no product inhibition. These findings suggest that rather than modular roles for the two domains, it is the interaction of both that contribute to the overall function of the enzyme.

One possible explanation for the intermediate activity of the FLuc/Ab chimera is that the AbLL C-terminal domain does not efficiently undergo the necessary conformational change between adenylation and oxidation. There could be residues that line the interface between it and the N-terminal domain that hinder its movement. For example, there is a loop that extends from the C-terminal domain of firefly luciferase into the N-terminal domain and positions K529 in the active site for adenylation (**Figure 8.1**). While K529 is conserved between ACSLs, the remaining residues of the loop are not. If the loop of an ACSL binds more tightly to the N-terminal domain of luciferase, it may hinder the conformational change between the adenylation and oxidation steps and lower the rate of catalysis.

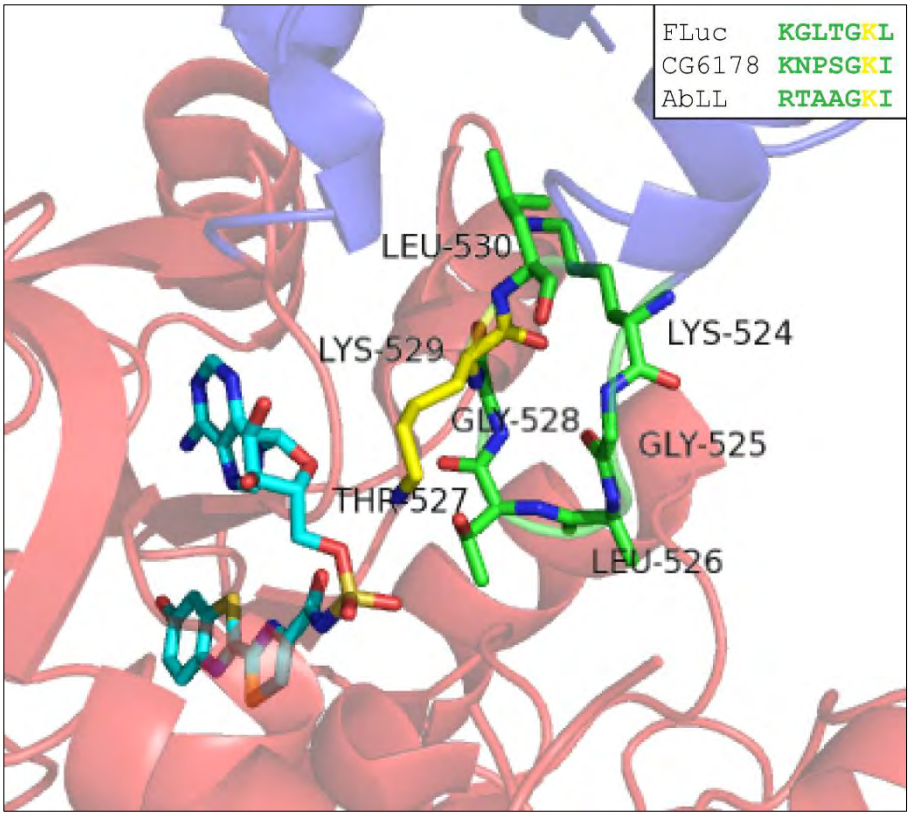

Figure 8.1. The loop in firefly luciferase that positions K529 is not well conserved in ACSLs. The loop (green) that extends from the C-terminal domain (blue) to the N-terminal domain (red) of luciferase to position K529 (yellow) for adenylation of the luciferin (cyan). The primary sequence of the loop residues is not conserved between ACSLs (insert). [Figure from PDB 4G36 (Sundlov et al., 2012)].

Additionally, we find that mutations that improved luciferase photon flux with synthetic luciferins did not readily translate to use with the C-terminal ACSL fusions. Neither the R218K point mutation nor the triple mutant synergized with the CG6178 and AbLL fusions as well as WT luciferase. These mutations were identified by saturating mutagenesis at specific sites in the luciferase active site. By re-screening using the chimera background instead of WT luciferase, it is

possible that there will be alternative mutations that will better cooperate with the new domain. Conceivably, the combination of direct mutation with chimeric enzymes may prove to be more beneficial than either one alone.

Apart from simply understanding and optimizing firefly bioluminescence, the aim of my work was to increase the applications of bioluminescence throughout biology. In CHAPTER VI, I sought to expand the bioluminescence toolkit by developing a sensor for fatty acid amide hydrolase (FAAH) (Mofford et al., 2015). FAAH is responsible for hydrolyzing fatty acid amide second messengers to their respective fatty acids (Cravatt et al., 1996). Based on the hypothesis that luciferase evolved from a fatty acyl-CoA synthetase (Day et al., 2009), and our discovery of two ACSLs that are able to catalyze light emission with a synthetic luciferin, we propose that D-luciferin and its analogs are essentially fatty acid mimics. We therefore hypothesized that a luciferin amide would mimic the native fatty acid amide substrates for FAAH and be hydrolyzed to release a proper luciferin. As expected, luciferin amides do not produce light as they are unable to be adenylated and thus are not substrates for luciferase. They are, however, extremely specific substrates for FAAH, readily translating from in vitro assays, to live cells, and finally to live mice (**Table 8.1**).

As discussed in CHAPTER II, we propose that the improved cell permeability and increased enzyme affinity of synthetic luciferins make them superior to D-luciferin for use in live cells and organisms. Consistent with this proposal, using the amide of our synthetic luciferin CycLuc1 allowed us to report

on FAAH activity in the brains of live mice, whereas the amide of D-luciferin was insufficient. FAAH may not be able to hydrolyze sufficient quantity of D-luciferin amide to overcome the higher K_m of D-luciferin. Moreover, the luciferin amide modification ameliorated cell permeability to a greater extent. In the brains of live mice, CycLuc1 amide increases photon flux over D-luciferin, even at 1,000-fold lower substrate dose. It is likely that the lack of an ionized carboxylate on the amides increases their cell permeability, while the membrane bound FAAH results in rapid hydrolysis. Therefore, as discussed in CHAPTER VII, luciferin amides are also ideal luciferin delivery vehicles for cells and tissues that express FAAH (Mofford and Miller, 2015).

By harnessing the intrinsic characteristics of luciferin analogs, and changing a single functional group, we have developed a sensor for a single enzyme in a live mouse. Further refinement of the luciferin structure and modification of the scissile bond should allow for the detection of other enzymatic activities, particularly those that release fatty acids. For example, one enzyme of interest is monoacylglycerol lipase (MAGL) (Blankman and Cravatt, 2013; Blankman et al., 2007). MAGL hydrolyzes the endocannabinoid 2-arachidonoyl glycerol to arachidonic acid (**Figure 8.2**) and is a drug target for the treatment of pain (Long et al., 2009). By replacing the free carboxylate of a luciferin with a glycerol ester, it should be possible to detect MAGL activity by bioluminescence. Structural optimization may be required to ensure selectivity, as there are a wide variety of esterases present in live cells and organisms and luciferin esters have

previously been used as luciferin delivery vehicles (Craig et al., 1991; Shinde et al., 2006). However, the successful detection of FAAH activity with our luciferin amides suggests that other enzymatic activities can be measured by employing other simple chemical modifications.

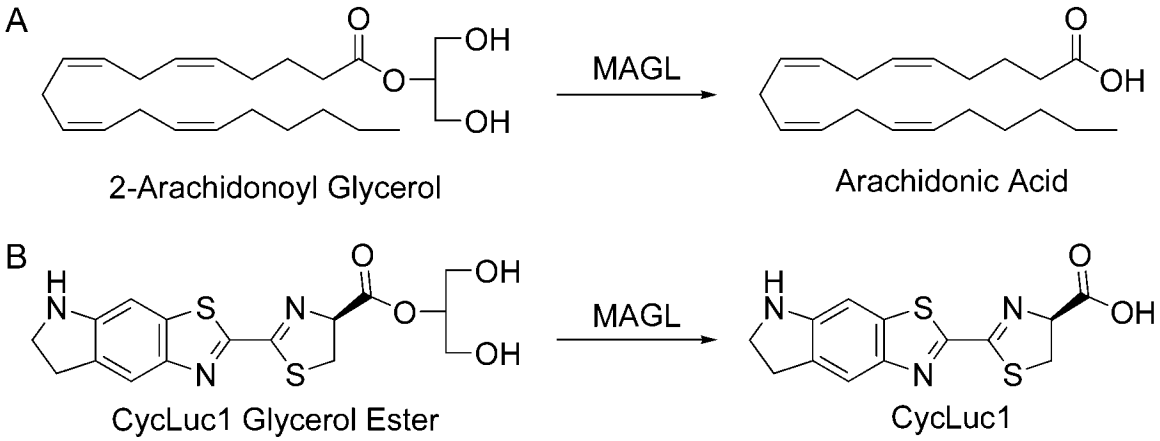

Figure 8.2. Proposed bioluminescence MAGL activity assay. (A) MAGL hydrolyzes 2-arachidonoyl glycerol to arachidonic acid. (B) Proposed bioluminescent activity assay where MAGL hydrolyzes the pro-luciferin CycLuc1 glycerol ester to release the luciferase substrate CycLuc1.

In summary, the work described herein harnesses the power of synthetic luciferin analogs to both understand the fundamental properties of bioluminescence and improve its practical applications. Our synthetic substrates combine with mutant luciferases to generally improve on current technologies. We show that latent luciferase activity exists in luciferase homologs, allowing us to explore the evolutionary origins of light emission and providing a platform to determine what defines a luciferase. Finally, we developed a pro-luciferin approach to detect enzymes that release fatty acid products, allowing us to probe

their enzymatic activity via light production and revealing the utility of our synthetic luciferins for exploring biological environments. It is clear that the only limit to bioluminescence applications is the imagination.

BIBLIOGRAPHY

Abell, L.M., and Schloss, J.V. (1991). Oxygenase side reactions of acetolactate synthase and other carbanion-forming enzymes. Biochemistry *30*, 7883–7887.

Adams, S.T., and Miller, S.C. (2014). Beyond D-luciferin: expanding the scope of bioluminescence imaging in vivo. Curr. Opin. Chem. Biol. *21*, 112–120.

Ahn, K., Johnson, D.S., Mileni, M., Beidler, D., Long, J.Z., McKinney, M.K., Weerapana, E., Sadagopan, N., Liimatta, M., Smith, S.E., et al. (2009). Discovery and characterization of a highly selective FAAH inhibitor that reduces inflammatory pain. Chem. Biol. *16*, 411–420.

Ando, Y., Niwa, K., Yamada, N., Enomoto, T., Irie, T., Kubota, H., Ohmiya, Y., and Akiyama, H. (2008). Firefly bioluminescence quantum yield and colour change by pH-sensitive green emission. Nat. Photonics *2*, 44–47.

Aswendt, M., Adamczak, J., Couillard-Despres, S., and Hoehn, M. (2013). Boosting bioluminescence neuroimaging: an optimized protocol for brain studies. PloS One *8*, e55662.

Atkins, R.L., and Bliss, D.E. (1978). Substituted coumarins and azacoumarins. Synthesis and fluorescent properties. J. Org. Chem. *43*, 1975–1980.

Auld, D.S., Zhang, Y.-Q., Southall, N.T., Rai, G., Landsman, M., MacLure, J., Langevin, D., Thomas, C.J., Austin, C.P., and Inglese, J. (2009). A basis for reduced chemical library inhibition of firefly luciferase obtained from directed evolution. J. Med. Chem. *52*, 1450–1458.

Ayzenberg, I., Schlevogt, S., Metzdorf, J., Stahlke, S., Pedreitturia, X., Hunfeld, A., Couillard-Despres, S., and Kleiter, I. (2015). Analysis of neurogenesis during experimental autoimmune encephalomyelitis reveals pitfalls of bioluminescence imaging. PloS One *10*, e0118550.

Badr, C.E., and Tannous, B.A. (2011). Bioluminescence imaging: progress and applications. Trends Biotechnol. *29*, 624–633.

Bandiera, T., Ponzano, S., and Piomelli, D. (2014). Advances in the discovery of N-acylethanolamine acid amidase inhibitors. Pharmacol. Res. Off. J. Ital. Pharmacol. Soc. *86*, 11–17.

Baron, R., Riley, C., Chenprakhon, P., Thotsaporn, K., Winter, R.T., Alfieri, A., Forneris, F., van Berkel, W.J.H., Chaiyen, P., Fraaije, M.W., et al. (2009). Multiple pathways guide oxygen diffusion into flavoenzyme active sites. Proc. Natl. Acad. Sci. U. S. A. *106*, 10603–10608.

Belov, V.N., Bossi, M.L., Fölling, J., Boyarskiy, V.P., and Hell, S.W. (2009). Rhodamine spiroamides for multicolor single-molecule switching fluorescent nanoscopy. Chem. Weinh. Bergstr. Ger. *15*, 10762–10776.

Van de Bittner, G.C., Bertozzi, C.R., and Chang, C.J. (2013). Strategy for dual-analyte luciferin imaging: in vivo bioluminescence detection of hydrogen peroxide and caspase activity in a murine model of acute inflammation. J. Am. Chem. Soc. *135*, 1783–1795.

Blankman, J.L., and Cravatt, B.F. (2013). Chemical probes of endocannabinoid metabolism. Pharmacol. Rev. *65*, 849–871.

Blankman, J.L., Simon, G.M., and Cravatt, B.F. (2007). A comprehensive profile of brain enzymes that hydrolyze the endocannabinoid 2-arachidonoylglycerol. Chem. Biol. *14*, 1347–1356.

Boger, D.L., Fecik, R.A., Patterson, J.E., Miyauchi, H., Patricelli, M.P., and Cravatt, B.F. (2000). Fatty acid amide hydrolase substrate specificity. Bioorg. Med. Chem. Lett. *10*, 2613–2616.

Bonger, K.M., Hoogendoorn, S., van Koppen, C.J., Timmers, C.M., Overkleeft, H.S., and van der Marel, G.A. (2009). Synthesis and pharmacological evaluation of dimeric follicle-stimulating hormone receptor antagonists. ChemMedChem *4*, 2098–2102.

Branchini, B.R., Hayward, M.M., Bamford, S., Brennan, P.M., and Lajiness, E.J. (1989). Naphthyl- and quinolylluciferin: green and red light emitting firefly luciferin analogues. Photochem. Photobiol. *49*, 689–695.

Branchini, B.R., Magyar, R.A., Murtiashaw, M.H., Anderson, S.M., and Zimmer, M. (1998). Site-Directed Mutagenesis of Histidine 245 in Firefly Luciferase: A Proposed Model of the Active Site. Biochemistry *37*, 15311–15319.

Branchini, B.R., Murtiashaw, M.H., Magyar, R.A., Portier, N.C., Ruggiero, M.C., and Stroh, J.G. (2002). Yellow-green and red firefly bioluminescence from 5,5-dimethyloxyluciferin. J. Am. Chem. Soc. *124*, 2112–2113.

Branchini, B.R., Southworth, T.L., Murtiashaw, M.H., Boije, H., and Fleet, S.E. (2003). A mutagenesis study of the putative luciferin binding site residues of firefly luciferase. Biochemistry *42*, 10429–10436.

Branchini, B.R., Southworth, T.L., Khattak, N.F., Michelini, E., and Roda, A. (2005a). Red- and green-emitting firefly luciferase mutants for bioluminescent reporter applications. Anal. Biochem. *345*, 140–148.

Branchini, B.R., Southworth, T.L., Murtiashaw, M.H., Wilkinson, S.R., Khattak, N.F., Rosenberg, J.C., and Zimmer, M. (2005b). Mutagenesis evidence that the partial reactions of firefly bioluminescence are catalyzed by different conformations of the luciferase C-terminal domain. Biochemistry *44*, 1385–1393.

Branchini, B.R., Ablamsky, D.M., Davis, A.L., Southworth, T.L., Butler, B., Fan, F., Jathoul, A.P., and Pule, M.A. (2010a). Red-emitting luciferases for bioluminescence reporter and imaging applications. Anal. Biochem. *396*, 290–297.

Branchini, B.R., Ablamsky, D.M., and Rosenberg, J.C. (2010b). Chemically modified firefly luciferase is an efficient source of near-infrared light. Bioconjug. Chem. *21*, 2023–2030.

Branchini, B.R., Southworth, T.L., Fontaine, D.M., Davis, A.L., Behney, C.E., and Murtiashaw, M.H. (2014). A Photinus pyralis and Luciola italica chimeric firefly luciferase produces enhanced bioluminescence. Biochemistry *53*, 6287–6289.

Branchini, B.R., Behney, C.E., Southworth, T.L., Fontaine, D.M., Gulick, A.M., Vinyard, D.J., and Brudvig, G.W. (2015). Experimental Support for a Single Electron-Transfer Oxidation Mechanism in Firefly Bioluminescence. J. Am. Chem. Soc. *137*, 7592–7595.

Cao, Y.-A., Wagers, A.J., Beilhack, A., Dusich, J., Bachmann, M.H., Negrin, R.S., Weissman, I.L., and Contag, C.H. (2004). Shifting foci of hematopoiesis during reconstitution from single stem cells. Proc. Natl. Acad. Sci. U. S. A. *101*, 221–226.

Carl, P.L., Chakravarty, P.K., and Katzenellenbogen, J.A. (1981). A novel connector linkage applicable in prodrug design. J. Med. Chem. *24*, 479–480.

Chang, K.H., Xiang, H., and Dunaway-Mariano, D. (1997). Acyl-adenylate motif of the acyl-adenylate/thioester-forming enzyme superfamily: a site-directed mutagenesis study with the Pseudomonas sp. strain CBS3 4-chlorobenzoate:coenzyme A ligase. Biochemistry *36*, 15650–15659.

Cheung, L., Yu, D.M.T., Neiron, Z., Failes, T.W., Arndt, G.M., and Fletcher, J.I. (2015). Identification of new MRP4 inhibitors from a library of FDA approved drugs using a high-throughput bioluminescence screen. Biochem. Pharmacol. *93*, 380–388.

Chintapalli, V.R., Wang, J., and Dow, J.A.T. (2007). Using FlyAtlas to identify better Drosophila melanogaster models of human disease. Nat. Genet. *39*, 715–720.

Clapper, J.R., Moreno-Sanz, G., Russo, R., Guijarro, A., Vacondio, F., Duranti, A., Tontini, A., Sanchini, S., Sciolino, N.R., Spradley, J.M., et al. (2010). Anandamide suppresses pain initiation through a peripheral endocannabinoid mechanism. Nat. Neurosci. *13*, 1265–1270.

Conley, N.R., Dragulescu-Andrasi, A., Rao, J., and Moerner, W.E. (2012). A selenium analogue of firefly D-luciferin with red-shifted bioluminescence emission. Angew. Chem. Int. Ed Engl. *51*, 3350–3353.

Conti, E., Franks, N.P., and Brick, P. (1996). Crystal structure of firefly luciferase throws light on a superfamily of adenylate-forming enzymes. Structure *4*, 287–298.

Conti, E., Stachelhaus, T., Marahiel, M.A., and Brick, P. (1997). Structural basis for the activation of phenylalanine in the non-ribosomal biosynthesis of gramicidin S. EMBO J. *16*, 4174–4183.

Craig, F.F., Simmonds, A.C., Watmore, D., McCapra, F., and White, M.R. (1991). Membrane-permeable luciferin esters for assay of firefly luciferase in live intact cells. Biochem. J. *276 (Pt 3)*, 637–641.

Cravatt, B.F., Giang, D.K., Mayfield, S.P., Boger, D.L., Lerner, R.A., and Gilula, N.B. (1996). Molecular characterization of an enzyme that degrades neuromodulatory fatty-acid amides. Nature *384*, 83–87.

Day, J.C., Tisi, L.C., and Bailey, M.J. (2004). Evolution of beetle bioluminescence: the origin of beetle luciferin. Lumin. J. Biol. Chem. Lumin. *19*, 8–20.

Day, J.C., Goodall, T.I., and Bailey, M.J. (2009). The evolution of the adenylate-forming protein family in beetles: multiple luciferase gene paralogues in fireflies and glow-worms. Mol. Phylogenet. Evol. *50*, 93–101.

Day, T.A., Rakhshan, F., Deutsch, D.G., and Barker, E.L. (2001). Role of fatty acid amide hydrolase in the transport of the endogenous cannabinoid anandamide. Mol. Pharmacol. *59*, 1369–1375.

DeLuca, M., and McElroy, W.D. (1974). Kinetics of the firefly luciferase catalyzed reactions. Biochemistry *13*, 921–925.

Dickason-Chesterfield, A.K., Kidd, S.R., Moore, S.A., Schaus, J.M., Liu, B., Nomikos, G.G., and Felder, C.C. (2006). Pharmacological characterization of endocannabinoid transport and fatty acid amide hydrolase inhibitors. Cell. Mol. Neurobiol. *26*, 407–423.

Evans, M.S., Chaurette, J.P., Adams, S.T., Reddy, G.R., Paley, M.A., Aronin, N., Prescher, J.A., and Miller, S.C. (2014). A synthetic luciferin improves bioluminescence imaging in live mice. Nat. Methods *11*, 393–395.

Fan, F., and Wood, K.V. (2007). Bioluminescent assays for high-throughput screening. Assay Drug Dev. Technol. *5*, 127–136.

Fernández-Suárez, M., and Ting, A.Y. (2008). Fluorescent probes for super-resolution imaging in living cells. Nat. Rev. Mol. Cell Biol. *9*, 929–943.

Fetzner, S., and Steiner, R.A. (2010). Cofactor-independent oxidases and oxygenases. Appl. Microbiol. Biotechnol. *86*, 791–804.

Fossey, J., Lefort, D., and Sorba, J. (1995). Free Radicals in Organic Chemistry (Chichester ; New York : Paris: Wiley).

Fraga, H. (2008). Firefly luminescence: a historical perspective and recent developments. Photochem. Photobiol. Sci. Off. J. Eur. Photochem. Assoc. Eur. Soc. Photobiol. *7*, 146–158.

Fraga, H., Fernandes, D., Fontes, R., and Esteves da Silva, J.C.G. (2005). Coenzyme A affects firefly luciferase luminescence because it acts as a substrate and not as an allosteric effector. FEBS J. *272*, 5206–5216.

Fraga, H., Fernandes, D., Novotny, J., Fontes, R., and Esteves da Silva, J.C.G. (2006). Firefly Luciferase Produces Hydrogen Peroxide as a Coproduct in Dehydroluciferyl Adenylate Formation. ChemBioChem *7*, 929–935.

Gibson, D.G., Young, L., Chuang, R.-Y., Venter, J.C., Hutchison, C.A., and Smith, H.O. (2009). Enzymatic assembly of DNA molecules up to several hundred kilobases. Nat. Methods *6*, 343–345.

Glasner, M.E., Gerlt, J.A., and Babbitt, P.C. (2006). Evolution of enzyme superfamilies. Curr. Opin. Chem. Biol. *10*, 492–497.

Greer, L.F., and Szalay, A.A. (2002). Imaging of light emission from the expression of luciferases in living cells and organisms: a review. Lumin. J. Biol. Chem. Lumin. *17*, 43–74.

Gulick, A.M., Starai, V.J., Horswill, A.R., Homick, K.M., and Escalante-Semerena, J.C. (2003). The 1.75 A crystal structure of acetyl-CoA synthetase bound to adenosine-5'-propylphosphate and coenzyme A. Biochemistry *42*, 2866–2873.

Haddock, S.H.D., Moline, M.A., and Case, J.F. (2010). Bioluminescence in the sea. Annu. Rev. Mar. Sci. *2*, 443–493.

Harvey, E.N. (1957). A history of luminescence from the earliest times until 1900. (Philadelphia: American Philosophical Society).

Harwood, K.R., Mofford, D.M., Reddy, G.R., and Miller, S.C. (2011). Identification of mutant firefly luciferases that efficiently utilize aminoluciferins. Chem. Biol. *18*, 1649–1657.

Hastings, J.W. (1983). Biological diversity, chemical mechanisms, and the evolutionary origins of bioluminescent systems. J. Mol. Evol. *19*, 309–321.

Hastings, J.W. (1996). Chemistries and colors of bioluminescent reactions: a review. Gene *173*, 5–11.

Hastings, J.W. (1998). Bioluminescence. In Cell Physiology, (Academic Press: New York), pp. 984–1000.

Hastings, J.W., McELROY, W.D., and Coulombre, J. (1953). The effect of oxygen upon the immobilization reaction in firefly luminescence. J. Cell. Physiol. *42*, 137–150.

Herring, P.J. (1979). Bioluminescence in Action (London ; New York: Academic Pr).

Hickson, J., Ackler, S., Klaubert, D., Bouska, J., Ellis, P., Foster, K., Oleksijew, A., Rodriguez, L., Schlessinger, S., Wang, B., et al. (2010). Noninvasive molecular imaging of apoptosis in vivo using a modified firefly luciferase substrate, Z-DEVD-aminoluciferin. Cell Death Differ. *17*, 1003–1010.

Hill, S.J., Baker, J.G., and Rees, S. (2001). Reporter-gene systems for the study of G-protein-coupled receptors. Curr. Opin. Pharmacol. *1*, 526–532.

Inagaki, K., Fuess, S., Storm, T.A., Gibson, G.A., Mctiernan, C.F., Kay, M.A., and Nakai, H. (2006). Robust systemic transduction with AAV9 vectors in mice: efficient global cardiac gene transfer superior to that of AAV8. Mol. Ther. J. Am. Soc. Gene Ther. *14*, 45–53.

Iwano, S., Obata, R., Miura, C., Kiyama, M., Hama, K., Nakamura, M., Amano, Y., Kojima, S., Hirano, T., Maki, S., et al. (2013). Development of simple firefly luciferin analogs emitting blue, green, red, and near-infrared biological window light. Tetrahedron *69*, 3847–3856.

Katoh, K., Misawa, K., Kuma, K., and Miyata, T. (2002). MAFFT: a novel method for rapid multiple sequence alignment based on fast Fourier transform. Nucleic Acids Res. *30*, 3059–3066.

Khersonsky, O., and Tawfik, D.S. (2010). Enzyme promiscuity: a mechanistic and evolutionary perspective. Annu. Rev. Biochem. *79*, 471–505.

Kojima, R., Takakura, H., Ozawa, T., Tada, Y., Nagano, T., and Urano, Y. (2013). Rational design and development of near-infrared-emitting firefly luciferins available in vivo. Angew. Chem. Int. Ed Engl. *52*, 1175–1179.

Larkin, M.A., Blackshields, G., Brown, N.P., Chenna, R., McGettigan, P.A., McWilliam, H., Valentin, F., Wallace, I.M., Wilm, A., Lopez, R., et al. (2007). Clustal W and Clustal X version 2.0. Bioinforma. Oxf. Engl. *23*, 2947–2948.

Long, J.Z., and Cravatt, B.F. (2011). The metabolic serine hydrolases and their functions in mammalian physiology and disease. Chem. Rev. *111*, 6022–6063.

Long, J.Z., Li, W., Booker, L., Burston, J.J., Kinsey, S.G., Schlosburg, J.E., Pavón, F.J., Serrano, A.M., Selley, D.E., Parsons, L.H., et al. (2009). Selective blockade of 2-arachidonoylglycerol hydrolysis produces cannabinoid behavioral effects. Nat. Chem. Biol. *5*, 37–44.

Long, J.Z., LaCava, M., Jin, X., and Cravatt, B.F. (2011). An anatomical and temporal portrait of physiological substrates for fatty acid amide hydrolase. J. Lipid Res. *52*, 337–344.

Matsuki, H., Suzuki, A., Kamaya, H., and Ueda, I. (1999). Specific and non-specific binding of long-chain fatty acids to firefly luciferase: cutoff at octanoate. Biochim. Biophys. Acta *1426*, 143–150.

McCutcheon, D.C., Paley, M.A., Steinhardt, R.C., and Prescher, J.A. (2012). Expedient synthesis of electronically modified luciferins for bioluminescence imaging. J. Am. Chem. Soc. *134*, 7604–7607.

McCutcheon, D.C., Porterfield, W.B., and Prescher, J.A. (2015). Rapid and scalable assembly of firefly luciferase substrates. Org. Biomol. Chem. *13*, 2117–2121.

McElroy, W.D., DeLuca, M., and Travis, J. (1967). Molecular uniformity in biological catalyses. The enzymes concerned with firefly luciferin, amino acid, and fatty acid utilization are compared. Science *157*, 150–160.

Mezzanotte, L., Que, I., Kaijzel, E., Branchini, B., Roda, A., and Löwik, C. (2011). Sensitive dual color in vivo bioluminescence imaging using a new red codon optimized firefly luciferase and a green click beetle luciferase. PloS One *6*, e19277.

Mileni, M., Johnson, D.S., Wang, Z., Everdeen, D.S., Liimatta, M., Pabst, B., Bhattacharya, K., Nugent, R.A., Kamtekar, S., Cravatt, B.F., et al. (2008). Structure-guided inhibitor design for human FAAH by interspecies active site conversion. Proc. Natl. Acad. Sci. U. S. A. *105*, 12820–12824.

Min, C., Ren, A., Li, X., Guo, J., Zou, L., Sun, Y., Goddard, J.D., and Sun, C. (2011). The formation and decomposition of firefly dioxetanone. Chem. Phys. Lett. *506*, 269–275.

Mobley, J., and Vo-Dinh, T. (2003). Optical properties of tissue. In Biomedical Photonics Handbook, (Boca Raton, Fla.: CRC Press), pp. 2–1 to 2–75.

Mofford, D.M., and Miller, S.C. (2015). Luciferins Behave Like Drugs. ACS Chem. Neurosci. *6*, 1273–1275.

Mofford, D.M., Reddy, G.R., and Miller, S.C. (2014a). Latent luciferase activity in the fruit fly revealed by a synthetic luciferin. Proc. Natl. Acad. Sci. U. S. A. *111*, 4443–4448.

Mofford, D.M., Reddy, G.R., and Miller, S.C. (2014b). Aminoluciferins extend firefly luciferase bioluminescence into the near-infrared and can be preferred substrates over D-luciferin. J. Am. Chem. Soc. *136*, 13277–13282.

Mofford, D.M., Adams, S.T., Reddy, G.S.K.K., Reddy, G.R., and Miller, S.C. (2015). Luciferin Amides Enable in Vivo Bioluminescence Detection of Endogenous Fatty Acid Amide Hydrolase Activity. J. Am. Chem. Soc. *137*, 8684–8687.

Moravec, R.A., O'Brien, M.A., Daily, W.J., Scurria, M.A., Bernad, L., and Riss, T.L. (2009). Cell-based bioluminescent assays for all three proteasome activities in a homogeneous format. Anal. Biochem. *387*, 294–302.

Nakamura, M., Maki, S., Amano, Y., Ohkita, Y., Niwa, K., Hirano, T., Ohmiya, Y., and Niwa, H. (2005). Firefly luciferase exhibits bimodal action depending on the luciferin chirality. Biochem. Biophys. Res. Commun. *331*, 471–475.

Nakatsu, T., Ichiyama, S., Hiratake, J., Saldanha, A., Kobashi, N., Sakata, K., and Kato, H. (2006). Structural basis for the spectral difference in luciferase bioluminescence. Nature *440*, 372–376.

Naumov, P., Ozawa, Y., Ohkubo, K., and Fukuzumi, S. (2009). Structure and spectroscopy of oxyluciferin, the light emitter of the firefly bioluminescence. J. Am. Chem. Soc. *131*, 11590–11605.

Oba, Y., Ojika, M., and Inouye, S. (2003). Firefly luciferase is a bifunctional enzyme: ATP-dependent monooxygenase and a long chain fatty acyl-CoA synthetase. FEBS Lett. *540*, 251–254.

Oba, Y., Ojika, M., and Inouye, S. (2004). Characterization of CG6178 gene product with high sequence similarity to firefly luciferase in Drosophila melanogaster. Gene *329*, 137–145.

Oba, Y., Sato, M., Ojika, M., and Inouye, S. (2005). Enzymatic and genetic characterization of firefly luciferase and Drosophila CG6178 as a fatty acyl-CoA synthetase. Biosci. Biotechnol. Biochem. *69*, 819–828.

Oba, Y., Sato, M., Ohta, Y., and Inouye, S. (2006a). Identification of paralogous genes of firefly luciferase in the Japanese firefly, Luciola cruciata. Gene *368*, 53–60.

Oba, Y., Tanaka, K., and Inouye, S. (2006b). Catalytic properties of domain-exchanged chimeric proteins between firefly luciferase and Drosophila fatty Acyl-CoA synthetase CG6178. Biosci. Biotechnol. Biochem. *70*, 2739–2744.

Oba, Y., Iida, K., Ojika, M., and Inouye, S. (2008). Orthologous gene of beetle luciferase in non-luminous click beetle, Agrypnus binodulus (Elateridae), encodes a fatty acyl-CoA synthetase. Gene *407*, 169–175.

Oba, Y., Iida, K., and Inouye, S. (2009). Functional conversion of fatty acyl-CoA synthetase to firefly luciferase by site-directed mutagenesis: a key substitution responsible for luminescence activity. FEBS Lett. *583*, 2004–2008.

Oba, Y., Kumazaki, M., and Inouye, S. (2010). Characterization of luciferases and its paralogue in the Panamanian luminous click beetle Pyrophorus angustus: A click beetle luciferase lacks the fatty acyl-CoA synthetic activity. Gene *452*, 1–6.

O'Brien, P.J., and Herschlag, D. (1999). Catalytic promiscuity and the evolution of new enzymatic activities. Chem. Biol. *6*, R91–R105.

Ohno, S. (1970). Evolution by Gene Duplication (Springer).

Okamoto, Y., Morishita, J., Wang, J., Schmid, P.C., Krebsbach, R.J., Schmid, H.H.O., and Ueda, N. (2005). Mammalian cells stably overexpressing N-acylphosphatidylethanolamine-hydrolysing phospholipase D exhibit significantly decreased levels of N-acylphosphatidylethanolamines. Biochem. J. *389*, 241–247.

Palanker, L., Tennessen, J.M., Lam, G., and Thummel, C.S. (2009). Drosophila HNF4 regulates lipid mobilization and beta-oxidation. Cell Metab. *9*, 228–239.

Panchuk-Voloshina, N., Haugland, R.P., Bishop-Stewart, J., Bhalgat, M.K., Millard, P.J., Mao, F., Leung, W.Y., and Haugland, R.P. (1999). Alexa dyes, a series of new fluorescent dyes that yield exceptionally bright, photostable conjugates. J. Histochem. Cytochem. Off. J. Histochem. Soc. *47*, 1179–1188.

Patricelli, M.P., and Cravatt, B.F. (1999). Fatty Acid Amide Hydrolase Competitively Degrades Bioactive Amides and Esters through a Nonconventional Catalytic Mechanism. Biochemistry *38*, 14125–14130.

Pauff, S.M., and Miller, S.C. (2011). Synthesis of near-IR fluorescent oxazine dyes with esterase-labile sulfonate esters. Org. Lett. *13*, 6196–6199.

Pfleger, K.D.G., Seeber, R.M., and Eidne, K.A. (2006). Bioluminescence resonance energy transfer (BRET) for the real-time detection of protein-protein interactions. Nat. Protoc. *1*, 337–345.

Pietrowska-Borek, M., Stuible, H.-P., Kombrink, E., and Guranowski, A. (2003). 4-Coumarate:Coenzyme A Ligase Has the Catalytic Capacity to Synthesize and Reuse Various (Di)Adenosine Polyphosphates. Plant Physiol. *131*, 1401–1410.

Prado, R.A., Barbosa, J.A., Ohmiya, Y., and Viviani, V.R. (2011). Structural evolution of luciferase activity in Zophobas mealworm AMP/CoA-ligase (protoluciferase) through site-directed mutagenesis of the luciferin binding site. Photochem. Photobiol. Sci. *10*, 1226–1232.

Prescher, J.A., and Contag, C.H. (2010). Guided by the light: visualizing biomolecular processes in living animals with bioluminescence. Curr. Opin. Chem. Biol. *14*, 80–89.

Purtov, K.V., Petushkov, V.N., Baranov, M.S., Mineev, K.S., Rodionova, N.S., Kaskova, Z.M., Tsarkova, A.S., Petunin, A.I., Bondar, V.S., Rodicheva, E.K., et al. (2015). The Chemical Basis of Fungal Bioluminescence. Angew. Chem. Int. Ed Engl. *54*, 8124–8128.

Ramarao, M.K., Murphy, E.A., Shen, M.W.H., Wang, Y., Bushell, K.N., Huang, N., Pan, N., Williams, C., and Clark, J.D. (2005). A fluorescence-based assay for fatty acid amide hydrolase compatible with high-throughput screening. Anal. Biochem. *343*, 143–151.

Reddy, G.R., Thompson, W.C., and Miller, S.C. (2010). Robust light emission from cyclic alkylaminoluciferin substrates for firefly luciferase. J. Am. Chem. Soc. *132*, 13586–13587.

Reed, M.C., Lieb, A., and Nijhout, H.F. (2010). The biological significance of substrate inhibition: a mechanism with diverse functions. BioEssays News Rev. Mol. Cell. Dev. Biol. *32*, 422–429.

Reger, A.S., Wu, R., Dunaway-Mariano, D., and Gulick, A.M. (2008). Structural characterization of a 140 degrees domain movement in the two-step reaction catalyzed by 4-chlorobenzoate:CoA ligase. Biochemistry *47*, 8016–8025.

Ribeiro, C., and Esteves da Silva, J.C.G. (2008). Kinetics of inhibition of firefly luciferase by oxyluciferin and dehydroluciferyl-adenylate. Photochem. Photobiol. Sci. *7*, 1085–1090.

Russell, G.A., and Bemis, A.G. (1966). The Oxidation of Carbanions. I. Oxidation of Triaryl Carbanions and Other Tertiary Carbanions1. J. Am. Chem. Soc. *88*, 5491–5497.

Seliger, H.H., and McElroy, W.D. (1962). Chemiluminescence of firefly luciferin without enzyme. Science *138*, 683–685.

Seliger, H.H., and McElroy, W.D. (1964). The colors of firefly bioluminescence: Enzyme configuration and species specificity. Proc. Natl. Acad. Sci. U. S. A. *52*, 75.

Shinde, R., Perkins, J., and Contag, C.H. (2006). Luciferin derivatives for enhanced in vitro and in vivo bioluminescence assays. Biochemistry *45*, 11103–11112.

Shoup, T.M., Bonab, A.A., Wilson, A.A., and Vasdev, N. (2014). Synthesis and Preclinical Evaluation of [18F]FCHC for Neuroimaging of Fatty Acid Amide Hydrolase. Mol. Imaging Biol. *17*, 257–263.

Stapleton, M., Carlson, J., Brokstein, P., Yu, C., Champe, M., George, R., Guarin, H., Kronmiller, B., Pacleb, J., Park, S., et al. (2002). A Drosophila full-length cDNA resource. Genome Biol. *3*, RESEARCH0080.

Sundlov, J.A., Fontaine, D.M., Southworth, T.L., Branchini, B.R., and Gulick, A.M. (2012). Crystal structure of firefly luciferase in a second catalytic conformation supports a domain alternation mechanism. Biochemistry *51*, 6493–6495.

Takakura, H., Sasakura, K., Ueno, T., Urano, Y., Terai, T., Hanaoka, K., Tsuboi, T., and Nagano, T. (2010). Development of luciferin analogues bearing an amino group and their application as BRET donors. Chem. Asian J. *5*, 2053–2061.

Takakura, H., Kojima, R., Urano, Y., Terai, T., Hanaoka, K., and Nagano, T. (2011). Aminoluciferins as functional bioluminogenic substrates of firefly luciferase. Chem. Asian J. *6*, 1800–1810.

Tracy, T.S., Wirthwein, D.P., and Hall, S.D. (1993). Metabolic inversion of (R)-ibuprofen. Formation of ibuprofenyl-coenzyme A. Drug Metab. Dispos. Biol. Fate Chem. *21*, 114–120.

Viviani, V.R. (2002). The origin, diversity, and structure function relationships of insect luciferases. Cell. Mol. Life Sci. CMLS *59*, 1833–1850.

Viviani, V.R., and Ohmiya, Y. (2000). Bioluminescence Color Determinants of Phrixothrix Railroad-worm Luciferases: Chimeric Luciferases, Site-directed Mutagenesis of Arg 215 and Guanidine effect. Photochem. Photobiol. Sci. *72*, 267–271.

Viviani, V.R., and Ohmiya, Y. (2006). Bovine serum albumin displays luciferase-like activity in presence of luciferyl adenylate: insights on the origin of protoluciferase activity and bioluminescence colours. Lumin. J. Biol. Chem. Lumin. *21*, 262–267.

Viviani, V.R., Bechara, E.J., and Ohmiya, Y. (1999). Cloning, sequence analysis, and expression of active Phrixothrix railroad-worms luciferases: relationship between bioluminescence spectra and primary structures. Biochemistry *38*, 8271–8279.

Viviani, V.R., Hastings, J.W., and Wilson, T. (2002). Two bioluminescent diptera: the North American Orfelia fultoni and the Australian Arachnocampa flava. Similar niche, different bioluminescence systems. Photochem. Photobiol. *75*, 22–27.

Viviani, V.R., Prado, R.A., Neves, D.R., Kato, D., and Barbosa, J.A. (2013). A route from darkness to light: emergence and evolution of luciferase activity in AMP-CoA-ligases inferred from a mealworm luciferase-like enzyme. Biochemistry *52*, 3963–3973.

Watkins, P.A., and Ellis, J.M. (2012). Peroxisomal acyl-CoA synthetases. Biochim. Biophys. Acta *1822*, 1411–1420.

Weissleder, R., and Ntziachristos, V. (2003). Shedding light onto live molecular targets. Nat. Med. *9*, 123–128.

Welsh, D.K., and Noguchi, T. (2012). Cellular Bioluminescence Imaging. Cold Spring Harb. Protoc. *2012*, pdb.top070607.

de Wet, J.R., Wood, K.V., DeLuca, M., Helinski, D.R., and Subramani, S. (1987). Firefly luciferase gene: structure and expression in mammalian cells. Mol. Cell. Biol. *7*, 725–737.

White, E.H., Wörther, H., Seliger, H.H., and McElroy, W.D. (1966). Amino Analogs of Firefly Luciferin and Biological Activity Thereof. J. Am. Chem. Soc. *88*, 2015–2019.

White, E.H., Rapaport, E., Seliger, H.H., and Hopkins, T.A. (1971). The chemi- and bioluminescence of firefly luciferin: An efficient chemical production of electronically excited states. Bioorganic Chem. *1*, 92–122.

White, E.H., Steinmetz, M.G., Miano, J.D., Wildes, P.D., and Morland, R. (1980). Chemi- and bioluminescence of firefly luciferin. J. Am. Chem. Soc. *102*, 3199–3208.

Williamson, N.M., and Ward, A.D. (2005). The preparation and some chemistry of 2,2-dimethyl-1,2-dihydroquinolines. Tetrahedron *61*, 155–165.

Wilson, T., and Hastings, J.W. (1998). Bioluminescence. Annu. Rev. Cell Dev. Biol. *14*, 197–230.

Wood, K.V., Lam, Y.A., Seliger, H.H., and McElroy, W.D. (1989). Complementary DNA coding click beetle luciferases can elicit bioluminescence of different colors. Science *244*, 700–702.

Woodroofe, C.C., Shultz, J.W., Wood, M.G., Osterman, J., Cali, J.J., Daily, W.J., Meisenheimer, P.L., and Klaubert, D.H. (2008). N-Alkylated 6'-aminoluciferins are bioluminescent substrates for Ultra-Glo and QuantiLum luciferase: new potential scaffolds for bioluminescent assays. Biochemistry *47*, 10383–10393.

Woodroofe, C.C., Meisenheimer, P.L., Klaubert, D.H., Kovic, Y., Rosenberg, J.C., Behney, C.E., Southworth, T.L., and Branchini, B.R. (2012). Novel heterocyclic analogues of firefly luciferin. Biochemistry *51*, 9807–9813.

Zhao, H., Doyle, T.C., Coquoz, O., Kalish, F., Rice, B.W., and Contag, C.H. (2005). Emission spectra of bioluminescent reporters and interaction with mammalian tissue determine the sensitivity of detection in vivo. J. Biomed. Opt. *10*, 41210.